Exploring the Role of the Insulin and Insulin-like Growth Factor Receptors in Vascular Regeneration and Aging

Andrew Michael Nicholas Walker

Submitted in accordance with the requirements for the degree of
Doctor of Philosophy

The University of Leeds

School of Medicine

Leeds Institute of Cardiovascular and Metabolic Medicine

August 2017

Intellectual Property and Publication

The candidate confirms that the work submitted is his own and that appropriate credit has been given where reference has been made to the work of others.

Figures 1.4, 1.8 and 1.12 have been produced using images from Servier Medical Art which is available through an open license agreement at http://smart.servier.com/

Assertion of moral rights:

The right of Andrew Michael Nicholas Walker to be identified as Author of this work has been asserted by him in accordance with the Copyright, Designs and Patents Act 1988.

Acknowledgements

Firstly I should like to acknowledge the British Heart Foundation who have funded my 4 years in the Leeds Institute of Cardiovascular and Metabolic Medicine (LICAMM). Without their investment I would not have been able to study for a PhD, and their generosity in funding my experiments has allowed me a fantastic opportunity to explore the fascinating world of insulin and insulin-like growth factor-1 biology across a diverse range of assays.

I owe a great deal of thanks to Dr Nadira Yuldasheva for her considerable expertise in performing the femoral artery wire injury and hind-limb ischaemia surgery, the results of which are crucial to my project. Her help and guidance throughout my PhD have been immensely valuable. I wish to thank Mrs Jessica Smith for her fantastic work with RNA extraction and qPCR, and for her ongoing efforts on the mountain of samples I have harvested. I have greatly enjoyed working with Dr Nicole Watt on the behavioural assays performed on my colony, and look forward to continuing to do so in future. At some point over the last 4 years I have been helped by all of the different members of our research group, and therefore I should like to acknowledge the diverse knowledge and expertise of (in no particular order) Anna Skromna, Natallia Makava, Stacey Galloway, Natalie Haywood, Romana Mughal, Alexander Bruns, Paul Cordell, Helen Imrie, Hema Viswambharan, Matthew Gage, Nele Warmke, Pooja Shah and Dr Stephen Wheatcroft. I should also like to thank Drs Ben Mercer, Kate Gatenby, Amir Aziz, Noman Ali, Peysh Patel, Katherine Bridge, Katherine Griffin, Marc Bailey, John Dalton, Michael Drozd, Thomas Slater, and Anshu Sengupta for

their excellent company in the lab and their help across the multiple disciplines of the research world.

I owe particular thanks to my supervisors Dr Richard Cubbon and Professor Mark Kearney. Without their help and support I would not have been awarded funding to study for my PhD, and their vast knowledge and expertise have been invaluable throughout my research. I have greatly enjoyed the opportunity to work within Team Kearney/Cubbon and look forward to continuing to do so in the years to come.

Finally, I'd like to acknowledge the contribution of my family and friends over the past 4 years to creating a happy environment in which to pursue my research, including the unwavering support of my wife Naomi.

Abstract

Insulin resistance is a key independent risk factor for cardiovascular disease. Our group has previously shown that the insulin-like growth factor-1 receptor (IGF-1R) is a negative regulator of insulin receptor (IR) signalling, by sequestering IR subunits in insulin resistant IR:IGF1R 'hybrid receptors'. By crossing IR haploinsufficient (IRKO) mice with IGF-1R haploinsufficient (IGF1Rko) mice (producing "double knockout" or DKO mice), our group has previously demonstrated rescue of the endothelial dysfunction caused by insulin resistance. Whether this is associated with wider benefits in vascular biology or aging is unclear.

Our hypothesis was that reduced expression of the IGF-1R in whole body insulin resistance would improve vascular repair and regeneration and prolong healthspan. Metabolic assessment included measurement of weight gain and glucose and insulin tolerance testing. We studied vascular repair and regeneration with *in vivo* models, complementing these studies with mechanistic work *in vitro*. 15 animals per group were aged until they met healthspan endpoints, with monitoring of metabolic status throughout.

Glucose and insulin tolerance tests were similar in young DKO and IRKO mice, with DKO and IRKO having improved glucose tolerance and insulin sensitivity compared with WT and IGF1Rko when tested at ≥80 weeks of age. Body weight was significantly lower in young DKO than IRKO, with IRKO and DKO remaining lighter than WT and IGF-1Rko littermates as they aged. DKO had superior recovery after induction of hind-limb ischemia versus both IRKO and WT. Re-

endothelialisation after denuding femoral artery wire injury was improved in the DKO group compared with IRKO. Healthspan was significantly prolonged in DKO versus WT

In conclusion, reduced IGF-1R expression improves vascular repair and regeneration in the context of whole-body insulin resistance, and also appears to promote healthy aging. Further work will aim to elucidate the possible mechanisms for these observations.

Table of Contents

List of Figures

List of Tables

Abbreviations

Akt	Protein binding kinase B
APC	Allophycocyanin
ATM	Ataxia telangiectasia mutated
BH_4	Tetrahydrobiopterin
BP	Base pairs
BS	*Bandeiraea simplicifolia*
BSA	Bovine serum albumin
CHF	Chronic heart failure
CFU	Colony forming units
CPC	Circulating progenitor Cell
DGAT1	Diacylglycerol O-acyltransferase
DiI-ac-LDL	1,1'-dioctadecyl-3,3,3',3'-tetramethylindocarbocyanine-labelled acetylated low-density lipoprotein
DKO	Double knockout
DLL4	Delta-like ligand 4
DM	Diabetes mellitus
DNA	Deoxyribonucleic acid
DPP-4	Dipeptidyl peptidase-4
EBM-2	Endothelial cell basal medium-2
EC	Endothelial cell
ECFC	Endothelial Colony Forming Cell
EEPC	Early outgrowth endothelial progenitor cell (see also MAC)
EGM-2	Endothelial cell growth medium-2
eNOS	Endothelial Nitric Oxide Synthase
EDTA	Ethylenediaminetetraacetic acid
EPC	Endothelial progenitor cell
ERK	Extracellular signal-regulated kinase
ET-1	Endothelin-1
FACS	Fluorescence-activated cell sorting (FACS)

FGF	Fibroblast growth factor
FIRKO	Fat-specific insulin receptor knockout
FITC	Fluorescein isothiocyanate
Flk-1	Foetal liver kinase 1 (see also KDR)
FOXO1	Forkhead box O1
GH	Growth hormone
GLP-1	Glucagon-like peptide-1
GLUT2	Glucose transporter 2
GSK3	Glycogen synthase kinase 3
GTT	Glucose tolerance test
HbA1c	Glycosylated haemoglobin
HBSS	Hank’s Buffered Saline Solution
HDL	High density lipoprotein
HLI	Hind-limb ischaemia
HPF	High-power field
HUVEC	Human umbilical vein endothelial cell
IGF-1	Insulin-like growth factor-1
IGF-1R	Insulin-like growth factor-1 receptor
IGF-1Rko	Insulin-like growth factor-1 receptor knockout
IP	Intraperitoneal
IR	Insulin Receptor
IRKO	Insulin Receptor knockout
IRS-1	Insulin receptor substrate-1
ITT	Insulin tolerance test
IVC	Inferior vena cava
kDa	kiloDalton
KDR	Kinase domain receptor (see also Flk-1)
LEPC	Late-outgrowth endothelial progenitor cell (see also OEC and ECFC)
LSK	Lin(-)Sca-1(+)c-Kit(+) cells

MAC	Myeloid Angiogenic Cell (See also EEPC)
MAPK	Mitogen-activated protein kinase
MI	Myocardial infarction
MMP	Matrix metalloprotease
MPS	Mucopolysaccharide
mRNA	Messenger ribonucleic acid
mTOR	Mammalian target of rapamycin
NAD	Nicotinamide adenine dinucleotide
NADPH	Nicotinamide adenine dinucleotide phosphate
NAFLD	Non-alcoholic fatty liver disease
NO	Nitric Oxide
NOX	Nicotinamide adenine dinucleotide phosphate oxidase
OEC	Outgrowth endothelial cell (see also LEPC and ECFC)
PBS	Phosphate buffered saline
PBMC	Peripheral blood mononuclear cell
PCR	Polymerase chain reaction
PI3K	Phosphatidylinositol 3’-kinase
PPAR-γ	Peroxisome proliferator-activated receptor-gamma
PTP1B	Protein-tyrosine phosphatase 1B
Rictor	Rapamycin-insensitive companion of mTOR
ROS	Reactive oxygen species
RPI	Relative perfusion index
Rpm	Revolutions per minute
Sca1	Stem cell antigen 1
SEM	Standard error of the mean
SGLT2	Sodium-glucose co-transporter-2
SOD	Superoxide dismutase
T2DM	Type 2 diabetes mellitus
TGF	Transforming growth factor
TNF	Tumour necrosis factor

Tris-HCl	2-Amino-2-(hydroxymethyl)-1,3-propanediol hydrochloride
UV	Ultraviolet
VE-cadherin	Vascular endothelial cadherin
VEGF	Vascular endothelial growth factor
WT	Wild type

Chapter 1 **Introduction**

1.1 Insulin Resistance and Cardiovascular Risk

1.1.1 Epidemiology of Diabetes and Insulin Resistance

The rising prevalence of diabetes mellitus (DM) has become a global health emergency [1]. Cases of the disease have nearly quadrupled since 1980, with an estimated 422 million people living with diabetes in 2015 [2]. 5 million people die from the condition each year with associated global healthcare costs estimated at $673 billion per year [1]. Current projections suggest that by 2040 expenditure could approach $1.5 trillion annually, as the number with DM is forecast to soar to 642 million people worldwide [1].

Whilst rates of type 1 diabetes have remained similar for many years, it is the rapid increase in the prevalence of type 2 diabetes (T2DM) which has fuelled the global surge in cases [2]. The first type results from autoimmune destruction of insulin-producing pancreatic β-cells in early adulthood and requires lifelong treatment with exogenous insulin. 90% of diabetes cases are due to T2DM, a condition characterised by resistance to insulin in its target tissues, with progressive β-cell dysfunction over the course of the disease. The biggest risk factor for T2DM is obesity; global changes in food consumption favouring the so-called, “Western Diet” of high calorie, high fat meals mirrored by a decrease in physical activity have fuelled the rise in T2DM [3].

Diabetes is a key risk factor for cardiovascular disease and much of the excess morbidity and mortality associated with the condition is linked to its effects on the

vasculature [4]. People with diabetes are twice as likely to suffer myocardial infarction (MI) and stroke and these events occur on average 15 years earlier than in the general population [5, 6]. As a result, despite a European prevalence of diabetes close to 10% [1], groups with established heart disease include a far greater proportion of people with DM than the general population: a quarter of patients with MI [7] and heart failure [8] have diabetes. Not only do cardiovascular events occur prematurely and more frequently in those with DM; patients have a far poorer prognosis if they develop heart disease, with double the risk of mortality following MI or in the setting of chronic heart failure (CHF) [9, 10]. As such, despite advances in the treatment and prevention of heart disease in recent years, there remain divergent outcomes in those with DM [9, 11].

1.1.2 Prediabetes

As T2DM develops, it is well-established that significant abnormalities of insulin and glucose homeostasis are seen many years before serum glucose levels become elevated and type 2 diabetes is diagnosed (see figure 1.1, adapted from [12]). It is estimated that 318 million people worldwide have impaired fasting glycaemia, with elevated serum glucose levels below the threshold for diagnosis of diabetes [1]. Importantly, this period of insulin-resistant “prediabetes”, prior to overt DM, also carries an increased risk of cardiovascular disease [13].

The metabolic syndrome describes a clustering of cardiovascular risk factors associated with obesity and insulin resistance (see figure 1.2). The association

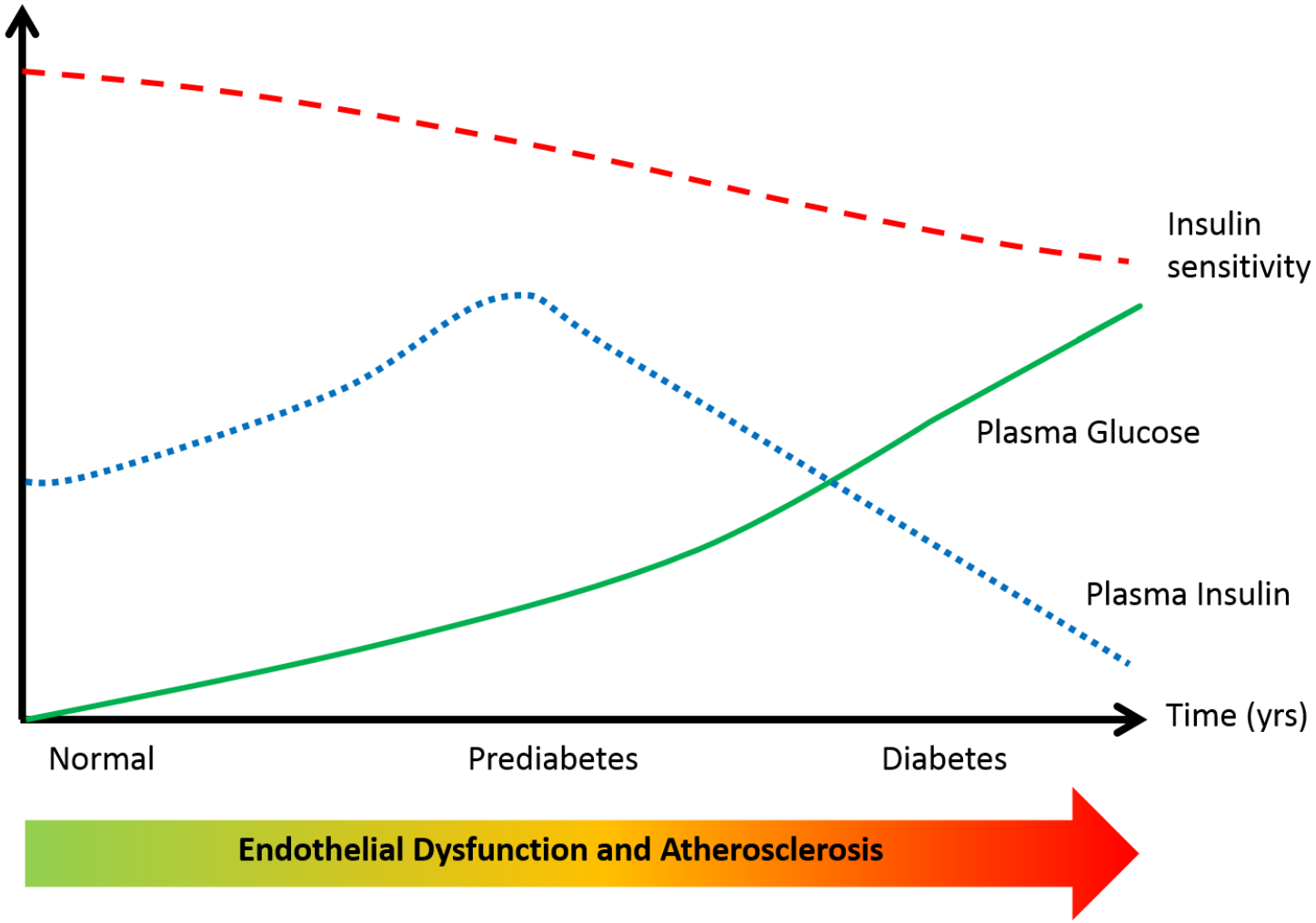

Figure 1.1 Glucose and Insulin Homeostasis in the Development of Diabetes

Insulin sensitivity decreases throughout the development of type II diabetes, mirrored by a gradual increase in plasma glucose which accelerates following a decline in plasma insulin levels. The risk of endothelial dysfunction and atherosclerosis increases throughout the period, meaning cardiovascular risk is elevated long before the diagnosis of diabetes.

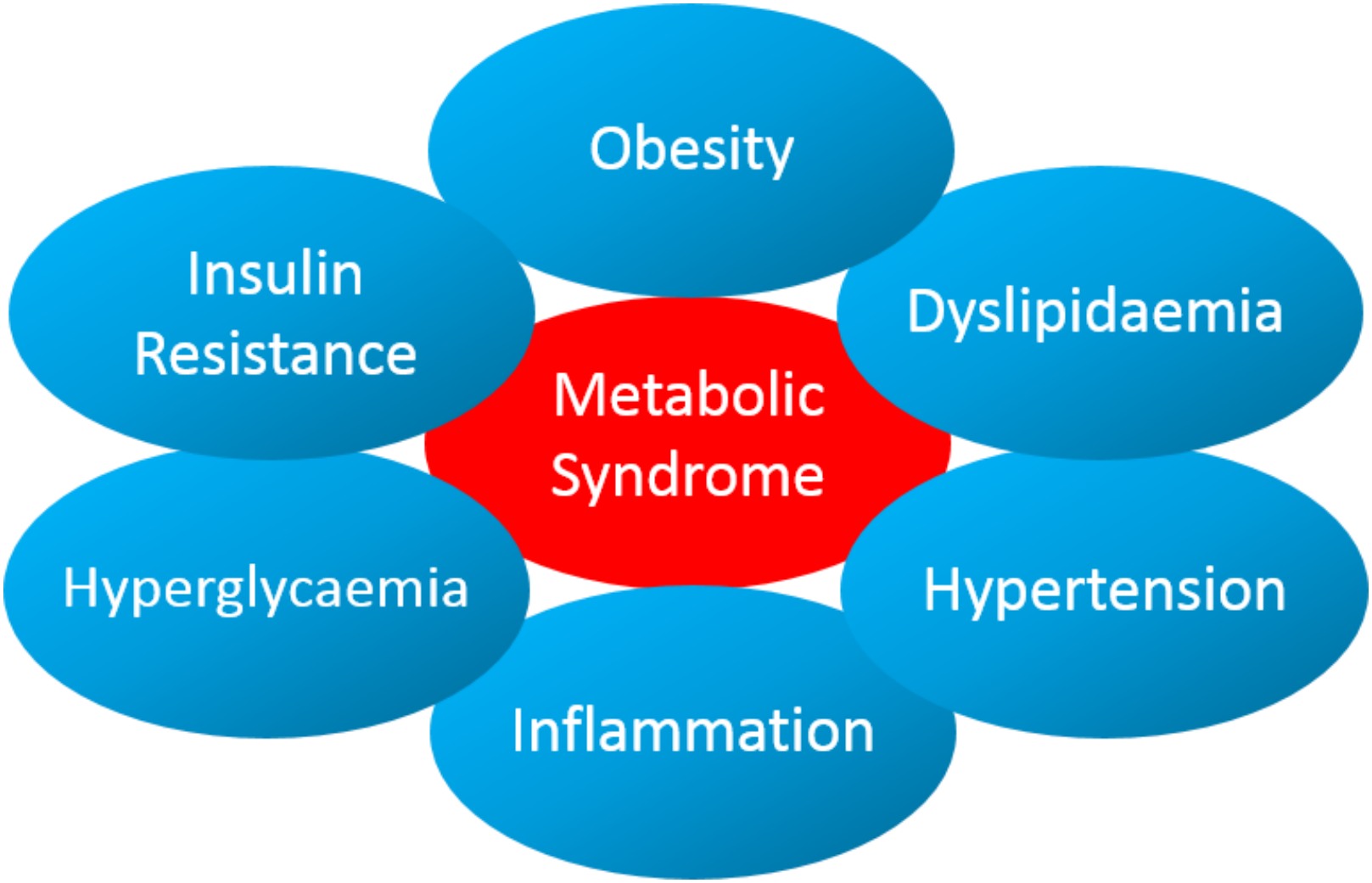

Figure 1.2: Features of the Metabolic Syndrome

Clustering of cardiovascular risk factors seen in the metabolic syndrome

between insulin resistance, hyperinsulinaemia, and established factors promoting cardiovascular disease, such as dyslipidaemia and hypertension, was first described in 1988 by Gerald Reaven [14]. Subsequently the metabolic syndrome, also known as syndrome X, has been defined as the presence of 3 or more of the following factors: elevated fasting glucose; hypertension; raised triglycerides; low serum levels of high density lipoprotein (HDL); and central obesity [15]. Impaired fasting glucose is now established as an independent risk factor for cardiovascular disease [13], though clearly the complex interactions between dysregulated glucose homeostasis, lipid metabolism, and blood pressure control in those with insulin resistant syndromes help create a powerfully pro-atherogenic environment.

1.1.3 Complications of Diabetes

Type 2 diabetes mellitus is a chronic multisystem disorder characterised by dysglycaemia and insulin resistance. The diverse complications of the condition are summarised in table 1.

Microvascular	Macrovascular	Other
Retinopathy	Ischaemic Heart Disease	Dementia
Nephropathy	Stroke	Thromboembolism
Neuropathy	Heart Failure	Dyslipidaemia
	Peripheral Vascular Disease	Hypertension
		Non-alcoholic Fatty liver Disease (NAFLD)

Table 1.1: Complications of Diabetes

Table adapted with permission from Walker *et al* [11]

1.1.4 Therapeutic Strategies

As outlined above, individuals with T2DM have a broad portfolio of metabolic perturbations. Clinicians have attempted to exploit these therapeutic targets to varying degrees of success.

1.1.4.1 Intensive Glucose Control

Hyperglycaemia is the most obvious metabolic difference between those with T2DM and the healthy population. It is long-established as an independent risk factor for cardiovascular disease [16] and there is a large body of evidence from clinical trials which demonstrates that ameliorating hyperglycaemia reduces microvascular complications of T2DM (reviewed in [11]). A landmark trial published in 1998 by the UK Prospective Diabetes Study (UKPDS) Group [17] showed that attempting to normalise serum glucose in individuals with T2DM can reduce the risk of retinopathy. Further evidence from the Action in Diabetes and Vascular Disease: Preterax and Diamicron Modified Release Controlled

Evaluation (ADVANCE) collaboration [18] demonstrated that intensive glycaemic control reduced the risk of nephropathy in their cohort of 11,140 patients with T2DM. That said, these studies and other large scale trials have failed to show a clear benefit of tight glycaemic control on the risk of macrovascular events [17-19]. Some evidence to suggest a modest benefit on cardiovascular endpoints was seen after very long term follow up (>10yrs) in the UKPDS study, although these findings should be treated with caution given that this was a *post hoc* analysis [20]. Indeed, aggressive glucose control may in fact be harmful; the Action to Control Cardiovascular Risk in Diabetes Study [21] was terminated prematurely due to excess mortality seen in the intensive treatment arm. Interestingly, this could not be fully explained by hypoglycaemia, highlighting the complexity in managing these high risk individuals [22].

1.1.4.2 Specific Hypoglycaemic Therapies

Specific therapies to manage T2DM have attempted to address the many elements of dysfunction within the glucoregulatory system. The biguanide Metformin is effective in lowering serum glucose and preventing microvascular outcomes [17]. Although research as part of the UKPDS study in the late 1990s suggested a benefit for the drug in reducing macrovascular outcomes in obese patients with T2DM [23], a more recent meta-analysis has cast doubt on these findings [24]. Boussageon *et al* highlighted the small sample size involved (342), the lack of blinding (amongst other methodological concerns), and noted that these results have not been replicated in subsequent trials. As such, the authors concluded that the current evidence base is insufficient to demonstrate a conclusive benefit of metformin for the reduction of cardiovascular risk in patients

with T2DM [24, 25]. Similarly, insulin secretagogues, such as the sulfonylurea Gliclazide, despite being first-line treatments for T2DM, are not effective in reducing the risk of cardiovascular disease [26].

Peroxisome proliferator-activated receptor (PPAR)-γ agonists are insulin-sensitising agents which have shown some beneficial effects in preclinical studies on factors such as vascular repair, endothelial function and endothelial progenitor cell activity, which might be expected to promote macrovascular health [27-30]. The most widely-prescribed of these drugs, Rosiglitazone, was famously withdrawn from clinical use in the US after increased rates of MI [31], heart failure [32], bone fractures [33], and death from cardiovascular causes [31] were noted. Whilst the FDA has now revised its position on the use of the drug as an oral hypoglycaemic, there is no evidence for any benefit of the medication on macrovascular outcomes in T2DM (reviewed in [11]). Pioglitazone, the other major PPAR-γ agonist, has remained in clinical use throughout, although there is conflicting evidence as to its efficacy in reducing cardiovascular outcomes in patients with T2DM [34-37]. A recent study demonstrated a benefit for the drug for secondary prevention after stroke or TIA in those with prediabetes [38], but whilst a small reduction in macrovascular events might be possible with this agent, any such benefit must be balanced against the potential for an increased risk of weight gain [34], bladder cancer [39], and worsening heart failure [40] associated with its use.

Incretin therapies exploit the activity of Glucagon-Like Peptide-1 (GLP-1) which is released in response to meals and augments the insulin response to promote

glucose absorption in peripheral tissues, thus lowering blood sugar levels. GLP-1 receptor agonists such as Exenatide and Liraglutide have been in clinical use for a number of years, and are effective hypoglycaemic drugs [41, 42]. Agents such as Sitagliptin inhibit the enzyme dipeptidyl peptidase-4 (DPP-4), which is responsible for the breakdown of GLP-1, thereby potentiating the effects of the endogenous hormone. There is some recent evidence for a beneficial effect on macrovascular events in patients with T2DM with Liraglutide [42], however similar trials with DPP-4 inhibitors [43-45] and a different GLP-1 agonist [46] have not demonstrated any superiority of these agents over placebo (discussed in [47]). As such, further work is required to establish the benefit of incretin therapies for reduction of cardiovascular risk in T2DM.

Sodium-glucose co-transporter-2 (SGLT2) inhibitors (gliflozins), such as Empagliflozin, are a relatively recent addition to the portfolio of hypoglycaemic agents. SGLT2 is expressed in the nephron, with gliflozins reducing sodium and glucose reabsorption in the proximal tubule, thereby leading to glycosuria, naturesis and hypoglycaemia [48]. Although these agents have only a modest hypoglycaemic effect and increase the risk of genital infection [49], they do offer some hope for the modification of macrovascular risk in diabetes. The recent EMPA-REG OUTCOME trial evaluating the safety of empagliflozin in patients with T2DM showed a reduction in macrovascular outcomes with this treatment versus placebo [49]. This finding was unexpected [50], given that reduction of serum glucose alone would not be expected to improve cardiovascular risk (see section 1.1.4.1). Subsequent studies have found that SGLT2 is also present within the glucagon-secreting alpha cells in the pancreatic islets [51], helping to explain the hyperglucagonaemia seen in patients treated with gliflozins. There

also appears to be a reduction in blood pressure associated with these agents [52, 53]. As such, wider metabolic effects may help explain the results of the EMPA-REG OUTCOME trial. The modest effect size on the primary outcome with empagliflozin (<2% absolute risk reduction) [49] and the lack of benefit seen for prevention of MI and stroke in secondary outcomes suggests that gliflozins alone will not abrogate the excess cardiovascular risk seen in T2DM, although they may be more useful in the setting of concomitant chronic heart failure [54]. Ongoing studies evaluating dapagliflozin (clinical trials number NCT01730534) and canagliflozin (NCT01032629) will further inform the evidence base on the utility of this class of drugs for preventing macrovascular outcomes in T2DM.

1.1.4.3 Other Treatments for Macrovascular Risk in Type II Diabetes

As one might expect, treatment for dyslipidaemia leads to improved macrovascular outcomes in T2DM [55], as does improving blood pressure control [56-58], although aggressive management may do more harm than good in those with established hypertension [59, 60]. Lifestyle modifications leading to weight loss might be expected to modify several elements of the metabolic syndrome and improve cardiovascular outcomes in patients with T2DM. Unfortunately, such interventions have not shown a long term benefit on cardiovascular outcomes, despite significant reductions in glycosylated haemoglobin (HbA1c) and weight [61].

As such, despite some encouraging results from recent clinical trials [38, 42, 49], there remains a significant challenge to the global healthcare community to abrogate the excess cardiovascular risk seen in patients with type II diabetes

mellitus [4]. The lack of success of strategies targeting established elements of the metabolic syndrome, such as hyperglycaemia and obesity, implies that a greater understanding of the other metabolic perturbations which affect people with insulin resistance is necessary. Work to elucidate the mechanisms which underpin the increased oxidative stress, abnormal growth factor signalling, adipocyte dysregulation, endothelial dysfunction, and impaired vascular repair and regeneration seen in T2DM (reviewed in [62]) could yield a broad portfolio of new targets to be exploited for future therapeutic development. A greater insight into these factors will be required if we are to realign the divergent macrovascular outcomes seen in those with and without diabetes [4, 9].

1.2 The Vascular Endothelium

1.2.1 Normal Endothelial Physiology

The intimal lining of blood vessels is far from a simple inert conduit through which blood is conveyed. The vascular endothelium is an exquisitely sensitive sensory organ which can detect minute changes in the circulatory environment. It employs powerful mechanisms to modify a diverse portfolio of processes which influence the absorption of key nutrients; regulate inflammation, thrombosis, and vessel tone; and co-ordinate vascular repair & regeneration. Given their potency in effecting change, both within the bloodstream and the vessels themselves, endothelial cells (ECs) are central to the maintenance of a healthy vasculature. When these cells become dysfunctional, their dysregulated actions can have serious, wide-ranging effects on the vascular system, and may promote atherosclerosis (see section 1.2.3) [63].

1.2.2 Nitric Oxide

Nitric Oxide (NO) is a key endothelial cell product, released by nitric oxide synthase (NOS) enzymes, principally endothelial NOS (eNOS), partly in response to signalling through the phosphatidylinositol 3'-kinase (PI3K)/Akt (protein binding kinase B) pathway (see section 1.3.3). NO is a hugely influential signalling radical, with wide-ranging effects on the vasculature. It is a potent direct vasodilator [64], and also has antithrombotic effects, both inhibiting platelet aggregation [65, 66] and thrombin-mediated platelet adhesion to the endothelium [67]. NO reduces leukocyte adhesion, thus playing a role in inflammation [68], but also negatively regulates endothelial cell growth [69] and inhibits proliferation of vascular smooth muscle cells (VSMC) [70]. NO contributes to vascular repair and regeneration by promoting angiogenesis and collateral formation after ischaemic injury [71]. The net effect of these vascular actions of NO is to protect against atherosclerosis [72]. Indeed, such is the importance of NO for vascular health that its deficiency is considered, "the hallmark of endothelial dysfunction" [73]. The vasodilatory effects of NO can be studied non-invasively in humans with techniques such as flow-mediated dilatation (FMD) [74]. Importantly, endothelial dysfunction as identified with FMD (i.e. insufficient NO to effect reactive hyperaemia following vascular occlusion [75]) is seen in those with risk factors for atherosclerosis who do not yet demonstrate macroscopic evidence of the disease [74]. As such, NO-deficient endothelial dysfunction is one of the earliest events in the atherosclerotic process.

Endothelial NOS (eNOS) is the primary enzyme responsible for the production of NO in the vasculature, although two other isoforms exist: inducible NOS

(iNOS), which is a minor producer of endothelial NO; and neuronal NOS (nNOS). Activated Akt can phosphorylate an eNOS dimer, which in the presence of haem and tetrahydrobiopterin (BH_4), sensitises eNOS to calcium/calmodulin activation [76]. Flavin adenine dinucleotide (FAD) and Flavin mononucleotide (FMN) are also essential cofactors [77]. eNOS then catalyses the conversion of L-arginine with oxygen and NADPH to L-citrulline, $NADP^+$ and nitric oxide, a process which again requires BH_4 as an essential cofactor (see figure 1.3) [78]. NO levels in the endothelium are determined by the scale of production of the radical itself by NOS enzymes, and also by the rate at which it is scavenged by reactive oxygen species, such as superoxide (O^-). As such, imbalance in endothelial cell signalling processes which influence eNOS function, such as those seen in insulin resistance (see section 1.3.7), can have major effects on the availability of NO [79], and therefore on endothelial function [80].

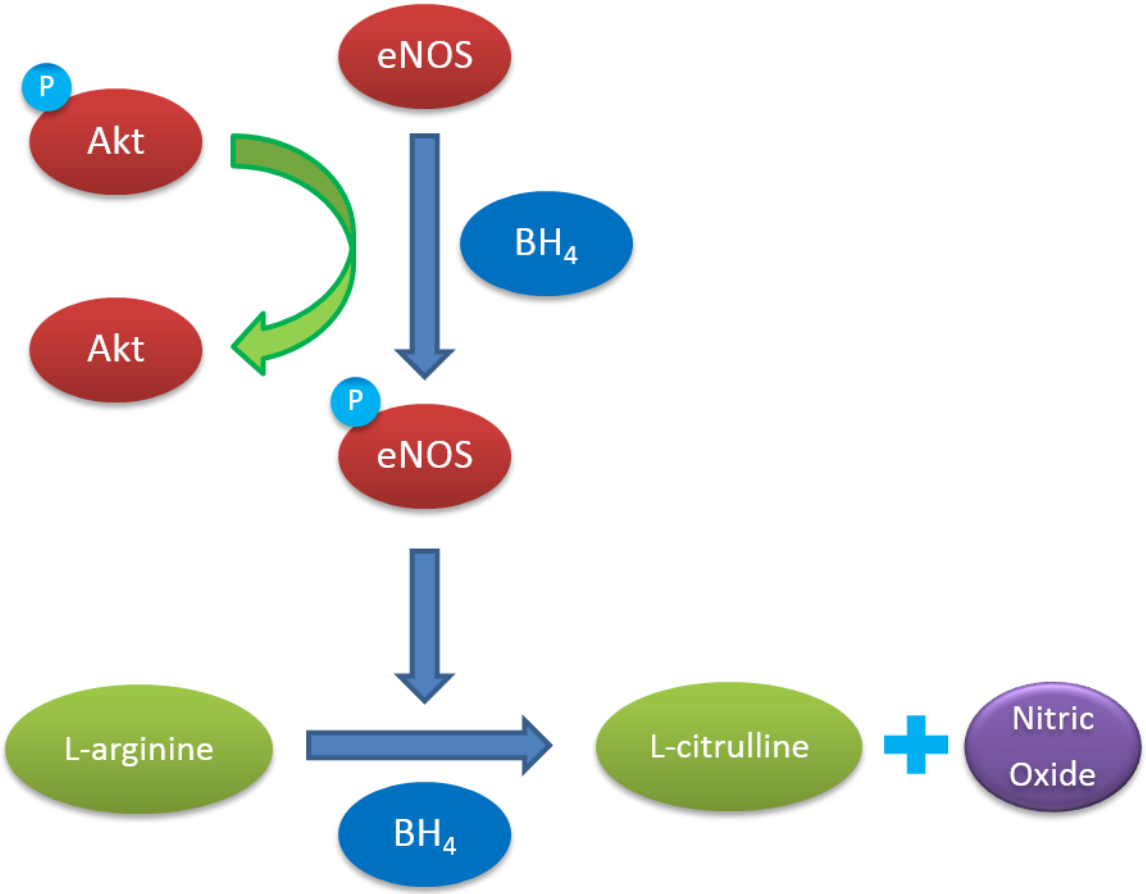

Figure 1.3: Nitric Oxide Production

Endothelial nitric oxide synthase (eNOS) is phosphorylated by phospho-Akt (protein binding kinase B) in the presence of tetrahydrobiopterin (BH_4). Flavin adenine dinucleotide (FAD) and Flavin mononucleotide (FMN) are also essential cofactors (not shown). BH_4, is also required for the conversion of L-arginine to L-citrulline and nitric oxide, catalysed by eNOS.

1.2.3 Atherosclerosis

Atherosclerosis is responsible for the vast majority of vascular disease. The term describes a chronic arterial inflammatory process characterised by the development of lipid-laden plaques (see figure 1.4) [81]. As mentioned above, endothelial dysfunction is the earliest step in this process, and may be precipitated by insulin resistance amongst many other stimuli. Dysfunctional or damaged endothelium expresses inflammatory molecules such as Intercellular Adhesion Molecule (ICAM) and selectins, and releases inflammatory cytokines such as TNF-α and a variety of interleukins [82]. The endothelium becomes more permeable to inflammatory cells and lipids, and the space between the intimal (endothelial) and medial (populated by vascular smooth muscle cells) layers begins to be infiltrated by inflammatory cells such as monocytes, and accumulates lipids (see figure 1.4). Monocytes differentiate to macrophages, and T-lymphocytes also play a role in the early development of a plaque. Macrophages accumulate lipid to become, “foam cells”, and by this stage the earliest macroscopic manifestation of atherosclerosis may be seen: the fatty streak [83]. Foam cells eventually undergo apoptosis, releasing powerful pro-inflammatory factors, and their lipid pools in the subendothelial space. As atherosclerosis progresses, a fibrous collagen cap forms and the plaque becomes more complex, with greater accumulation of cholesterol-rich lipids, and increased infiltration by macrophages, T-cells, and vascular smooth

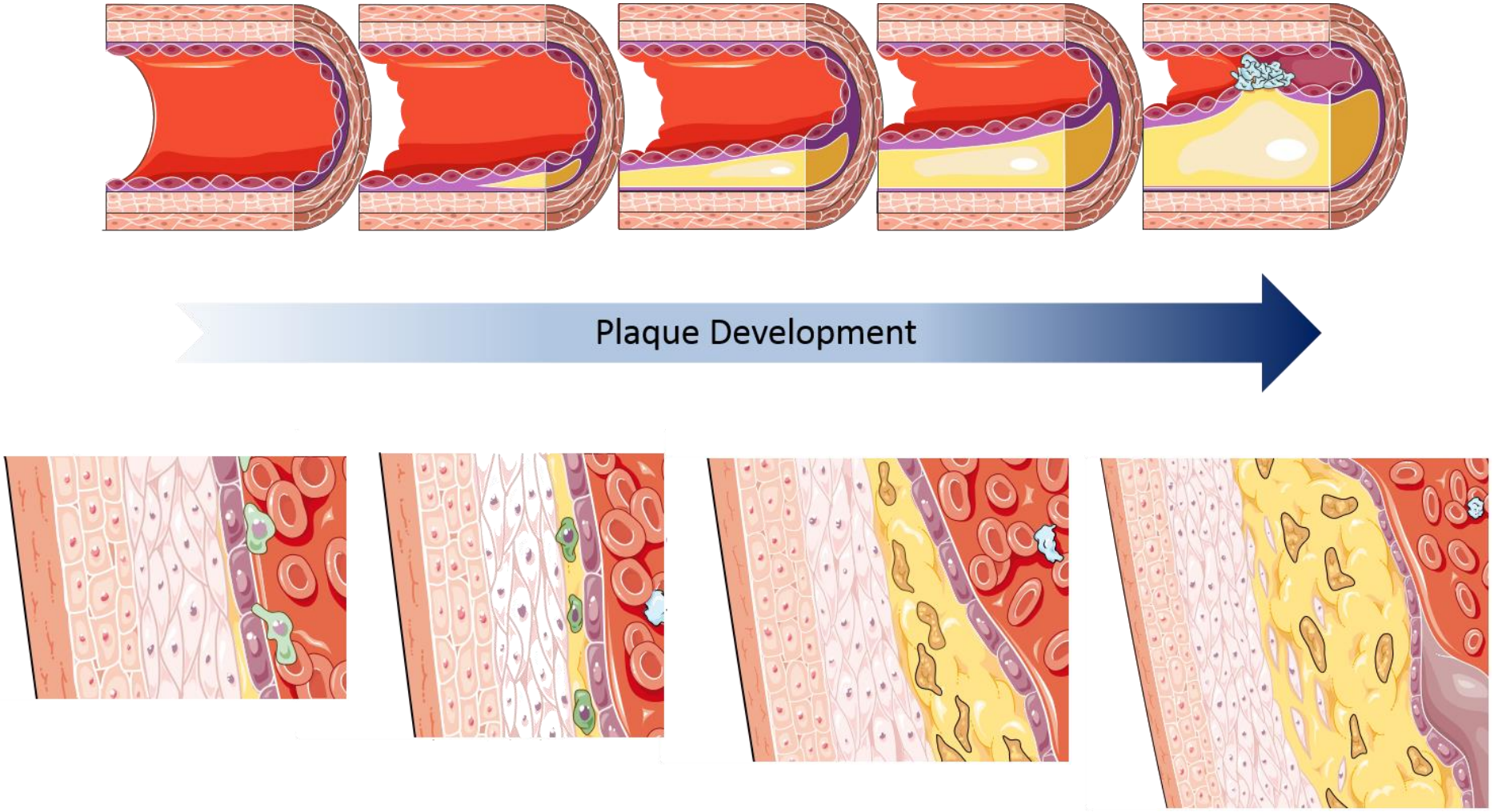

Figure 1.4: The Pathogenesis of Atherosclerosis

From left to right: monocytes (in green) pass through the endothelial barrier into the subendothelial space. Monocytes differentiate to macrophages and absorb the accumulating lipid to become foam cells. Eventually plaques become more cellular and complex with the involvement of vascular smooth muscle cells prior to atherothrombosis.

muscle cells [81]. Collagen, elastin and mucopolysaccharide (MPS) are found in increasing abundance and the plaque begins to calcify. This strongly pro-inflammatory, ischaemic milieu drives the development of neovessels within the plaque itself, which are of insufficient quality to provide purposeful perfusion, and instead lead to plaque haemorrhage. By this stage, the now unstable plaque is replete with thrombogenic and inflammatory factors. Plaque rupture liberates these contents into the circulation, leading to rapid, potent activation of the clotting cascade, platelet recruitment and thrombus formation, with vessel occlusion culminating in ischaemia or infarction of the tissue perfused by the vessel. This process, termed atherothrombosis, is responsible for the vast majority of acute coronary syndromes, and has been extensively studied in order to gain insights that have eventually improved outcomes in those patients with atherosclerotic vasculopathy. Whilst modern advances, such as angioplasty and stenting, have revolutionised the care of patients with established ischaemic heart disease, prevention is always superior to a ‘cure’. Therefore treatments which target the earliest stages of atherosclerosis, such as endothelial dysfunction, hold enormous therapeutic potential.

1.3 Insulin and Insulin-Like Growth Factor-1 Signalling

1.3.1 Insulin Biosynthesis and Secretion

Insulin is the key endogenous hypoglycaemic hormone, and is crucial for glucose homeostasis. First isolated by Banting and Best in the early 20th century, the protein provided a treatment for type I diabetes mellitus which had, until this point, been rapidly fatal. It was the first protein to have its amino acid structure

sequenced [84], and much of our current understanding of polypeptide biology stemmed from research into the hormone (reviewed in [85]).

The insulin gene is situated on chromosome 11 and insulin mRNA leads to production of the precursor protein, preproinsulin in the rough endoplasmic reticulum [86]. This is cleaved to proinsulin by a signal peptidase, then packaged into secretory vesicles at the Golgi apparatus (reviewed in [87]). Once within these vesicles, proinsulin is cleaved to insulin and C-peptide. Following consumption, glucose is absorbed through the gut via active transport through sodium/glucose cotransporters [88], but also by facilitated diffusion through glucose transporter 2 (GLUT2) channels [89]. Once in the circulation, extracellular glucose levels rise in the pancreas, and the molecule is transported into β-cells via the GLUT2 channel [87]. Rising intracellular glucose levels lead to increased production of ATP via glycolysis, and then interact with ATP-sensitive potassium channels, leading to plasma membrane depolarisation and calcium influx through voltage-dependent channels. Increased intracellular glucose also stimulates insulin production [90]. Calcium influx leads to exocytosis of the secretory vesicles containing insulin and C-peptide.

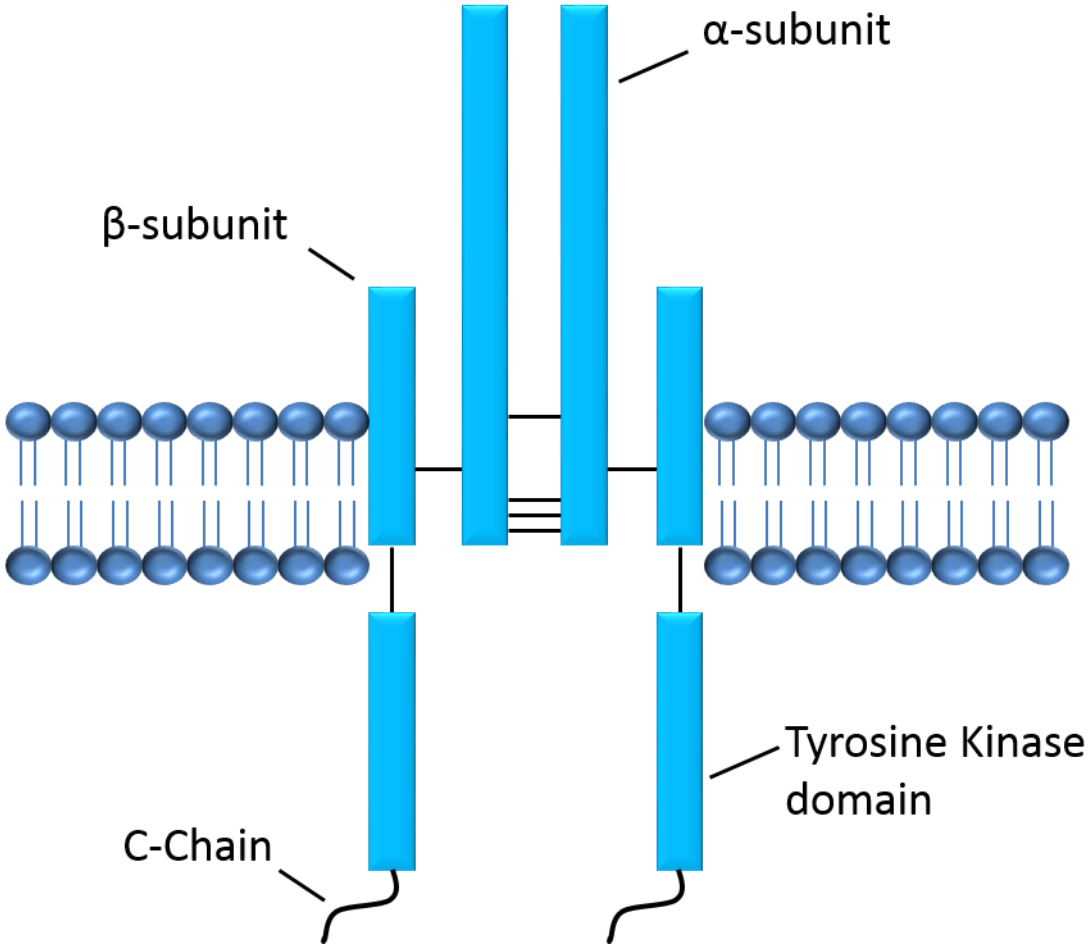

Figure 1.5: Structure of the Insulin Receptor

The insulin receptor comprises two predominantly extracellular α-subunits and two transmembrane β-subunits containing tyrosine kinase domains which project intracellularly. The two αβ subunits are linked by disulphide bonds.

1.3.2 The Insulin Receptor

The insulin receptor (IR) is a receptor tyrosine kinase comprising two αβ subunits linked by disulphide bonds (see figure 1.5). The prepro-receptor is translated as a single chain, then glycosylated and folded before dimerization to the homodimeric protein, chaperoned by calnexin and calreticulin [91]. The protein is then transported to the Golgi apparatus for further processing into the mature $\alpha_2\beta_2$ tetrameric receptor [92]. Once expressed on the plasma membrane the alpha subunits are largely extracellular, with a transmembrane portion linked to the beta subunits which project intracellularly and carry the tyrosine kinase domain. Two splice variants of the IR exist: IR-A and IR-B. These differ through the presence of a 12-amino acid segment, encoded by exon 11 of the insulin receptor gene, occurring exclusively in the IR-B variant, found between residues 716 and 717 of the IR-A [93].

The IR is widely expressed, and is a fundamental coordinator of nutrient sensing and metabolism, highly conserved through evolution [94]. A common precursor of the structurally similar IR and insulin-like growth factor-1 receptor (IGF-1R) has been identified in primitive organisms, such as *Caenorhabditis elegans,* and plays a key role linking nutrient intake with protein production and longevity [93, 95].

1.3.3 Insulin Receptor Signalling

Interactions between the alpha and beta subunits of the insulin receptor prevent spontaneous tyrosine kinase activity in the resting state [96]. Stimulation with

insulin induces conformational change within the IR, leading to autophosphorylation of the tyrosine kinase domain [97]. This process is highly regulated, with several factors influencing activation of the IR in response to ligand binding [98]. These include the particular splice isoform of the receptor itself [99], the ligand (IGF-1 may also stimulate IR activity, but has far lower affinity for the receptor [100]), and regulatory proteins such as protein-tyrosine phosphatase 1B (PTP1B) which is a negative regulator of insulin signalling [101]. IR activity is also regulated by ligand binding itself, as internalisation and degradation follow activation of the receptor by insulin or IGF-1 [102].

As described above, stimulation of the IR with insulin leads to autophosphorylation of the intracellular tyrosine kinase domain [97], which then activates two key pathways: the phosphatidylinositol 3'-kinase (PI3K)/Akt (protein binding kinase B) cascade and the Ras/ERK (extracellular signal-regulated kinase) pathway (see figure 1.6).

The interplay between these signalling processes is highly complex and influences a diverse range of cellular processes (reviewed in [98]). Central to the action of insulin as a hypoglycaemic hormone is that stimulation of its cognate receptor leads to upregulation of GLUT4 translocation to the cell surface membrane [103], thus facilitating greater glucose uptake by the cell. This action is dependent on the PI3K/Akt pathway, as are a broad portfolio of other processes which govern glucose metabolism including glycogen synthesis, regulated by glycogen synthase kinase 3 (GSK3), and gluconeogenesis, influenced by forkhead box O1 (FOXO1) [98].

1.3.4 Insulin Signalling and Vascular Function

Beyond the role of insulin signalling in glucose homeostasis, both PI3K/Akt signalling and the Ras/ERK cascade influence vascular function (see section 1.3.7). Akt stimulates endothelial nitric oxide synthase (eNOS) activity in endothelial cells, increasing production of the key signalling radical nitric oxide (NO). NO is a potent vasodilator and has a broad portfolio of effects on the vasculature including anti-inflammatory and anti-atherosclerotic actions [104] (see section 1.2.2). Ras/ERK signalling in the microvasculature counterbalances the actions of the PI3K/Akt pathway to a certain extent, favouring vascular smooth muscle cell proliferation and increasing endothelin-1 (ET-1) release, which promotes vasoconstriction. In heath, an appropriate balance is maintained between these competing pathways; however in the setting of insulin resistance and hyperglycaemia there is a shift towards increased Ras/ERK signalling mirrored by a decrease in PI3K/Akt activity [72]. The resultant reduction in NO production and bioavailability is thought to be a key precipitator of the increased atherosclerotic burden seen in insulin resistant syndromes.

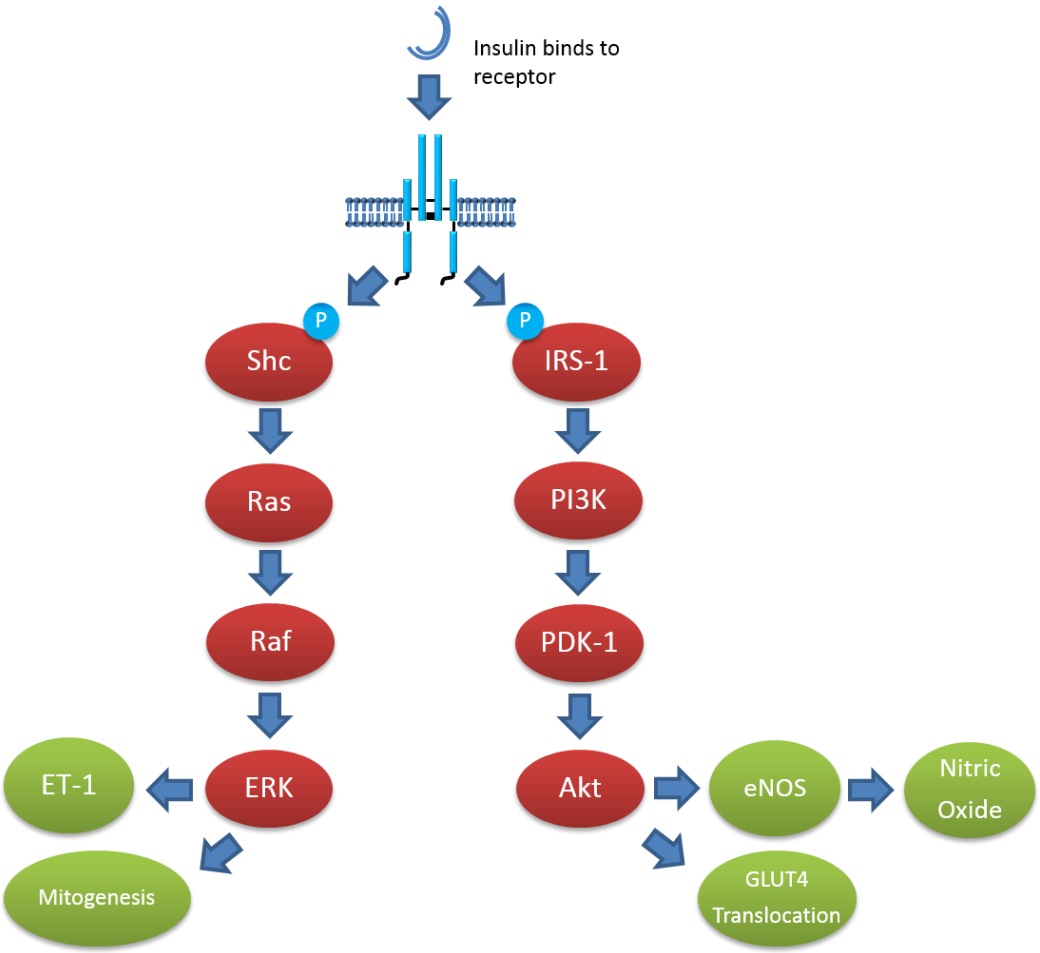

Figure 1.6: Insulin Signalling

Ligand binding stimulates autophosphorylation of the insulin receptor tyrosine kinase domains. These then phosphorylate insulin receptor substrates (IRS) to activate the PI3K (Phosphatidylinositol 3'-kinase)/Akt (protein binding kinase B) pathway. Akt stimulates translocation of glucose transporter 4 (GLUT4) to the cell membrane and stimulates eNOS (endothelial nitric oxide synthase) to produce nitric oxide. Phosphorylation of Shc leads to activation of the Ras/ERK (extracellular signal-regulated kinase) pathway which stimulates endothelin-1 (ET-1) production and has mitogenic effects.

1.3.5 Insulin-Like Growth Factor-1

Insulin-like growth factor-1 (IGF-1), as its name suggests, is a protein similar to insulin in structure and function. It is primarily synthesised by the liver, a process which is regulated by growth hormone (GH), although it is also produced in a growth factor-independent manner in peripheral tissues as a paracrine signal [105]. IGF-1 plays a key role in growth and development, as evidenced by the severely growth restricted phenotype seen in Laron syndrome, a rare condition caused by a primary deficiency in IGF-1 [105]. An important role for IGF-1 in glucose homeostasis is hinted at by the close link between acromegaly and type II diabetes. Acromegaly is generally caused by a GH hypersecreting pituitary adenoma, leading to increased serum IGF-1 levels, which are diagnostic for the condition [106]. The acromegalic phenotype, featuring large extremities, contrasts with that seen in Laron syndrome. People with acromegaly are insulin resistant, and often develop type II diabetes.

The actions of IGF-1 are intimately related to glucose and insulin homeostasis. Hepatic glucose release is decreased by IGF-1, and it also modulates free fatty acid metabolism [107]. Administration of IGF-1 has been trialled as a treatment strategy for patients with diabetes, leading to improved glycaemic control and a decreased requirement for exogenous insulin [108]. Unfortunately, side effects such as facial and peripheral oedema, arthralgia, myalgia, and tachycardia have limited its use as a therapeutic, but it is clear that a greater understanding of the relationship between IGF-1, insulin and glycaemic control represents an important avenue of study for the development of novel treatments to manage insulin resistant syndromes.

IGF-1 levels are closely related to cardiovascular disease. Low serum IGF-1 in otherwise healthy individuals is associated with a doubled risk of ischaemic heart disease [109]. Indeed a 38% increased risk of death due to coronary artery disease was seen for every 40ng/ml decrement in IGF-1 in a large American cohort study [110]. Across the Atlantic, a European population study has linked high IGF-1 levels with a lower risk of acute coronary syndromes [111]. Interestingly, a more complex, “U-shaped” relationship between IGF-1 levels and cardiovascular disease has been identified by other groups [112, 113]. As such, a greater understanding of the effects of IGF-1 on the vasculature is clearly warranted.

1.3.6 The Insulin-like Growth Factor-1 Receptor and Insulin Receptor Hybridisation

The insulin-like growth factor-1 receptor (IGF-1R) shares approximately 70% DNA sequence homology with the insulin receptor [114] and developed from a common evolutionary precursor [115]. As such, the downstream actions of the activated IR and IGF-1R are intimately related, yet differ in several important respects (see section 1.3.7). A fundamental difference between the two receptors and hormones is their ability to effect NO generation in endothelial cells. Studies *in vitro* with human umbilical vein endothelial cells (HUVECs) have shown that stimulation with IGF-1 results in only 40% of the nitric oxide produced by stimulation of such cells with an equimolar concentration of insulin [116]. Further data indicate IGF-1 receptors are far more numerous than insulin receptors (by up to a factor of ten depending on whether endothelial cells are

derived from the micro- or macrovasculature [116]). As such, endothelial cells are in other regards relatively insulin resistant [117].

A concept which is crucial to the understanding of the interplay between IR and IGF-1R biology is that of IR:IGF-1R hybridisation (see figure 1.7). Due to the structural homology between the two receptors, αβ dimers from each of the IR and IGF-1R can heterodimerise to form so-called, “hybrid” receptors. Critically, these hybrids have an affinity for IGF-1 similar to that of its canonical receptor, but do not respond to insulin except at supraphysiological concentrations [117-119]. Increased hybrid receptor expression is seen in obesity and type II diabetes and levels correlate inversely with insulin sensitivity [120], demonstrating the potential importance of this phenomenon in human disease. If IR αβ heterodimers are sequestered into hybrid receptors in these disease states, this may help to explain the resistance to insulin of these cells, and therefore the endothelial dysfunction and subsequent accelerated atherogenesis which is a hallmark of these conditions.

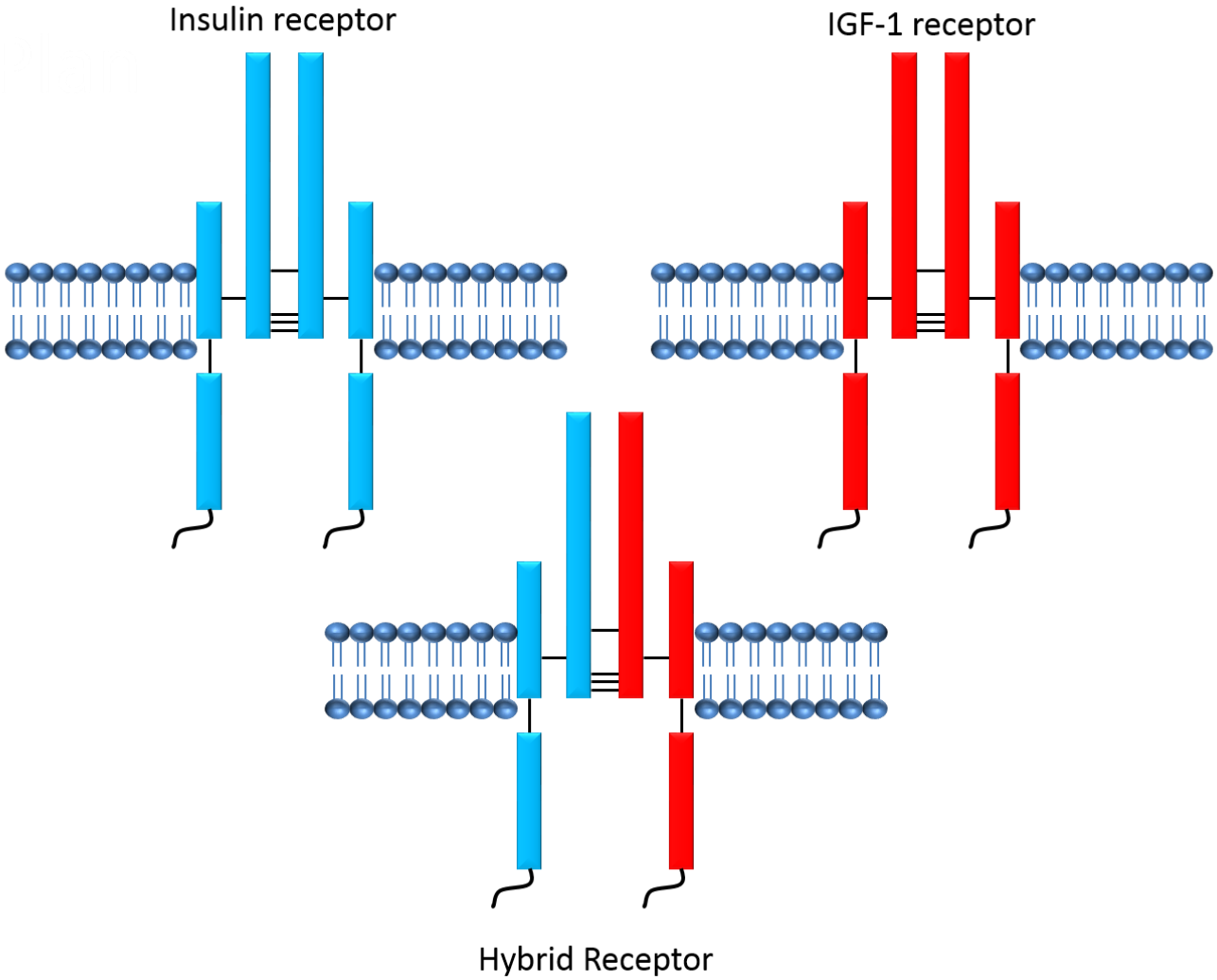

Figure 1.7: Insulin and IGF-1 Receptor Hybrids

Hybrid receptors are formed through heterodimerisation of an insulin receptor αβ subunit (blue) and an insulin-like growth factor-1 receptor αβ subunit (red).

The precise mechanism by which hybrid receptor expression is regulated remains unclear; however, there are several factors which have been shown to be important for the process. Work by Federici *et al* has shown hybrid receptor expression is higher in the setting of hyperinsulinaemia [121], and also with hyperglycaemia [120, 122]. Work from this lab has demonstrated the importance of the molar ratio of the different receptors in the endothelium for hybrid receptor formation [123, 124]. Transgenic mice haploinsufficient for the insulin receptor ($IR^{+/-}$, or insulin receptor knockout (IRKO)) display increased hybrid receptor expression [123], an observation which is associated with decreased NO bioavailability [125] and deficient vascular repair [80]. In animals haploinsufficient for both the IR and IGF-1R, so-called, “double knockout” (DKO) mice ($IR^{+/-}$/$IGF\text{-}1R^{+/-}$), this relative difference in hybrid receptor expression is abrogated, with NO bioavailability restored to wild type (WT) levels [123]. The converse is true in animals overexpressing the IGF-1R in the endothelium, with increased hybrid receptor expression and diminished NO bioavailability seen [124]. As such, expression of the IGF-1R appears to be an important determinant of hybrid receptor expression, and consequently of endothelial function and insulin sensitivity.

1.3.7 IR/IGF-1R Signalling in Health and Disease

Studies examining the pathophysiology of insulin resistance have identified important differences in insulin and IGF-1 signalling in disease states such as obesity and type II diabetes [126]. Although each receptor activates both pathways to a certain degree, activation of the IR preferentially stimulates the PI3K/Akt cascade [93, 126-129], influencing key glucose homeostatic processes

and favouring NO production, thereby promoting normal endothelial function. By contrast, the IGF-1R appears to favour stimulation of the Ras/ERK system to influence mitogenesis and promote ET-1 production. A shift towards maintained Ras/ERK signalling, with diminished PI3K/Akt activity is seen in insulin resistant states [126, 130]. This leads to diminished eNOS activity and an imbalance towards increased ET-1 production and therefore endothelial dysfunction. The precise mechanisms for this shift are complex, with a range of factors thought to influence the process [131]. Certainly, the concept of IR:IGF-1R hybrids, increased levels of which are associated with insulin resistant disease states, represents an important possible mechanism for the imbalance between PI3K/Akt and Ras/ERK signalling seen in T2DM [94]. Other authors have postulated that these differences may be related to divergent IRS1 and IRS2 expression in the setting of sustained hyperinsulinaemia and subsequent divergence of their downstream signalling cascades [132]. However, it is important to consider further evidence that insulin resistance occurs at multiple nodes in the signalling cascade in pathological states, with a wide variety of proteins implicated [98]. PTP1B levels in brain [133], muscle [101], and liver [134] have been shown to have an important influence on glucose homeostasis, while the roles of PI3K and AKT themselves are central to effective glucose handling [98]. As such, a difference in the expression or activity of any of these molecules is likely to have an important influence on the sensitivity of cells to insulin.

The influence of different IR splice variants on downstream signalling has been described [93], and there is evidence that expression of IR-A and IR-B is altered in insulin resistant states [135-137]. Although insulin receptor mutations do not

appear to contribute meaningfully to the T2DM epidemic [138] the importance of the precise IR structure for appropriate signal transduction has been extensively studied. Recent research from the Kahn group has highlighted the importance of structural differences between the IR and IGF-1R in their divergent signalling properties [127]. Cai *et al* used an elegant approach to investigate the roles of the IR and IGF-1R, employing modified forms of each receptor with either swapped or mutated intracellular or extracellular domains. These studies were conducted in cells featuring only one of each type of receptor, thus examining the roles of each receptor tyrosine kinase in isolation, and without the possibility for IR:IGF-1R hybridisation. The intracellular domain was found to be the most influential portion of the receptors in determining downstream signalling. Indeed the authors identified a single amino acid in the juxtamembrane region of the IR (Leucine^{973}) which, when substituted for the corresponding residue in the IGF-1R (Phenylalanine), shifted the activity of the receptor towards Ras/ERK stimulation and away from PI3K/Akt signalling. The authors noted that whilst the tyrosine kinase domains of the two receptors are virtually identical, differences elsewhere in the beta subunit appear to alter the docking potential for the various potential substrates of phosphorylation. As such, these structural differences may help explain the apparent propensity for the IR and IGF-1R to preferentially regulate particular downstream signalling pathways.

This study provides important insights within the confines of a much-simplified model environment. In human physiology the complex interactions between the PI3K/Akt and Ras/ERK systems are likely to be influenced to a greater or lesser extent by a combination of each of the above factors. Given the importance of IR and IGF-1R signalling in health and disease, further study is required in order

to translate these interesting observations towards future therapies for insulin resistant syndromes.

1.3.8 Animal Models of Insulin and Growth Factor Resistance

1.3.8.1 Models of Insulin Resistance

More than 40 different animal models of insulin resistance and diabetes have been described, spanning a broad range of phenotypes (reviewed in [139], [12], [140]). Streptozotocin, a substance which leads to pancreatic beta-cell destruction, can be administered to mice, resulting in reduction or failure of insulin production and consequent diabetes [141]. This model emulates the type I diabetes phenotype, with resultant diabetic ketoacidosis if high doses are given. Particular breeds of mice have a greater propensity to develop diabetes, such as the C57/Bl6 strain. High fat diet feeding leads to obesity, glucose intolerance, and insulin resistance in these animals, mirroring the phenotype seen in patients with type II diabetes [142]. Other approaches involve manipulation of the action of the adipokine leptin, which is crucial for satiety. Strains such as leptin-deficient ob/ob [143] and leptin receptor-deficient db/db mice offer alternative murine experimental models of type II diabetes. Models such as these display many of the physiological and phenotypic abnormalities we associate with human T2DM; however, due to their complexity, other approaches specifically targeting the insulin receptor allow more precise study of pre-diabetic insulin resistance. Homozygous insulin receptor null animals have been generated using targeted disruption of the insulin receptor gene via a homologous recombination approach [144, 145]. These animals survive to term, but die roughly 7 days *post-partum* due to diabetic ketoacidosis. By contrast, mice haploinsufficient for the insulin

receptor gene, known as insulin receptor knockout (IRKO) mice [145] ($IR^{+/-}$), exhibit a milder phenotype of insulin resistance, with the only significant metabolic abnormality being elevated plasma insulin levels after glucose challenge [146]. These animals offer a model of human prediabetes, as despite only a limited perturbation in glucoregulation, they have a significant impairment in vasomotor function [146] and NO bioavailability [147], highlighting the importance of insulin signalling for normal endothelial function. Additionally, IRKO mice exhibit attenuated endothelial recovery after vascular injury (see section 1.4.2), which is associated with decreased number and function of endothelial progenitor cells (EPCs) (see section 1.4.4) [80]. These animals also have significantly greater expression of IR/IGF-1R hybrid receptors in the endothelium than wild type controls [123]. As such, they are one of the models chosen for this study in order to investigate the contribution of IR and IGF-1R signalling to vascular regeneration.

1.3.8.2 Mouse models to investigate the role of the IGF-1R in vascular repair and regeneration

Work from this lab has investigated the role of the IGF-1R in glucose homeostasis, endothelial function and vascular repair. Transgenic mice with endothelial-specific overexpression of the human IGF-1R have increased hybrid receptor expression, with a corresponding decrease in insulin-stimulated eNOS activity and basal NO production [124]. Mice heterozygous for the IGF-1R gene (IGF1Rko) are mildly glucose intolerant, yet have improved basal and insulin-stimulated NO production, as compared to WT counterparts [123], mirrored by a decrease in hybrid receptor expression. Consistent with this apparently

favourable vascular phenotype, these animals have improved recovery after femoral arterial wire injury (see section 1.4.2) and have augmented circulating progenitor cell (CPC) function *in vitro* and *in vivo* [148] (see section 1.4.4). Animals haploinsufficient for both the IR and IGF-1R (IRKO-IGF1Rko or DKO) have been studied in this lab to investigate the effect of IGF-1R deficiency in the setting of insulin resistance [123]. Hybrid receptor expression in these mice is consistent with WT levels, abrogating the excess expression of these IR/IGF-1R heterodimers seen in IRKO mice. These animals also have improved vasomotor function and NO bioavailability compared with IRKO littermates [123]. As such, IR/IGF-1R hybrid biology appears closely associated with endothelial function and vascular repair, and further insights in this area may be key to understanding the pathophysiology of the excess cardiovascular risk seen in insulin resistant syndromes.

1.4 Vascular Repair and Regeneration

1.4.1 Introduction

The development of the vascular system has allowed evolution from simple forms of life to the complex multicellular organisms which inhabit the Earth today. The delivery of oxygen and substrates of metabolism to cells via blood vessels is crucial to their survival. Therefore, the processes by which arteries and veins are formed, maintained, and remodelled are essential for multicellular life. Angiogenesis was first identified as a target for therapeutics in the 1970s, when it was discovered to be a key determinant of cancer growth [149]. As such, antiangiogenic therapies (reviewed in [150]) have been developed to combat

malignant disease and other conditions characterised by excessive blood vessel development such as wet age-related macular degeneration.

Diabetes is a condition which exemplifies disordered blood vessel development and maintenance. In some tissue beds such as the retina, excessive, poor-quality blood vessel development is seen, whereas in other organs insufficient angiogenesis contributes to a failure of patients with DM to recover from acute limb ischaemia and to heal soft tissue wounds (reviewed in [62], [151]). As such, the simple distinction between more or less angiogenesis is not sufficient to understand or treat the full spectrum of angiogenic disorders seen in diabetes and insulin resistance. Rather, a more nuanced approach to promote healthy angiogenesis appears to hold the key to manipulation of the process for therapeutic ends.

1.4.2 Vascular repair

Vascular repair and regeneration are related but different processes which are crucial to the recovery of the vasculature after damaging stimuli. Vascular repair specifically refers to the process of re-endothelialisation which occurs after injury to a blood vessel resulting in denudation of the endothelial monolayer. This may be due to atherosclerosis, or via iatrogenic damage from catheter-based procedures such as angioplasty [62]. Animal models such as murine femoral artery wire injury (see section 4.4.1) have been used to study this process and to help understand the factors which may enhance or inhibit recovery from endothelial damage [124].

Several cellular processes are likely to contribute to vascular repair. Endothelial cells residing close to the denuded area of the vessel may activate, proliferate, then migrate to fill the gap and restore the endothelial barrier: a process which is influenced by VEGF [152]. There is also a body of work to suggest that marrow-derived progenitor cells are important for this process [80, 153, 154] (see section 4.8). Work by Hagensen *et al* indicated that progenitor cells from bone marrow may exert their beneficial effects via paracrine mechanisms [154, 155], rather than by contributing directly to the regenerated endothelium. That said, *in vivo* studies from this lab and others have shown that transplanted circulating progenitor cells (CPCs) [148, 156], myeloid angiogenic cells (MACs) [157], and endothelial colony forming cells (ECFCs) do at least transiently reside in the vasculature of the recipient [153]. Indeed, our work has shown clear evidence demonstrating ECFCs directly form new intima and capillaries [153]. As such, perturbations in the abundance or function of such cells have an important influence on the process of vascular repair. This will be discussed in greater detail in section 1.4.6.

1.4.3 Vascular Regeneration

Whilst vascular repair describes the recovery of the endothelial monolayer after vascular injury, vascular regeneration is a far more complex process involving not just endothelial cells, but vascular smooth muscle cells (VSMC), and pericytes to re-establish a vascular plexus in an area deprived of perfusion [158]. *Vasculogenesis* is the process by which new blood vessels form *de novo* from progenitor cells [159]. This process has only been formally observed *in utero*. It is important to distinguish vasculogenesis from *angiogenesis*, which refers

specifically to the sprouting of neovessels from existing blood vessels and will be a focus for study in this project. Angiogenesis may be termed developmental when it occurs as part of normal blood vessel formation *in utero* or during organismal growth, or pathological when induced by disease. *Arteriogenesis* is the related process by which microvessels mature into conduit arteries, with enlargement of the lumen and the establishment of a surrounding network of VSMCs to support the endothelium.

1.4.3.1 Angiogenesis

The complex processes of angiogenesis are crucial for normal vascular development and maintenance, as well as for an effective response to tissue damage. Inadequate perfusion leads to hypoxia and nutrient depletion, resulting in acidosis and an increased nicotinamide adenine dinucleotide (NAD^+)/NADH ratio. A range of mechanisms detect these disturbances then effect changes in cellular metabolism, promote VEGF generation and signalling, and enhance Delta-like ligand 4 (DLL4)/Notch activity [160] (see figure 1.8).

Exposure to VEGF causes activation of quiescent endothelial cells (ECs) (see figure 1.9), leading to the development of fine protrusions called filopodia (see figure 1.10 – confocal image from mouse retina) which aid in the sensing of angiogenic stimuli. Activated ECs secrete enzymes such as matrix metalloprotease-1 (MMP-1) which break down the capillary basement membrane [160]. Angiopoetin 2, released from EC Weibel-Palade bodies [161], promotes detachment of mural cells such as VSMCs and pericytes [162], with the result that endothelial cells are exposed to greater concentrations of VEGF

and other proangiogenic factors. Further EC activation follows, which is then tempered through the process of lateral inhibition to favour the emergence of tip and stalk cells, with concomitant suppression of those cells which are less responsive to VEGF (see figure 1.11) [163, 164]. A feature of healthy angiogenesis is that an effective balance is achieved between activation and suppression of ECs in order to promote good quality vascular development and patterning. As such, DLL4/Notch signalling is crucial for effective angiogenesis, as an excess of either the tip or stalk phenotype would result in abnormal sprout formation and flow. Indeed, genetic deletion of either DLL4 or Notch-1 in mouse embryos leads to intrauterine death [165].

Tip cells migrate along the VEGF gradient, leading stalk cells to protrude from the established endothelium, thereby producing an angiogenic sprout. Sprouts from neighbouring vessels may then fuse, through the formation of VE-cadherin junctions on the tip cells (see figure 1.9, step 5), in a process facilitated by tissue macrophages [166]. Stalk cells facilitate lumen formation via cell and cord hollowing to create a new conduit for blood flow [167]. Mural cells are then recruited and a basement membrane established, leading to completion of a mature vessel as the endothelial cells return to quiescence. Finally, there is provision for remodelling of the vascular plexus in response to low flow, leading to regression of redundant vessels through decreased levels of shear stress and resultant diminished Krüppel-like factor 2 (KLF2) signalling [160].

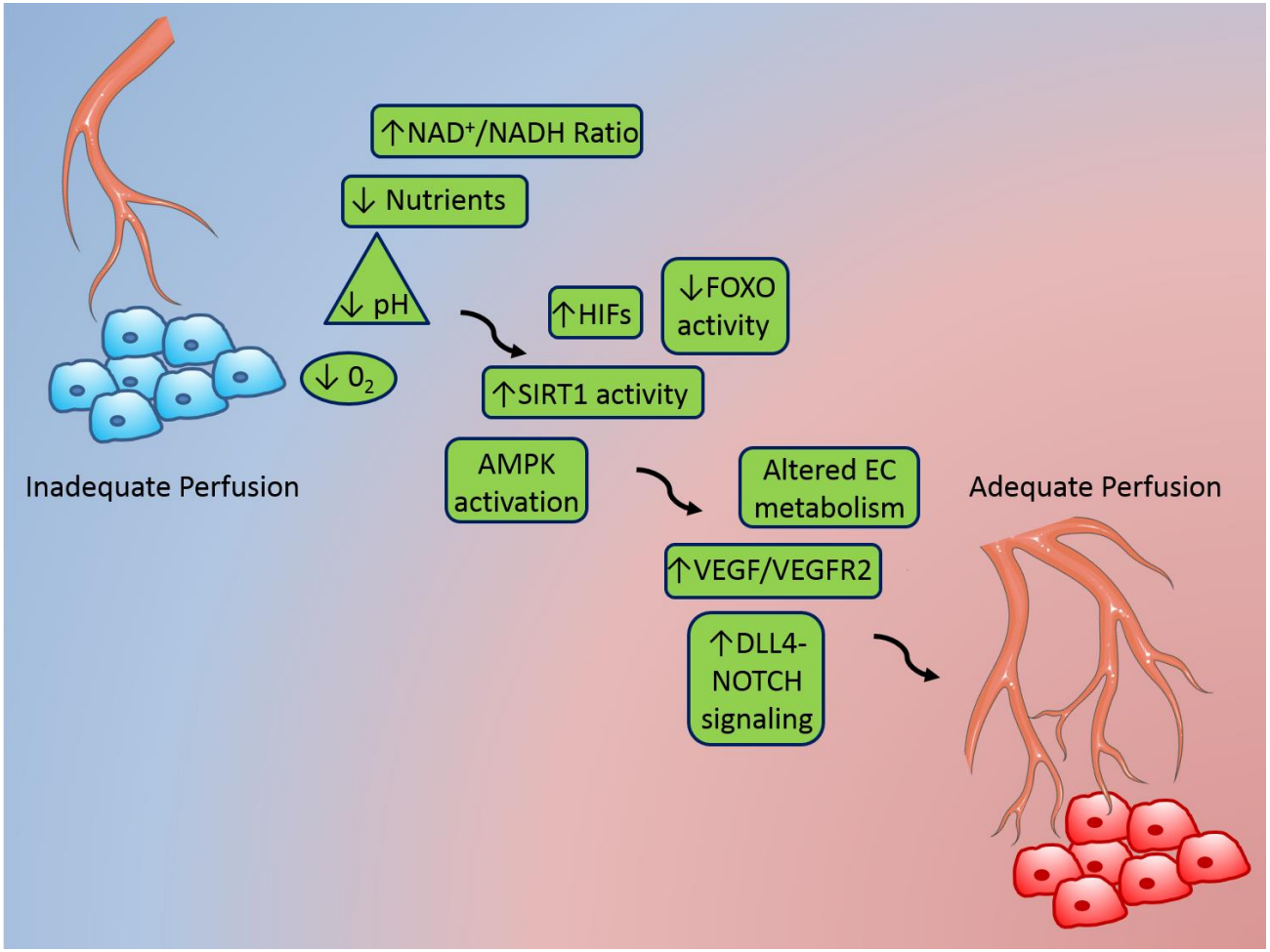

Figure 1.8 Vascular Responses to Impaired Perfusion

Inadequate tissue perfusion results in hypoxia, acidosis, nutrient scarcity, and rising NAD+/NADH ratio (reflecting reduced catabolism of metabolic substrates). These phenomena are detected by an array of molecular sensors (a small selection of which are illustrated), including hypoxia inducible factors (HIFs), AMP-dependent protein kinase (AMPK), NAD+-dependent deacetylases (e.g., Sirtuin1 or SIRT1), and Forkhead transcription factors (FOXOs). Cumulatively, these sensors orchestrate a molecular response, including increased VEGF production and signalling, increased Dll4/Notch signalling, and altered endothelial cell (EC) metabolism, which promote angiogenesis, and aim to restore adequate tissue perfusion.

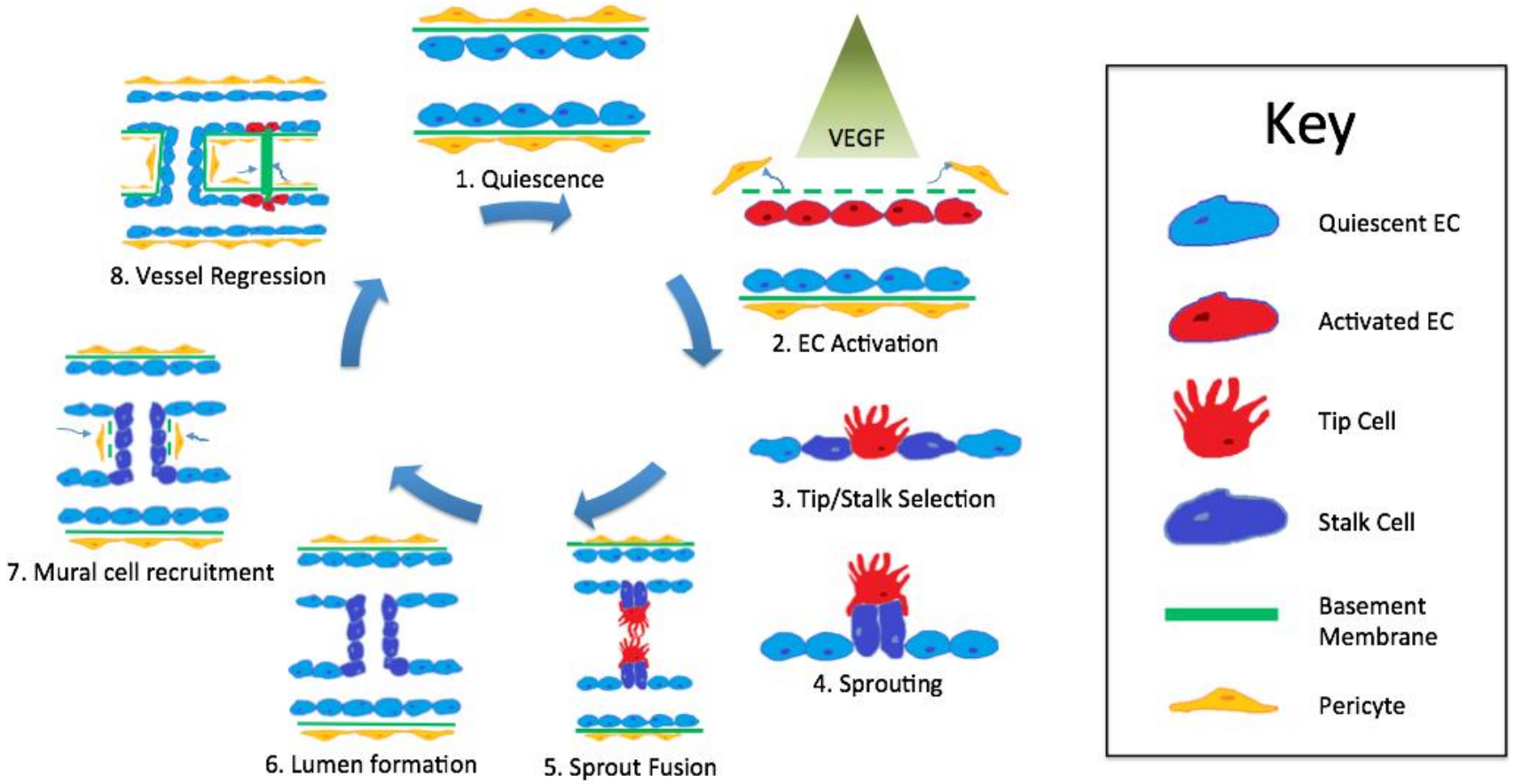

Figure 1.9: Sprouting Angiogenesis

Progression from vascular sprout to mature vessel. When a quiescent vessel (1) experiences increased concentrations of proangiogenic growth factors (2), endothelial cells (EC) become activated, releasing cytokines and enzymes that promote pericyte shedding and basement membrane degradation. EC with the highest levels of VEGF signalling become selected as tip cells, which actively induce stalk cell phenotype in their neighbours (3 - see also Fig. 1.11). Tip cells migrate toward the greatest concentrations of proangiogenic growth factors, with following stalk cells proliferating to form a vascular sprout (4). Sprouts then anastomose (5) with the assistance of macrophages to form vascular loops, which then form perfused lumens (6) that mature as migrating pericytes envelop the vessel and contribute to basement membrane deposition (7). Finally, neovessels experiencing low flow selectively regress (8), with this cycle continuing iteratively until a mature vascular plexus is formed, which matches local blood supply to demand.

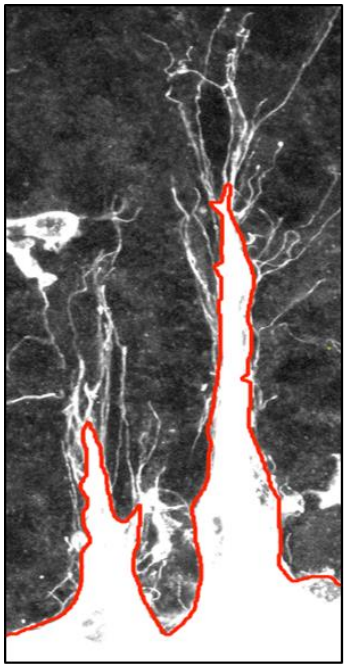

Tip Cells
Outlined in Red

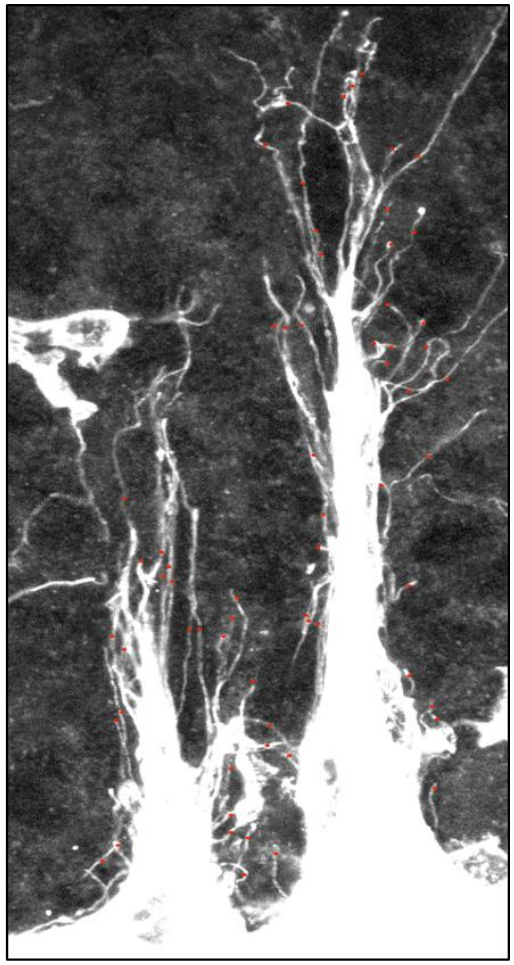

Filopodia Marked With
Red Dots

Figure 1.10: Tip Cells and Filopodia

Image courtesy of Dr Richard Cubbon. Taken with confocal microscopy at 400x magnification

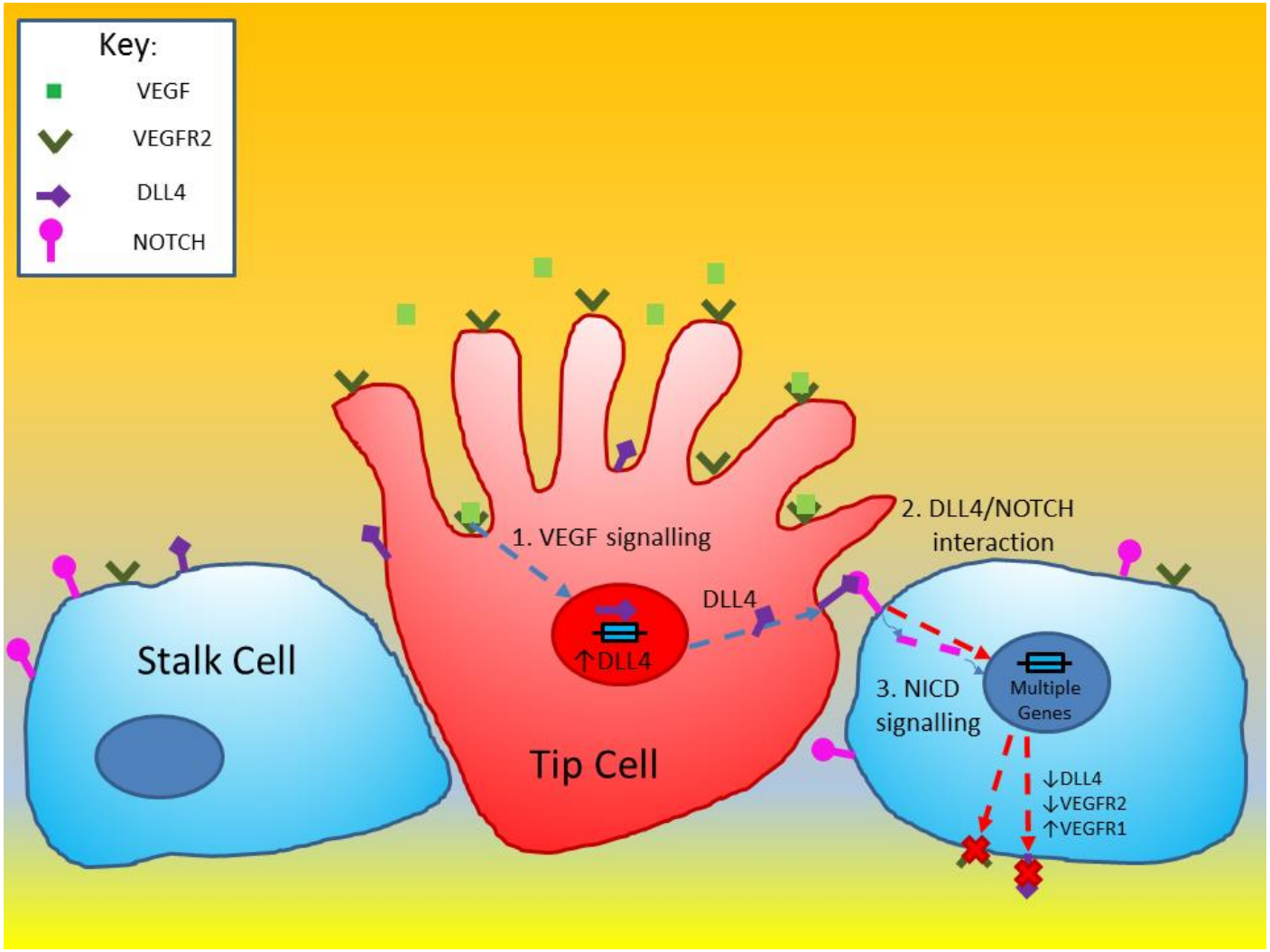

Figure 1.11: Lateral inhibition

Lateral inhibition during tip/stalk selection. During angiogenic sprouting, endothelial cells (EC) with higher levels of VEGF signalling express greater concentrations of cell surface Dll4, which interacts with Notch on neighbouring EC. This molecular interaction results in cleavage of the Notch intracellular domain (NICD), which translocates to the nucleus and modulates gene expression, resulting in suppression of VEGFR2 and Dll4, along with increased expression of the antiangiogenic VEGF receptor VEGFR1. This communication is dynamic and bidirectional, with the cells expressing most Dll4 at any instant becoming tip cells, which actively inhibit tip cell fate in their neighbours.

1.4.4 Endothelial Progenitor Cells (EPCs)

As mentioned above, the classical paradigm of vascular repair holds that damaged endothelium is repaired by migration and proliferation of neighbouring quiescent endothelial cells to re-establish the disrupted monolayer [168, 169]. Whilst this process is certainly important, other factors have since been implicated in this process and in vascular regeneration [170]. Asahara *et al* published a seminal study of cells expressing the human haematopoietic stem cell marker CD34, isolated from the mononuclear fraction of blood via immuno-magnetic separation [156]. These cells, and separately those expressing VEGF receptor 2 (also known as kinase insert domain receptor [KDR] in human cells [Flk-1: foetal liver kinase is the murine equivalent]), after a period of *ex vivo* cell culture were found to behave as, “putative endothelial progenitor cells”: augmenting angiogenesis after hind-limb ischaemia in mice and co-localising with capillaries. The abundance of non-culture expanded circulating CD34+/KDR+ cells has been shown to predict adverse cardiovascular outcomes in patients with confirmed coronary artery disease, highlighting the potential importance of such progenitors for vascular health [171]. Given that some mature endothelial cells co-express these markers [62], it has been proposed that circulating CD34+/KDR+ cells also expressing the haematopoietic marker CD133 represent a less mature progenitor population for study [172]. In mice, CD117, also known as c-kit, is a recognised haematopoietic stem cell marker and when bone marrow-derived CD117+ cells obtained via magnetic separation are transfused into animals which have undergone femoral artery wire injury they accelerate endothelial repair [148]. There is a lack of consistency in nomenclature describing putative endothelial progenitors across publications, and terminology is often misleading in implying unproven functional roles or

lineages [173]. For the avoidance of confusion, such cells identified from peripheral blood mononuclear cells (PBMCs) either by magnetic separation or by flow cytometry, and without *in vitro* manipulation, will hereafter be termed circulating progenitor cells (CPCs) in this thesis.

1.4.5 Cell Culture-Derived Endothelial Progenitor Cells

Alternative methods to study cells which may contribute to vascular regeneration have been described [174]. Culture of PBMCs in endothelial growth medium with different protocols produces 3 broad groups of cells which may contribute to vascular repair. These methods are summarised in figure 1.12. In each method, PBMCs are initially plated down and cultured. In the protocol described by Hill *et al*, cells non-adherent at 48hrs are re-plated for further culture [175]. Colonies, now understood to comprise haematopoietic cells including T-lymphocytes, monocytes and myeloid angiogenic cells (MACs) [174, 176], form in these samples at day 4-9 and are termed, “colony forming units (CFU)” or CFU-Hill. The abundance of CFUs cultured from patients is inversely correlated with combined Framingham risk factor score [175]. That said, these cells display few of the characteristics one would expect from putative endothelial progenitor cells in that they do not incorporate into newly-forming vasculature [174], whereas they readily phagocytose bacteria – a function one would associate with cells of a myeloid lineage rather than with endothelial cells [177]. As such, although these cells may be important for maintenance of a healthy vasculature, with their actions presumably effected in paracrine fashion [178], they are not truly endothelial progenitor cells.

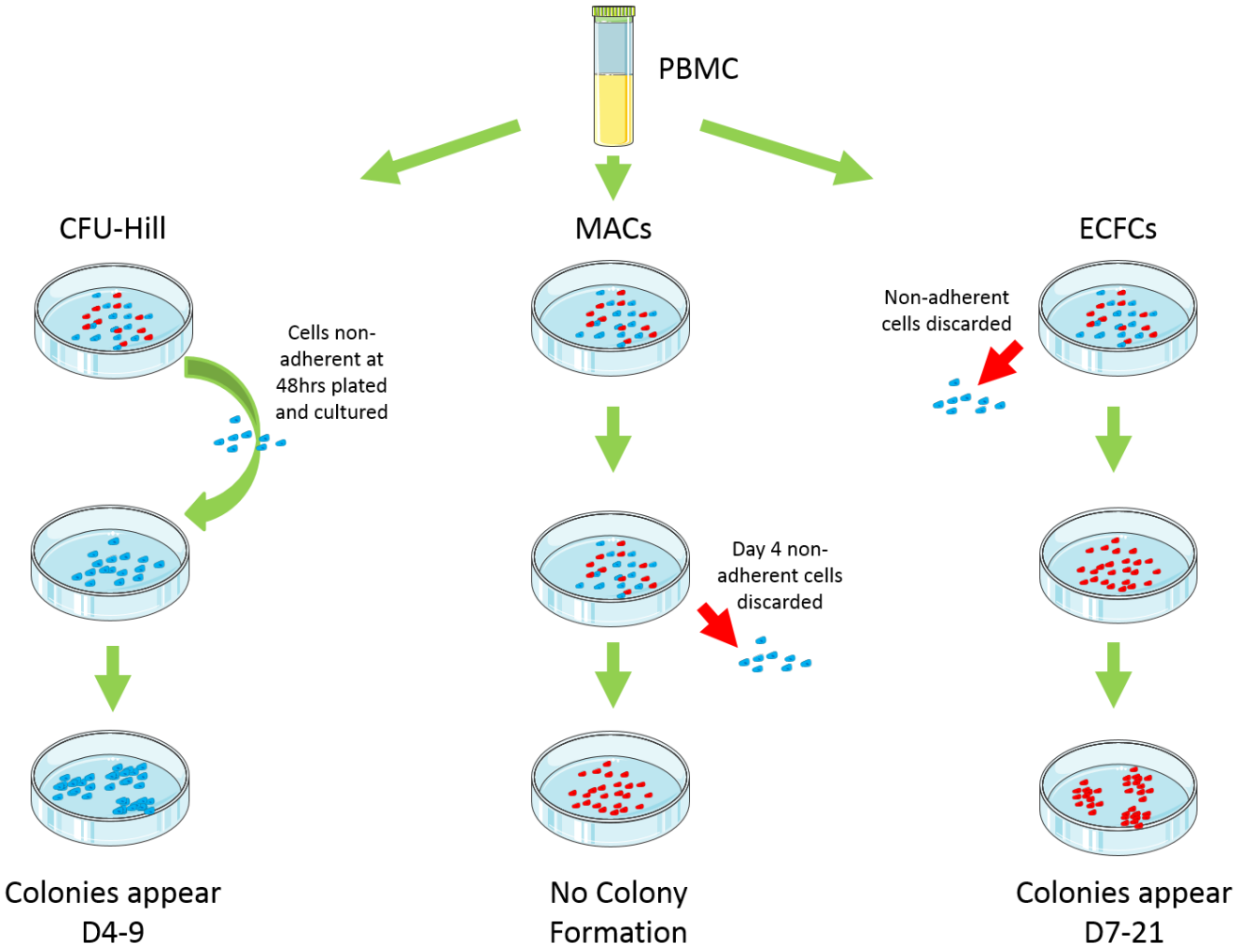

Figure 1.12: Angiogenic and Colony-Forming Cell Derivation Methods

PBMC (peripheral blood mononuclear cell), CFU (colony forming unit), MAC (myeloid angiogenic cell), ECFC (endothelial colony forming cell)

The second method displayed in figure 1.12, also pioneered by the Asahara group [157], derives cells initially referred to as early outgrowth EPCs (EEPCs). Circulating levels of these cells are inversely correlated with coronary artery disease and associated risk factors [157]. These cells were found to express KDR and other endothelial cell markers, however this has subsequently been proven to be a cell culture artefact due to ingestion of platelets in culture [179]. These cells may only be expanded to a limited degree *ex vivo* and have not been shown to contribute directly to neovessels. Due to inconsistencies in nomenclature in the literature, a recent consensus statement has recommended the term myeloid angiogenic cells (MACs) be used to describe these cells, as this better describes their phenotype and function [173] in that they are not truly endothelial progenitors, but do contribute to angiogenesis via paracrine mechanisms [180].

The third protocol included in figure 1.12 was first described by Lin *et al* [181]. This prolonged culture of PBMCs produces cells which form colonies after 7-21 days and may then be expanded through serial passage *ex vivo*. These cells express endothelial markers, and behave as putative endothelial cells: directly forming capillary-like structures *in vitro* and when transplanted *in vivo*, showing a progenitor hierarchy in single cell clonal assays, and augmenting vascular regeneration and repair *in vivo* [178, 182], reviewed in [62]. These cells, formerly known as late outgrowth EPCs (LEPCs), or outgrowth endothelial cells (OECs) are now termed endothelial colony forming cells ECFCs, again to reflect their phenotype and function compared with MACs [173].

1.4.6 Progenitor Cells and Insulin Resistance

Work from this lab has investigated how CPCs and ECFCs are affected by insulin resistance. In health CPCs are mobilised to the circulation from the bone marrow in response to exercise. Studies have shown that there is a mobilisation defect in insulin resistant, but otherwise apparently healthy South Asian men [183]. This impairment is nitric oxide dependent. Another study has shown that ECFCs from insulin resistant, but otherwise apparently healthy, South Asian men have impairment of both *in vitro* and *in vivo* functionality as compared with cells from healthy Caucasians [182]. This impairment is due to reduced Akt signalling in the insulin resistant cells and is abrogated when this signalling is restored. Given the abnormalities in PI3K/Akt signalling and eNOS function seen with insulin resistance (see section 1.3.7), the importance of these processes for mobilisation and function of CPCs and ECFCs may explain some of the adverse phenotype of vascular repair and regeneration seen in insulin resistant individuals. As such, treatments which may improve the mobilisation and function of such cells represent an attractive therapeutic target.

1.4.7 Monocytes and Macrophages in Vascular Regeneration

A broad body of work has investigated the role of monocytes and macrophages in recovery after ischaemic injury [184, 185]. Monocytes are derived from myeloid haematopoietic cells in the bone marrow, and the classical paradigm holds that they are then transformed into macrophages once they have manoeuvred from the bloodstream into tissue [186]. Recent studies have significantly advanced our understanding beyond this original template. In fact, haematopoietic progenitors can be found in the circulation, and differentiation to

monocytes can occur outside of the marrow itself [187]. Moreover, monocytes are not exclusively found in the circulation: they also reside in niches such as the spleen without differentiation to a macrophage phenotype and may be mobilised from these reservoirs in response to myocardial injury [188].

Monocytes can be divided into two key subtypes which differ both functionally and phenotypically: the classical, “inflammatory” type; and the so-called, “patrolling”, or non-classical monocyte [185]. In mice, these groups are differentiated by their expression of Ly-6C, with high levels (Ly-6C^{high}) seen in the inflammatory type and low levels (Ly-6C^{low}) in the patrolling type [184, 185]. The corresponding monocyte phenotypes in human cells are identified by the expression or absence of CD16 and CD14 [185]. Inflammatory monocytes are relatively short-lived within the circulation, whereas the patrolling type may persist in the bloodstream for some time and are less prone to accumulation in areas of inflammation [185]. Interestingly, rather than being produced from separate progenitors, Ly-6C^{low} cells appear to be derived from Ly-6C^{high} monocytes [189, 190]. This process is regulated by the vascular endothelium, with the Notch ligand DLL1 being shown to influence monocyte fate [191].

Macrophages may be classified in two subgroups in similar fashion to monocytes: M1 macrophages are considered inflammatory as they result from the, “classical” activation of monocytes with interferon-γ or lipopolysaccharide; M2 macrophages are derived through, “alternative” activation of monocytes via exposure to interleukin (IL)-4 or IL-10 [185]. However, this distinction has been criticised for being overly simplistic, and may be context dependent. M1

macrophages develop from Ly-6C^{high} monocytes and accumulate in damaged myocardium within a few minutes following ischaemic injury [192]. They contribute to the initial inflammatory response following MI, phagocytosing dead cells and releasing powerful cytokines such as TNF-α [184]. M2 macrophages start to accumulate in the infarct zone after the initial inflammatory phase, around 4 days following myocardial injury. They contribute to the resolution phase of wound healing and release substances such as VEGF which is crucial for vascular regeneration (see section 1.4.3) [184].

It appears the balance between the levels of monocyte subtypes is important during recovery after ischaemic injury. A skewing, or polarisation, in monocyte fractions towards a greater proportion of the inflammatory subset is associated with poorer outcomes for patients after MI [193]. Interestingly, recent human studies have shown that patients with diabetes have a marked decrease in circulating levels of, “patrolling” type cells, with a resultant imbalance in the levels of the two monocyte groups [194]. This pro-inflammatory shift may help explain the divergent outcomes in patients with DM following ischaemic injury. Indeed, recent work has linked ERK activity with monocyte differentiation itself, thereby implicating the IR/IGF-1R axis in both atherogenesis and vascular regeneration [195]. As such, further investigation into the role of these cells in vascular repair, and the influence of insulin and IGF-1 signalling on their abundance and function is clearly warranted.

1.5 Aging and the Vasculature

1.5.1 The Aging Population

Advances in medicine over the last half of a century have helped shape a dramatic demographic shift in Western populations. Within the next three years there are expected to be more adults over the age of 60 worldwide than there are children younger than 5 years old [196]. In the UK, the number of men aged 75 or above has increased by 149% since 1974, with the median age of the population rising from 34 to 40 years over the four decades to 2014 [197]. These remarkable improvements in longevity have not been without cost, however. As patients survive diseases which would have led to their death as recently as the mid-1970s, the prevalence of multi-morbidity and frailty has increased dramatically, presenting an enormous challenge to health and social care provision in the UK in the coming years. Age-related diseases such as dementia, arthritis and sensorineural hearing loss have a huge impact on the quality of life of older people. As advances in lifespan have outstripped improvements in healthspan, the challenge for researchers is to develop treatments which promote, “healthy aging”.

1.5.2 Aging and the Vasculature

Increasing age is a key determinant of cardiovascular risk [198, 199], and vascular disease remains the most common cause of death in the Western world [200-202]. Ischaemic heart disease (IHD), stroke, vascular dementia, renovascular atherosclerosis with resultant chronic kidney disease, aortic aneurysm, systolic and diastolic heart failure, valvular calcification and hypertension are all major cardiovascular consequences of aging [196]. As the

population grows older, the American Heart Association forecasts that there will be 8 million additional cases of IHD, 4 million more strokes, 2 million with a new diagnosis of heart failure, and a staggering 27 million extra cases of hypertension in the US by 2030 [199].

Two key processes are thought to dictate the adverse vascular phenotype seen with increasing age: progressive central arterial stiffness; and widespread endothelial dysfunction [203, 204]. As people age, changes in the vessel wall of the large arteries such as the aorta lead to a decrease in elastin with increasing collagen accumulation. This process appears to be related to the activity of transforming growth factor (TGF)-β and the influence of several enzymes such as matrix metalloproteases (MMPs)-19 and 12, neutrophil elastase, and cysteine cathepsins [205]. As vessel stiffness rises, the loss of vascular compliance leads to systolic hypertension. If left untreated, this increase in afterload leads to left ventricular hypertrophy, diastolic and eventually systolic dysfunction. The wider effects of hypertension on the vasculature are legion, but it is well-established that increases in shear stress are closely linked to endothelial dysfunction and the development of atherosclerosis [206].

Aside from the influence of hypertension, endothelial dysfunction becomes more prevalent with age [204] largely due to a deficiency in NO (see section 1.2.2) [207, 208]. A key factor in this process is the phenomenon known as, “eNOS uncoupling” [209]. Preclinical studies have identified a reduction in BH_4 levels associated with aging which, given it is an essential cofactor for eNOS activity, leads to decreased production of NO, instead favouring release of superoxide

anion (O_2^-), a powerful oxidative agent [210]. It has also been proposed that increased activity of the enzyme arginase observed with aging contributes to eNOS uncoupling as it competes with eNOS for L-arginine, the substrate for NOS-derived NO production [211]. Aging is associated with increased expression of nicotinamide adenine dinucleotide phosphate (NADPH) oxidase (NOX), possibly related to increased TNF-α levels which appear to rise with age [196]. As such, this creates an atmosphere of increased oxidative stress, which predisposes to both reduced NO production, and also a further increase in the generation of reactive oxygen species (ROS) such as peroxynitrite ($ONOO^-$) and superoxide anion (O_2^-) [212]. Such an excess of ROS is associated with DNA damage, aging and endothelial dysfunction [213]. It should be noted that the phenomenon of, “eNOS uncoupling” is but one of many theories to explain cardiovascular aging. Many others exist, with factors such as mitochondrial oxidative stress, chromatin remodeling, a senescence-associated secretory phenotype [214], and genomic instability (reviewed in [196]) likely to contribute to deterioration of the vasculature over time as part of a complex multifactorial pathogenic process.

1.5.3 Insulin/IGF-1 Signalling and Aging

The provision of nutrition is a key determinant of growth and repair. As such, insulin has wider actions than those purely governing glucose homeostasis and vascular function. Indeed, insulin is a growth factor and therefore can also influence cell fate. Moreover, patients with diabetes exhibit evidence of premature cardiovascular disease, with macrovascular events occurring on average 15 years earlier than in those without the condition [6]. As such, the

links between insulin and IGF-1 signalling, longevity, and cardiovascular aging are key to the understanding of the phenotype of diabetes and will be important for the development of new therapies to address the marked disparity in outcomes between those with and without the condition [9].

Calorie restriction is well-established to increase longevity [215, 216], having been first identified in 1935 as a powerful environmental determinant of aging [217]. Recently, animal models of accelerated aging have helped elucidate this phenomenon. Mice lacking the DNA excision-repair gene Ercc1 display accelerated aging as they are unable to maintain the fidelity of their genome appropriately [218]. They have a decreased lifespan, living for between 4-6 months, but incredibly this is doubled when their calorie intake is restricted by 30%. Improvements were also seen in measures of both neurocognitive and physical function, effectively extending the healthspan of these animals. Crucially, calorie restriction reduces insulin and IGF-1 signalling [219, 220], and this is one possible mechanism for the differences in longevity seen in animals with reduced energy intake.

Given the poor prognosis seen in obese patients and those with T2DM, it is not surprising that altered insulin and IGF-1 signalling has been linked to lifespan. Studies in supercentenarian humans have highlighted genetic variants in the insulin/IGF-1 axis associated with longevity [221] [222]. Further work in animal models has explored this in greater detail with seminal studies in transgenic mice showing a key role of both the IR [223] and IGF-1R [224] in lifespan. Holzenberger *et al* published a paper in 2003 using mice haploinsufficient for the

IGF-1R (IGF-1R$^{+/-}$) to investigate the effects of diminished signalling through this axis on longevity and resistance to oxidative stress [224]. The female IGF-1R$^{+/-}$ animals lived around a third longer than their WT counterparts, and survived longer after paraquat injection, an inducer of oxidative stress. A trend towards an increase in longevity was also seen in the male animals, although this did not reach statistical significance. Of note, fewer male animals were studied compared to the female cohort, meaning that type II error is a possibility.

Research from the laboratory of Ronald Kahn demonstrated a significant survival advantage in mice with fat-specific IR knockout (FIRKO) [223]. These animals were lighter than controls by 15-25% over the course of their lifespan, and leaner with a >50% reduction in adiposity as estimated by perigonadal fat pad mass. Interestingly the FIRKO mice had a 55% higher intake of food per gram of body weight than controls, indicating that leanness and/or decreased insulin signalling was responsible for the changes in metabolism and longevity rather than reduced caloric intake. More recent work from this group has shown that fat-specific inducible deletion of both the IR and IGF-1R results in rapid and extensive apoptosis of fat cells, followed by a brief period during which the animals display features of the metabolic syndrome [225]. As such, insulin and IGF-1R signalling are required for maintenance and survival of mature adipocytes. More nuanced reduction in IR and IGF-1R signalling is therefore likely to have important effects on longevity, body weight and glucose homeostasis.

It is interesting to note that PTP1B knockout animals (i.e. with increased insulin and IGF-1 signalling) have reduced longevity compared with wild type mice

[226]. Moreover, the authors of this study noted that male IRKO mice appeared to have increased maximum lifespan compared to WT, indicating contrasting effects of increased versus decreased insulin signalling on longevity in these models. Further downstream of the IR and IGF-1R, the Ras/ERK signalling axis is strongly implicated in mitogenesis, with Ras activity highly upregulated in many cancer cell types [227]. Conversely, decreased Ras signalling has been shown to increase longevity, with RasGrf1$^{-/-}$ (a guanine nucleotide-releasing factor for Ras) transgenic mice living 20% longer than wild type (WT) littermates, and with better-preserved motor function [228]. This finding is consistent with research in *Drosophila,* which employed pharmacological inhibition of Ras/ERK signalling, leading to significant increases in lifespan [229]. This research, and others, has also highlighted the role of forkhead box O (FOXO) transcription factors as key determinants of cell aging [230]. Reduced signalling through the IR/IGF-1R pathways increases FOXO activity, with resultant increases in lifespan seen across different species [231-234] (reviewed in [235]). Importantly the link between caloric restriction and aging also appears to be dependent on FOXO, at least in mice, emphasising the links between nutrient availability, IR/IGF-1R signalling, and longevity [236]. In humans, FOXO has been implicated in aging with mutations in the FOXO3 gene being associated with exceptional longevity [230, 237]. Moreover, FOXOs are now understood to have wide-ranging effects on a variety of cellular processes which have the combined effect of protecting against type II diabetes, cardiovascular disease, cancer and neurological degeneration, thereby promoting healthy aging (reviewed in [237]). Research from Webb *et al* studying the direct targets of FOXO transcription factors across different species has identified a range of genes conserved throughout evolution which influence key processes determining longevity and healthspan [230].

Several other proteins which have been found to influence longevity and healthspan are linked with insulin and IGF-1 signalling. One such factor is the mammalian target of rapamycin (mTOR) (reviewed in [235]). TOR inhibition with rapamycin increases lifespan in mice and more primitive organisms [235], and associations between reduced mTOR signalling and human longevity have also been noted [238]. Interestingly, the effects of inhibiting the TOR pathway closely mimic those of dietary restriction, and indeed insulin signalling via the PI3K/Akt pathway increases mTOR activity to promote protein synthesis, cell growth and differentiation [98]. The mitochondrial adaptor protein p66Shc has also been linked to lifespan [239], which is particularly important given that levels of the protein are elevated in older people and those with diabetes [240]. It appears to have a crucial role in protection from oxidative stress, with $p66Shc^{-/-}$ mice showing resistance to paraquat [239] and reduced ROS production in response to insulin *in vitro* [241]. These animals are also resistant to diet-induced obesity and are more insulin sensitive than their WT counterparts [241].

To conclude, it is interesting to consider that insulin resistance is associated with an unfavourable vascular phenotype [80, 153], yet reduced insulin signalling may be associated with longevity [223]. Indeed, there appears to be a similarly complex relationship with IGF-1R signalling [112, 224]. As such, this may suggest as yet unappreciated roles of the ligands or receptors themselves, the divergent effects of excessive versus reduced signalling, the balance between pathway-specific and global signalling effects and spatial and temporal differences in signalling in various settings. As such, further research into this fascinating area of biology is clearly warranted in order to delineate the complex associations between the IR, IGF-1R and their influences on vascular function

and longevity. Overall, much as a delicate balance between the two key IR/IGF-1R signalling pathways must be maintained for vascular health, conditions which particularly favour either the PI3K/Akt cascade or the Ras/ERK pathway have the potential to have a profound influence on the trade-off between healthy growth and repair and the aging process.

Chapter 2 **Hypotheses**

The key hypothesis tested in the first part of this project is that decreased IGF-1R expression in the setting of insulin resistance leads to an improved phenotype of vascular repair and regeneration. I plan to investigate this by addressing the following questions:

1. Does decreasing IGF-1R expression in the setting of whole body haploinsufficiency of the IR lead to differences in growth, development and metabolism?
2. Does decreasing IGF-1R expression in the setting of whole body haploinsufficiency of the IR augment vascular repair?
3. Does decreasing IGF-1R expression in the setting of whole body haploinsufficiency of the IR leads to improved vascular regeneration?

The second part of this thesis examines the following hypothesis: haploinsufficiency of both the IR and IGF-1R influences growth and metabolism over the lifespan of the animals and increases their healthspan. I will investigate this by addressing the following questions:

1. Does decreasing IGF-1R expression in the setting of whole body haploinsufficiency of the IR lead to differences in growth, development and metabolism as mice age?
2. Does decreasing IGF-1R expression in the setting of whole body haploinsufficiency of the IR increase healthspan?

3. Does the expression of FOXO targets (known to influence the aging process [230]) differ between animals with haploinsufficiency of the IR, IGF-1R or both compared with wild type mice?

Chapter 3 **Materials**

3.1 Animal Husbandry

- Chow diet — B&K Universal Ltd.; Hull UK

3.2 Genotyping

- Sodium hydroxide — Fisher; Loughborough, UK
- EDTA — Sigma-Aldrich; St Louis, USA
- Tris-HCl — Fisher; Loughborough, UK
- Molecular grade H_2O — BD Biosciences; Nottingham, UK
- Primers (see Chapter 4) — Invitrogen; Carlsbad, USA
- Biomix^{TM} Red — Bioline; London, UK
- PCR tubes — Fisher; Loughborough, UK
- PTC- 200 Thermal Cycler — MJ Research; Ramsey USA
- Tris base — Fisher; Loughborough, UK
- Glacial acetic acid — Fisher; Loughborough, UK
- Agarose — Bioline; London, UK
- Ethidium bromide — Sigma-Aldrich; St Louis, USA
- 100 base pair ladder — Thermo Scientific; Rockford, USA
- G-box imaging system — Syngene; Cambridge, UK

3.3 Glucose Homeostasis Assessments

- CODA Blood Pressure system — Kent Scientific; Torrington, USA

- Accu-Chek™ Aviva Plus test strips — Aviva; Mannheim, Germany
- Accu-Chek™ Aviva Plus glucometer — Aviva; Mannheim, Germany
- D-glucose — Sigma; St Louis, USA
- Actrapid™ insulin — Novo-Nordisk; Bagsvaerd, Denmark
- Dulbecco's phosphate-buffered saline — Sigma; St Louis, USA

3.4 Vascular Injury

- Povidone-Iodine 0.75% — Sigma; St Louis, USA
- Vannas spring scissors — Fine Science Tools; Germany
- Angioplasty guidewire: Hitorque Cross-it 200XT — Abbot Vascular; USA
- Buprenorphine — Alsatoe Animal Health; York, UK
- Evans blue dye — Sigma; St Louis, USA
- 4% paraformaldehyde — Fisher; Loughborough, UK
- ImagePro Plus 6.2 — Media Cybernetics; Cambridge UK
- QiCam — Olympus; Tokyo, Japan

3.5 Hind-limb Ischaemia

- Veet — Reckitt Benckiser; UK
- Povidone-iodine 0.75% — Sigma; St Louis, USA

- Laser Doppler imager (LD12) Moor Clinical; UK
- Moor LDI V5.3 imaging software Moor Clinical; UK

3.6 Enumeration of Murine CPCs

- Microvette® tube Sarstedt; Nümbrecht, Germany
- Heparin 1000IU/ml Wockhardt; Wrexham, UK
- Pharmlyse® BD Biosciences; Nottingham, UK
- Dulbecco's phosphate-buffered Saline Sigma; St Louis, USA
- Foetal calf serum Sigma; St Louis, USA
- Bovine serum albumin Sigma; St Louis, USA
- Fc block (CD16/CD32 rat anti-mouse; 553142) BD Biosciences; Nottingham
- FITC (rat IgG2a Isotype Control; 553929) BD Biosciences; Nottingham
- Sca1-FITC (rat IgG2a κ Ly6A/E; 557405) BD Biosciences; Nottingham
- PE rat (IgG2a κ Isotype Control; 553930) BD Biosciences; Nottingham
- Flk1-PE (Flk1 VEGFR2; 555308) BD Biosciences; Nottingham
- APC (rat IgG2b κ Isotype Control; 553991) BD Biosciences; Nottingham
- APC (rat anti-mouse CD117; 553356) BD Biosciences; Nottingham

- FACSCalibur Flow Cytometer — BD Biosciences; Nottingham

3.7 Murine MAC Culture

- Isoflurane — Abbott Logistics BV; USA
- Insulin syringe/29Gx13mm needle — Terumo; Bagshot, UK
- Sodium citrate from 4mL blood collection tubes — Greiner Bio-One; Austria
- 4mL EDTA blood tube — Greiner Bio-one; Austria
- Phosphate Buffered Saline — Sigma; St Louis, USA
- 23G needle — Terumo; Bagshot, UK
- 70µm nylon cell strainer — Greiner Bio-one; Austria
- 5cm Petri dish — BD Falcon; Oxford, UK
- Histopaque-1083 — Sigma; St Louis, MO
- EGM-2 basal medium/bullet kit — Lonza; Blackley, UK
- Foetal calf serum — Sigma; St Louis, USA
- Trypan blue — Sigma; St Louis, USA
- Neubauer Counting Chamber — Hawksley; Lancing, UK
- 24-well/6-well fibronectin coated cell culture plates — BD Biocoat; Redford, MA
- DiI-ac-LDL — Life Technologies; Paisley, UK
- BS-1 Lectin-FITC — Sigma; St Louis, USA

- Image J — National Institutes of Health; USA

3.8 Quantification of Leukocyte Populations

- Isoflurane — Abbott Logistics BV; USA
- Insulin syringe/29Gx13mm needle — Terumo; Bagshot, UK
- Pharmlyse® — BD Biosciences; Nottingham, UK
- Dulbecco's phosphate-buffered Saline — Sigma; St Louis, USA
- Foetal calf serum — Sigma; St Louis, USA
- Bovine serum albumin — Sigma; St Louis, USA
- EDTA — Sigma; St Louis, USA
- CD16/32 FcR block — BD Biosciences; Nottingham, UK
  Cat No. BD 553142
- anti-CD45-VioBlue — Miltenyi Biotec; Cologne, Germany
  Cat No. 130-110-802
- VioBlue Isotype control — Miltenyi Biotec; Cologne, Germany
  Cat No. 130-103-083
- anti-CD11b-FITC — Miltenyi Biotec; Cologne, Germany
  Cat No. 130-081-201
- FITC Isotype control — Miltenyi Biotec; Cologne, Germany

Cat No. 130-103-088

- anti-Ly6G-PE Miltenyi Biotec; Cologne, Germany

  Cat No. 130-107-913

- PE Isotype control Miltenyi Biotec; Cologne, Germany

  Cat No. 130-104-628

- Ly6C-APC eBioscience; San Diego, USA

  Cat No. 17-5932-82

- APC Isotype control Miltenyi Biotec; Cologne, Germany

  130-103-085

- anti-c-Kit-PE Miltenyi Biotec; Cologne, Germany

  Cat No. 130-102-542

- anti-Sca-1-APC Miltenyi Biotec; Cologne, Germany

  Cat No. 130-106-425

- Lineage eFluor450 eBioscience; San Diego, USA

  Cat No. 88-7772-72 ,

- F4/80-APC Miltenyi Biotec; Cologne, Germany

  Cat No. 130-102-379

3.9 Isolation of Murine Pulmonary Endothelial Cells (PEC)

- Hank’s Buffered Saline Solution Sigma; St Louis, USA

- 5mm Petri Dish — Sigma; St Louis, USA
- Scalpel blades size 22 — Swann-Morton; Sheffield, UK
- Corning Centrifuge tubes — Sigma; St Louis, USA
- MACSmix tube rotator — Miltenyi Biotec; Cologne, Germany
- Bovine serum albumin 7.5% — Sigma; St Louis, USA
- Antibiotic/antimycotic supplement — Invitrogen; USA
- Foetal bovine serum — Biosera; Boussens, France
- Endothelial cell growth medium MV2 plus endothelial supplement — PromoCell; Germany
- 14G Cannula — BD Biosciences; Nottingham
- Bovine skin gelatin — Sigma; St Louis, USA
- CD146 (LSEC) microbeads, mouse — Miltenyi Biotec; Cologne, Germany
- T25 Corning® cell culture flask — Sigma; St Louis, USA
- Trypsin-EDTA 0.25% — Sigma; St Louis, USA
- OctoMACS manual separator — Miltenyi Biotec
- MACS MS cell separation columns — Miltenyi Biotec
- Type II collagenase — Gibco, Life Technologies; USA

3.10 Scratch Wound Assay

- ImageLock Plate — Essen Bioscience; USA
- Woundmaker — Essen Bioscience; USA
- IncuCyte Zoom — Essen Bioscience; USA
- Endothelial cell growth medium — PromoCell; Germany

MV2 +/- endothelial supplement

- Antibiotic/antimycotic supplement Invitrogen; USA
- Foetal bovine serum Biosera; Boussens, France

3.11 Angiogenic Bead Assay

- EGM-2 BulletKit Media Lonza; Basel, Switzerland
- T25 Corning® cell culture flask Sigma; St Louis, USA
- Trypsin-EDTA 0.25% Sigma; St Louis, USA
- Cytodex-3 beads (17-0485-01) GE Healthcare; UK
- Aprotinin (A-1153) Sigma; St Louis, USA
- Thrombin (T-3399) Sigma; St Louis, USA
- Fibrinogen Type I (F-8630) Sigma; St Louis, USA

3.12 Quantitative PCR

- Tissue Lyser Qiagen; Netherlands
- 6mm cone balls (RS.22.455.0003C) Retsch
- RNAse Away spray Molecular Bio Products
- TRIzol® (Tri reagent) Sigma; St Louis, USA
- Phenol chloroform Sigma; St Louis, USA
- Isopropanol Sigma; St Louis, USA
- Ethanol Fisher; USA
- RNAse free H2O Life Technologies; USA
- NanoDrop® ND1000 Spectrophotometer Thermo Scientific; USA

- ND-1000 v3.1 software — Thermo Scientific; USA
- High capacity cDNA reverse transcription kit — Applied Biosystems; USA
- 96 well optical reaction plate — Applied Biosystems; USA
- ABI Prism 7900 HT PCR cycler — Applied Biosystems; USA
- LightCycler 480 PCR cycler — Roche; Switzerland
- SDS v2.2 software — Applied Biosystems; USA
- RT-PCR primers (SYBR green) — Invitrogen; USA
- Taqman® Gene Expression Mastermix — Applied Biosystems; USA
- RT-PCR primers (Taqman®) — Applied Biosystems; USA
- Molecular grade H_2O — BD Biosciences; Nottingham
- ATM TaqMan Probe Mm01177457_m1 — Thermofisher; USA
- Catalase TaqMan Probe Mm00437992_m1C — Thermofisher; USA
- SOD2 TaqMan Probe Mm01313000_m1 — Thermofisher; USA
- Rictor TaqMan Probe Mm01307318_m1 — Thermofisher; USA
- Dgat1 TaqMan Probe Mm00515643_m1 — Thermofisher; USA
- Frataxin TaqMan Probe Mm00784016_s1 — Thermofisher; USA
- Myc TaqMan Probe — Thermofisher; USA

Mm00487804_m1

- β-Actin TaqMan Probe Thermofisher; USA

  Mm02619580_g1

3.13 Nesting Studies

- Nestlets International Product Supplies;

  Product code: EE-NEST-C London

Chapter 4 **Methods**

4.1 Animal Husbandry

4.1.1 General

Murine work was carried out in accordance with The Animals (Scientific Procedures) Act 1986 (Amended 2012). Mice were kept in the University of Leeds animal facility under standard conditions, including a 12-hour sleep/wake cycle, with access to water and chow diet *ad libitum* unless otherwise stated. Experiments were conducted under Home Office Project License P144DD0D6. All studies were approved by the University of Leeds Ethics Committee. Male animals were ear notched at weaning, with these samples being used for genotyping (see section 4.2). Female mice were not used for experiments to exclude the endothelial effects of oestrogens at different points in the menstrual cycle. Female animals were culled at weaning by a suitable method as described in Schedule 1 of The Animals (Scientific Procedures) Act 1986 (Amended 2012) unless required for breeding.

4.1.2 IRKO-IGF1Rko mice

IRKO-IGF1Rko mice, as described in section 1.3.8, were obtained from established local colonies. IRKO animals were originally sourced from the Medical Research Council Mammalian Genetics Unit (Harwell, Oxfordshire, U.K.) and backcrossed onto the C57BL/6 background. These animals were originally described as part of a study which generated $IR^{-/-}$ mice [144]. These animals are non-viable, and die from ketoacidosis within 48-72hrs, whereas their IR haploinsufficient littermates ($IR^{+/-}$, IRKO) have grossly normal development

and can be bred for research purposes. Accili *et al* used electroporation to transfect murine embryonic stem cells with a vector containing a premature chain termination mutation downstream from codon 306 in exon 4 of the murine IR gene, with incorporation via homologous recombination. Mutant cells were selected with neomycin (the vector also encoded neomycin resistance), injected into mouse embryos at day 3.5, and then implanted into C57Bl6 females. This approach rendered homozygous animals IR-null, with the heterozygous IRKO animals with one null insulin receptor allele expressing around 50% of IR protein compared to WT littermates. Male IGF1Rko mice [224] sourced from The European Mutant Mouse Archive (Munich, Germany; http://www.emmanet.org) were also bred with C57BL/6 females to establish a heterozygous colony. The male IRKO mice were then bred with IGF1Rko females to produce offspring of four possible genotypes: wild type (WT); IRKO; IGF-1Rko; and IRKO-IGF1Rko (from now on referred to as DKO, or double knock-out). Appropriate knockdown of IR and IGF-1R in this colony has been confirmed in previous work from our lab (see [123]).

4.2 Genotyping

4.2.1 DNA Extraction

As previously mentioned, ear notches used for mouse identification were taken at weaning and used for genotyping. Samples were incubated in 100µL 25mM Sodium hydroxide / 0.2mM Ethylenediaminetetraacetic acid (EDTA) for 20mins at 95°C before the addition of 100µL 40mM Tris-HCl. The samples were then vortexed for 20s before being stored at -20°C.

4.2.2 IRKO Polymerase Chain Reaction (PCR)

PCR was used to genotype mice. 10µL BioMix Red® was added to 12.5µL distilled water with 0.5µL of each of the following commercially sourced primers:

TTA AGG GCC AGC TCA TTC CTCC (forward – for WT locus)

AGC TGT GCA CTT CCC TGC TCAC (forward – for IRKO locus)

TCT TTG CCT GTG CTC CAC TCT CA (reverse).

1µL of extracted DNA was added to this mixture and the resultant 25µL volume was placed in a thermal cycler with the following program:

1 denaturation cycle: 94°C for 4 minutes

31 amplification cycles: 94°C for 1 minute, 62°C for 1 minute then 72°C for 1 minute

1 completion cycle: 72°C for 4 minutes.

PCR products were then added to a 1.5% agarose gel (total volume 120ml) containing 3µL ethidium bromide. Electrophoresis identified bands visible on ultraviolet (UV) imaging at 232 base pairs (bp) for WT animals with bands present at 232bp and 255bp for IRKO mice (see section 5.1 for sample image).

4.2.3 IGF1Rko PCR

DNA samples (see above) were incubated with 10µL Biomix Red® and 13µL distilled water with 0.5µL of each of the following two commercially sourced primers (Invitrogen):

5' CCATGGGTGTTAAATGTTAATGGC 3'

5' ATGAATGCTGGTGAGGGTTGTCTT 3’

PCR was then performed with the following program:

1 denaturation cycle: 94°C for 5 minutes

35 amplification cycles: 94°C for 30 seconds,

57 °C for 30 seconds, 72°C for 1 minute.

1 completion cycle 72°C for 5 minutes

Agarose gel electrophoresis was performed as described in section 3.2.1 and bands were identified at 871bp (WT) and 202bp (IGF-1Rko) (see section 5.1 for sample image).

4.3 Metabolic phenotyping

4.3.1 Body Weight

Mice were weighed weekly from weaning (~3-4 weeks of age) until they were 13 weeks old. In the case of the aging cohort, animals were weighed weekly from weaning until their death.

4.3.2 Systolic Blood Pressure

Mice underwent non-invasive tail cuff plethysmography using the CODA system (Kent Scientific) as previously described [242]. Briefly, animals underwent 2 training sessions before a test session was recorded. Mice were held under conscious restraint in an environment maintained at 32°C for a minimum of 15mins prior to a test session. The session protocol comprised 10 acclimatisation cycles, followed by 18 test recordings. An average of at least 5 readings was used to produce mean systolic blood pressure values for each mouse.

4.3.3 Glucose Tolerance Testing (GTT)

Animals were fasted overnight with access to water *ad libitum*. The following morning they were weighed before being placed under conscious restraint. A small incision was made in the distal lateral part of the tail of each animal in order to obtain a tail vein blood sample of 1-2µL. This was analysed with a glucometer and testing strips. Mice were then treated with 200mg/mL glucose solution (1mg per gram of body weight in distilled, sterile-filtered water) administered via intraperitoneal injection. Repeat tail vein blood samples were taken at 30 minute intervals until 120mins after the initial injection. Between measurements animals had free access to water and were not restrained.

4.3.4 Insulin Tolerance Testing (ITT)

This experiment was conducted in similar fashion to the GTT (section 4.3.3) except that animals were fasted for four hours, rather than overnight (or 2 hours in the case of the aging cohort). Mice then underwent intraperitoneal (IP) injection of insulin at a dose of 0.75IU per gram of body weight with tail vein blood glucose measurements taken at the same time intervals as for GTT. Animals were monitored closely for any signs of hypoglycaemia throughout the experiment. No mice required treatment with IP glucose to correct hypoglycaemia.

4.4 Vascular Injury

Surgery was performed by Dr N Yuldasheva as previously published [80].

4.4.1 Femoral Artery Wire Injury

Animals were anaesthetised with isofluorane 3-4% and supplemental oxygen. They were then secured to an operating table heated to 37°C and maintained under anaesthesia throughout the procedure via a nose cone. After disinfection of the target area with povidone-iodine 0.75% a small incision was made to expose the femoral artery, and a suture and clamp were used to occlude carefully the proximal vessel. Arteriotomy was performed using vannas spring scissors and an angioplasty guide wire 0.014 inches in diameter was inserted and advanced 3cm into the artery. This was repeated three times to ensure complete endothelial denudation. The artery was then ligated and the wound closed. A sham procedure without passage of the angioplasty wire was performed on the contralateral limb to act as a control sample. Postoperative analgesia was provided with buprenorphine (0.25mg/kg) injected subcutaneously at the wound site and mice were warmed in a recovery area after cessation of anaesthesia.

4.4.2 Assessment of Vascular Repair

Mice were sacrificed at day 4 post-procedure after perfusion with Evans blue dye then 4% paraformaldehyde for fixation. Evans blue stains subendothelial structures, thus highlighting areas where re-endothelialisation has not occurred following denuding arterial injury. Femoral arteries were removed bilaterally and were imaged at 20X magnification on a QiCam camera. A segment 5mm in

length was then identified 5mm from the aortic bifurcation and this was analysed using ImagePro Plus to quantify the percentage area stained blue by the dye. This was then subtracted from 1 to derive the proportion of re-endothelialisation.

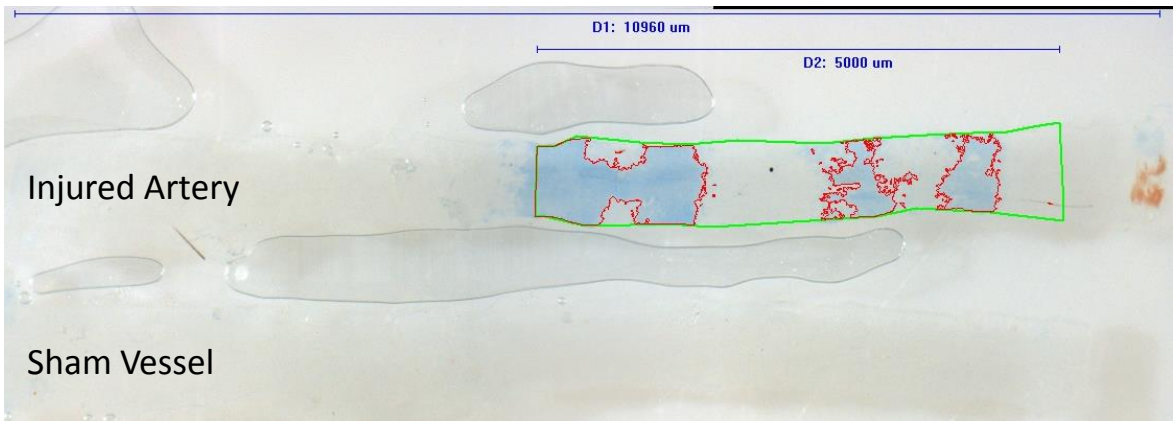

Figure 4.1: Femoral Artery Wire Injury

Representative image of murine femoral arteries. The top image has had denuding artery injury with the sham operated vessel shown below. D1 is the total vessel length, with D2 the 5mm area analysed for re-endothelialisation. Evans blue stain (blue) indicates subendothelial, i.e. not re-endothelialised areas, with the endothelium remaining unstained.

4.5 Hind-limb ischaemia

Surgery was performed by Dr N Yuldasheva as previously described [153].

4.5.1 Femoral Artery Ligation and Excision

Prior to the procedure animals were shaved from the waist down with an electric razor and hair removal cream. Mice were then anaesthetised with isoflurane 3-4% with supplemental oxygen before being secured to an operating table heated to 37°C and maintained under anaesthesia throughout the procedure via a nose cone. After disinfection of the target area with povidone-iodine 0.75% a small

incision was made to expose the left femoral artery. Sutures were used at the level of the inguinal ligament proximally and at the level of the bifurcation of the saphenous and popliteal vessels distally to ligate the femoral artery. The intervening section of vessel was then excised and the wound closed.

4.5.2 Laser Doppler Imaging

Mice were anaesthetised with isoflurane and laid supine on a light absorbing mat. Anaesthesia was maintained throughout the procedure through a nose cone with supplemental oxygen. The hind-limbs were extended and supinated, and this position was maintained using double-sided adhesive tape applied to the dorsal aspects of the paws to secure the limbs to the mat. The hind-limbs were scanned using a laser Doppler imager. Images were processed using compatible software and the area from the ankle joint down to the toes was chosen for quantification of perfusion in each hind-limb. The values for the ischaemic limb were divided by the value from the contralateral unoperated limb to produce a relative perfusion index (RPI). Images were taken 90 mins post-operatively to confirm ischaemia, then at 7 day intervals thereafter up to 28 days. The animals were then sacrificed with gastrocnemius muscles harvested bilaterally after perfusion fixation with 4% paraformaldehyde. These samples were suspended in 4% paraformaldehyde for another 24hrs after tissue harvest before being blocked in paraffin for histological sectioning.

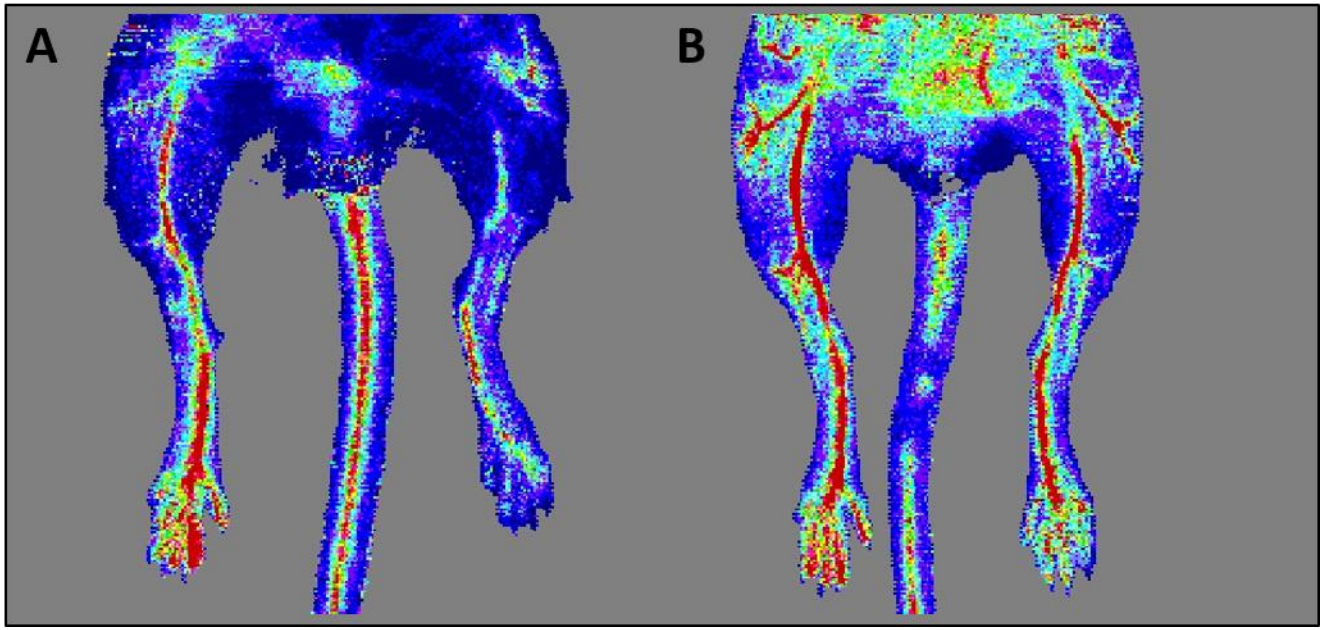

Figure 4.2: Representative Laser Doppler Images of HLI

Image A taken at day 0, shortly after femoral artery surgery. Image B is the same animal at 21 days following surgery, with recovery of perfusion seen in the animal's left leg to approximately 80% of that seen in the right hind-limb.

4.6 Enumeration of Murine CPCs

4.6.1 Blood sampling

Blood samples were taken from mice via saphenous venous puncture. 150µL blood was collected into a Microvette® tube (Sarstedt) containing 50µL heparin (1000 IU/ml). Samples were then transferred into 3mL Pharmlyse® red cell lysis buffer at 1:10 dilution with any clots removed with a pipette tip prior to further processing. The solution was incubated at room temperature for 10 minutes before being centrifuged at 300g, 18°C for 10 minutes. The pellet was then resuspended in 1ml fluorescence-activated cell sorting (FACS) buffer from stock solution consisting of 500mL phosphate-buffered saline, 2.5mL foetal calf serum and 2.5g bovine serum albumin. This was then centrifuged with the same settings for 10 minutes.

4.6.2 Antibody Labelling

Cells were resuspended in 1:10 Fc block diluted in FACS buffer with either antibody or isotype control added at a concentration of 1:50. The following 3 antibodies (or their isotype controls) were added to each sample:

1. Stem cell antigen (Sca1) with fluorescein isothiocyanate (FITC)
2. Kinase domain receptor/VEGF receptor 2 (KDR/Flk-1) with R-phycoerythrin
3. c-kit with allophycocyanin (APC).

Samples were then incubated in the dark at 4°C for 10 minutes before a further centrifugation and re-suspension in FACS buffer. They were then transferred to the flow cytometer on ice.

4.6.3 Flow Cytometry

Flow cytometry was performed with a BD LSR-Fortessa cytometer to enumerate $Sca1^{+}KDR^{+}$ cells and c-kit^{+} cells as a percentage of 100,000 events recorded in the lymphocyte gate, defined by typical light scatter properties. Isotype control specimens were used to define the threshold of antigen expression and also to subtract non-specifically fluorescent events.

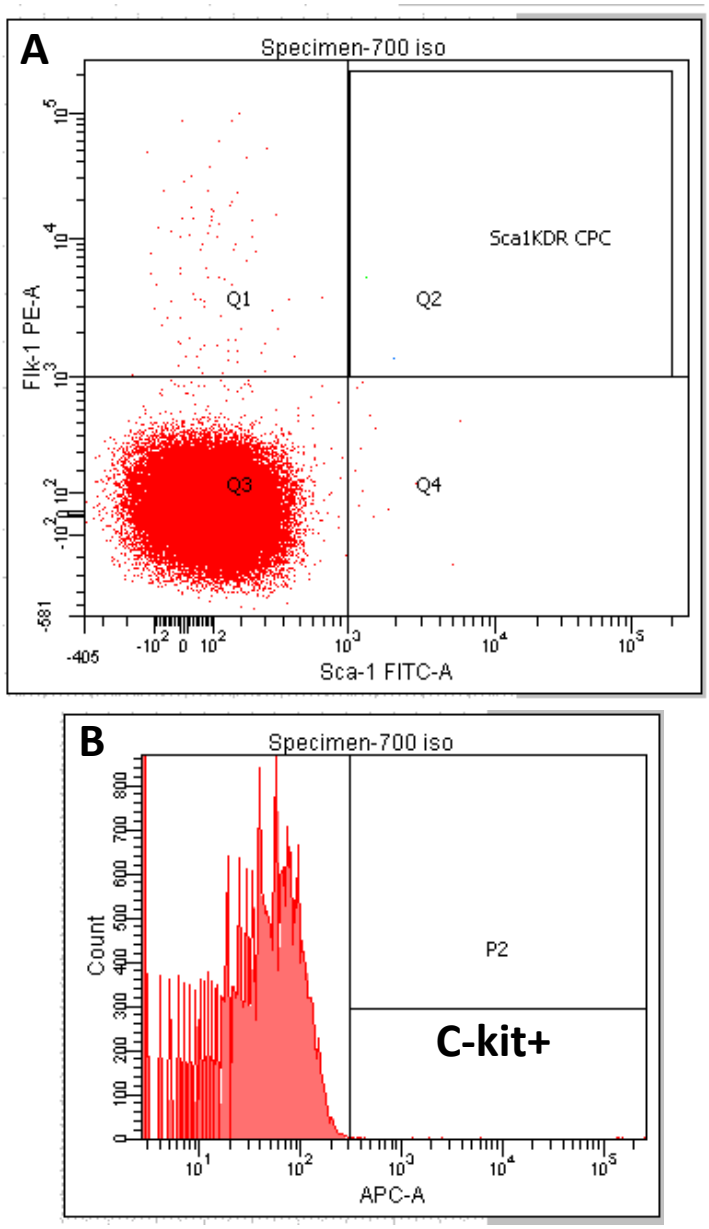

Figure 4.3: Sample Image of Isotype Control CPC Flow Cytometry Gating

Image A plots Stem cell antigen-1 (Sca-1) fluorescence with FITC (fluorescein isothiocyanate) on the x-axis against kinase domain receptor/VEGF receptor 2 (KDR/Flk-1) fluorescence with R-phycoerythrin on the y-axis. This isotype control shows few cells strongly expressing both antigens (Q2). Image B plots C-Kit fluorescence with allophycocyanin (APC) on the x-axis with cell count on the y-axis. The box labelled, "C-kit+" includes cells with strong fluorescence for the antigen, which are few in number in this isotype control.

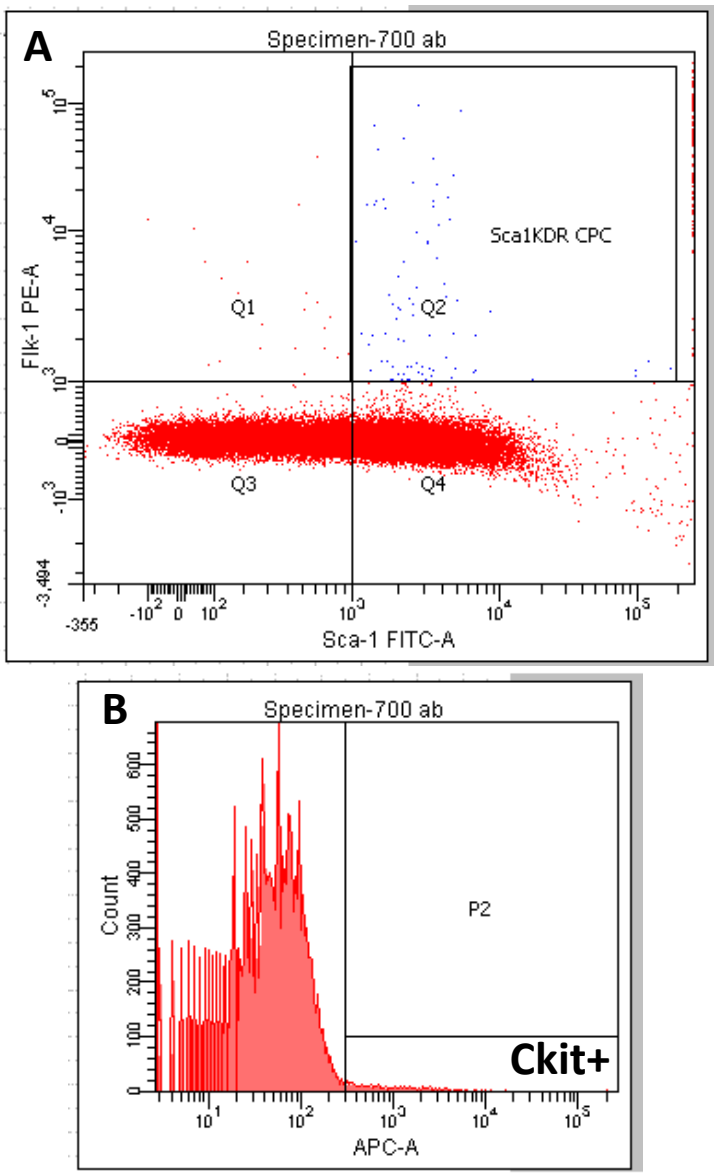

Figure 4.4: Sample Image of Antibody-Labelled CPC Flow Cytometry Gating

Image A plots Stem cell antigen-1 (Sca-1) fluorescence with FITC (fluorescein isothiocyanate) on the x-axis against kinase domain receptor/VEGF receptor 2 (KDR/Flk-1) fluorescence with R-phycoerythrin on the y-axis. This sample shows cells strongly expressing both antigens are rare, but there are significantly more than in the isotype control sample (see figure 4.3) (Q2). Image B plots C-Kit fluorescence with allophycocyanin (APC) on the x-axis with cell count on the y-axis. The box labelled, “C-kit+” includes cells with strong fluorescence for the antigen, which are rare in this sample, but again significantly greater in number than in the isotype control (see figure 4.3).

4.7 Murine MAC Culture

4.7.1 Tissue Harvest

Terminal anaesthesia with isoflurane was used for harvest of blood, spleen and bone marrow samples from mice. A midline laparotomy incision was made once animals were anaesthetised and blood was taken via inferior vena cava (IVC) puncture into a 1ml insulin syringe pre-filled with 50µL sterile sodium citrate. A 1ml sample was obtained, then added to 4ml sterile PBS. Splenectomy was then performed, with the sample stored in 5ml sterile PBS. Bone marrow was then extracted from the femur and tibia bilaterally after these bones were dissected from the animal, cut at the proximal and distal ends and flushed with 5ml sterile PBS with a 23G needle and syringe. Samples were stored on ice for transfer to the main laboratory.

4.7.2 Isolation of Mononuclear Cells

Samples were processed under aseptic conditions in a tissue culture laboratory within a laminar flow hood. Blood was passed through a 70µm cell strainer into a 50ml centrifuge tube. Bone marrow and spleen samples were minced mechanically with syringe plungers into 3ml sterile PBS, then passed through 70µm cell strainers into 50ml centrifuge tubes. Filtrates were washed with 2ml sterile PBS before undergoing density gradient centrifugation after being layered onto 5ml Histopaque-1083. Samples were spun for 30 minutes at 400g, 18°C with the brake turned off to ensure preservation of the density gradient. The buffy layer was aspirated from each sample with a pipette into another 50ml

centrifuge tube with two further wash steps in sterile PBS for marrow and spleen samples and three washes for the blood samples.

4.7.3 MAC Culture

Samples were suspended in MAC growth medium made with EBM-2 basal medium with an EGM-2 bullet kit, and 20% foetal calf serum. A 20µL sample from each tube was then stained with trypan blue and viable cells were counted using a haemocytometer. Cells were seeded onto fibronectin-coated 24-well plates at a density of $5x10^6$ per well for blood, $8x10^6$ per well for spleen and $1x10^6$ per well for marrow. Samples were incubated in standard conditions in a cell culture incubator (37°C, 5% CO2) for 7 days with a PBS wash and media change on day 4.

4.7.4 MAC Enumeration

After culture for 7 days, cells were washed with PBS then incubated in the dark for 3 hours in a 10µg/ml solution of 1,1'-dioctadecyl-3,3,3',3'-tetramethylindocarbocyanine-labelled acetylated low-density lipoprotein (DiI-ac-LDL) diluted in MAC media. Samples were then fixed in 4% paraformaldehyde for 10 minutes at room temperature. After a PBS wash, a 10µg/ml solution of BS-1 Lectin-FITC was then added to the cells and they were then left for 1 hour at room temperature. Cells were visualised at 10x magnification with a fluorescence microscope and phase-contrast, green fluorescence (lectin-FITC) and red fluorescence (DiI) images were taken using Cell B software. Images were recorded from 5 high-power fields (HPF) per well with a minimum of 2 wells imaged for each mouse sample. A macro was then used to overlay each of the

three images per HPF within Image J software. MACs were counted as those staining co-staining red and green (i.e. yellow) in these composite images and mean numbers per HPF were recorded.

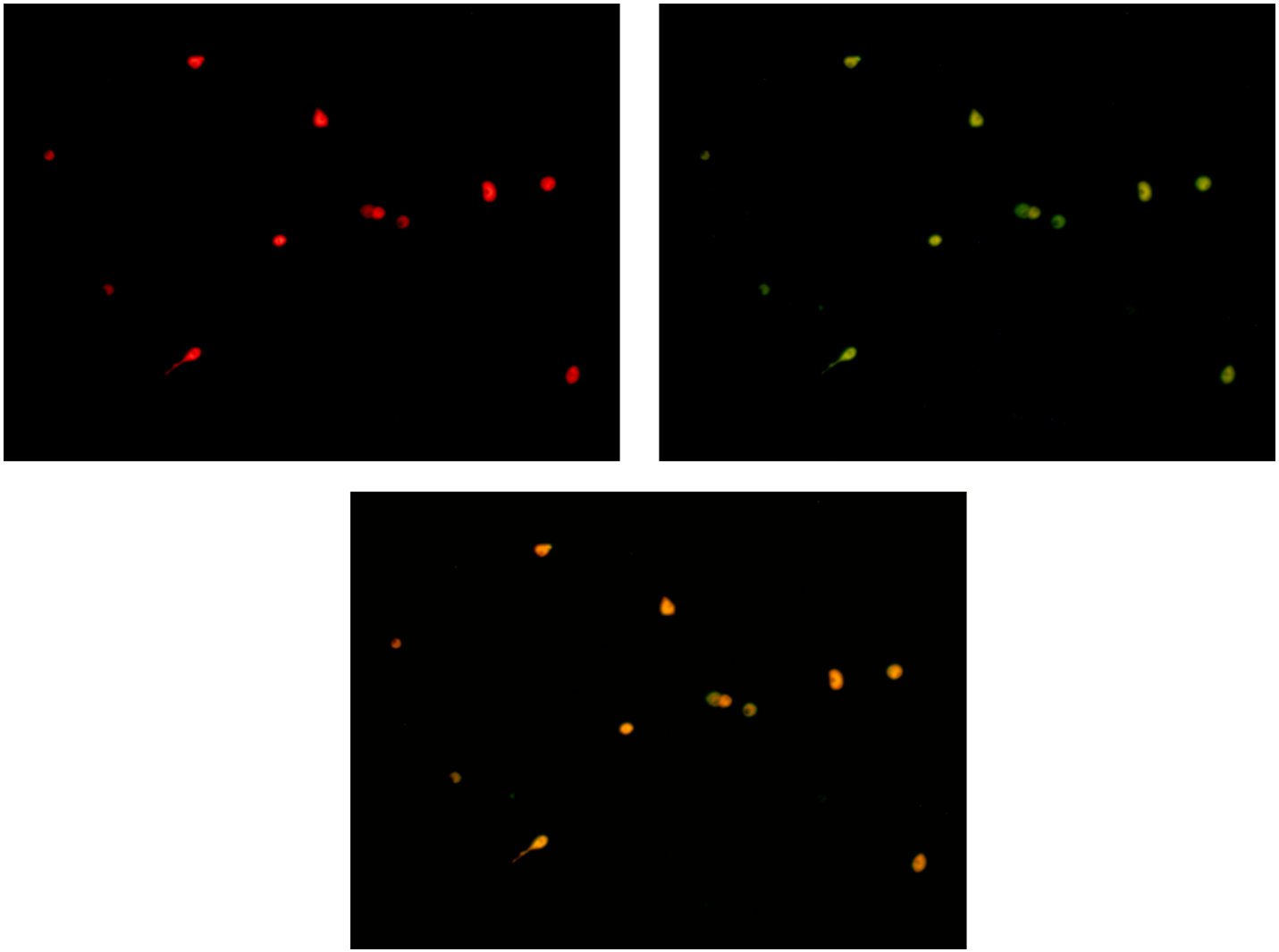

Figure 4.5: Representative Images of Marrow-Derived MAC Enumeration

Myeloid angiogenic cells (MACs) stained with DiI-ac-LDL (red, top left), Lectin (green, top right), and Dual Stained (yellow, bottom). 100X magnification.

4.8 Quantification of Leukocyte Populations

4.8.1 Blood and Bone Marrow Harvesting

Terminal anaesthesia with isoflurane was used for harvest of blood, and bone marrow samples from mice. A midline laparotomy incision was made once animals were anaesthetised and blood was taken via inferior vena cava (IVC) puncture into a 1ml insulin syringe pre-filled with 100µL sterile heparin. A 1ml sample was obtained, then added to 20ml 1:10 Pharmlyse® red cell lysis buffer solution (in distilled water). Bone marrow was then extracted from both femurs after these bones were dissected from the animal, cut at the proximal and distal ends and flushed with 5ml phosphate-buffered saline (PBS) containing 0.5% bovine serum albumin (BSA) and 2mM EDTA using a 23G needle and syringe. Samples were stored on ice for transfer to the main laboratory.

4.8.2 Sample Processing

After washing and resuspending bone marrow cells in PBS with 0.5% BSA and 0.5% foetal calf serum, cells were incubated at 4ºC with CD16/32 Fc block, then ten minutes later with anti-CD45-VioBlue, anti-CD11b-FITC, anti-Ly6G-PE and Ly6C-APC, for a further ten minutes, prior to washing unbound antibodies. Some bone marrow cells were separately stained with anti-lineage cocktail-eFluor450, anti-c-Kit-PE, and anti-Sca-1-APC for ten minutes. Paired samples were prepared with corresponding isotype-specific controls.

4.8.3 Flow Cytometry

Flow cytometry was performed to acquire leukocytes based on typical light scatter properties, with further gating used to define the following subsets: total leukocytes - $CD45^+$; myeloid cells - $CD45^+CD11b^+$; monocytes - $CD45^+CD11b^+Ly6G^-Ly6C^+$; neutrophils - $CD11b^+Ly6G^{hi-}Ly6C^{hi}$; 'inflammatory' monocytes - $CD11b^+Ly6G^-Ly6C^{hi}$; 'patrolling' monocytes - $CD11b^+Ly6G^-Ly6C^{lo}$; haematopoietic stem cells - $Lin^-Sca\text{-}1^+c\text{-}Kit^+$. Known sample volumes were processed, allowing absolute population counting, and isotype controls were used to define the threshold of antigen expression. All populations are expressed as cells/ml for blood or cells/femur for bone marrow.

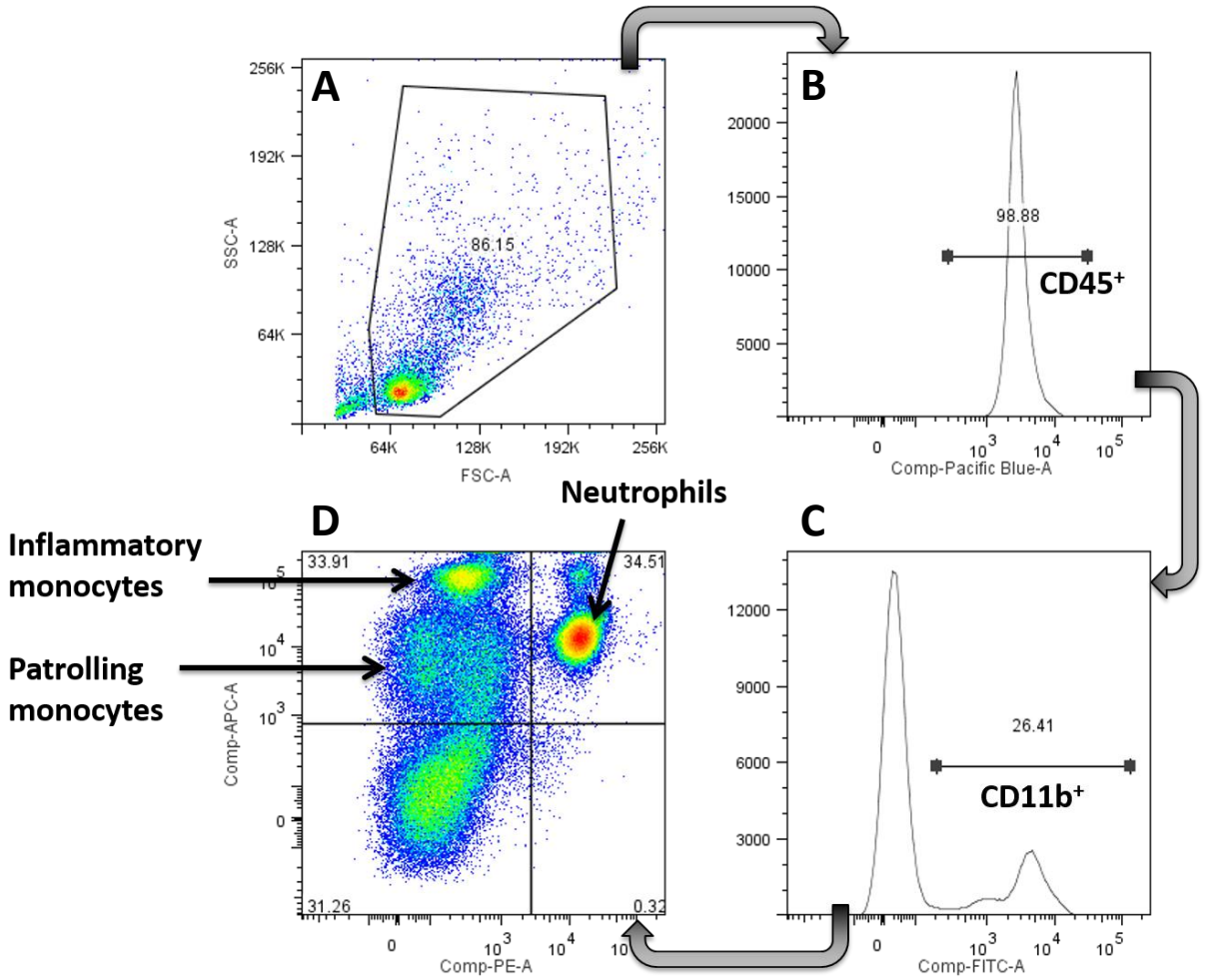

Figure: 4.6: Blood Leukocyte Gating on Flow Cytometry

Panel A shows forward scatter on x-axis and side scatter on y-axis, with the outlined area encompassing the single cell population (debris is to the bottom left). Panel B shows pacific blue fluorescence for CD45 expressing cells on the x-axis with the CD45+ population highlighted. Panel C shows fluorescence for FITC (fluorescein isothiocyanate)-labelled cells, indicating CD11b expression (highlighted) in the CD45+ cells. Panel D shows the CD11b positive population further subdivided. It highlights neutrophils showing strong R-phycoerythrin (PE) fluorescence (i.e. $Ly6G^{hi}$), and inflammatory and patrolling monocytes which have little PE fluorescence ($Ly6G^{-}$) and high ($Ly6C^{hi}$) or low ($Ly6C^{lo}$) APC (allophycocyanin) fluorescence respectively.

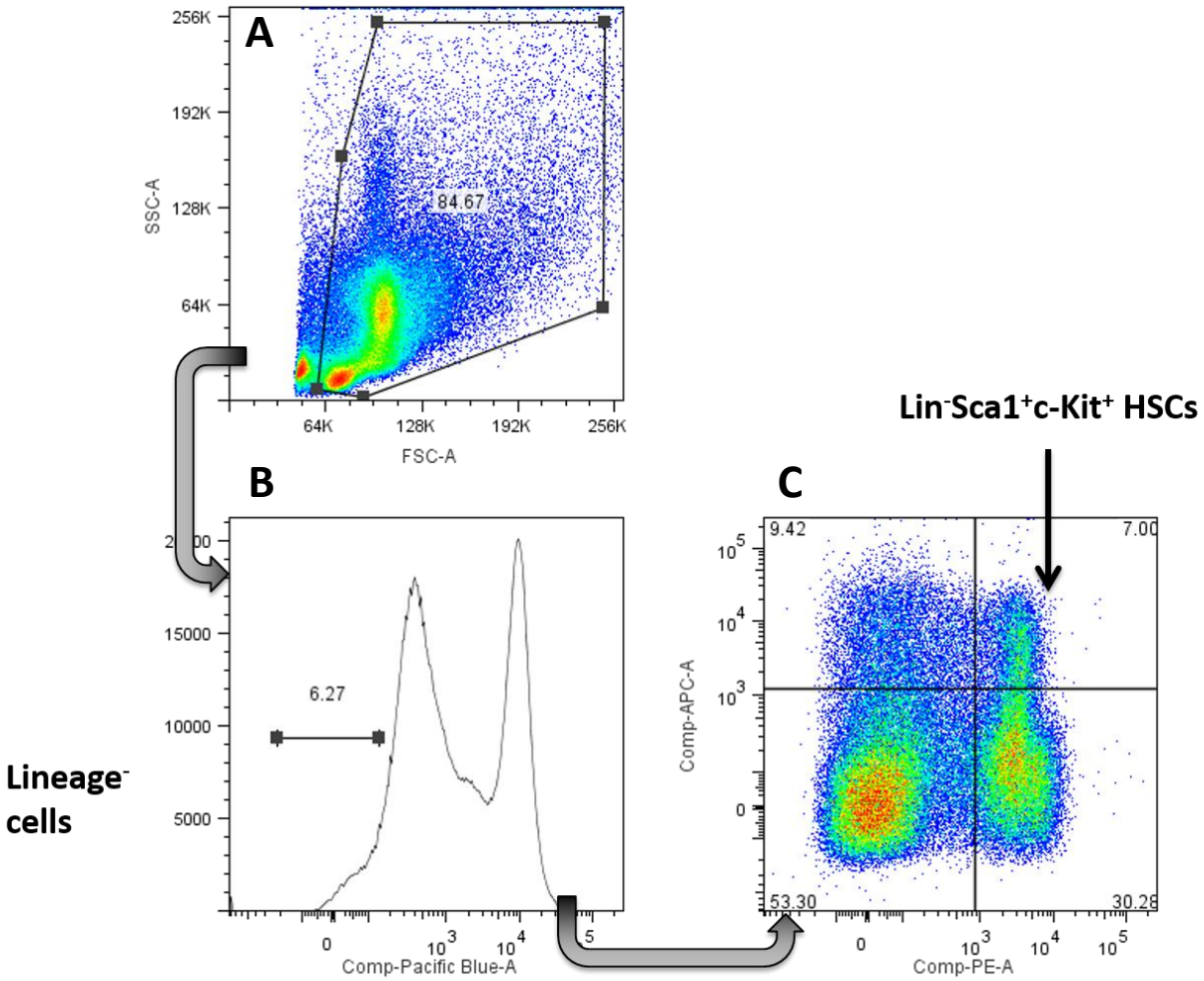

Figure 4.7: Gating Strategy for Bone Marrow on Flow Cytometry

Panel A shows forward scatter on the x-axis and side scatter on the y-axis with the single cell population outlined. The x-axis of panel B shows fluorescence for pacific blue (lineage cocktail), with cells negative for the stain (i.e. lineage$^-$) highlighted. These cells are then further subdivided in panel C, with the x-axis showing fluorescence for R-phycoerythrin (PE) (c-Kit) and the y-axis showing fluorescence for APC (allophycocyanin) (Sca1). As such, the top right quadrant contains HSCs which are Lineage$^-$Sca1$^+$c-Kit$^+$.

4.9 Isolation of Murine Pulmonary Endothelial Cells

Animals were sacrificed via cervical dislocation, then midline sternotomy was performed followed by dissection and removal of the lungs into Hank's Buffered Saline Solution (HBSS). Samples were transferred on ice to the tissue culture laboratory, with all subsequent steps being performed in a laminar flow hood. Lungs were added to a petri dish (5mm diameter) containing 1ml type II collagenase dissolved in HBSS (1mg/ml) then minced with 2 scalpel blades until a paste was formed. Samples were then transferred into 15ml centrifuge tubes and made up to a total volume of 10ml of the collagenase/HBSS solution and incubated at 37°C for 45mins on a MACSmix rotator.

Samples were transferred to a sterile 50ml centrifuge tube and the contents were then aspirated through a 14G cannula attached to a 5ml stripette. The contents were alternately aspirated then expelled into the centrifuge tube (~ 15 times) in order to reduce any tissue aggregates and to aid in producing a single cell suspension. The solution was then passed through a 70µM cell strainer into a fresh 50ml centrifuge tube. The strainer was washed with 10ml 0.5% bovine serum albumin (BSA) in phosphate buffered saline (PBS). Samples were then centrifuged at 2000rpm for 5mins to pellet the cell suspension. Cells were resuspended in 5ml BSA/PBS solution then spun again for 5mins at 2000rpm.

Samples were resuspended in 300 microlitres BSA/PBS then transferred to a 1.5ml microcentrifuge tube. 15µL of CD146 microbead solution was added to each tube, with samples then being incubated for 20 mins at 4°C on the

MACSmix rotator. After incubation, cell suspensions were washed by adding 500µl of PBS/BSA, spun at 4000rpm for 5 mins, then the supernatant was discarded. This wash step was repeated, after which MiniMACS columns were set up on a magnetic stand and primed with 500µL BSA/PBS. Samples were applied to the columns through a 30µM cell strainer with the non-endothelial cell fraction collected in 15ml centrifuge tubes. Columns were rinsed five times with BSA/PBS once the contents had drained through. The columns were then removed from the magnetic stand and placed into 15ml centrifuge tubes. 1ml BSA/PBS was added then the plunger from the kit was applied forcibly through the column to extract the endothelial cells. Samples were centrifuged for 5 mins at 4000rpm then resuspended in 500µL BSA/PBS and applied to MiniMACS columns as previously described. The final endothelial samples were centrifuged at 4000rpm for 5 mins then resuspended in endothelial cell growth medium containing 10% foetal calf serum, 5ml antibiotic/antimycotic solution, and 10ml endothelial growth supplement (MV2) before being plated onto tissue culture flasks coated with 0.1% gelatin (in distilled water). A full media change was performed 2hrs following isolation to remove cell debris, with half media changes every 2 days thereafter. Flasks were typically confluent within 2-3 weeks, at which point cells were trypsinised and seeded onto new plates for functional assays. As such, all PEC functional assays were done with P1 cells. Purity of samples produced with this method was assessed in PECs from a separate colony of reporter mice: VE-cadherin-Cre IGF-1Rlox mTmG, treated with tamoxifen, leading to endothelial-specific green staining, with non-endothelial cells remaining red in colour.

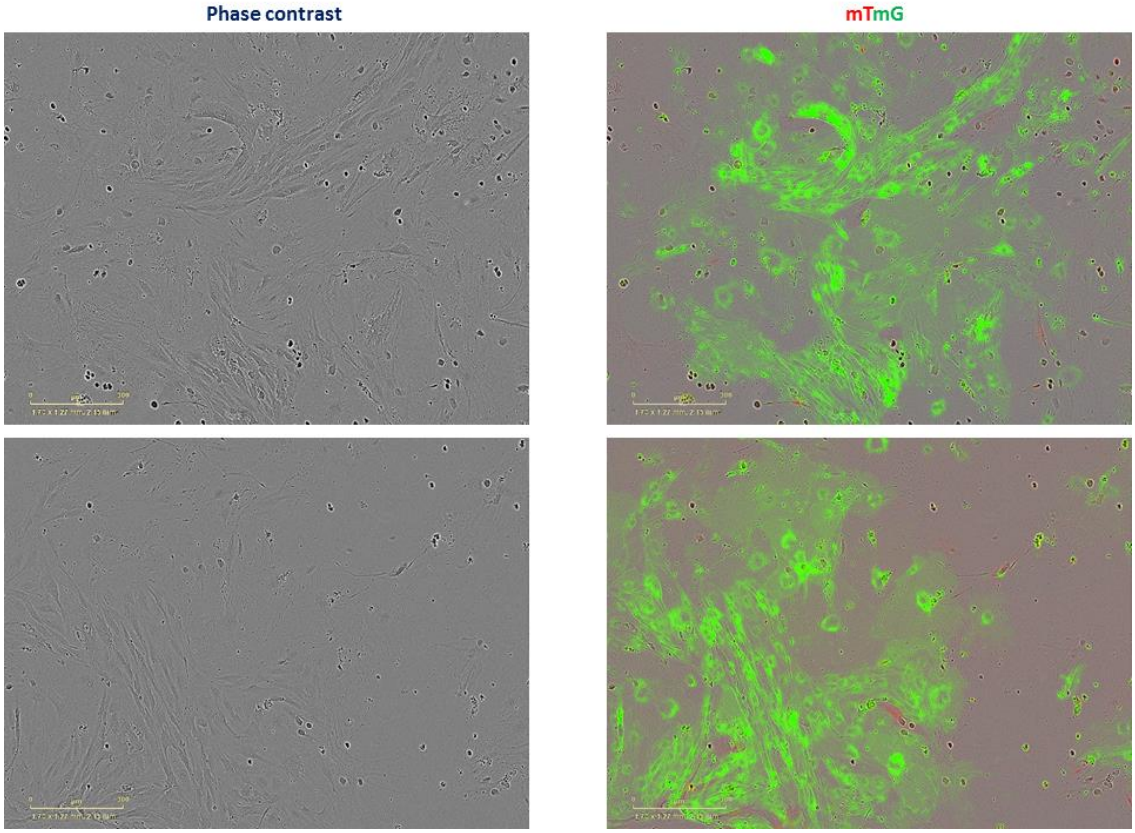

Figure 4.8: Pulmonary Endothelial Cell Purity

Image courtesy of Dr Katherine Paradine, PECs kindly donated by Dr Marc Bailey. Endothelial cells are green-staining, with non-endothelial cells seen in red.

4.9.1 Scratch Wound Assay

The entire assay was conducted in a laminar flow tissue culture hood. Pulmonary endothelial cells were passaged (P1) and resuspended in endothelial cell growth medium. 40,000 cells were added to each of six wells of an ImageLock 96 well cell culture plate per sample. The total volume of cells and medium per well was 100 µL.

Cells were left to achieve confluence overnight, then serum starved in basal medium containing no growth factors or serum for 4hrs. After this, a Woundmaker was used to remove a band of cells from the centre of each well.

Wells were washed twice with PBS, then media containing 2% serum was added and the dish. The wells were imaged at 100X magnification (2 images per well), and the plate was then incubated at 37°C and imaged again 18hrs later. Image J software was used to calculate the cell-free area immediately following scratch wound creation, with the area at 18hrs subtracted from then divided by the initial value to give the proportion of scratch area recovered.

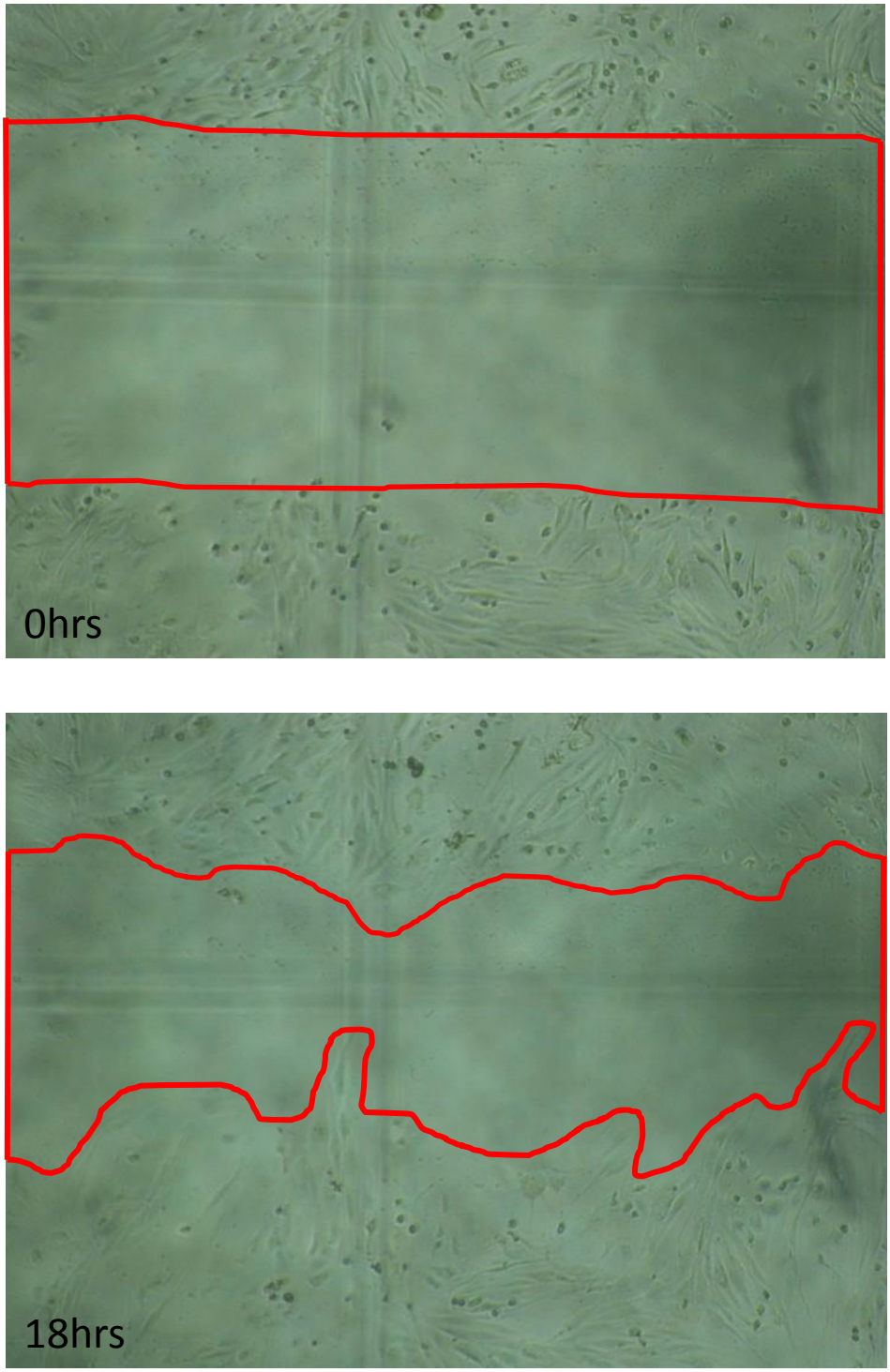

Figure 4.9 Scratch Wound Closure Method

Border of confluence highlighted in red – area within red margin quantified using ImageJ software. Images taken at 100X magnification.

4.9.2 Angiogenic Bead Assay

This method was adapted from the assay first described by Nakatsu *et al* [243]. The entire assay is conducted in a laminar flow tissue culture hood. Pulmonary endothelial cells were cultured with endothelial cell growth medium containing growth factors including VEGF and FGF (EGM-2 Bulletkit, Lonza) for a minimum of 48hrs prior to passage (P1). Cells were trypsinised, pelleted and then resuspended in EGM-2 and counted with a haemocytometer. 500,000 cells were suspended in 1.5ml media, then added to a 1.5ml microcentrifuge tube containing 1250 Cytodex-3 beads (21µL of stock solution at 60,000 beads/mL washed first with 1mL EGM-2). The bead/cell solution was then transferred to a sterile FACS tube and incubated at 37°C for 4hrs with agitation every 20 mins. Following this the coated bead solution was transferred to a T25 cell culture flask, made up to a total of 7ml with media. This was then incubated overnight to allow unattached cells to come out of solution onto the plate.

The next day the T25 was gently agitated, with the beads removed with a strippette and transferred into a 15ml centrifuge tube. The T25 was washed twice with medium to ensure all beads were removed. The bead suspension was allowed to settle for a minimum of 5 mins, after which the media was aspirated to leave the beads at the bottom of the tube. Beads were gently resuspended in 1ml EGM-2 then transferred to a 1.5ml microcentrifuge tube. The beads were allowed to settle for 5mins, with the media then aspirated and replaced to wash the beads. This process was repeated 3 times, after which the beads were resuspended in a solution containing fibrinogen 2mg/ml and

aprotinin 0.15 units/mL. 2.5 mL of this solution was used for each sample of 500,000 cells with 1250 beads. 12.5µL thrombin 50 units/mL was added to the centre of each well of a 24-well cell culture plate. Following this, 500µL of the bead/fibrinogen solution was added to each well after careful mixing with a 1000µL pipette. There were therefore 5 wells of beads per sample, each containing ~ 250 beads. Once all wells were complete, the plate was left undisturbed for 5 mins to allow the matrix to coagulate. The plate was then moved to the incubator at 37°C and left for a further 10mins until the fibrin clots were set. 1mL of EGM-2 was then added to each well drop-wise with the plate then being returned to the incubator for 24hrs prior to imaging. Imaging was performed with phase-contrast microscopy at 10x magnification with a minimum of 25 beads per sample photographed. Images were then analysed offline using Image J, with sprouts counted and their length measured. Divergent sprouts were counted as two separate entities if the length distal to their branching point was >50% of the total sprout length.

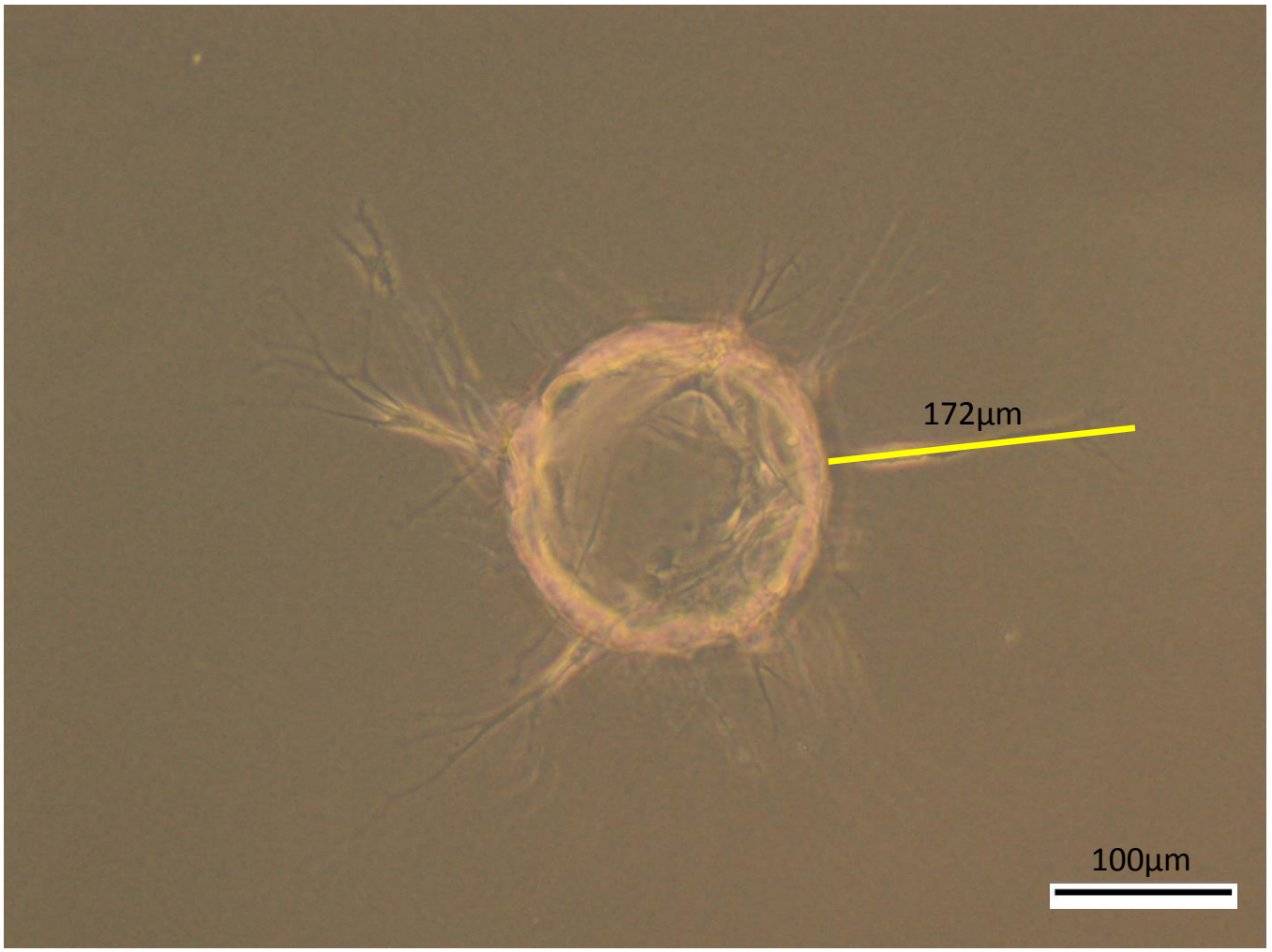

Figure 4.10: Representative Image of Angiogenic Bead Sprouting Assay

Image taken at 100X magnification, ImageJ software used for measurements – sprout length shown in yellow.

4.10 Aging Studies

4.10.1 Establishment of Aging Colony

Animals were bred from the IRKO-IGF1Rko colony as previously described in section 4.1. Genotyping was performed at weaning (age 3-4 weeks), and 15 consecutively born mice were selected for each of the four possible genotypes: WT; IRKO; IGF1Rko; and DKO. Animals were housed with littermates where

possible. Mice were kept in the University of Leeds animal facility under standard conditions, including a 12-hour sleep/wake cycle, with access to water and chow diet *ad libitum* unless otherwise stated.

4.10.2 Metabolic Phenotyping

Animals were weighed weekly from age 4 weeks until their death. Fasting glucose and glucose and insulin and insulin tolerance tests were performed at age > 80 weeks as described in sections 4.3.3 and 4.3.4, although prior to ITTs in this colony mice were fasted for 2hrs rather than 4hrs so as to avoid severe hypoglycaemia following insulin administration.

4.10.3 Healthspan

Assessment of healthspan was made according to criteria provided by a Home Office approved Veterinary Surgeon to ensure animal welfare throughout the study [244]. Animals were considered to have reached their healthspan endpoint if one or more of the following conditions was met:

1. Spontaneous death before one of the following endpoints.
2. Body condition score 2 to 1 out of 5 [244].
3. Body weight loss of ≥15% of the average highest body weight.
4. Hunched posture/starry coat/abnormal gait of more than 48 hours duration regardless of body weight loss.
5. Any subcutaneous lump/swelling regardless of body weight loss.
6. Excessive hair loss. Any hair loss monitored over a one week period.

Assessment to confirm whether an animal had met a healthspan endpoint was made by two independent observers except in the case of spontaneous death or body weight loss of ≥15% of the average highest body weight, which were considered independent of inter-observer variability. Animals were culled in accordance with Schedule 1 of The Animals (Scientific Procedures) Act 1986 (Amended 2012) once a healthspan endpoint was reached, with tissue harvested for later analysis. Post-mortem examinations were performed in order to assist in determination of cause of death, in particular the presence or absence of any macroscopically visible tumours was recorded. In keeping with our Home Office Project License (P144DD0D6) stipulations, any animals considered to be experiencing excessive pain or distress (outside of the criteria mentioned above) were culled after assessment by two independent observers blinded to genotype.

4.10.4 Quantitative Polymerase Chain Reaction of RNA samples

4.10.4.1 RNA Extraction

Samples were harvested by myself with RNA extraction, Reverse Transcriptase PCR and quantitative PCR performed by Mrs Jessica Smith.

Samples were harvested from young mice from the IRKO:IGF1Rko colony aged 8-15 weeks following sacrifice by appropriate Schedule 1 method. It should be noted that these animals were not part of the separate aging cohort (see section 4.10.1). Tissue was placed in a tube with a metal lysis bead and 1ml Trizol Reagent was added to each sample. Tubes were then placed in a tissue lyser and agitated at 30Hz for 3 x 2 minute sessions. The resultant liquid was transferred to 1.5ml centrifuge tubes then spun at 10000g (4°C) for 10 minutes.

The supernatant was transferred to new centrifuge tubes with the pellet discarded. 200 microlitres of chloroform was added to each tube, which were then vortexed then left to settle for 3 minutes at room temperature. The tubes were spun at 12000g (4°C) for 15 minutes with the supernatant then transferred to new tubes. 500 microlitres of isopropanol was added to each tube then gently mixed before being left to stand on ice for 10min. The samples were then spun for 10min at 12000g (4°C), with the supernatant discarded following this. The pellets were resuspended in 1ml of 70% ethanol (in dH_2O) before a further spin at 7500g (4°C) for 5min. The supernatant was removed carefully, then 20 microlitres of RNA-free distilled water was added to each sample. After leaving the samples on ice for 20 minutes, RNA was quantified using a NanoDrop® and ND-1000 (V3.1.0) software. Samples were diluted to a total volume of 10 microlitres with RNA-free distilled water.

4.10.4.2 Reverse Transcriptase PCR

A master mix was made using the following:

Constituent	Volume (µL)
Buffer	2
Random Primers	2
Multiscribe	1
DNTP	0.8
Distilled Water	4.2

Table 4.1: Reverse Transcriptase PCR Mastermix Constituents

10µL of mastermix was mixed with the 10µL RNA sample in a PCR plate then transferred to a thermal cycler with the following programme:

1. 25°C for 10 minutes
2. 37°C for 2 hours
3. 85°C for 5 minutes
4. 4°C for 30 minutes

4.10.4.3 Real Time PCR

Following reverse transcriptase PCR, cDNA products were transferred to new vessels, with 2 microlitres then added to a new PCR plate containing 10µL of TaqMan gene expression master mix, 1µL of the probe (see section 3.12 for list) and 7µL of molecular grade distilled water. A LightCycler was used to process the samples in triplicate. The cycle threshold (CT) values from the gene of interest were compared with those from the housekeeper gene (beta actin), with

delta (Δ) CT calculated and $2^{-\Delta CT}$ used to normalise to beta actin, expressed as a percentage.

4.10.5 Nesting Studies

Preserved cognitive function, motivation, planning skills, coordination, manual dexterity, and physical strength, amongst other attributes, are important features of healthy aging in mice [245]. As such, we conducted a gross assessment of these abilities in the mice from the aging cohort. Nesting studies were performed by Dr Nicole Watt, with scoring performed by myself, Dr Watt and two other independent researchers all blinded to genotype, with a mean score produced from the four assessors' marks.

Mice were caged individually and left overnight with a nestlet. The next morning the cage was examined for the presence of a nest and images taken to quantify nest building according to an established protocol [245]. Images were taken by a blinded researcher, with the nest photographs subsequently being scored by a total of 4 researchers per mouse, also blinded to genotype. Scoring criteria were as follows:

1. Nestlet not noticeably touched (more than 90% intact).
2. Nestlet partially torn (50–90% remaining intact).
3. Nestlet mostly shredded but often no identifiable nest site: less than 50% of the Nestlet remains intact, but less than 90% is within a quarter of the cage floor area; i.e., the cotton is not gathered into a nest but is spread around the cage. The material may sometimes be in a broadly defined

nest area, but the critical definition here is that 50–90% has been shredded.

4. An identifiable but flat nest: more than 90% of the Nestlet is torn and the material is gathered into a nest within a quarter of the cage floor area, but the nest is flat, with walls higher than mouse body height (of a mouse curled up on its side) for less than 50% of its circumference.
5. A (near) perfect nest: more than 90% of the Nestlet is torn and the nest is a crater, with walls higher than mouse body height for more than 50% of its circumference.

Representative images are shown below:

Figure 4.11: Representative Images of Nesting Scores

4.11 Statistics

All data are presented as mean +/- standard error of the mean (SEM) with statistical significance considered $P < 0.05$: this is denoted with an asterisk. As our hypothesis was that DKO would have improved vascular repair and regeneration compared with IRKO, data from these groups in chapter 5 are compared with unpaired Student's t-tests, unless otherwise stated. WT results are therefore provided for reference only. In chapter 6 the Log-Rank test has been used to analyse the four genotypes on the Kaplan-Meier plots for healthspan, with the largest difference (WT versus DKO) being analysed with the same test separately. Other data in chapter 6 are hypothesis-generating, with ANOVA p-values provided, and post-hoc student's t-tests without correction for multiple testing performed to indicate possible differences between groups on which to base future experiments. Comparison of groups in the nesting studies in chapter 6 was made using the Mann-Whitney U test, as these data are not normally distributed [246]. Analysis was performed using GraphPad Prism or Microsoft Excel except for analysis of healthspan, which was made using Statistical Package for the Social Sciences (SPSS) software (IBM), with Log-Rank tests used to compare groups on Kaplan-Meier survival plots.

Chapter 5 **Results: Vascular Repair and Regeneration**

5.1 Genotyping

Figure 5.1 shows a representative image taken following gel electrophoresis for the IRKO transgene, with figure 5.2 displaying a typical gel for IGF-1R electrophoresis. A 1000 base pair (bp) ladder is shown on the left of each image for reference.

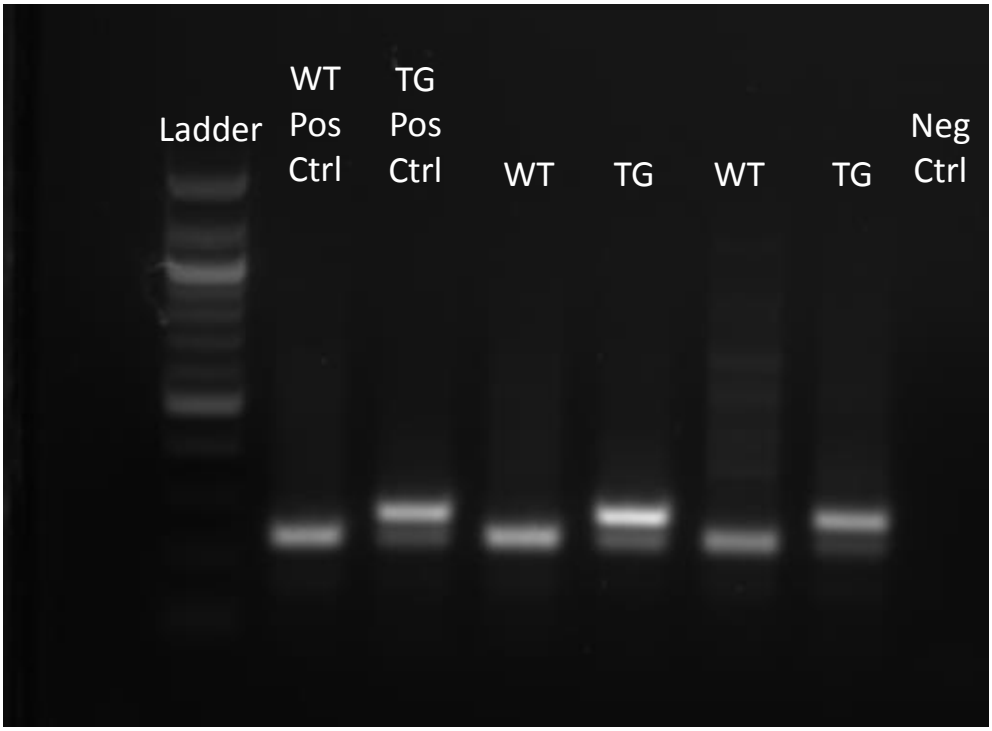

Figure 5.1: IRKO Genotyping

Single band at 235 base pairs (bp) denotes wild type (WT), with bands at 235 and 255bp denoting IRKO transgene (TG). Negative and positive controls are included for reference.

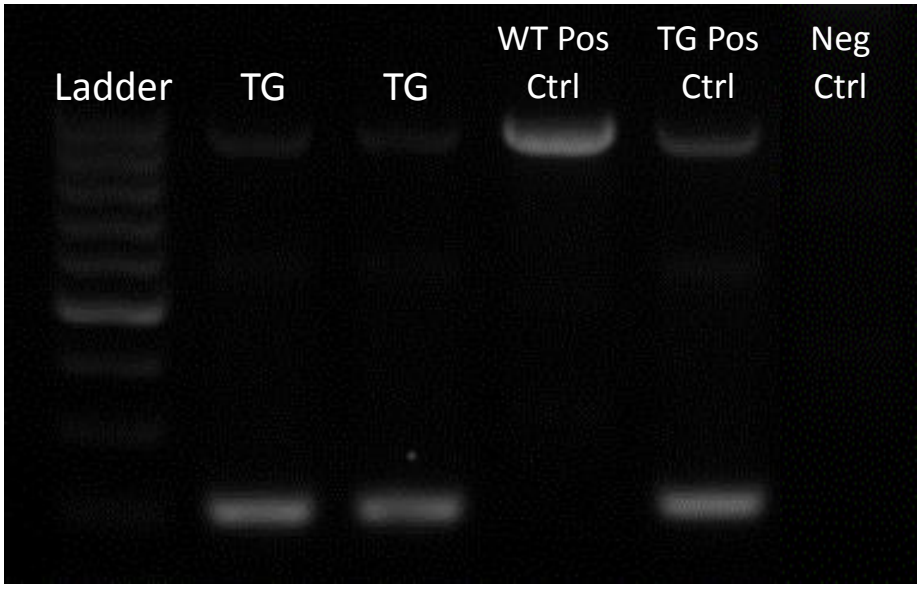

Figure 5.2: IGF-1R Genotyping

Agarose gel electrophoresis with wild type (WT) bands identified at 871bp and IGF-1Rko (TG – transgenic) at 202bp. Positive and negative controls are provided for reference.

5.2 Metabolic Phenotyping

Given the importance of insulin and IGF-1 signalling in growth, vascular function, and glucose metabolism, we studied a range of indices to investigate the effect of haploinsufficiency of both IR and IGF-1R.

5.2.1 Body Weight

Animals were weighed weekly from the age of 8 weeks until 13 weeks of age. Both IRKO and DKO mice were significantly lighter than their WT littermates, with DKO also being lighter than IRKO.

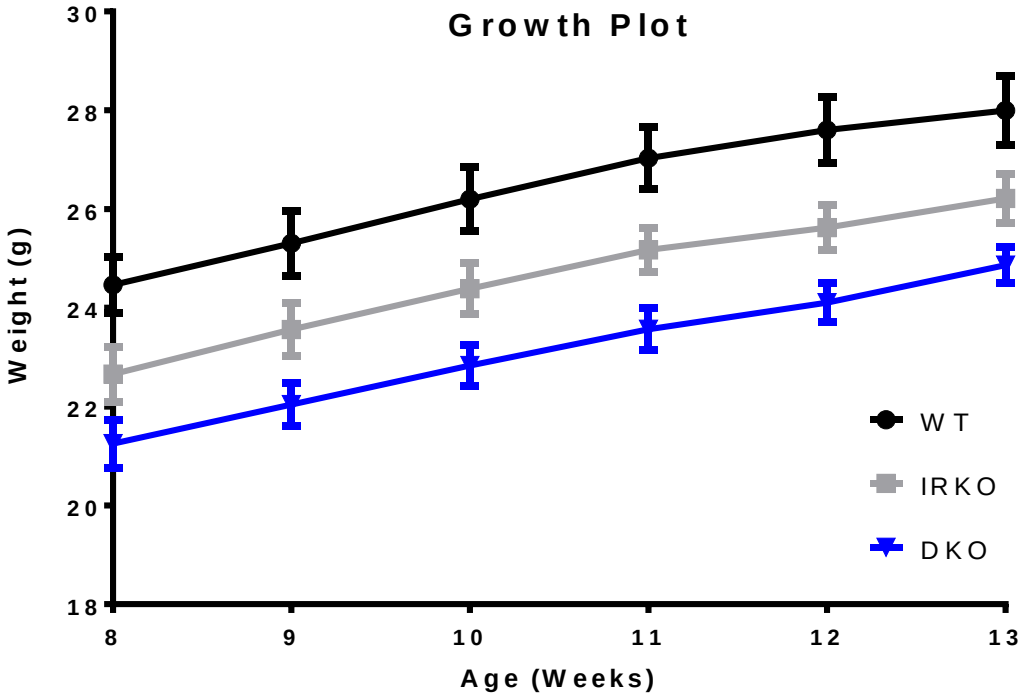

Figure 5.3: Body Weight

Mouse body weight was recorded weekly from age 8 to 13 weeks. N=15 for each group.

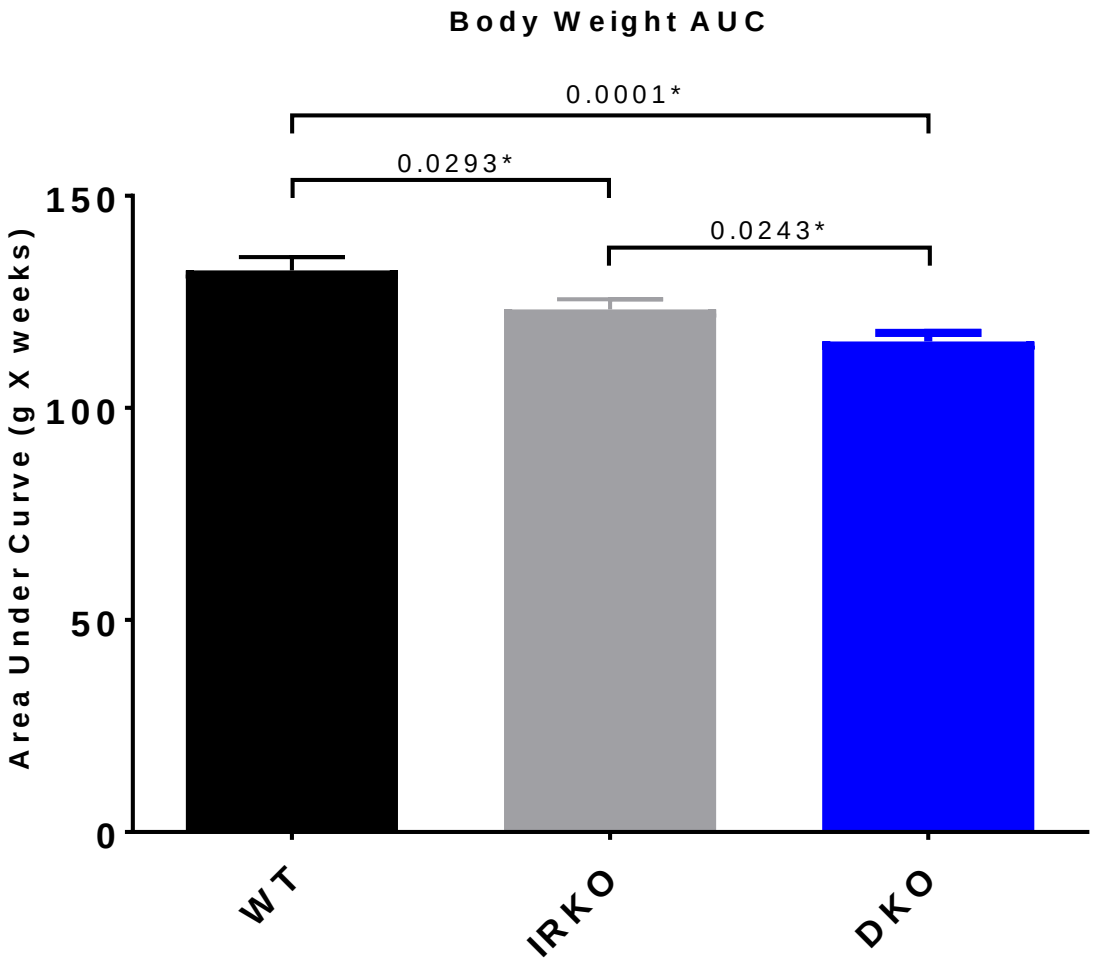

Figure 5.4: Area under the curve for body weight age 8-13 weeks
N=15 for each group.

5.2.2 Systolic Blood Pressure

It has previously been noted that IRKO animals have an elevated blood pressure (BP) compared with WT littermates [146]. We hypothesised that DKO animals would have a normalised BP, given their increased nitric oxide bioavailability and improved vascular reactivity to insulin compared with IRKO [80]. The results did not differ between groups in this study.

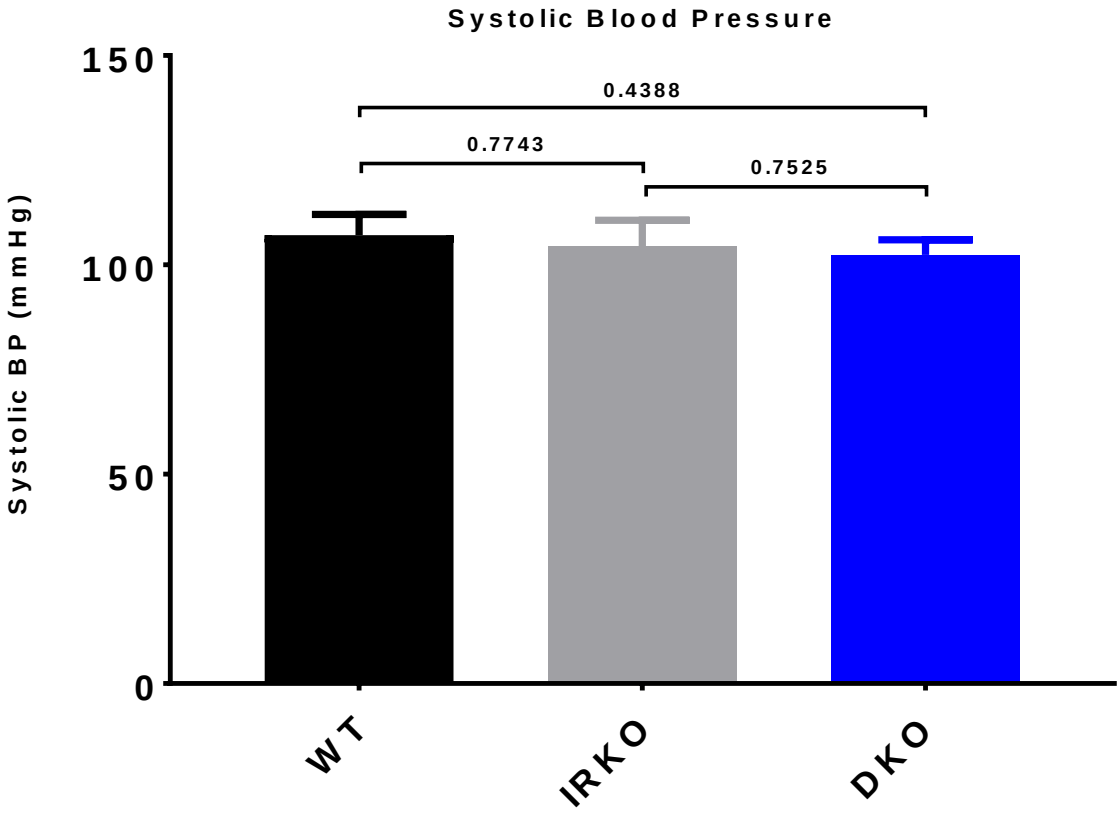

Figure 5.5: Systolic Blood Pressure

Systolic blood pressure was recorded for each group. N= 11 (WT), 10 (IRKO), 16 (DKO).

5.2.3 Fasting Blood Glucose

No significant difference was observed between groups on fasting plasma glucose testing performed via tail-vein sampling after overnight fast.

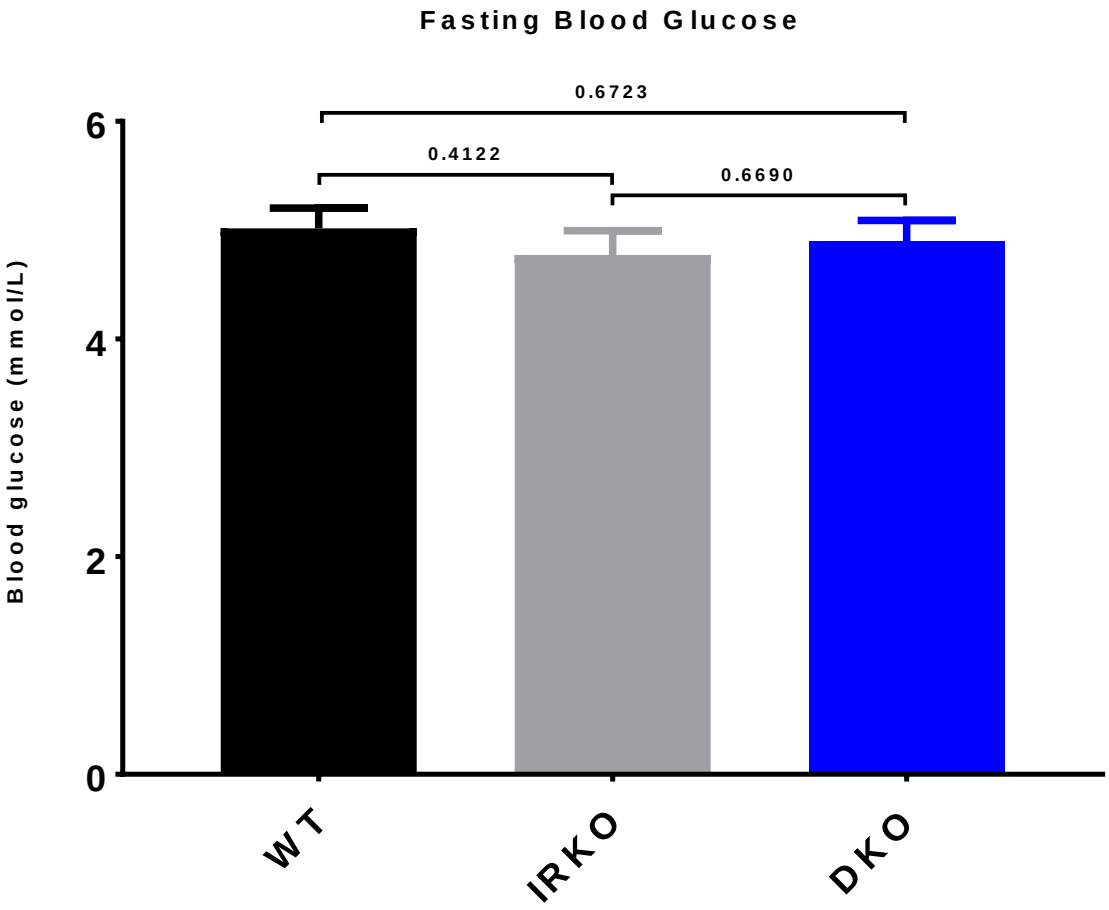

Figure 5.6: Fasting Blood Glucose

Fasting blood glucose measurements were recorded following an overnight fast. N=13 (WT), 11(IRKO), 11(DKO).

5.2.4 Glucose and Insulin Tolerance Testing

Previous work in our lab has assessed glucose and insulin tolerance in DKO animals compared with IRKO, finding no significant difference between the two genotypes [123]. Given the possibility of genetic drift in transgenic mouse colonies, we decided to assess these parameters in the current cohort of animals to ensure they were adequately phenotyped. In keeping with previous results, no difference was noted between genotypes on either glucose or insulin tolerance testing (GTT and ITT respectively). Data are displayed as glucose

plots covering the duration of each experiment (figures 5.7, 5.9), and as area under the curve (AUC) (figures 5.8, 5.10).

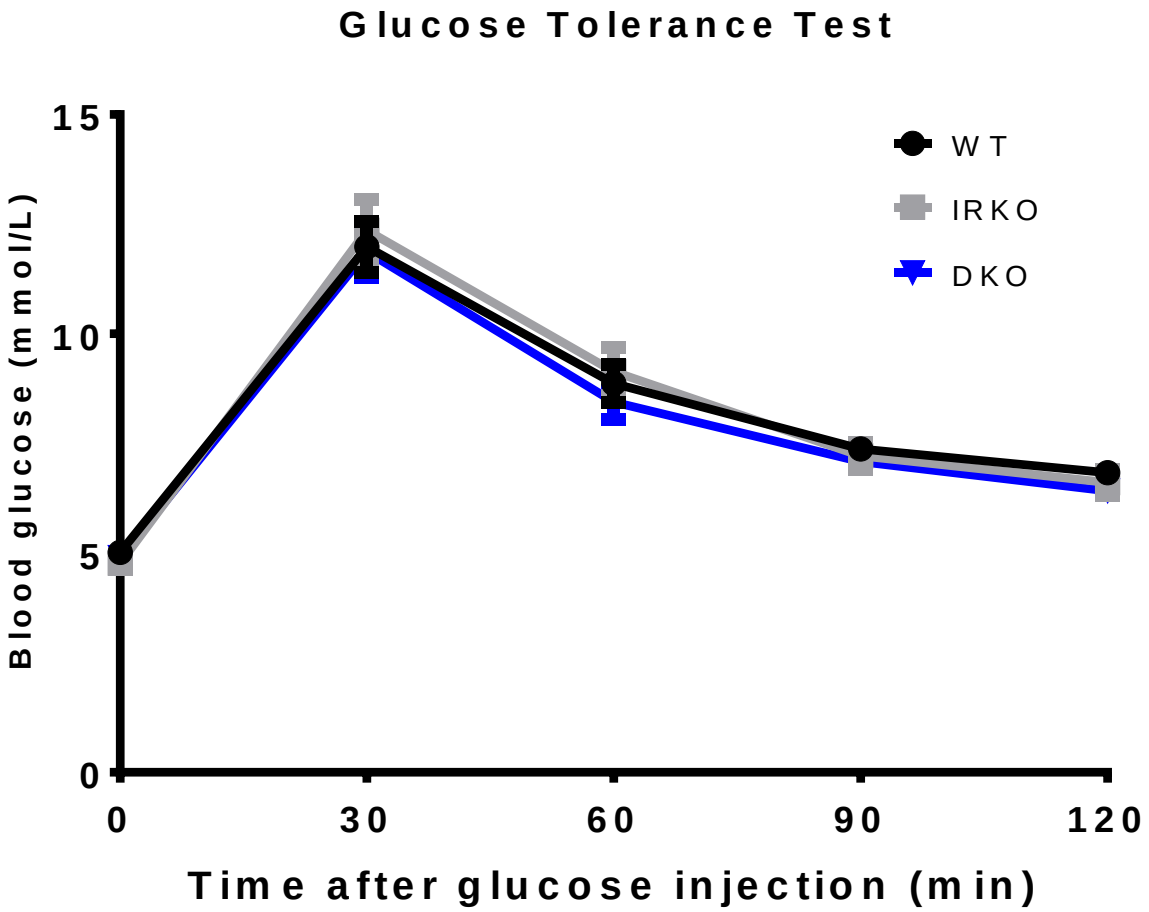

Figure 5.7: Glucose Tolerance Test (GTT)

Mice were fasted overnight then injected with intraperitoneal glucose 1mg/g of body weight. Capillary glucose measurements were made at 30 minute intervals for 2 hours following injection. N= 13 (WT), 11 (IRKO), 11(DKO).

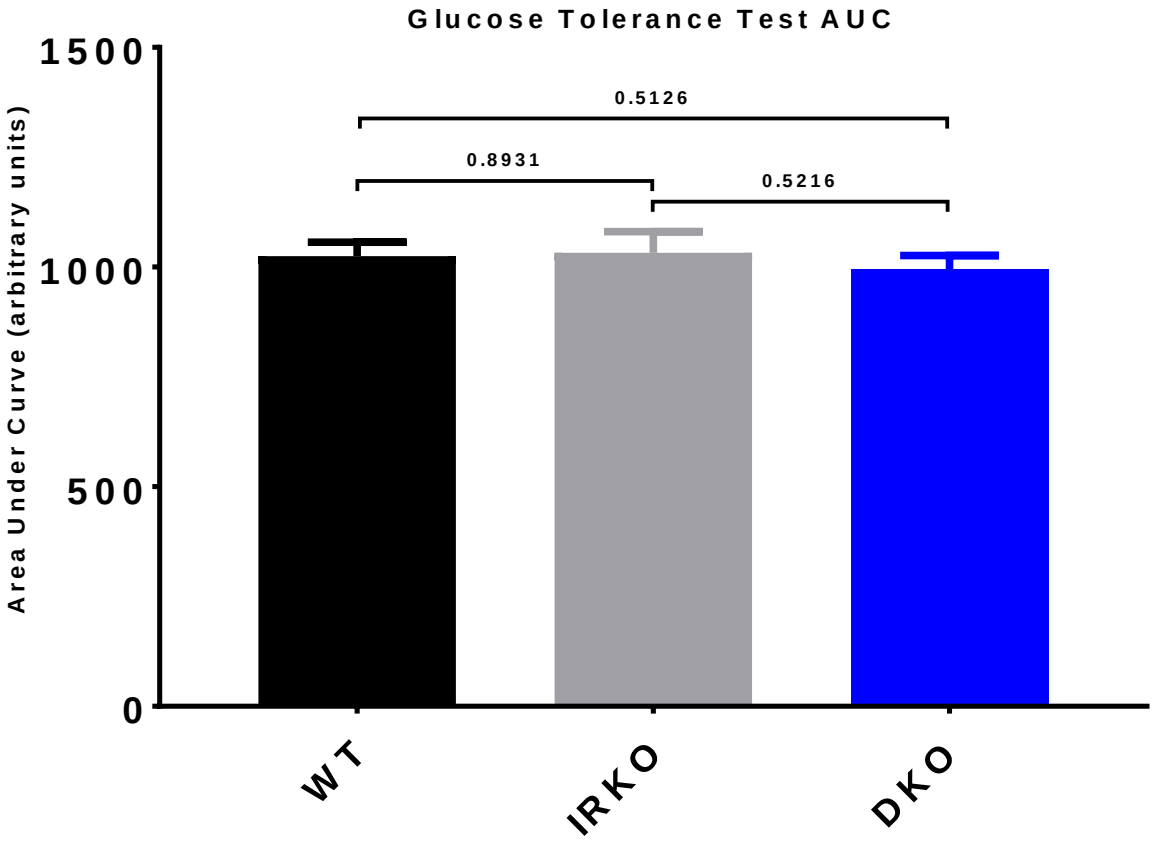

Figure 5.8: Glucose Tolerance Test Area Under the Curve (AUC)
N= 13 (WT), 11 (IRKO), 11(DKO).

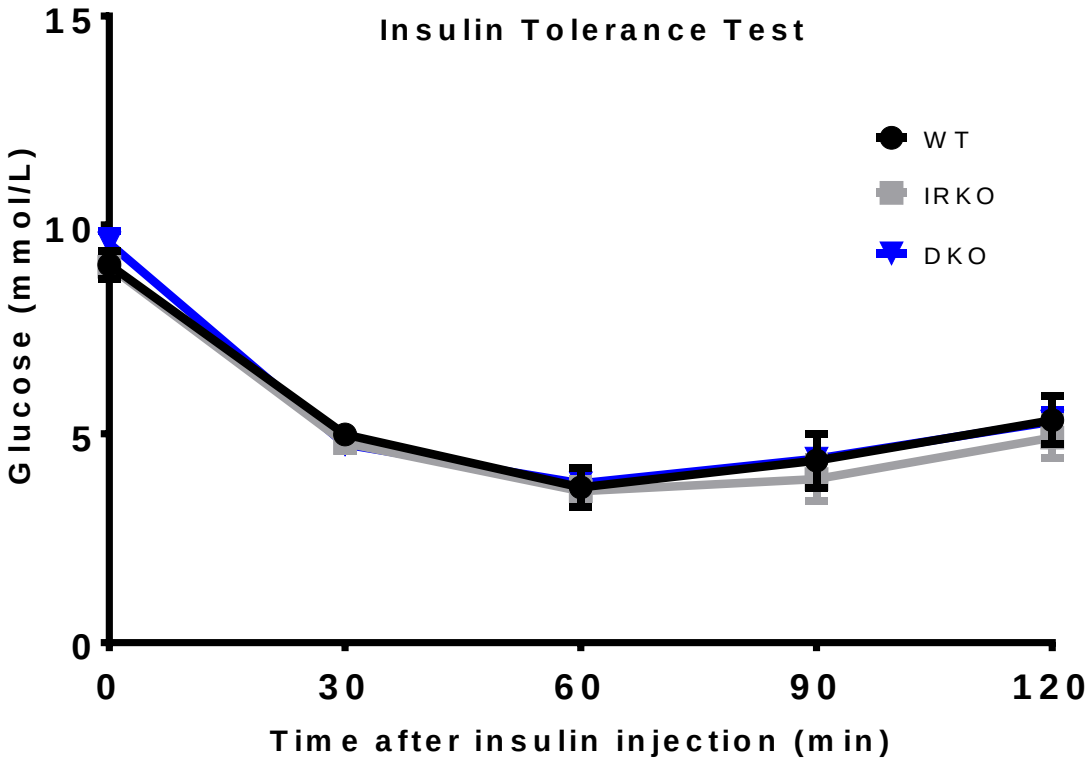

Figure 5.9: Insulin Tolerance Test (ITT)

Mice were fasted for 4hrs then injected with intraperitoneal insulin 0.75IU per gram of body weight. Tail vein blood samples were taken at 30 minute intervals with capillary glucose recorded for 2hrs following injection. N=12 (WT), 10 (IRKO), 13 (DKO).

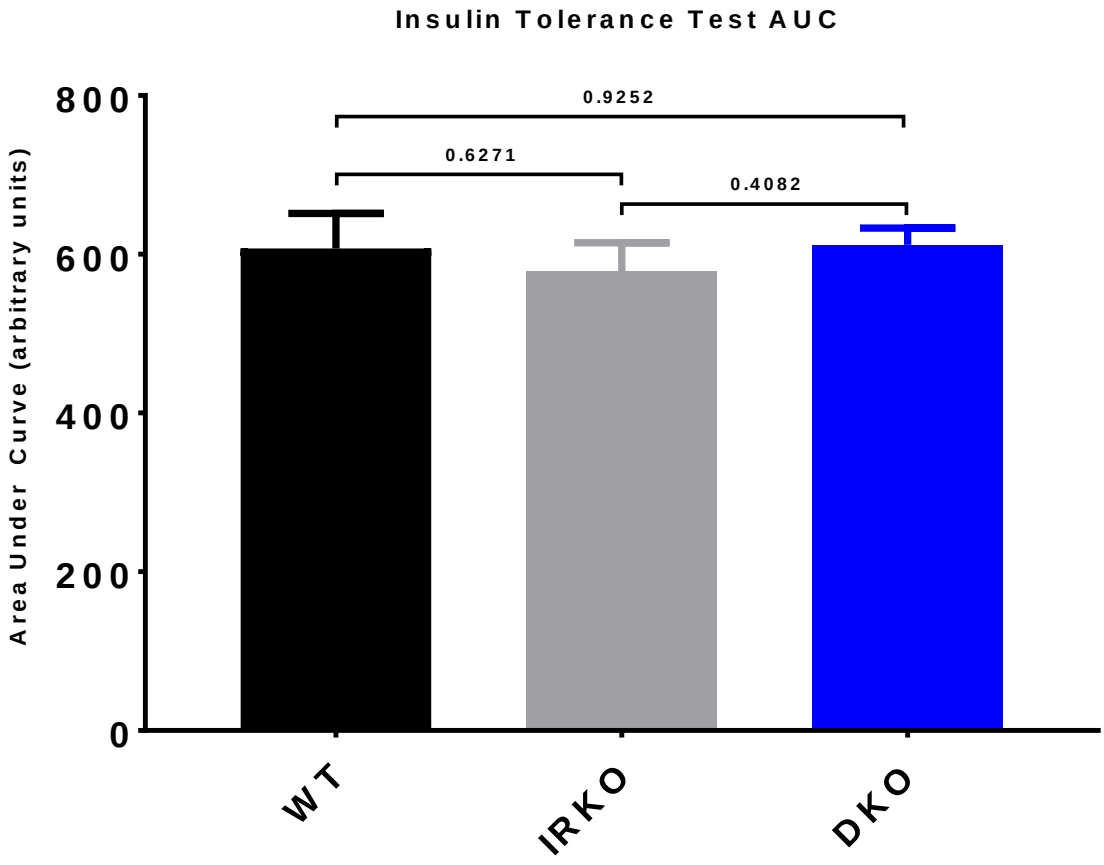

Figure 5.10: Insulin Tolerance Test Area Under the Curve
N=12 (WT), 10 (IRKO), 13 (DKO).

5.3 Vascular Injury

Deficient vascular repair has been observed in IRKO animals compared with WT littermates [80]. We hypothesised that DKO animals would have augmented vascular repair, given their more favourable vascular phenotype [123] (see section 1.3.8). In keeping with previous data, the proportion of recovered endothelium was lower in IRKO compared with WT (0.46 [0.02] Vs 0.60 [0.04], p=0.0081). DKO had a significantly greater proportion of recovered endothelium compared with IRKO (0.55 [0.04] Vs 0.46 [0.02] p=0.047), and did not differ significantly from WT.

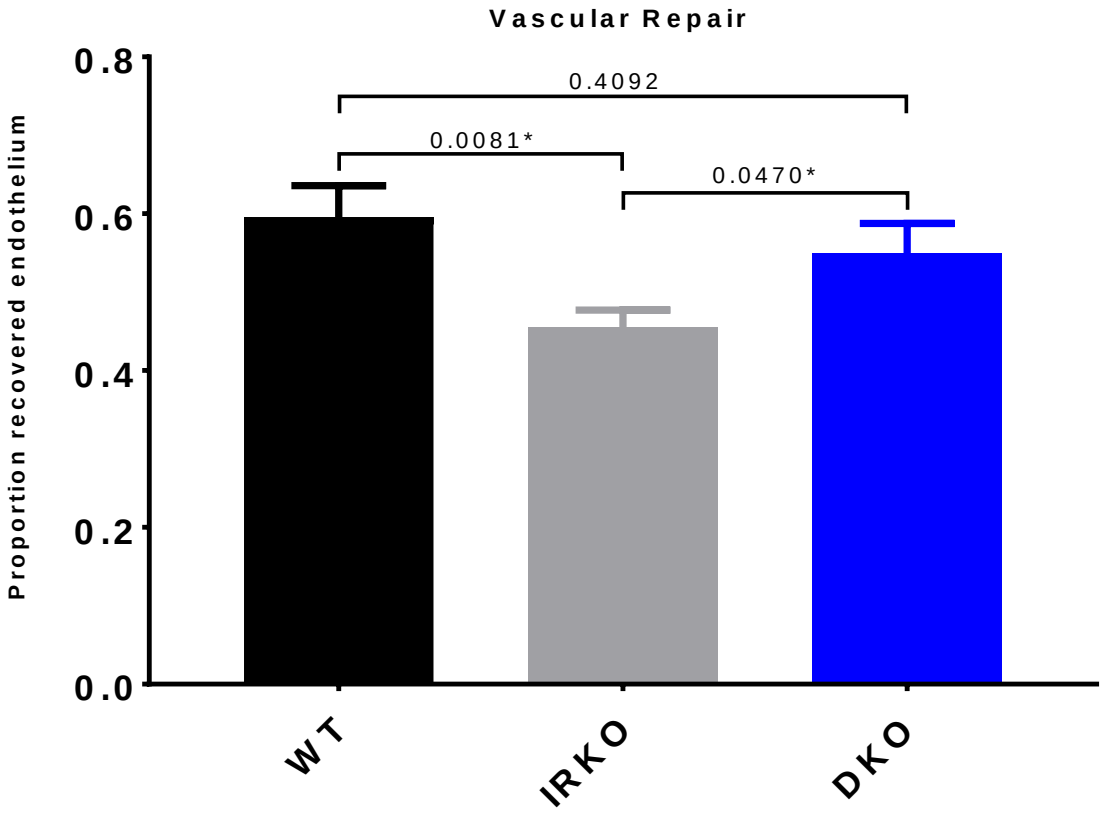

Figure 5.11: Vascular Repair

The proportion of recovered endothelium was recorded 4 days following denuding femoral artery wire injury (see figure 5.12). N=10 (WT), 8 (IRKO), 14 (DKO)

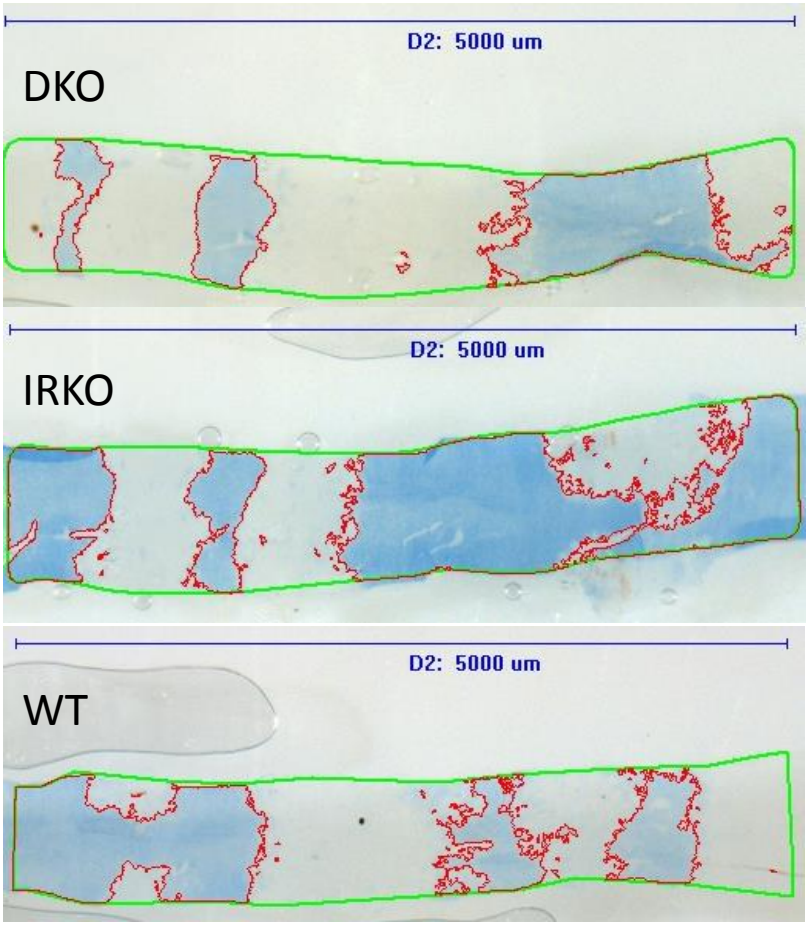

Figure 5.12: Vascular Repair Images

Representative images of femoral arteries 4 days following denuding wire injury photographed at 20x magnification. Evans blue dye highlights subendothelial structures (blue), i.e. areas not yet re-endothelialised.

5.4 Vascular Regeneration

Previous work from our department has indicated that IRKO mice have impaired recovery following induction of hind-limb ischaemia (HLI) [247]. Given the effect of reduced IGF-1R expression on vascular repair, we investigated whether vascular regeneration could be augmented in similar fashion. In keeping with the vascular repair data, DKO animals displayed a significantly greater recovery of perfusion on laser Doppler imaging at 21 days following surgery compared with IRKO (ischaemic/non-ischaemic limb perfusion ratio 0.75 [0.06] Vs 0.40 [0.03], $p<0.0001$). Remarkably, DKO animals also had superior recovery to WT

animals at the same time point (ischaemic/non-ischaemic limb perfusion ratio 0.75 [0.06] Vs 0.55 [0.04], p=0.0097). These data are displayed graphically across the time course of the experiment (figure 5.13) and at day 21 following induction of HLI (figure 5.14).

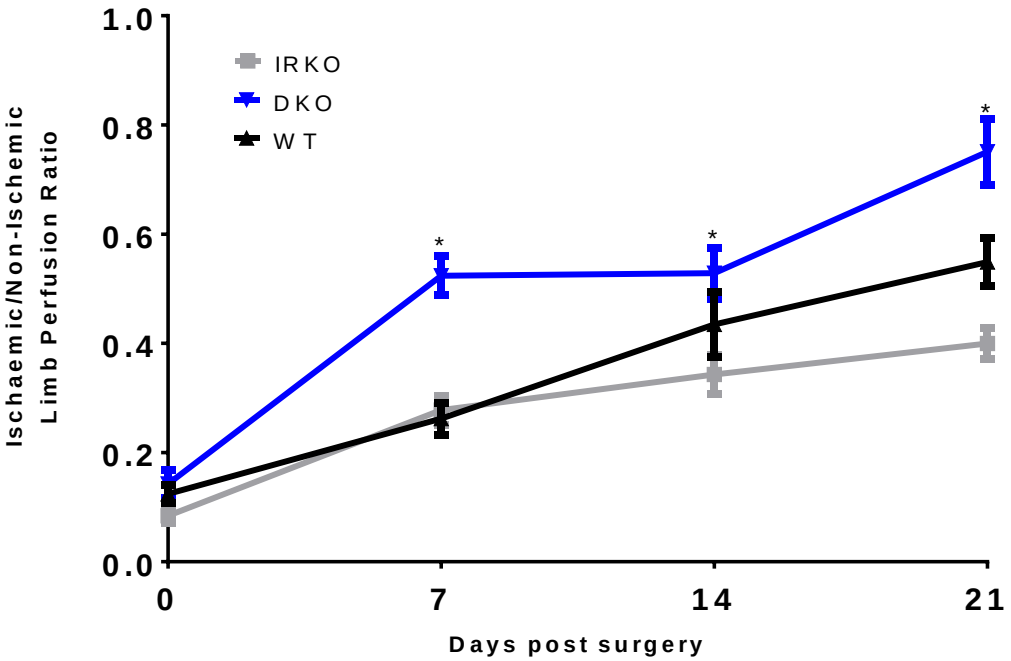

Figure 5.13: Hind-limb Ischaemia IRKO Vs DKO

Laser Doppler flux assessment was performed immediately after left femoral artery ligation and excision and weekly thereafter. Results were compared with those from the sham-operated right leg and are displayed as a ratio of ischaemic (left)/ non-ischaemic (right) limb perfusion. N=19 (IRKO), 12 (DKO), 18 (WT). * denotes statistical significance (P<0.05) for difference between IRKO and DKO. WT data provided for reference.

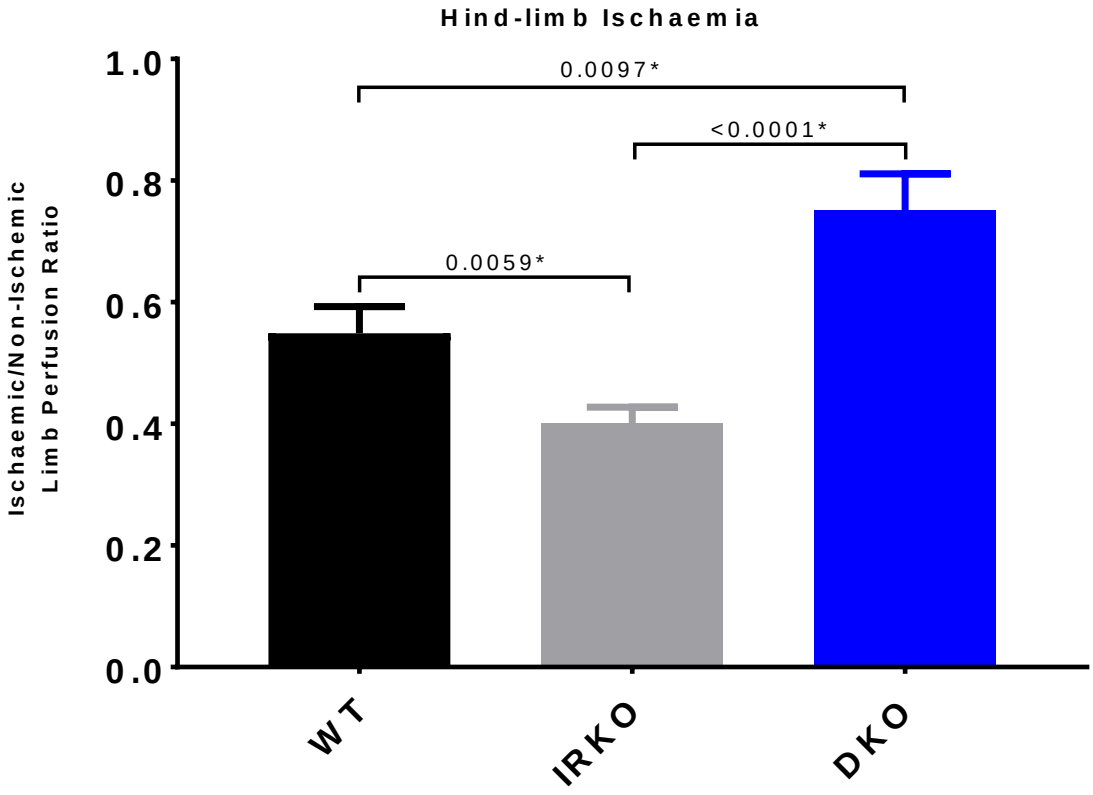

Figure 5.14: Hind-limb Ischaemia at Day 21

Laser Doppler flux results at day 21 for each group. N= 18 (WT), 19 (IRKO), 12 (DKO)

5.5 *In Vitro* Assays

Having established that DKO animals exhibit a favourable phenotype of vascular repair and regeneration, we next sought to examine some of the possible mechanisms for these observations. In the first instance, we investigated the potential role of progenitor cells. Previous work from our department has indicated that reduced numbers of blood-derived myeloid angiogenic cells (MACs) and circulating progenitor cells (CPCs) in IRKO may be responsible for the deficient vascular repair exhibited by these animals [80]. As such, we sought to quantify these cells in the present colony.

5.5.1 Enumeration of Murine Circulating Progenitor Cells

Blood samples were collected from mice, then processed as described in section 4.6. There were no significant differences in the number of $Sca1^+/Flk1^+$ or c-kit^+ cells across the different genotypes studied. For $Sca1^+/Flk1^+$ cells: WT mean events per 100,000 cells 141.7 (13.1) Vs IRKO 141.2 (11.7) p=0.9788; IRKO 141.2 (11.7) Vs DKO 154.9 (14.2) p=0.4684; WT 141.7 (13.1) Vs DKO 154.9 (14.2) p=0.5046. For c-kit^+ cells: WT mean events per 100,000 cells 200.5 (22.0) Vs IRKO 279.6 (71.4) p=0.2548; IRKO 279.6 (71.4) Vs DKO 193.6 (25.7) p=0.2299; WT 200.5 (22.0) Vs DKO 193.6 (25.7) p=0.8420.

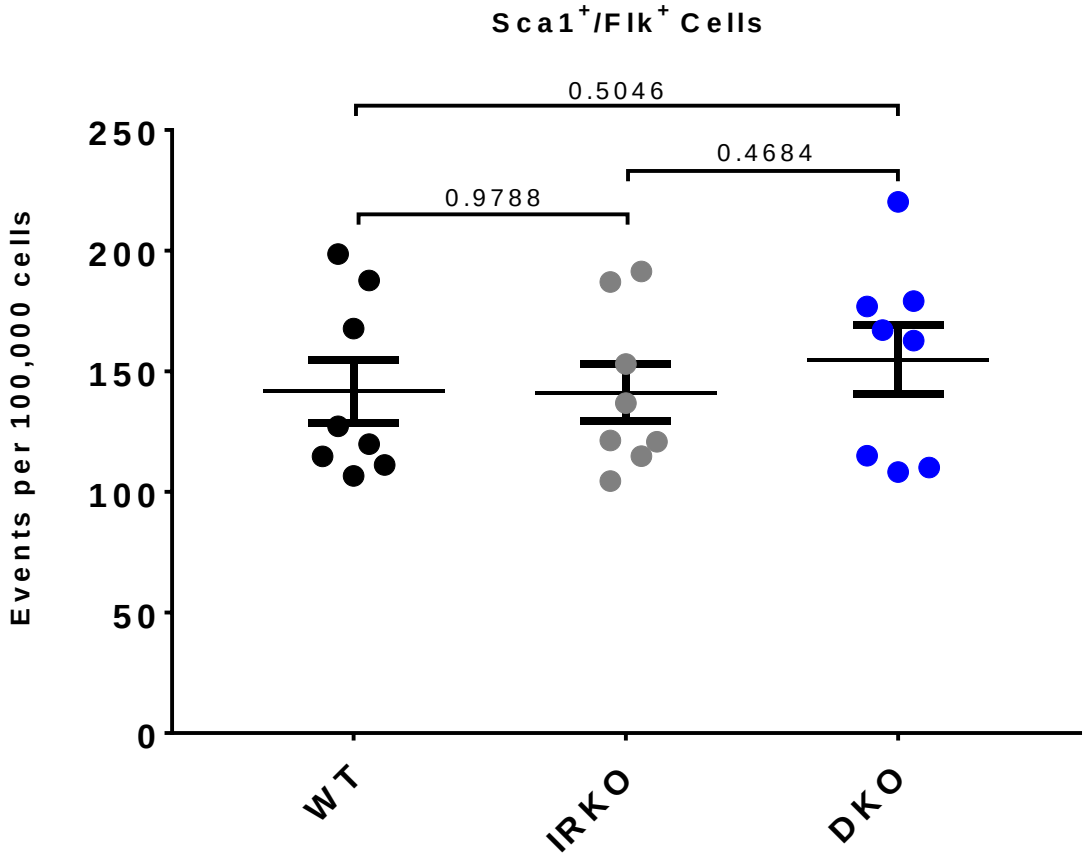

Figure 5.15: $Sca1^+/Flk1^+$ Cells

Events per 100,000 cells recorded for cells expressing stem cell antigen-1 (Sca1) and foetal liver kinase (Flk) 1. N=8 for all genotypes

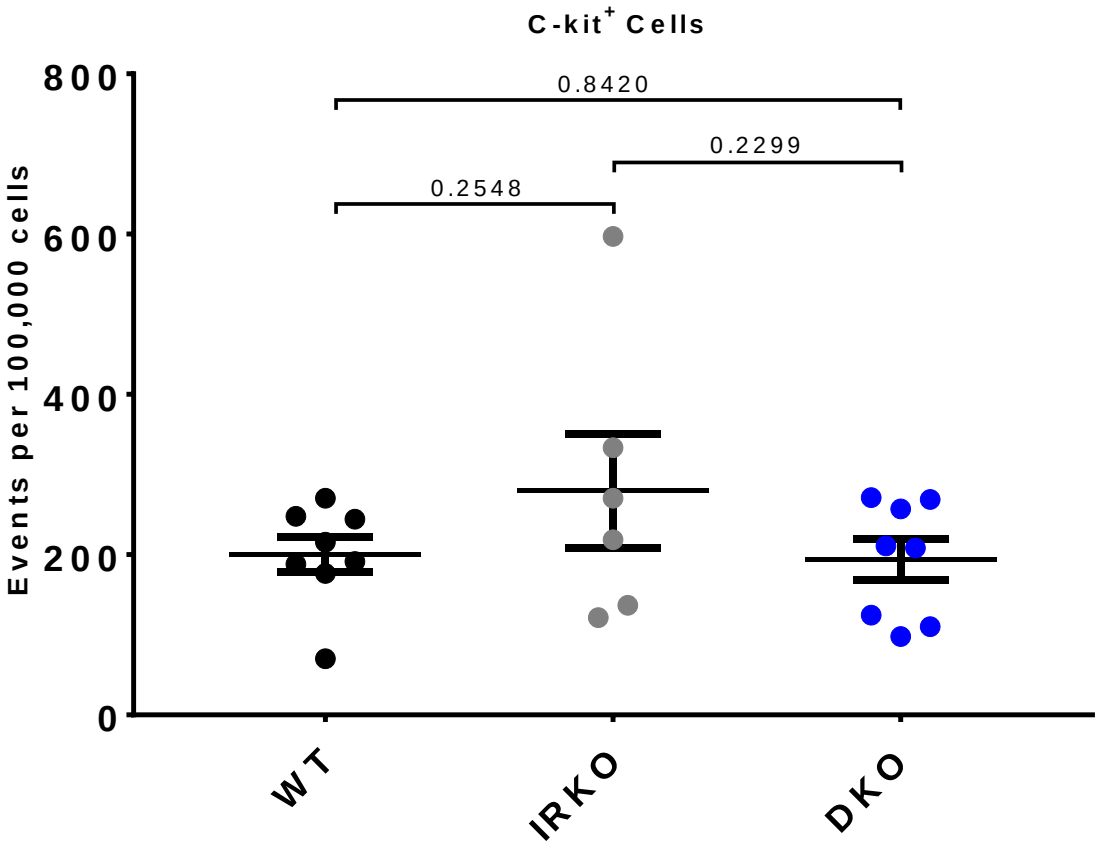

Figure 5.16: C-kit⁺ Cells

Events per 100,000 cells recorded for cells expressing C-kit. N=8 (WT), 6 (IRKO), 8 (DKO)

5.5.2 Murine Myeloid Angiogenic Cell Culture

Mononuclear cells were isolated from blood, spleen and bone marrow, as described in section 4.7. There were no significant differences between genotypes in the number of MACs cultured after 7 days in samples from blood and spleen. There were significantly more MACs cultured from the bone marrow of DKO animals than from IRKO (29.9 [6.5] Vs 12.9 [1.6], p=0.0235), although the number of cells cultured did not differ between IRKO and WT (12.9 [1.6] Vs 16.9 [5.9] p=0.5207) or DKO and WT (29.9 [6.5] Vs 16.9 [5.9], p=0.1596).

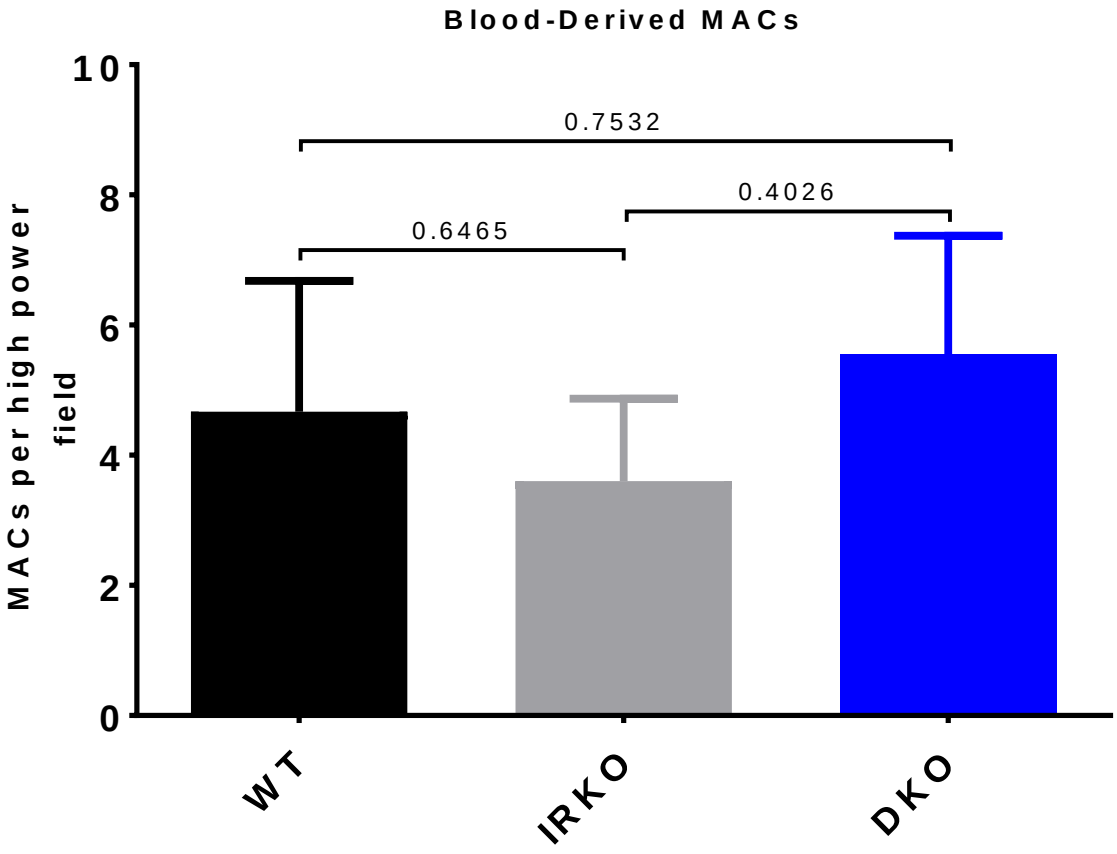

Figure 5.17: Blood-Derived MACs

Murine peripheral blood monocytes were cultured in vitro. Cells staining positive for DiI-ac-LDL and FITC-labelled BS1 Lectin (Myeloid Angiogenic Cells) were counted at 7 days. N= 6 (WT), 8 (IRKO), 9 (DKO)

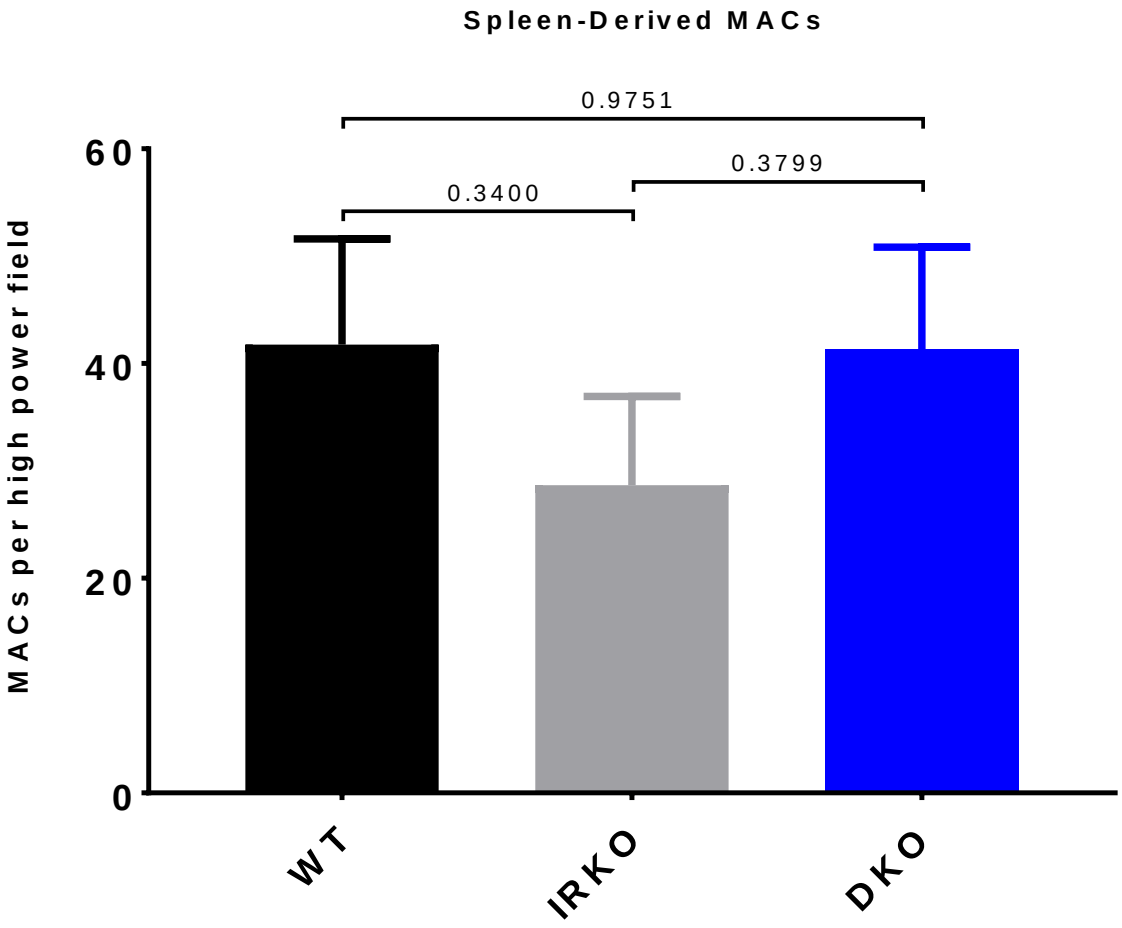

Figure 5.18: Spleen-Derived MACs

Murine spleen-derived monocytes were cultured in vitro. Cells staining positive for DiI-ac-LDL and FITC-labelled BS1 Lectin (Myeloid Angiogenic Cells) were counted at 7 days. N= 7 (WT), 6 (IRKO), 10 (DKO)

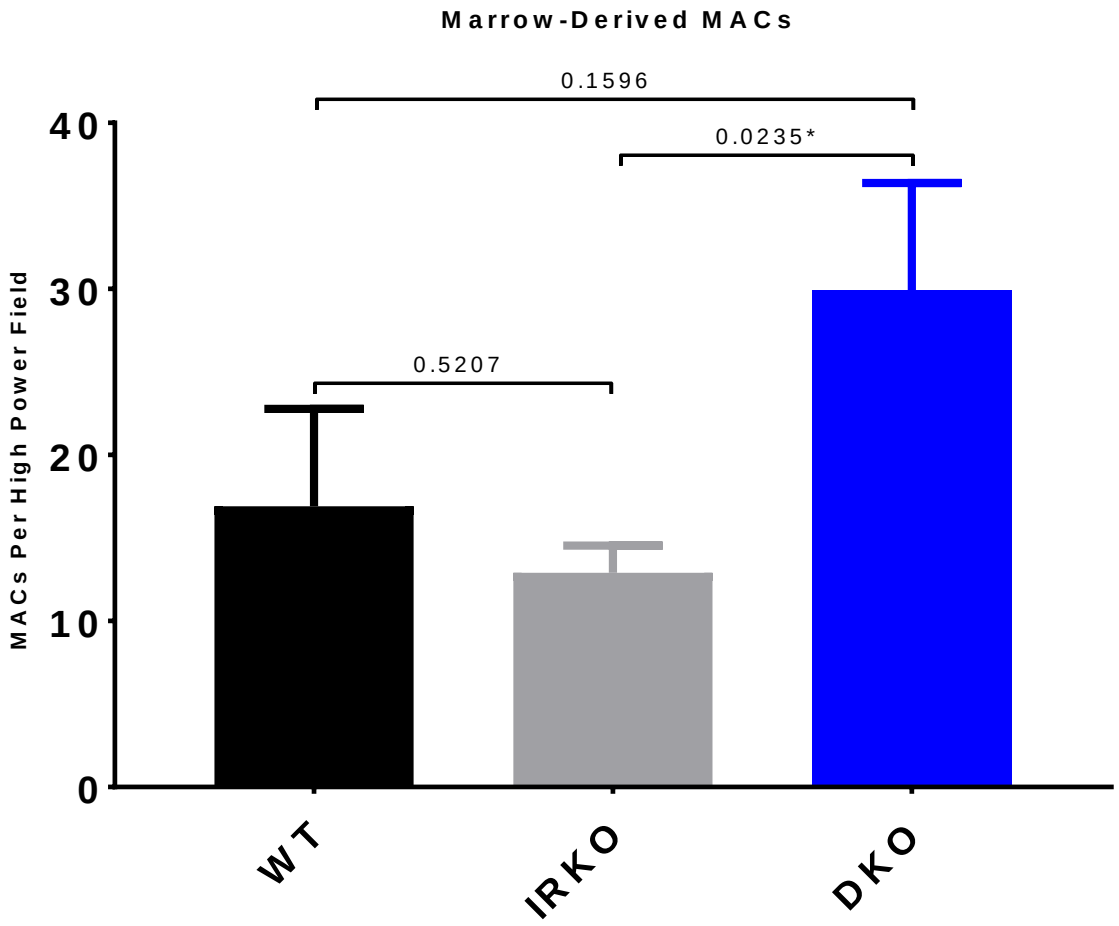

Figure 5.19: Bone Marrow-Derived MACs

Murine bone marrow-derived monocytes were cultured in vitro. Cells staining positive for DiI-ac-LDL and FITC-labelled BS1 Lectin (Myeloid Angiogenic Cells) were counted at 7 days. N= 8 for all genotypes.

5.5.3 Quantification of Leukocyte Populations

Given the observed differences between the number of MACs grown from bone marrow-derived mononuclear cells in DKO compared with IRKO, we decided to examine the populations of leukocytes in the blood and marrow in further detail using flow cytometry (see section 4.8).

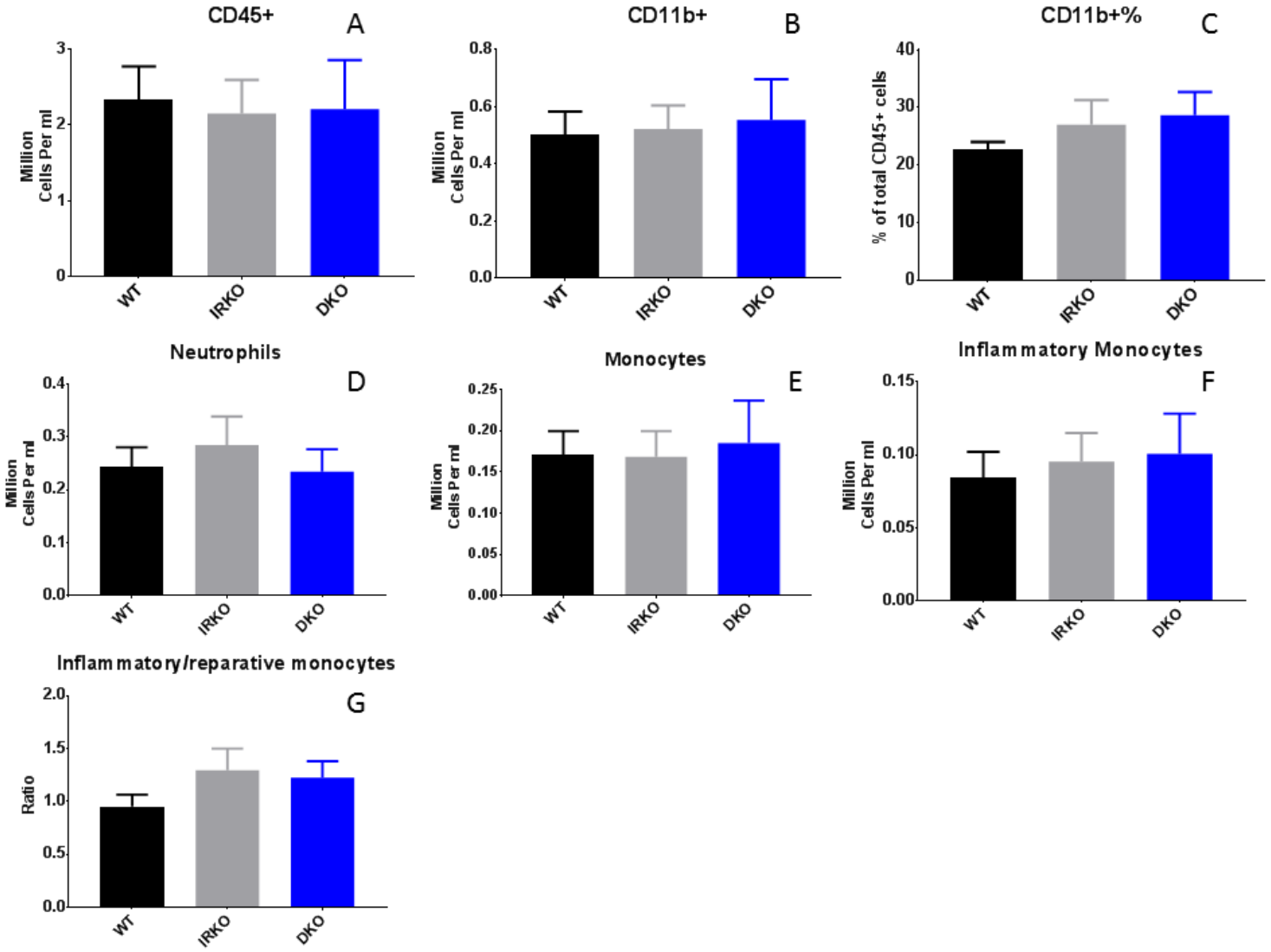

Figure 5.20: Blood Leukocyte Quantification

Murine blood leukocyte subsets were quantified using flow cytometry (see section 4.8). N= 7 (WT), 6 (IRKO, 6 (DKO). P values listed where P<0.1, * denotes statistical significance (P<0.05)

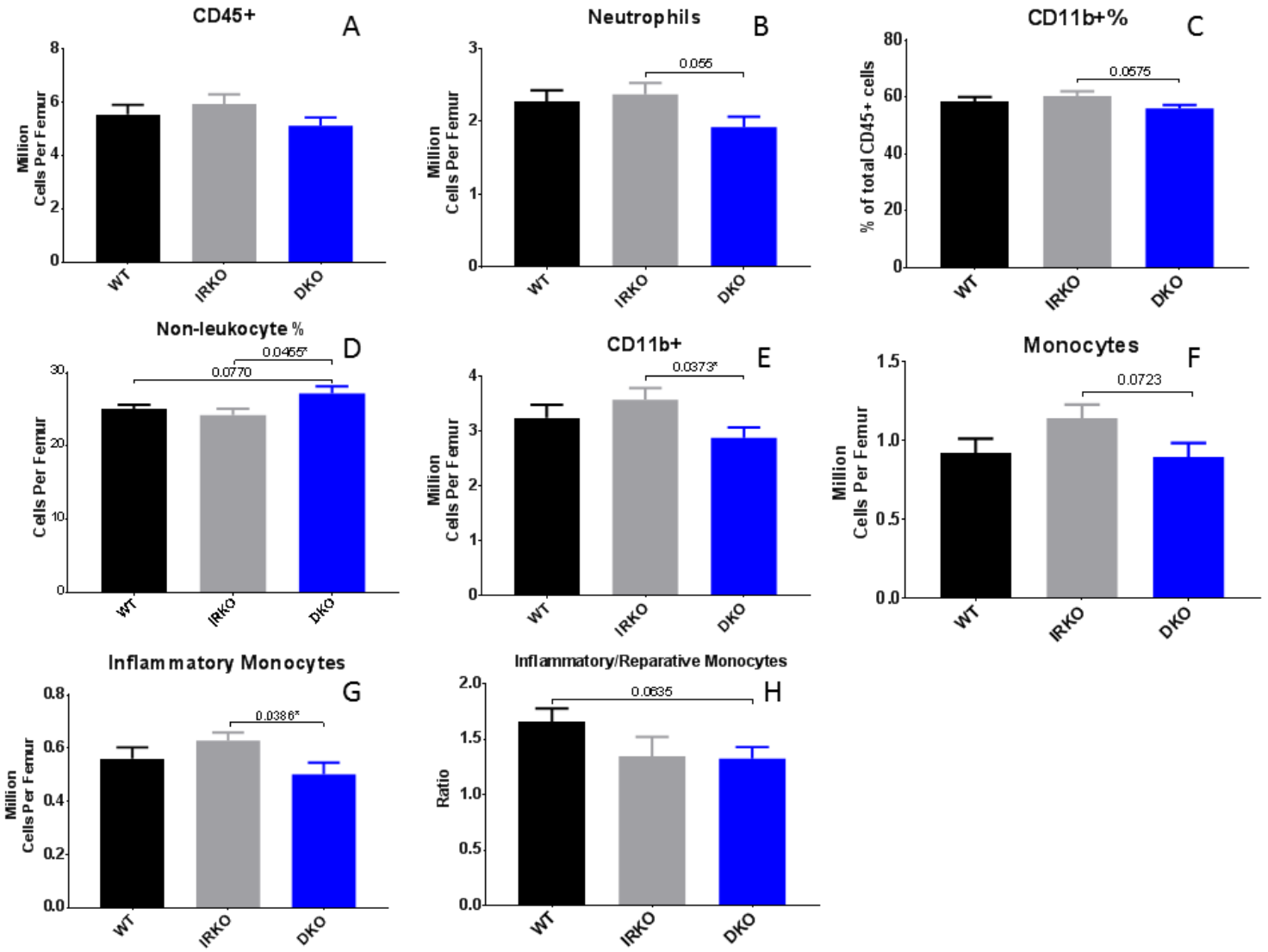

Figure 5.21: Marrow Leukocyte Quantification

Murine marrow leukocyte subsets were quantified using flow cytometry (see section 4.8). N= 7 (WT), 6 (IRKO), 6 (DKO). P values listed where P<0.1, * denotes statistical significance (P<0.05)

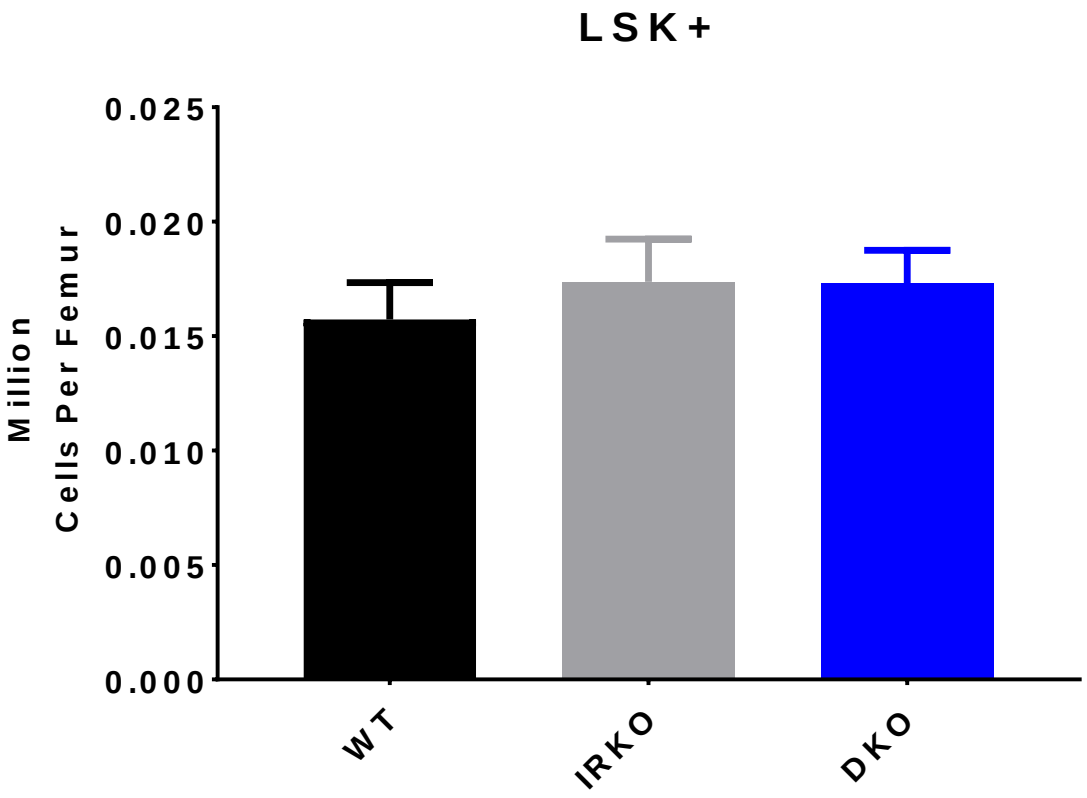

Figure 5.22: Bone Marrow Lin(-)Sca-1(+)c-Kit(+) (LSK) Cell Quantification

Lineage-negative bone marrow leukocytes expressing Sca-1 and C-Kit (LSK) cells were quantified using flow cytometry (see section 4.8) N= 7 (WT), 6 (IRKO), 6 (DKO). P values listed where P<0.1

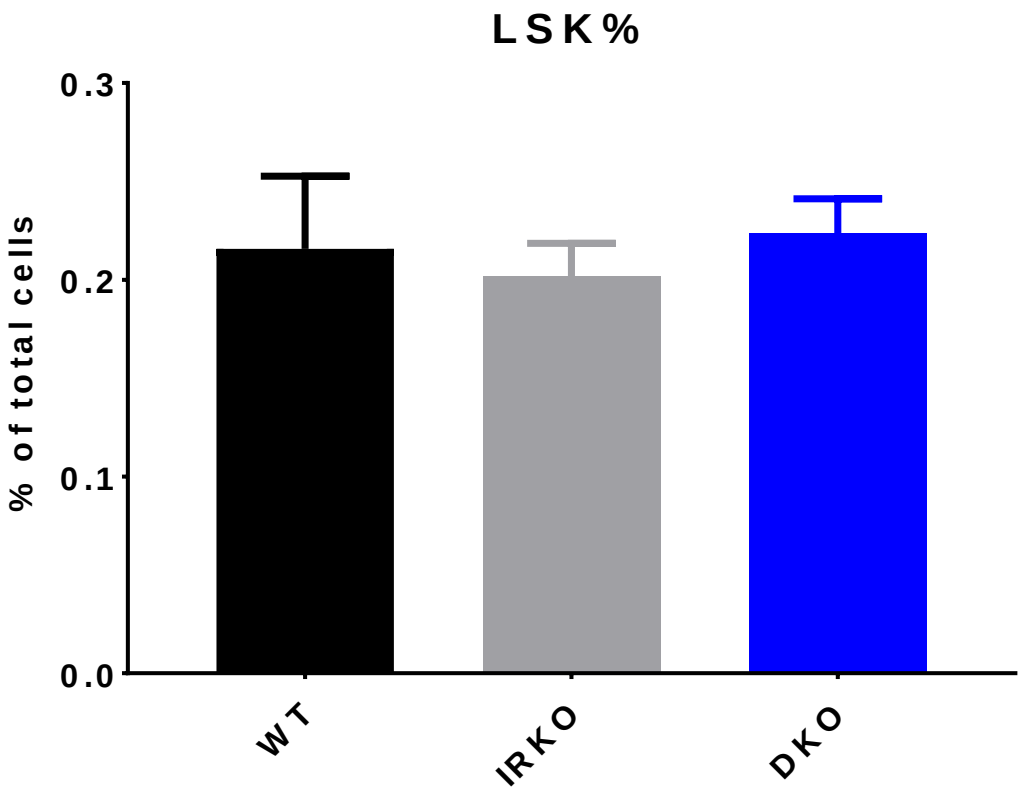

Figure 5.23: Bone Marrow Lin(-)Sca-1(+)c-Kit(+) (LSK) Cell Proportion
N= 7 (WT), 6 (IRKO), 6 (DKO). P values listed where P<0.1

There were no significant differences between genotypes in the numbers of cells from any of the leukocyte populations studied in blood samples (Figure 5.20). The bone marrow samples yielded some interesting findings (Figure 5.21), with panel B showing a trend towards fewer neutrophils in DKO compared with IRKO (1.9 [0.14] Vs 22.4 [0.15], p= 0.055), significantly fewer CD11b+ cells in DKO than IRKO (panel E) (2.87 [0.19] Vs 3.57 [0.22], p=0.0373) and a trend towards a lower proportion of CD11b+ cells percentage of total CD45+ cells (panel C) (DKO 56.2% [1.17%] Vs IRKO 60.5% [1.65%], p=0.0575). Interestingly there was a significant increase in the proportion of non-leukocyte cells (panel D) in the DKO marrow compared with IRKO (27.2% [0.97%] Vs 24.2% [0.87%] p=0.0455), with a trend towards a similar increase compared with WT (DKO

27.2% [0.97%] Vs WT 25.0% [0.61%] p=0.0770). There was a further trend towards DKO having fewer monocytes (panel F) than IRKO (0.90 [0.09] Vs 1.14 [0.09], p= 0.0723). Intriguingly DKO had significantly fewer (panel G) inflammatory monocytes (i.e. Ly-6C^{high}) than IRKO (0.50 [0.04] Vs 0.63 [0.03], p=0.0386), with a trend towards (panel H) a lower ratio of inflammatory to reparative monocytes in DKO compared with IRKO (1.33 [0.10] Vs 1.66 [0.12], p=0.0635). Mirroring the earlier findings from blood CPC enumeration (section 5.5.1), there were no significant differences in the number (Figure 5.22) or proportion (Figure 5.23) of Lin(-) Sca-1(+) c-Kit(+) (LSK) cells in the bone marrow samples. It should be noted that this dataset is incomplete and further work is ongoing to complete this experiment. As such, these data only represent preliminary results.

5.5.4 Studies with Murine Pulmonary Endothelial Cells

Our findings detailed in sections 5.3 and 5.4, demonstrating superior recovery following vascular injury and induction of hind-limb ischaemia in DKO animals compared with IRKO, led us to explore whether differences in endothelial cell phenotype might help explain some of these observed differences in vascular repair and regeneration.

5.5.4.1 Scratch Wound Closure

A fundamental property of endothelial cells is the ability to migrate and proliferate to cover an area denuded of endothelium, as seen in the femoral artery wire injury model (see section 5.3). *In vivo* multiple factors may contribute to vascular repair other than endothelial cells alone, including the influence of progenitor

cells [80]. As such, we wanted to investigate the specific role of the endothelium in this process and therefore undertook a scratch wound assay (see section 4.9.1) to examine the properties of migration and proliferation *in vitro* with PECs.

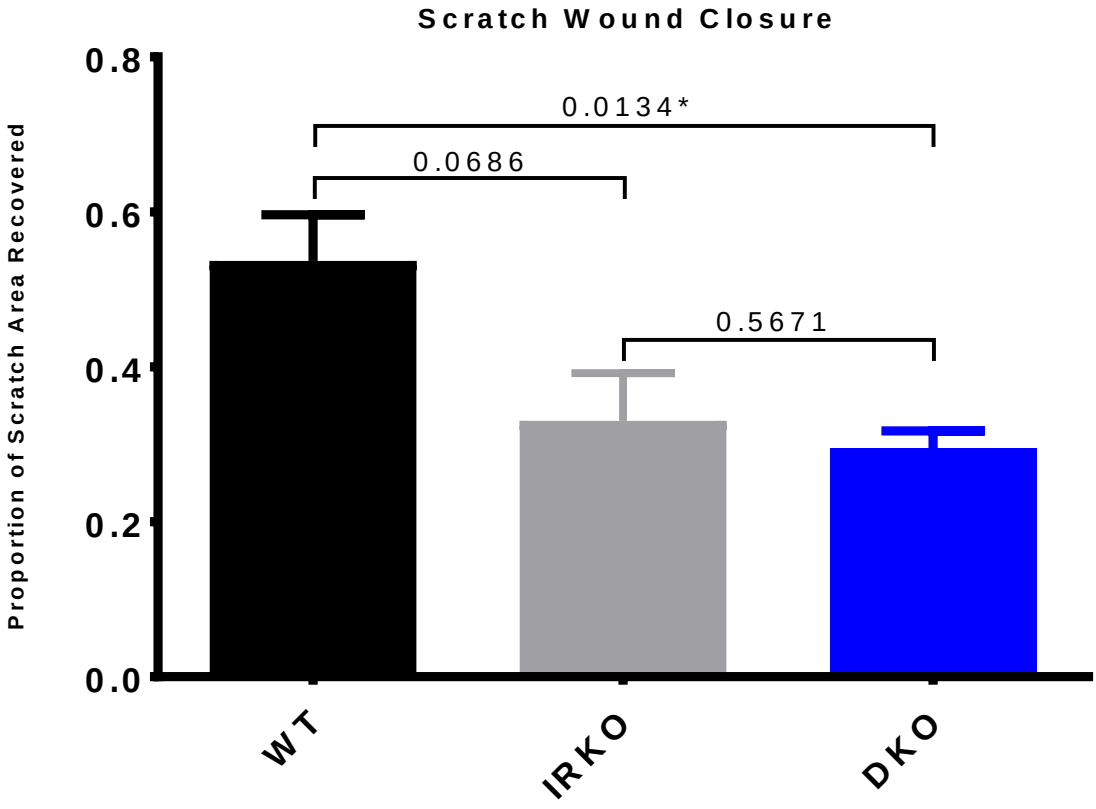

Figure 5.24: Scratch Wound Closure

Confluent pulmonary endothelial cells were scratched with a Woundmaker then incubated for 18hrs with 2% serum media. Images taken at 18hrs were compared with those from time zero and a proportion of scratch area recovered was calculated (see section 4.9.1). N= 6(WT), 3(IRKO), 4(DKO)

Scratch wound closure was significantly delayed in DKO PECs compared with WT (proportion recovered DKO 0.30 [0.02] Vs WT 0.54 [0.06], p=0.0134), with a trend towards a similar impairment in IRKO vs WT (0.33 [0.06] Vs 0.54 [0.06], p=0.0686).

5.5.4.2 Angiogenic Bead Assay

We developed an assay based on a sprouting angiogenesis experiment first described by Nakatsu *et al* [243] to investigate whether differences in endothelial sprouting might contribute to the previously noted positive vascular reparative phenotype in DKO animals. We used murine pulmonary endothelial cells (PECs) to coat Cytodex-3® beads, then suspended them in a fibrin matrix covered with media containing growth factors such as VEGF (see section 4.9.2). Sprouting was assessed 24 hours following fibrin clot formation. Sprout length was significantly shorter in PECs from IRKO animals compared to WT (82.7µm [5.0] Vs 102.5µm [23], p=0.0086) (Figure 5.24). This difference was abrogated in the DKO samples (DKO 110.6µm [5.4] Vs WT 82.7µm [5.0], p=0.3159), with DKO cells having significantly longer sprouts than IRKO (DKO 110.6µm [5.4] Vs 82.7µm [5.0], P= 0.0014).

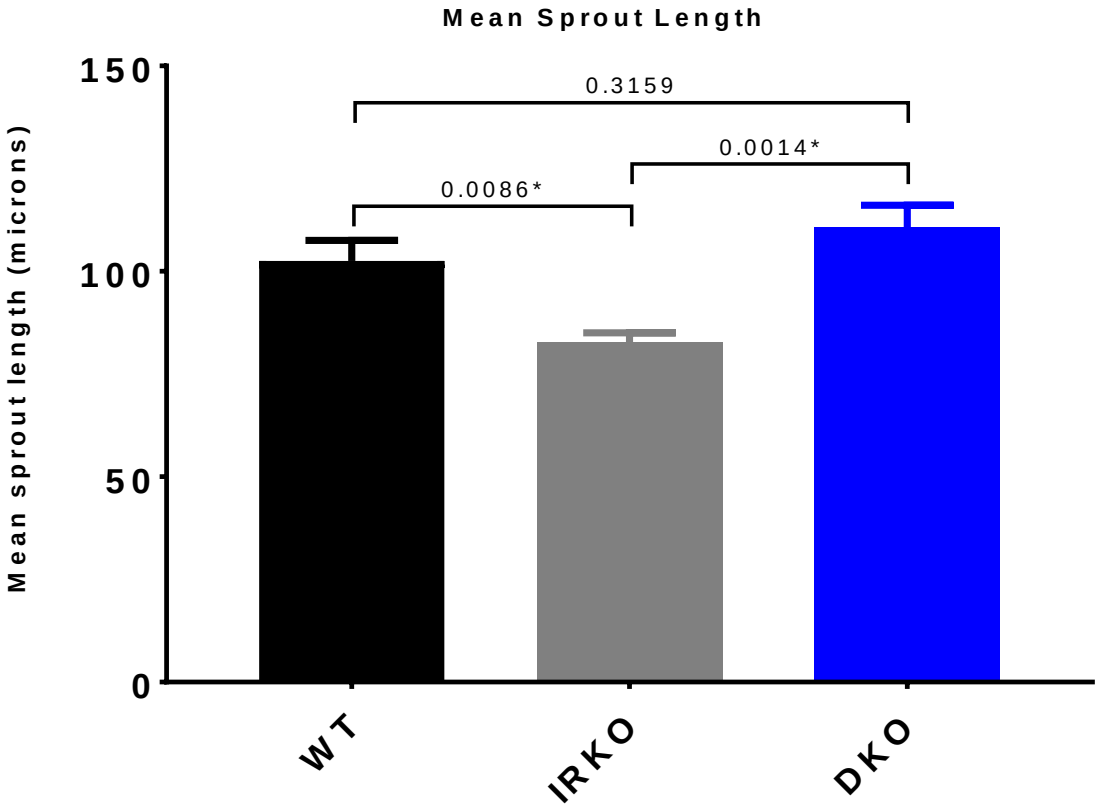

Figure 5.25: Mean Sprout Length

The length of every sprout on a minimum of 25 beads per mouse was measured using ImageJ software 24 hours after fibrin matrix formation (see section 4.9.2). N= 6 (WT), 5 (IRKO), 4 (DKO) mice per group.

No significant difference was noted in the mean number of sprouts per bead in samples from each genotype: IRKO 17.4 (3.6) Vs WT 15.1 (2.1), p=0.5826; DKO 21.5 (3.5) Vs WT 15.1 (2.1), p=0.1361; DKO Vs IRKO p=0.4589.

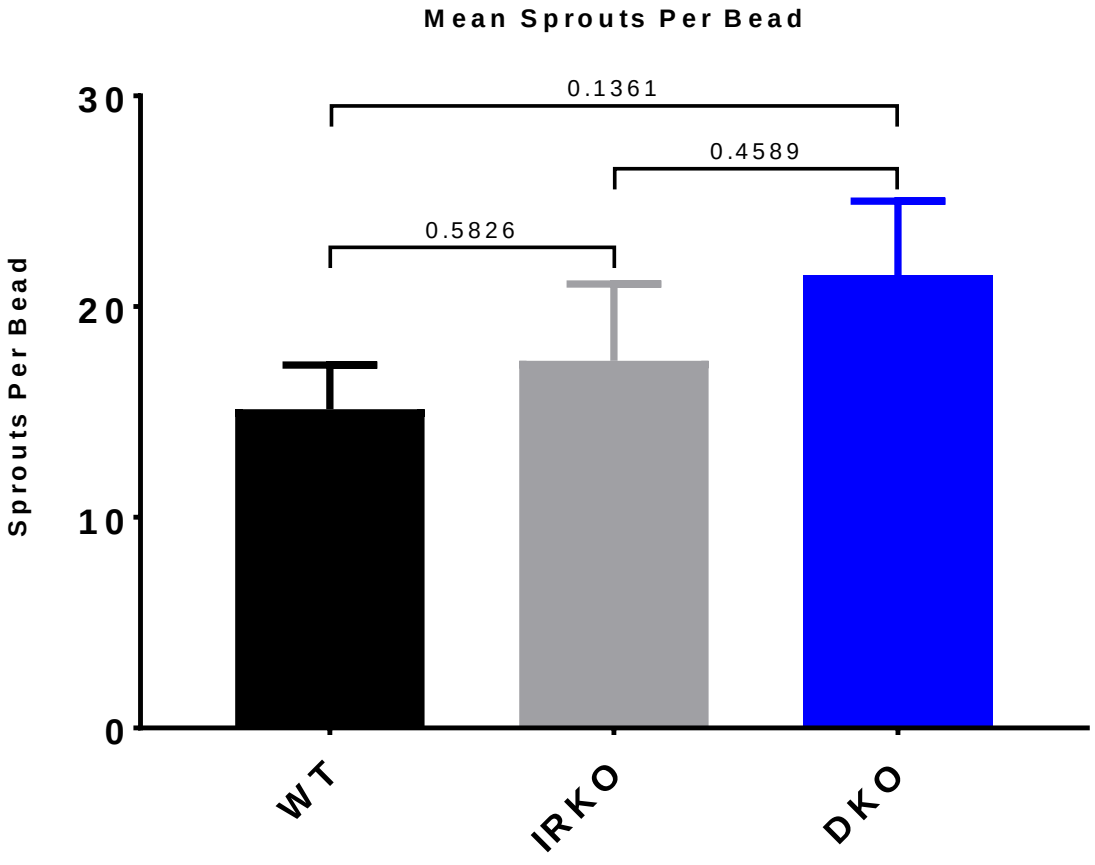

Figure 5.26: Mean Sprouts Per Bead

The number of sprouts per bead on a minimum of 25 beads per mouse was counted using ImageJ software 24 hours after fibrin matrix formation (see section 4.9.2). N= 6 (WT), 5 (IRKO), 4 (DKO) mice per group

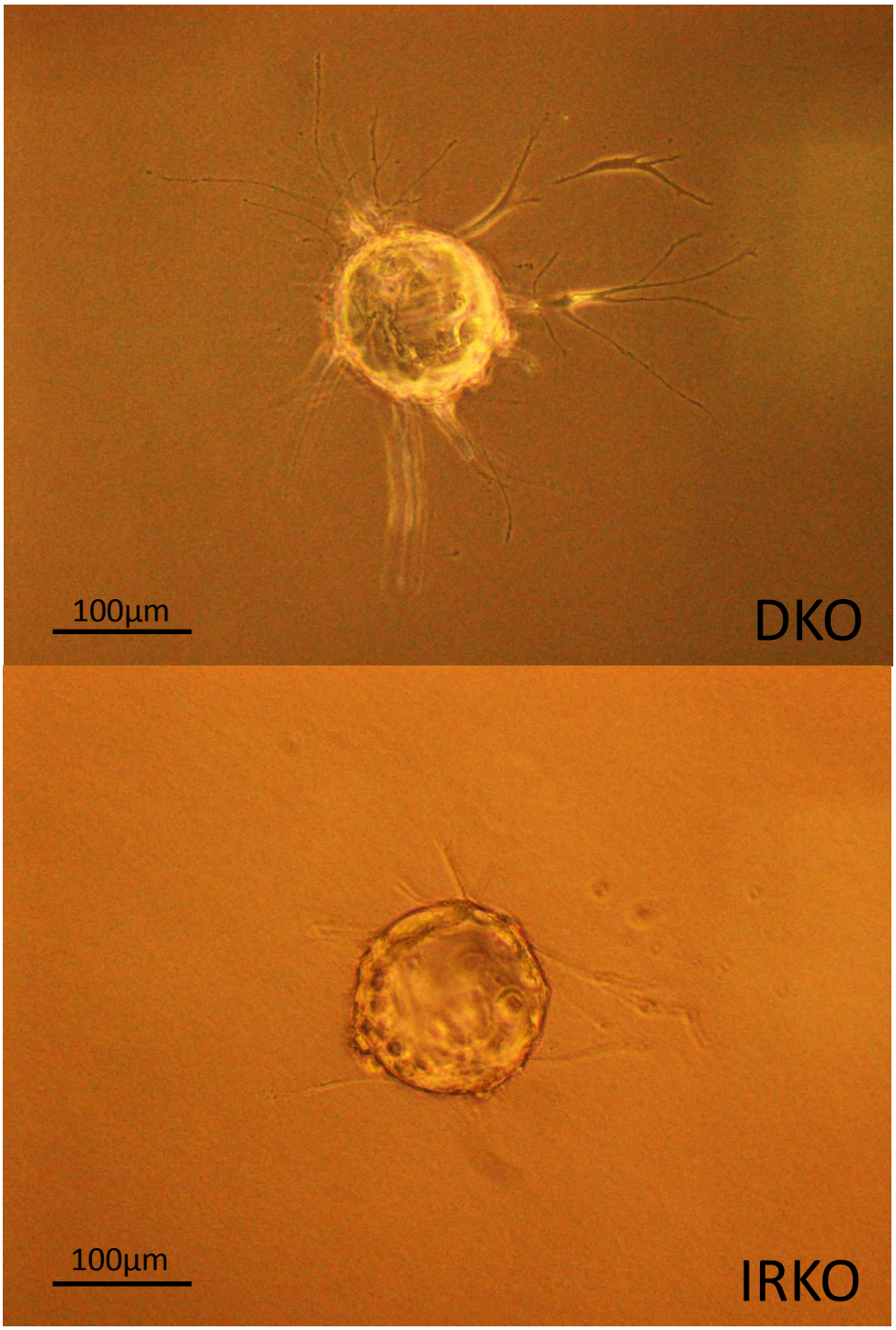

Figure 5.27: Representative Images of Angiogenic Beads

See section 4.9.2 for methodological details. Images taken at 100X magnification.

Chapter 6 **Results: Aging Studies**

It is well-established that globally reduced IGF-1R expression [224], and tissue-specific reduced IR expression [223] are associated with increased longevity in mice. Our group has previously documented a negative vascular phenotype in animals with global haploinsufficiency for the IR [80], with some of these differences abrogated in DKO ($IR^{+/-}$/$IGF\text{-}1R^{+/-}$) mice [123]. As such, we wanted to investigate the consequences of long-term reduction in IR and IGF-1R expression on mouse growth, glucose and insulin homeostasis, and healthspan.

6.1 Establishment of Aging Cohort

We decided to breed a cohort of mice from the IRKO-IGF1Rko colony for study throughout their healthspan. We selected 15 male animals born consecutively from each of the following genotypes: wild type (WT); insulin receptor haploinsufficient (IRKO); IGF-1R haploinsufficient (IGF1Rko); and dual IR and IGF-1R haploinsufficient (DKO). Mice were weaned and genotyped at age 3-4 weeks then housed with littermates under standard conditions (see section 4.1)

6.2 Metabolic Phenotyping

6.2.1 Body weight

Animals were weighted weekly from the age of 4 years until their death or healthspan endpoint (see section 4.10.3). Area under the curve calculated in early adulthood, between the age of 8 and13 weeks, showed a significant difference between groups with ANOVA analysis ($p<0.0001$) with both IRKO and DKO animals to be significantly lighter than WT (Figure 6.1) on t-testing, with

DKO being the lightest genotype overall. Data also shown as a growth plot (Figure 6.2).

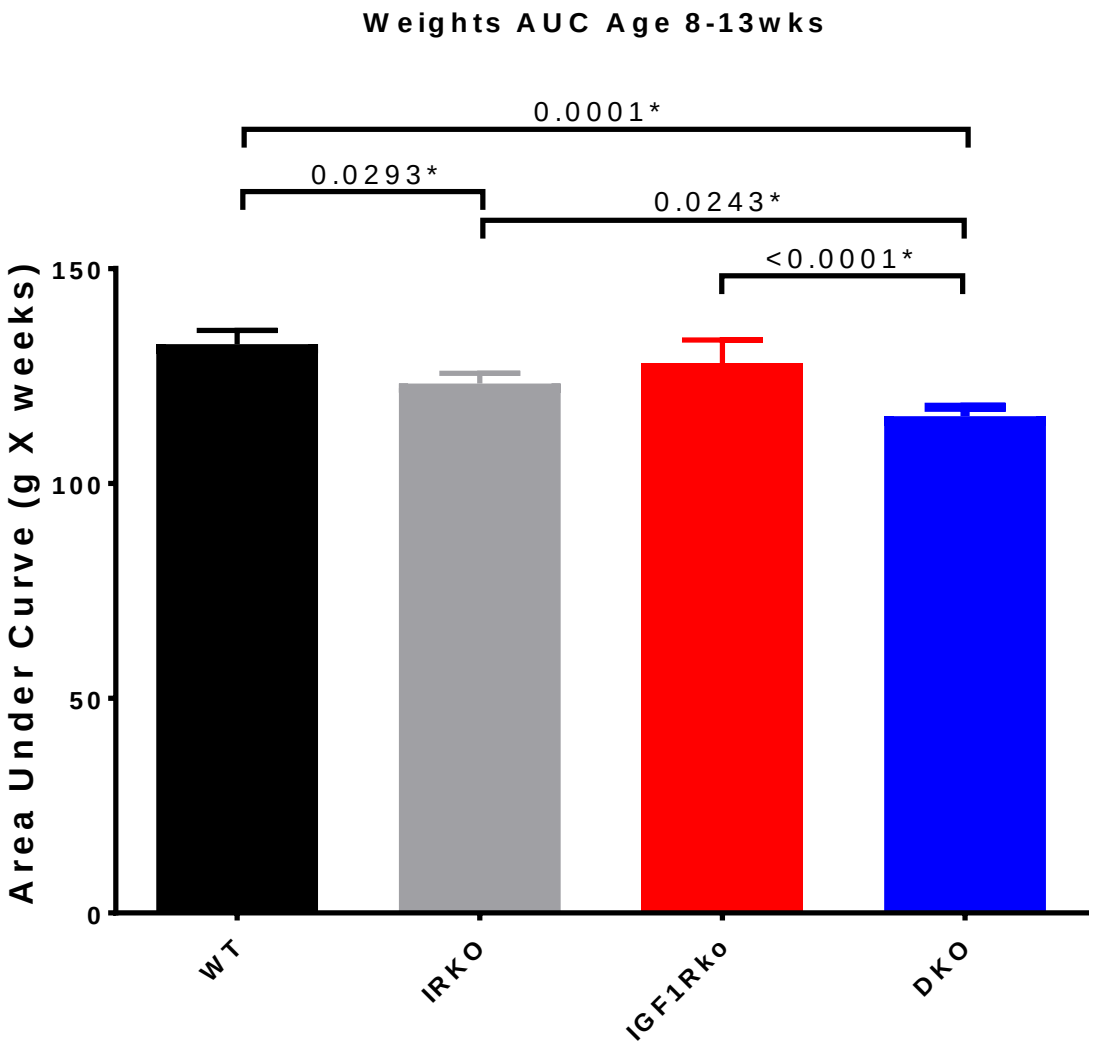

Figure 6.1: Body Weight Area under Curve at age 8-13 weeks

Mice were weighed weekly. N= 15 mice per group. P values <0.1 included on the figure, with significance (P<0.05) highlighted with an asterisk.

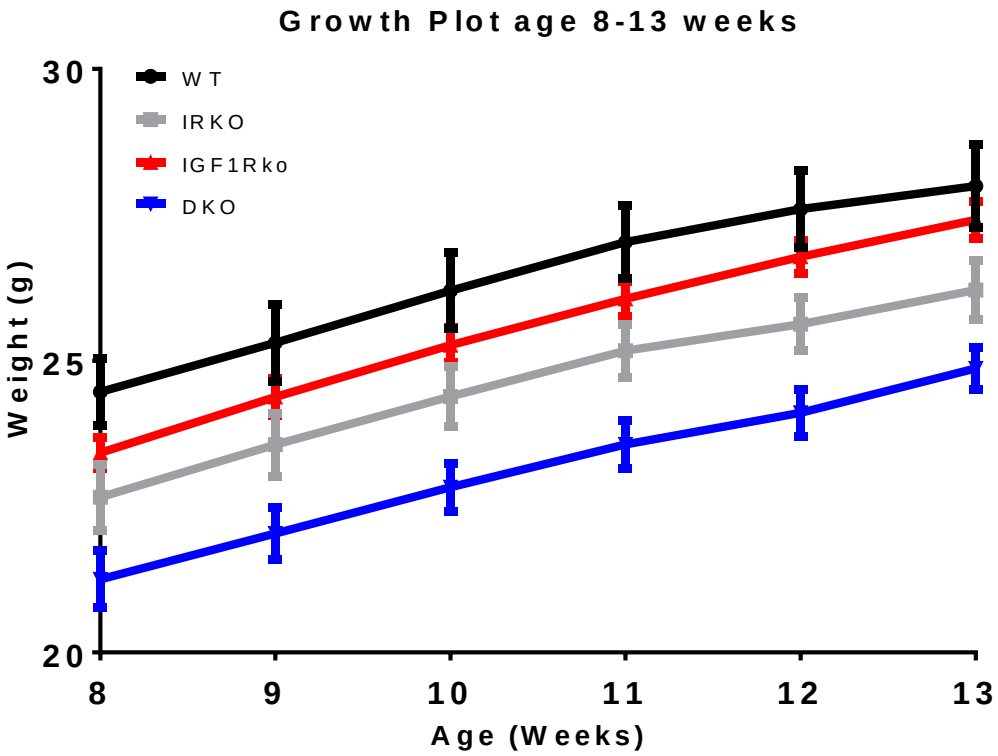

Figure 6.2: Growth Plot Age 8-13 weeks

N=15 mice per group.

Figure 6.3 shows data across the entire healthspan of the animals studied, correct as of 01/08/2017. At this time point there are 1 WT, 1 IGF1Rko, 4 IRKO and 3 DKO animals still alive.

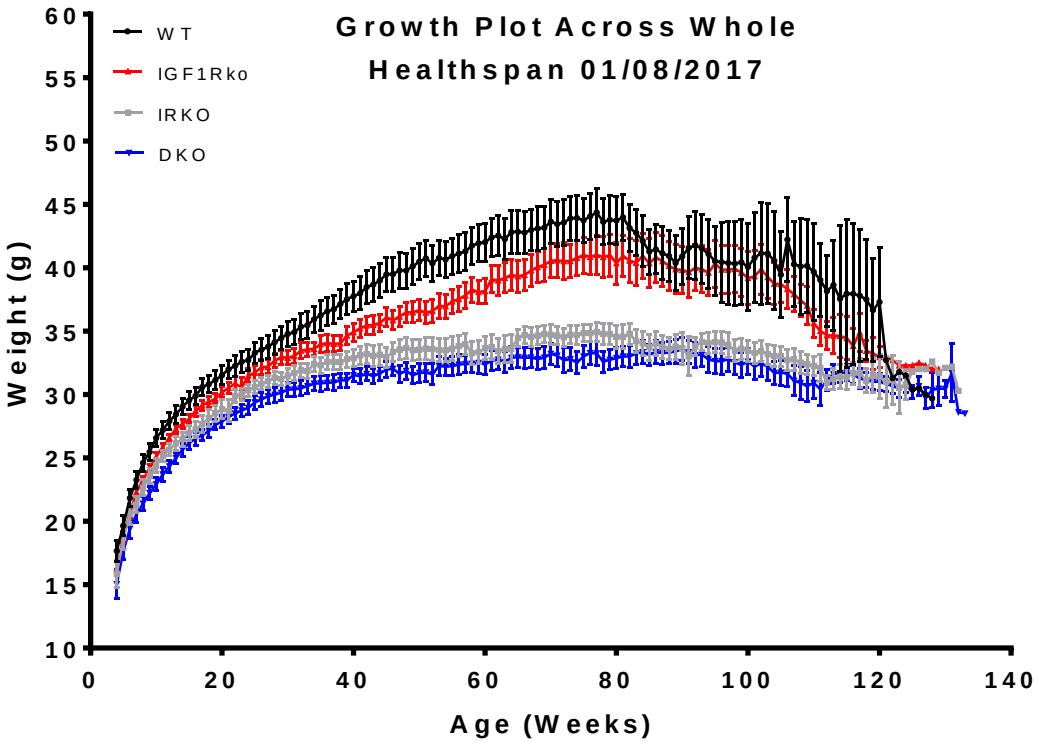

Figure 6.3: Growth Plot Across Whole Healthspan

N=15 mice per group

Weight appears to peak around 18 months of age in the IGF1Rko and WT groups, with subsequent falls in weight leading to animals meeting their healthspan endpoint (see section 4.10.3) and exiting the study. As such, area under the curve data up until 01/08/2017 are misleading as they include progressively fewer values as animals' healthspan ends. As such, figure 6.4 presents area under the curve data for animals to 72 weeks (i.e. 18 months) of age. At this time point only one mouse from each of the WT, IGF1Rko, and DKO groups had exited the study, with 2 having reached their healthspan endpoint in the IRKO group. As such, these data provide a reasonable assessment of peak body weight across genotypes.

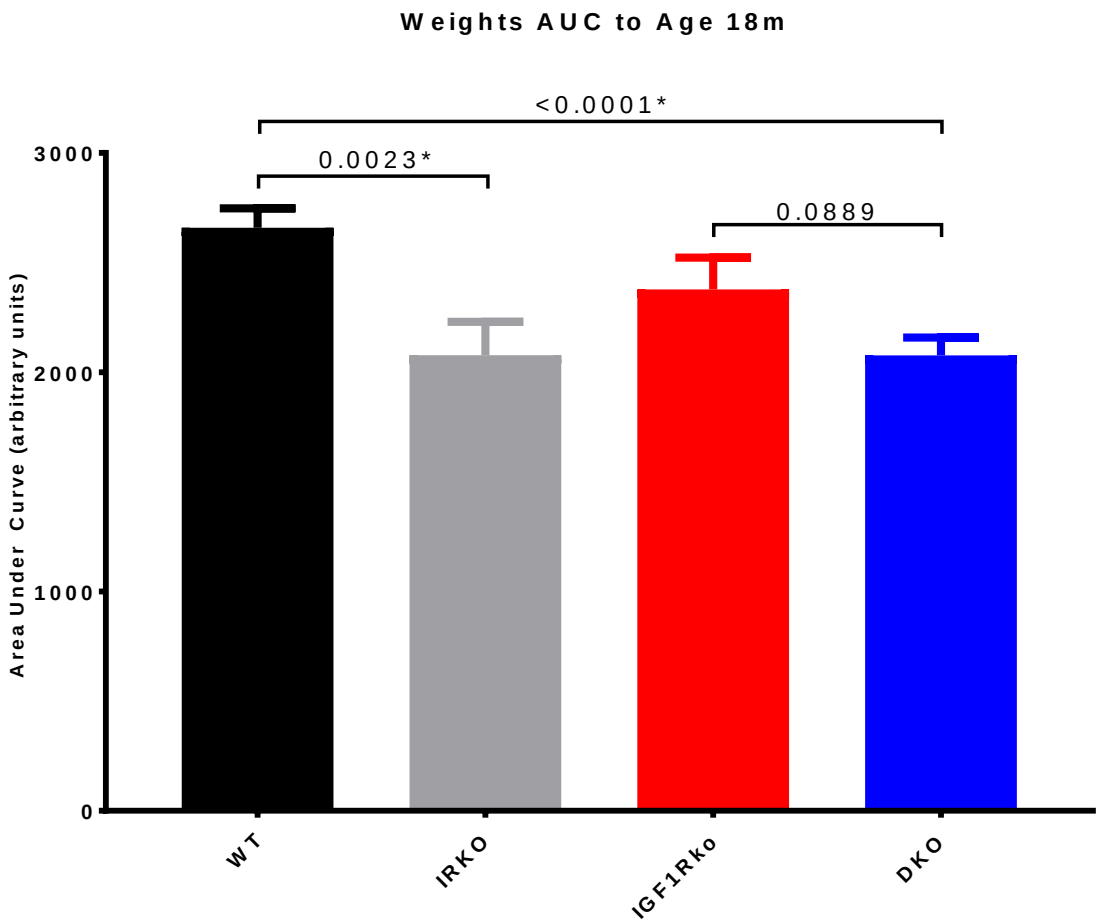

Figure 6.4: Body Weight Area Under the Curve to Age 72 Weeks

N= 14 (WT, IGF1RKO, DKO), 13 (IRKO). P values <0.1 included on the figure, with significance (P<0.05) highlighted with an asterisk.

Data from figure 6.4 indicate significant between group differences (ANOVA p=0.0027) with t-tests suggesting body weight is significantly higher in WT animals than IRKO (AUC 2659 [87.9] Vs 2077 [152], p=0.0023), and DKO (AUC 2659 [87.9] Vs 2076 [82.1], p<0.0001) at age 72 weeks. No other significant differences were noted between genotypes, although there is a trend towards the IGF1Rko mice also having higher body weight than DKO (p=0.0889). Interestingly, the heaviest mice in the colony (weight >45g on at least 2 consecutive weeks) were all from the WT (9 mice) and IGF1Rko (5 mice) groups. The highest individual body weight recorded for a WT mouse was 59.1g, only

just surpassing the highest weight for an IGF1Rko at 57.3g. The highest individual weights for IRKO and DKO were nearly 20 grams less than these at 40.7g and 39.8g respectively.

6.2.2 Fasting Blood Glucose

We measured fasting blood glucose once mice exceeded 80 weeks of age (mean 86.2 weeks [0.8]), with 46 results available from the mice surviving to this time point.

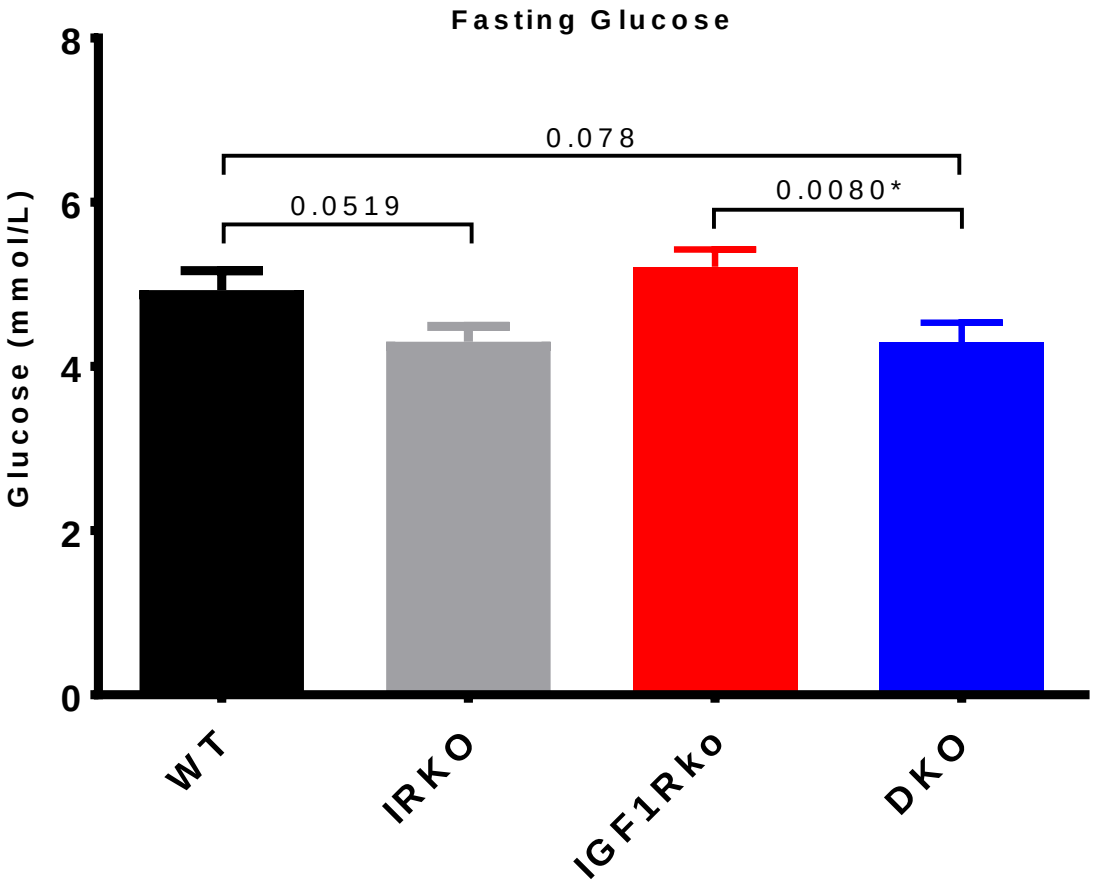

Figure 6.5: Fasting Blood Glucose at Age ≥80 weeks

Blood glucose measurements were made following overnight fast. N= 10 (WT and IRKO),13 (IGF1Rko and DKO). P values <0.1 included on the figure, with significance (P<0.05) highlighted with an asterisk.

ANOVA analysis indicated significant inter-group differences (P=0.0080) and t-tests indicated DKO had significantly lower fasting glucose than IGF1Rko (4.3mmol/L[0.24] Vs 5.2mmol/L[0.2]), with trends towards lower fasting glucose in DKO and IRKO when compared with WT.

6.2.3 Glucose and Insulin Tolerance Testing

Glucose tolerance tests (GTTs) were performed at age >80 weeks of age (mean 86.2 weeks [0.8]), with insulin tolerance testing (ITT) completed 2 weeks following the initial GTT. Figures 6.6-6.9 show glucose plots and area under the curve (AUC) for these experiments.

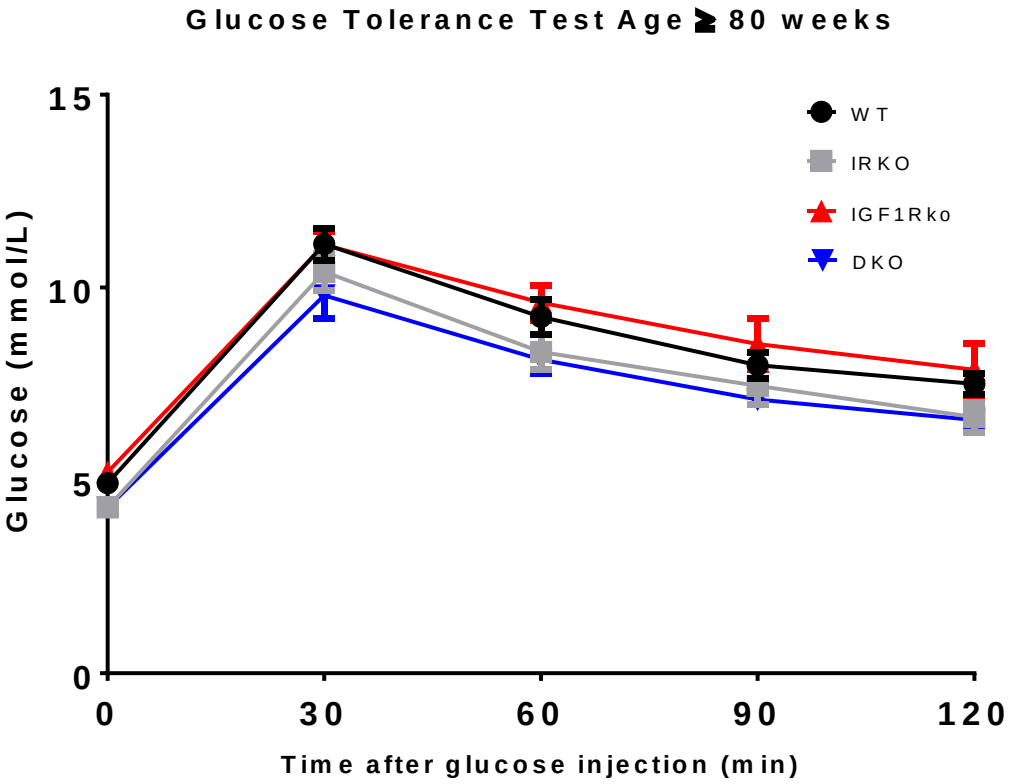

Figure 6.6: Glucose Tolerance Test at Age ≥80 weeks

Mice were fasted overnight, then injected (intraperitoneally) with glucose 1mg per gram of body weight. Capillary glucose measurements were taken at 30 minute intervals for 2hrs following injection. N= 10(WT, IRKO), 13(IGF1Rko, DKO)

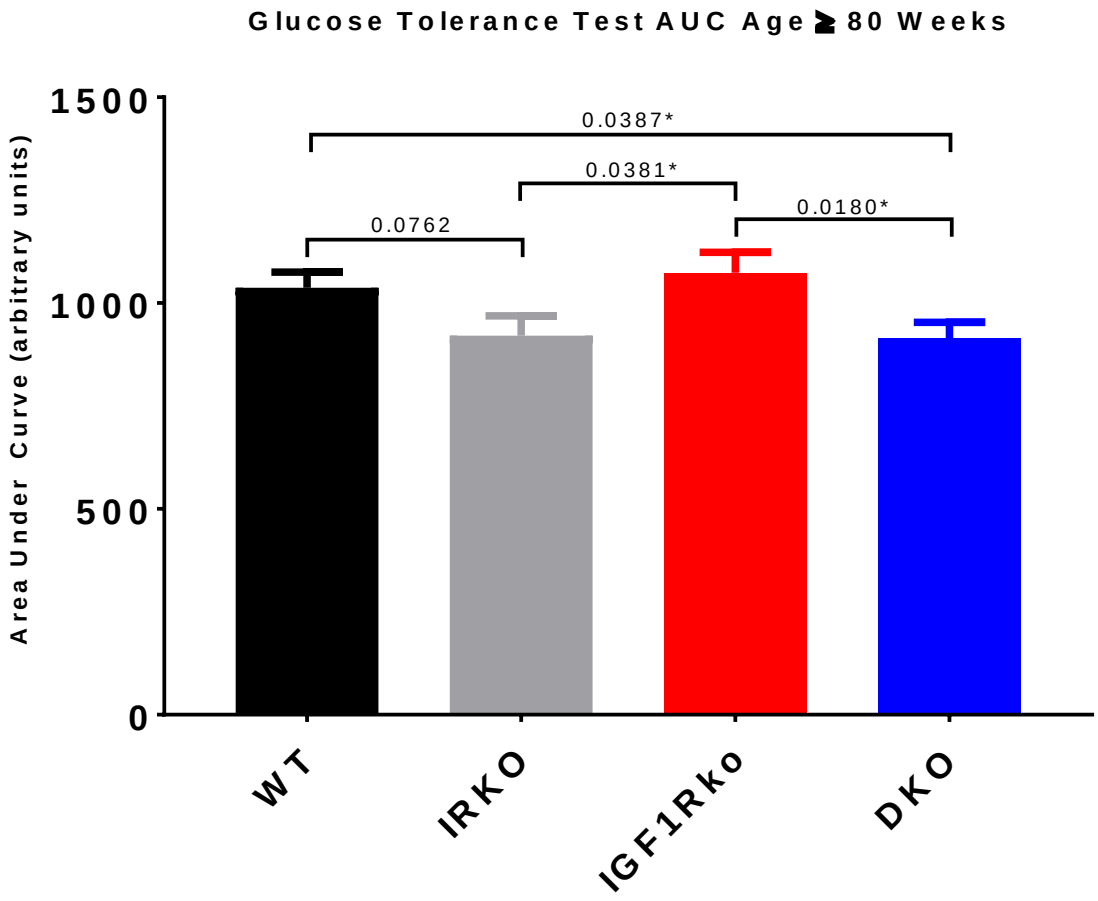

Figure 6.7: Area Under Curve for Glucose Tolerance Test Age ≥80 weeks

N= 10(WT, IRKO), 13(IGF1Rko, DKO). P values <0.1 included on the figure, with significance (P<0.05) highlighted with an asterisk.

Results differed significantly between groups (ANOVA p=0.0248) and t-tests indicated glucose tolerance was significantly better in DKO than WT (DKO 913.8 [39.4] Vs WT 1037[37.9], p=0.0387) and IGF1Rko (DKO 913.8 [39.4] Vs IGF1Rko 1074[49.2], p=0.0180). A similar (non-significant) trend was seen in IRKO compared with WT, with IRKO having significantly lower glucose AUC over the duration of the experiment than IGF1Rko (IRKO 920.6 [48.2] Vs IGF1Rko 1074 [49.2], p=0.0381).

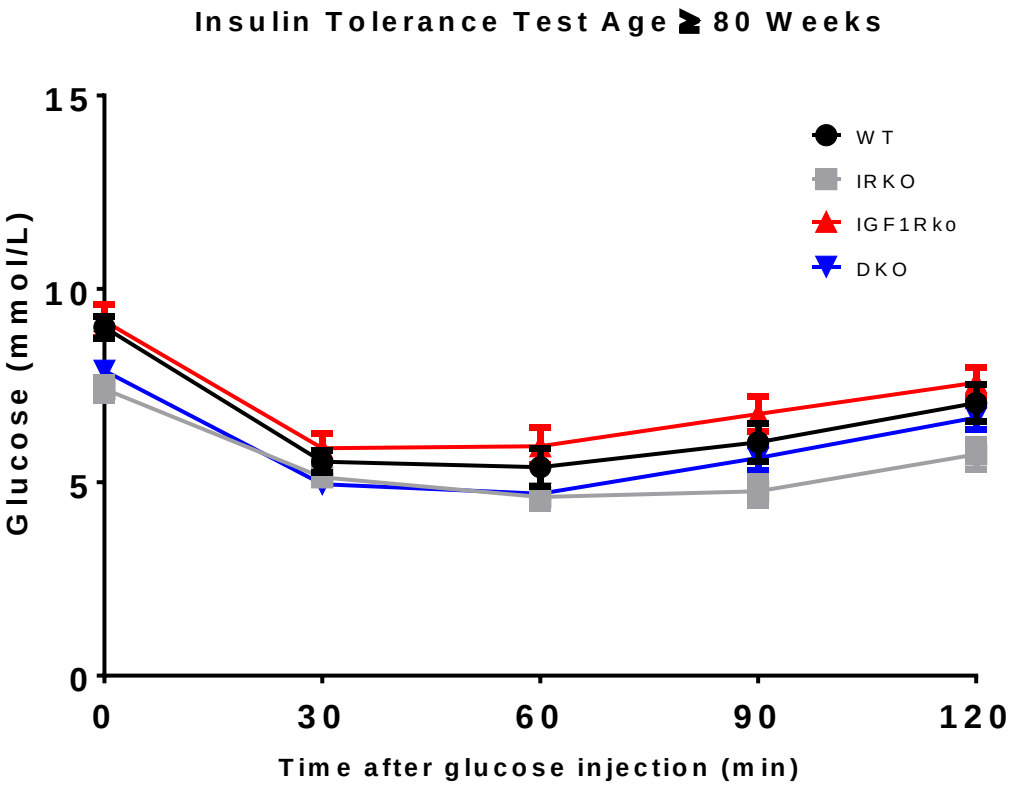

Figure 6.8: Glucose Tolerance Test at Age ≥80 weeks

Mice were fasted for 2hrs, then injected (intraperitoneally) with insulin 0.75IU per g of body weight. Capillary glucose measurements were taken at 30 minute intervals for 2hrs following injection. N=10(WT, IRKO), 13(IGF1Rko, DKO).

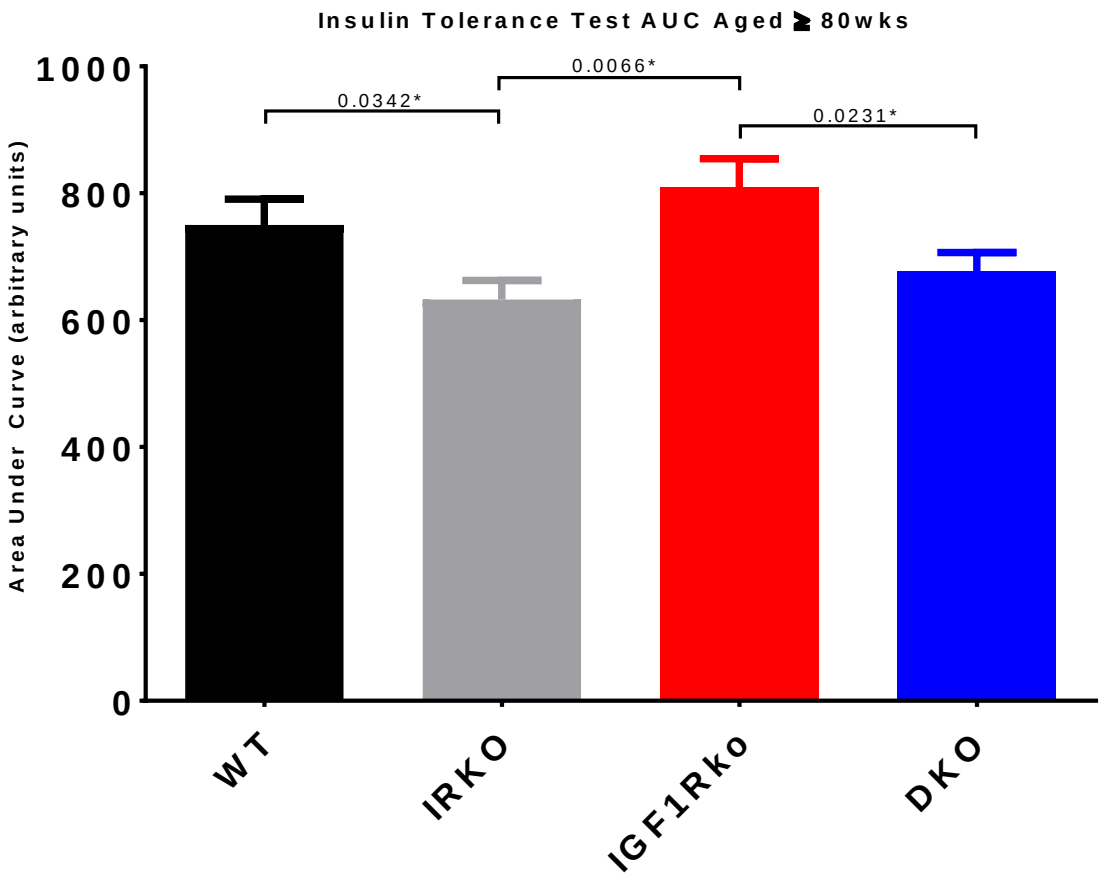

Figure 6.9: Insulin Tolerance Test Area Under Curve at Age ≥80 weeks

N= 10(WT, IRKO), 13(IGF1Rko, DKO). P values <0.1 included on the figure, with significance (P<0.05) highlighted with an asterisk.

Insulin tolerance testing showed a significant difference between groups on ANOVA analysis (P=0.0106), with t-tests indicating significant increases in insulin sensitivity in IRKO compared with WT and IGF1Rko, and in DKO versus IGF1Rko, with a similar non-significant trend seen between DKO and WT.

We noted a significant difference in body weight between groups with ANOVA analysis (p=0.0002) when performing the ITTs and GTTs (Figure 6.10). T-tests indicated both IRKO and DKO were significantly lighter than WT and IGF1Rko counterparts,

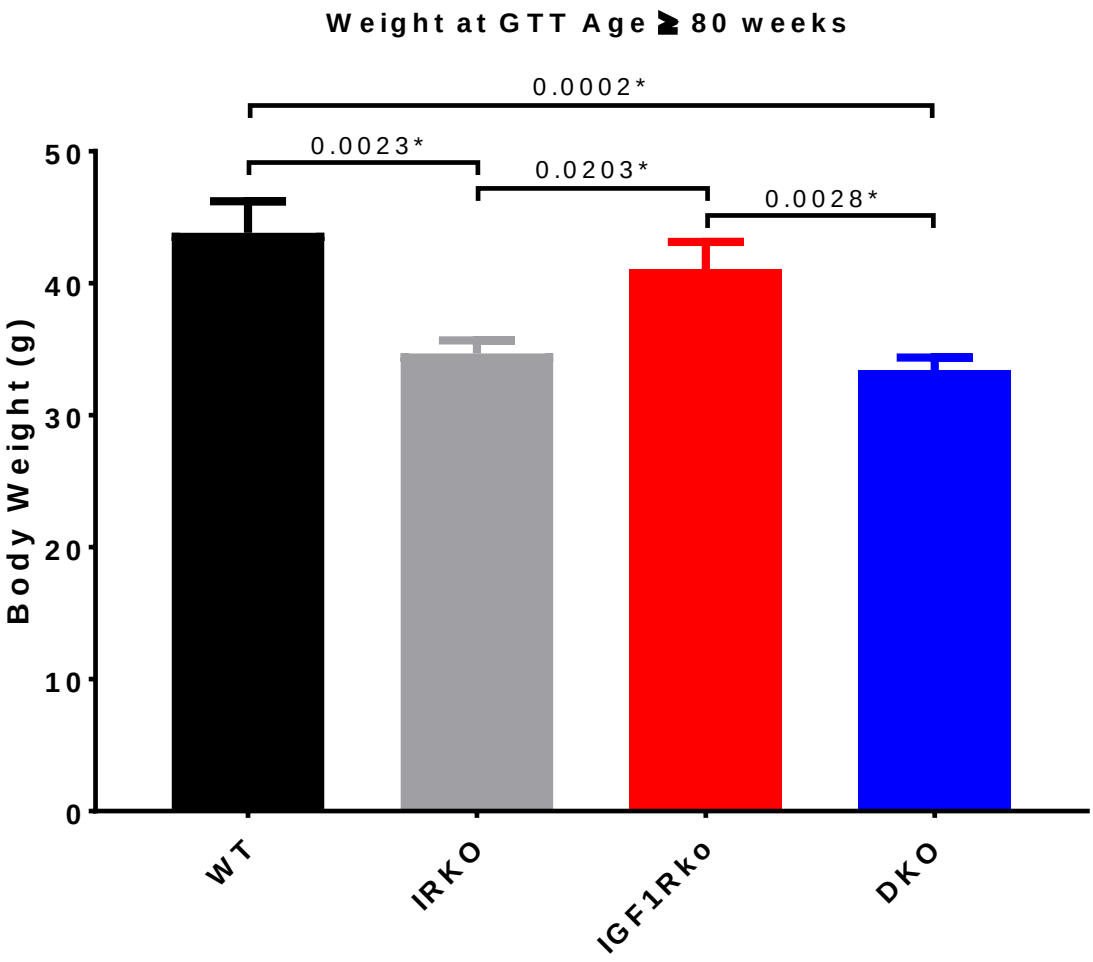

Figure 6.10: Weights at Glucose Tolerance Testing Age ≥80 weeks

N= 10(WT, IRKO), 13(IGF1Rko, DKO). P values <0.1 included on the figure, with significance (P<0.05) highlighted with an asterisk.

Given these differences in body weight at the time of GTT and ITT, we decided to investigate a correlation between body weight and glucose and insulin tolerance in these mice.

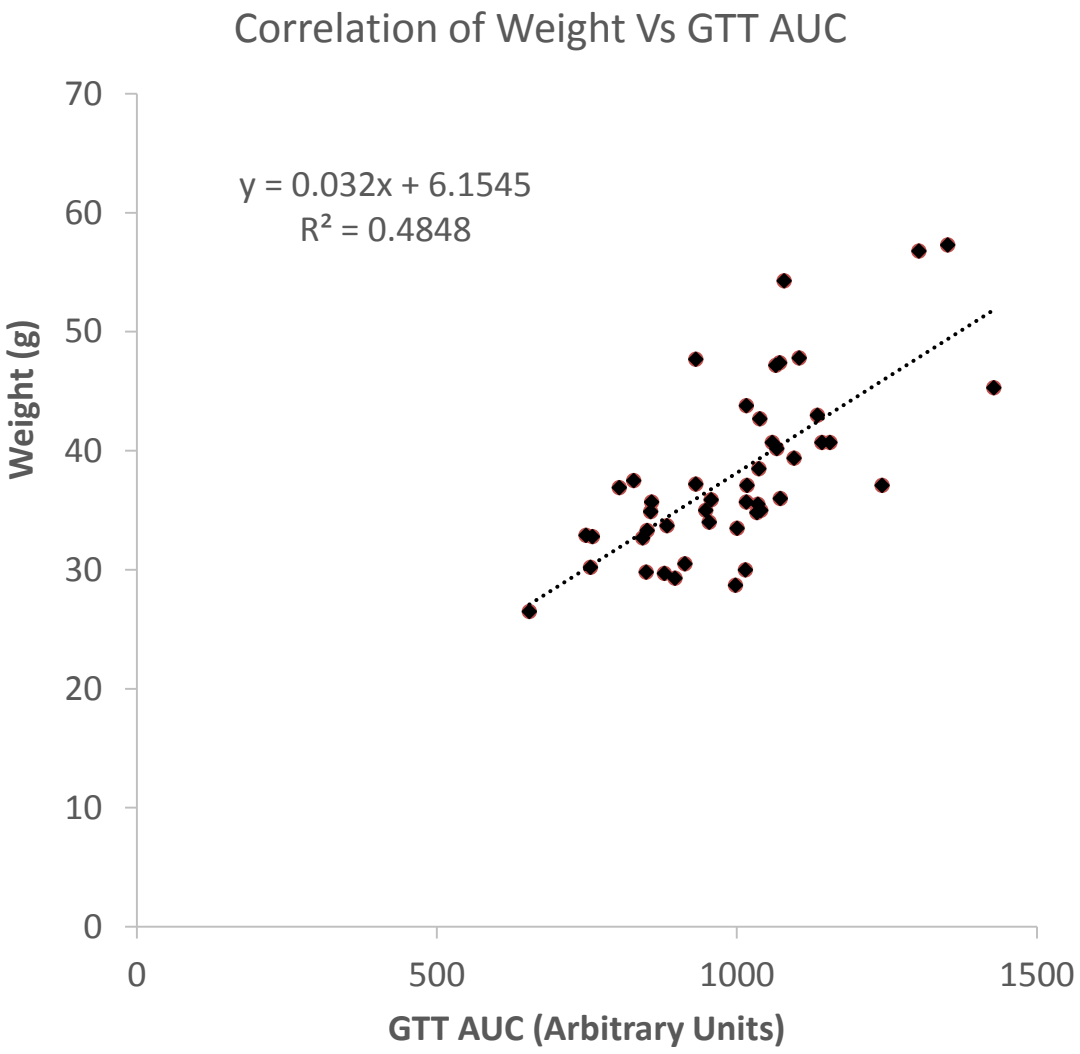

Figure 6.11: Correlation Between Weight and Glucose Tolerance Test Area Under Curve

N= 46 mice (10 WT, 10 IRKO, 13 IGF1Rko, 13 DKO)

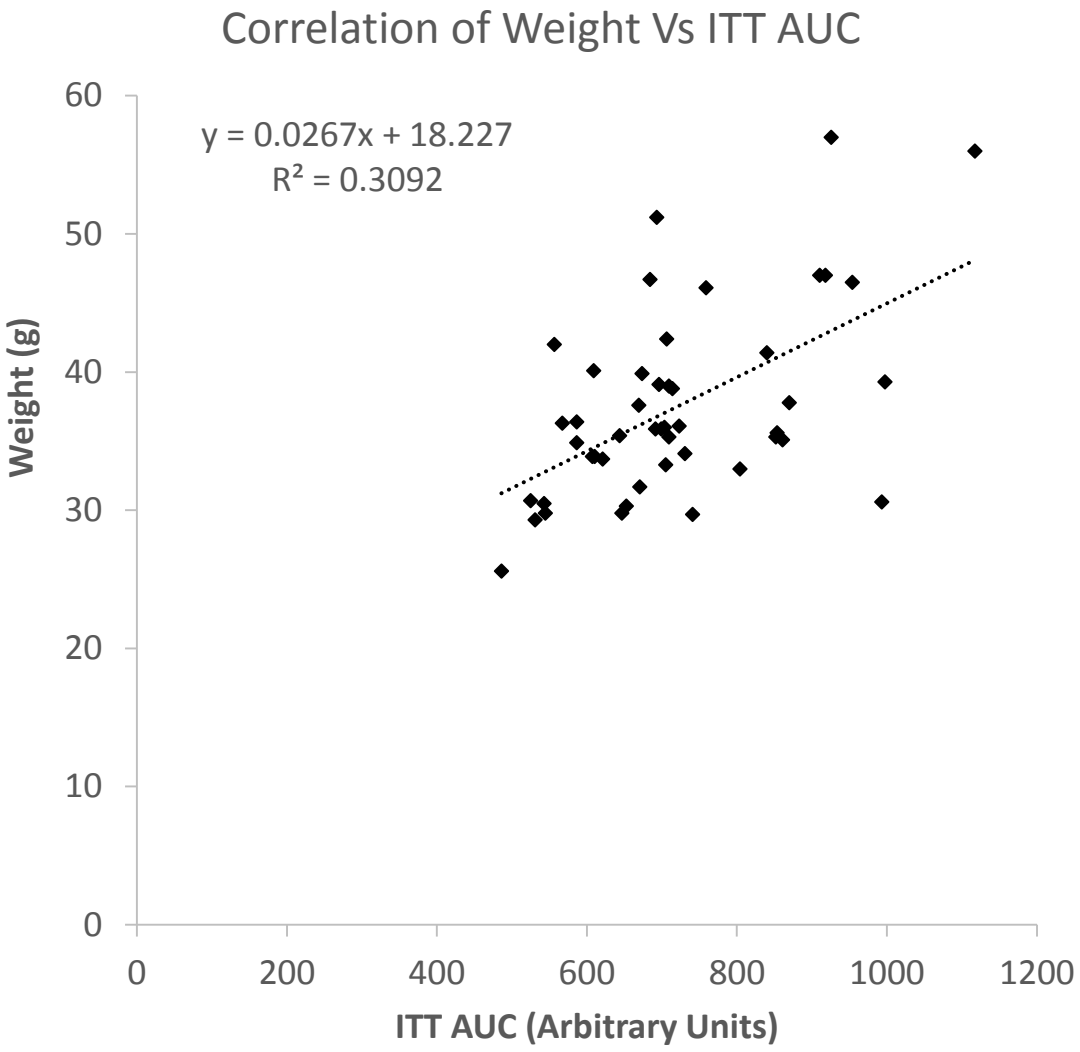

Figure 6.12: Correlation Between Weight and Glucose Tolerance Test Area Under Curve

N= 46 mice (10 WT, 10 IRKO, 13 IGF1Rko, 13 DKO)

There was a strong positive correlation between GTT area under curve and body weight (R^2 =0.48), with a similar, if slightly weaker correlation seen between ITT area under curve and body weight (R^2=0.31).

6.3 **Healthspan**

As outlined in section 4.10.3, we studied a cohort of mice throughout the course of their healthspan.

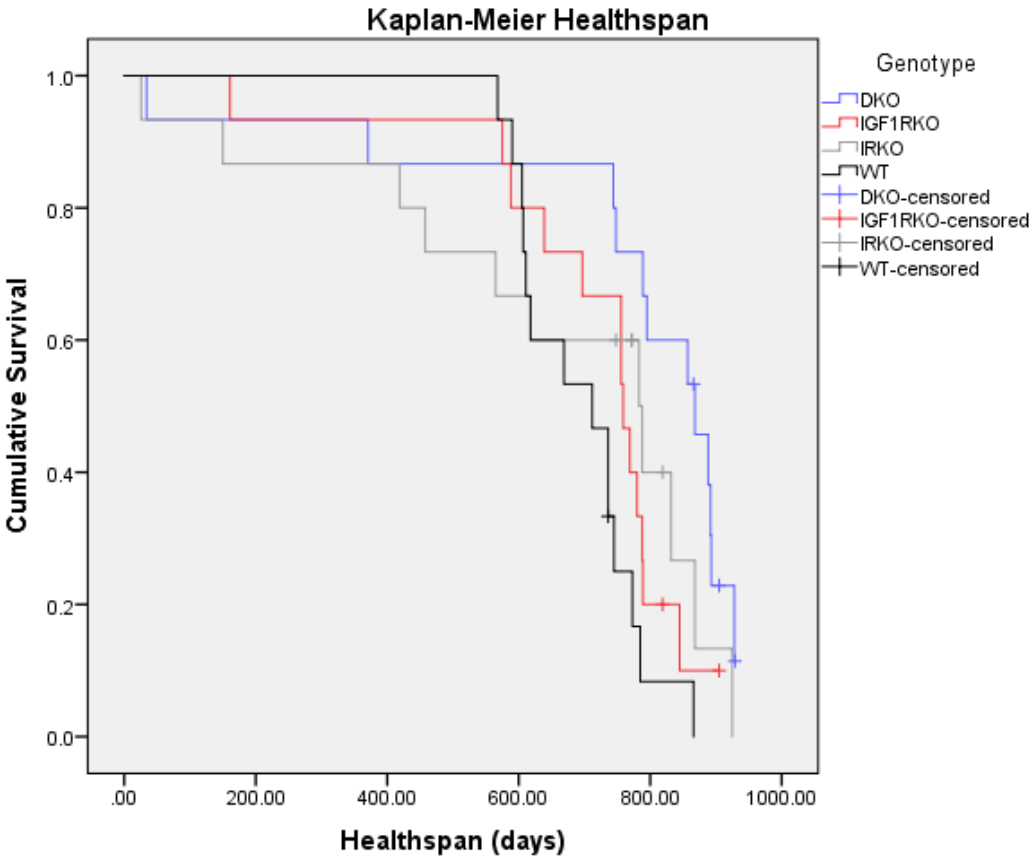

Figure 6.13: Kaplan-Meier Survival Plot for Healthspan

Kaplan-Meier Survival Plot for mouse healthspan – see section 4.10.3 for criteria used. N=15 per group, plot correct as of 1/8/17. Data censored for animals still within their healthspan. P= 0.006* by Log-Rank (Mantel-Cox) test.

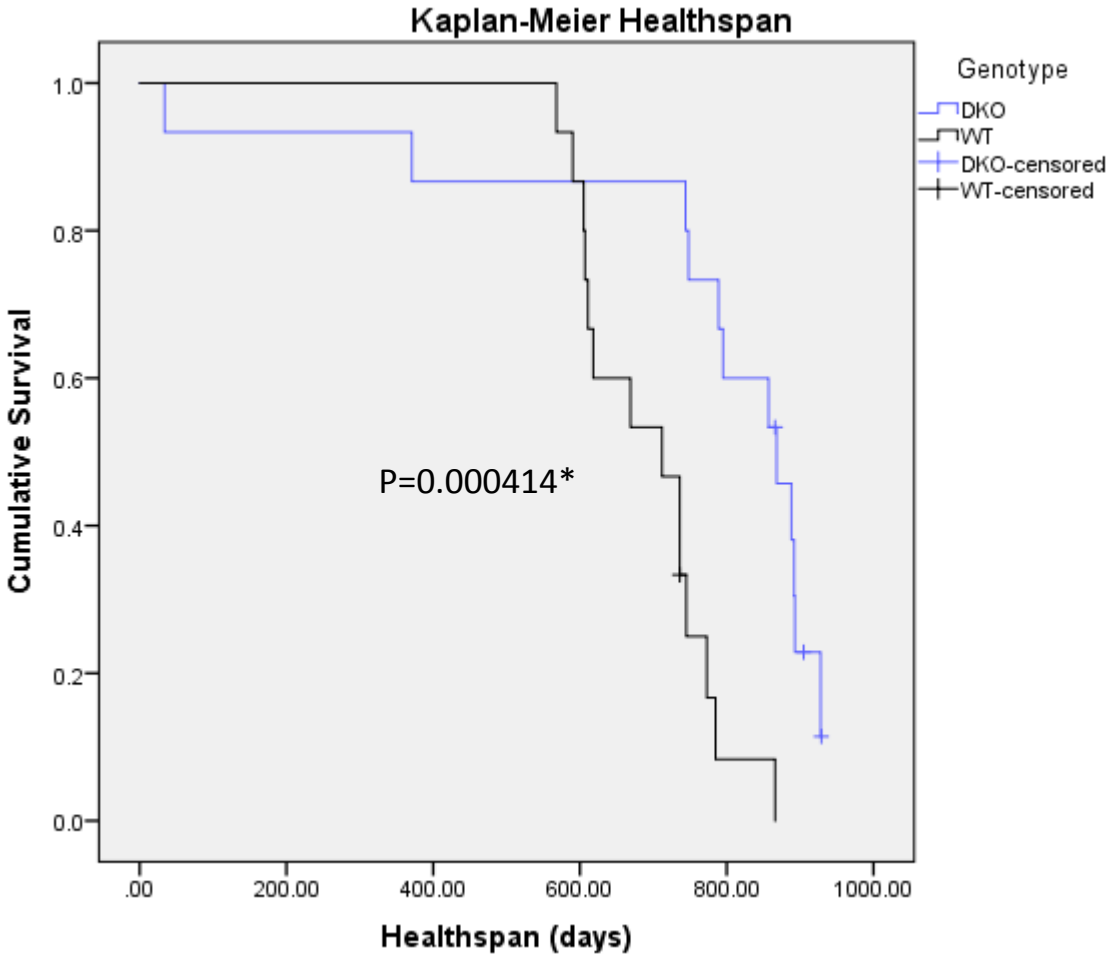

Figure 6.14: Healthspan Kaplan-Meier Survival DKO Versus WT

N=15 per group, plot correct as of 1/8/17. Data censored for animals still within their healthspan

Figures 6.13 and 6.14 display healthspan results for the aging cohort correct as of 1/8/17. At this time point there were 1 WT, 4 IRKO, 2 IGF1Rko and 3 DKO still alive and within their healthspan. DKO healthspan was significantly longer than WT (mean survival 771 days [62] Vs 694 days [24], p=0.000414 by Log-Rank Test. There were no other significant inter-group differences.

Genotype	Spontaneous Death No Cause Identified	Spontaneous Death Tumour Present	Culled for Wt. Loss	Culled for Welfare	Totals
WT	3	1	10	0	14
IRKO	1	1	7	2	11
IGF1Rko	0	0	12	1	13
DKO	3	2	6	1	12

Table 6.1: Cause of Death in Aging Cohort

Genotype	Tumour Present	Tumour Absent	Total
WT	4	10	14
IRKO	2	9	11
IGF1Rko	5	8	13
DKO	2	10	12

Table 6.2: Probable Tumour Prevalence in Aging Cohort

Tables 6.1 and 6.2 show cause of death and probable tumour prevalence data respectively. No significant differences were identified between groups (p-values not listed). All healthspan endpoints met were for weight loss >15% maximum average body weight except in 4 cases, where trauma due to in-fighting, a dental abscess causing significant distress, a severe rectal prolapse, and abdominal distension and distress (large abdominal tumour identified on post mortem) were the reasons for euthanasia.

6.4 Quantitative Polymerase Chain Reaction Studies for FOXO targets

IR and IGF-1R signalling influence the function forkhead box O (FOXO) transcription factors through the action of AKT [98, 235]. Phosphorylation of FOXO through this process leads to inhibition of its ability to promote transcription by precluding its passage to the nucleus. As such, the IR and IGF-1R are negative regulators of FOXO signalling. FOXO transcription factors have a broad spectrum of targets, many of which influence aging [230]. Indeed, diminished FOXO signalling is associated with longevity across species [230]. As such, we decided to perform exploratory analyses involving quantitative polymerase chain reaction (qPCR) on samples from the IRKO-IGF1Rko colony in order to measure the RNA levels of a range of FOXO targets. We selected a range of targets conserved across species based on studies performed by Webb *et al* [230] in order to assess the impact of decreased IR and IGF-1R expression on a range of processes which influence longevity. We measured: Ataxia telangiectasia mutated (ATM), a gene associated with DNA repair; catalase, and superoxide dismutase 2 (SOD2), enzymes which regulate oxidative stress; Diacylglycerol O-acyltransferase 1 (Dgat1) and Frataxin (Fxn), involved in fat and

iron metabolism respectively; rictor (Rapamycin Insensitive – Companion of the mammalian Target Of Rapamycin [mTOR]), involved in protein synthesis and aging; and myc, involved in cell proliferation and highly expressed in many cancer cells [248]. Figures 6.15a and b display results from qPCR of aortic RNA, with figures 6.16a and b showing results from fat samples.

Aorta qPCR

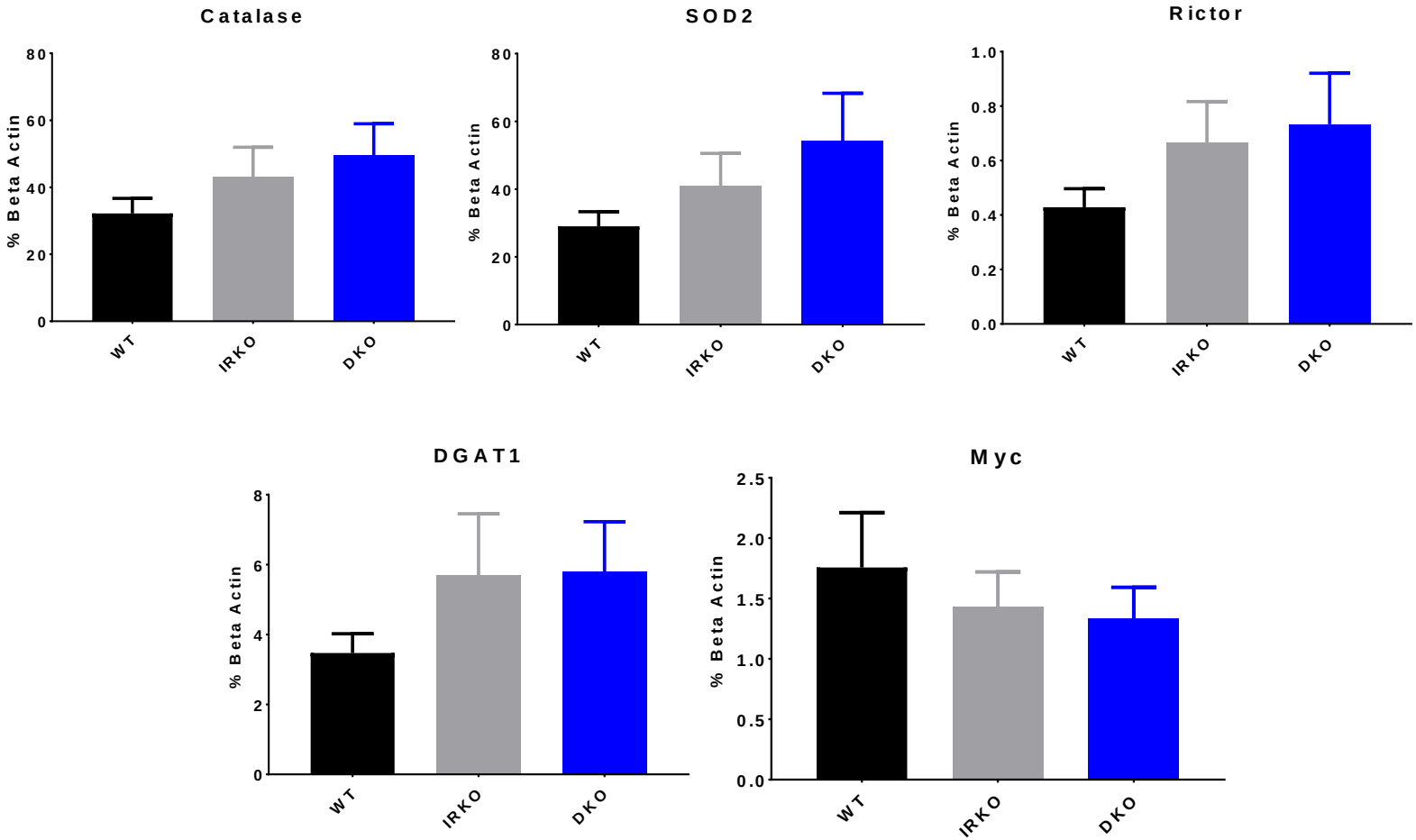

Figure 6.15a: Quantitative PCR from Aortic RNA Samples

N= 7 (WT), 6 (IRKO), 6 (DKO). P values listed where P<0.1, significance (P<0.05) denoted with an asterisk

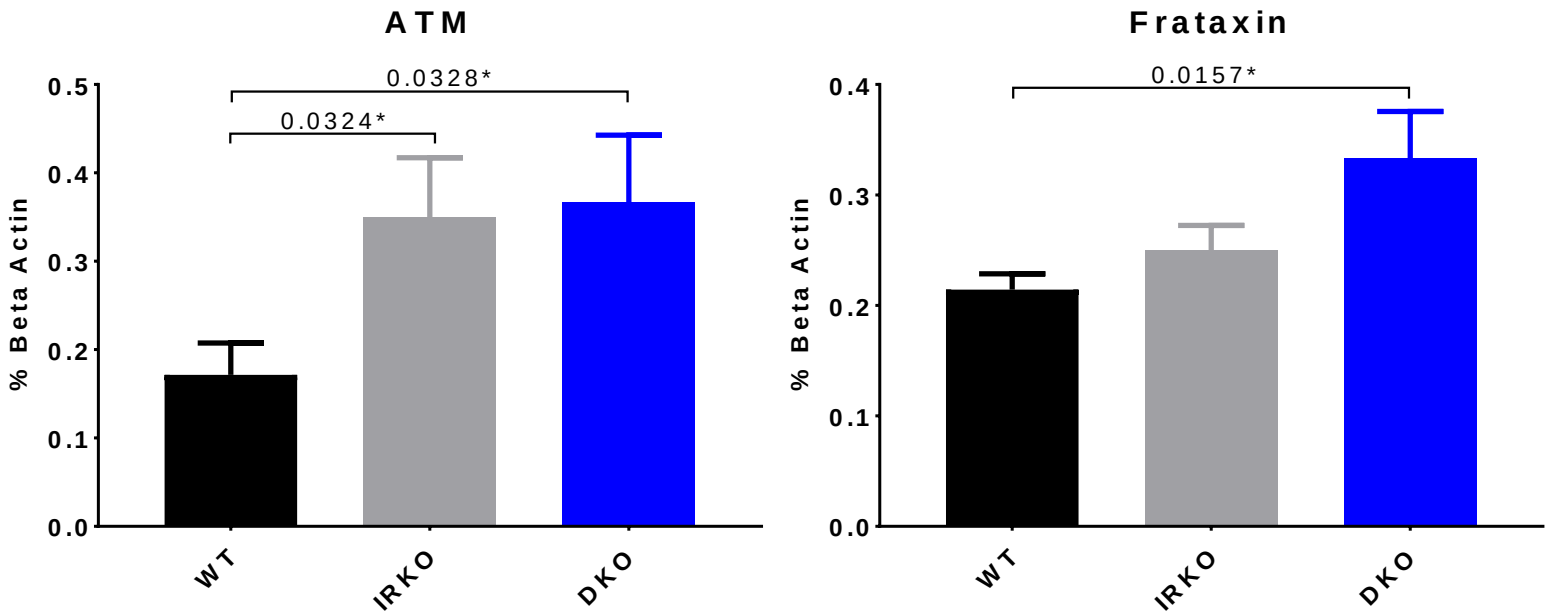

Figure 6.15b: Quantitative PCR from Aortic RNA Samples

N= 7 (WT), 6 (IRKO), 6 (DKO). P values listed where P<0.1, significance (P<0.05) denoted with an asterisk

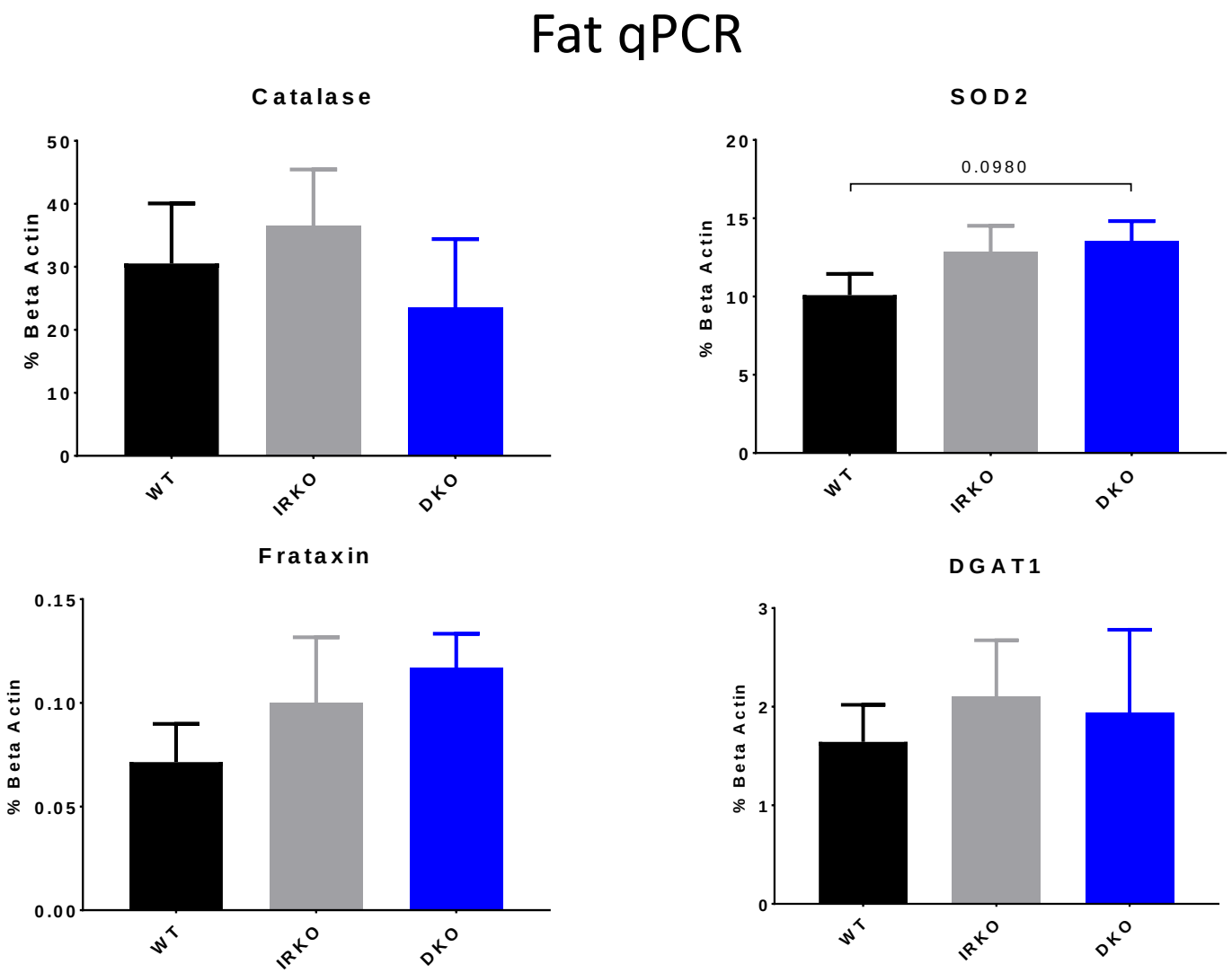

Figure 6.16a: Quantitative PCR from Fat RNA Samples

N= 7 (WT), 6 (IRKO), 6 (DKO). P values listed where P<0.1, significance (P<0.05) denoted with an asterisk

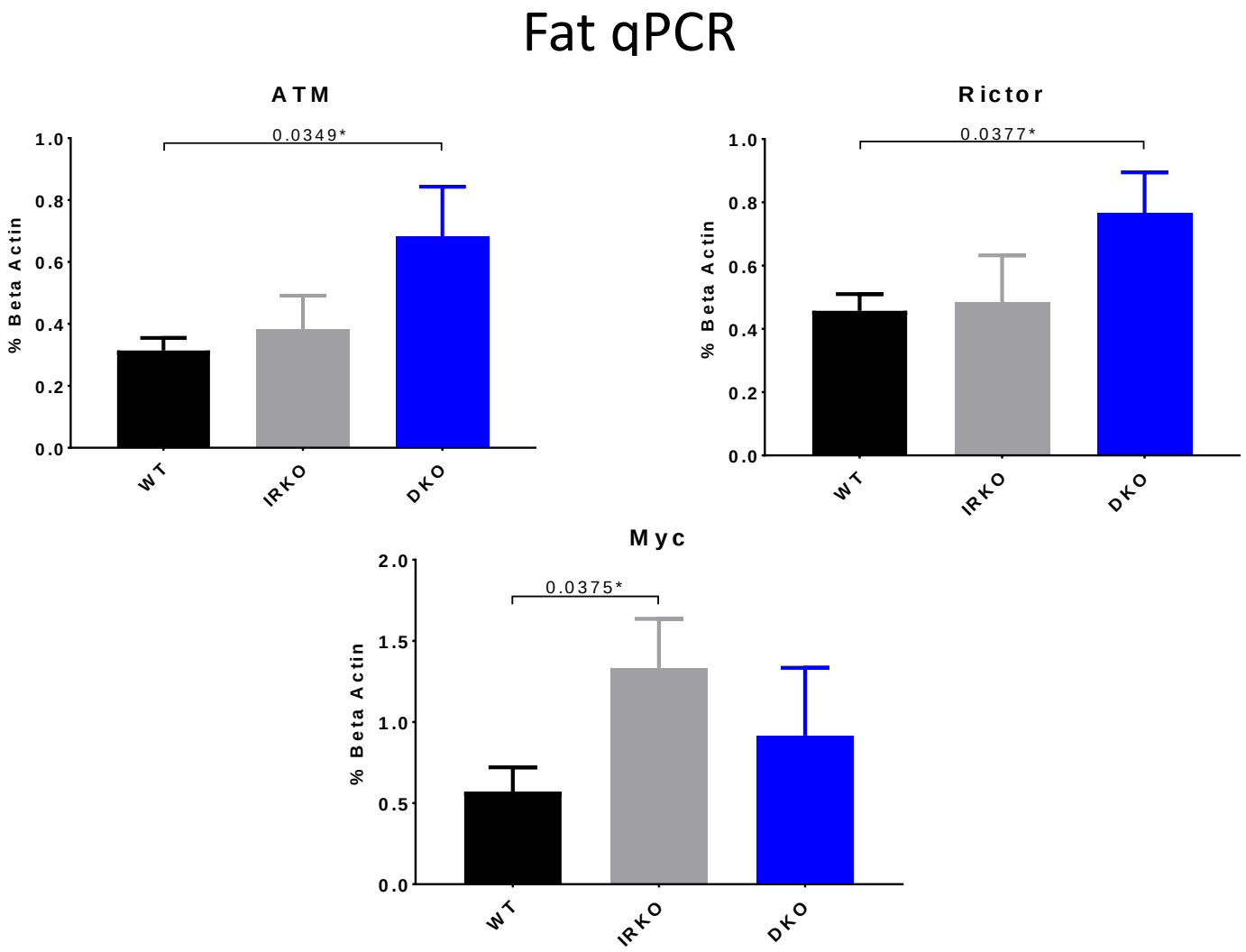

Figure 6.16b: Quantitative PCR from Fat RNA Samples

N= 7 (WT), 6 (IRKO), 6 (DKO). P values listed where P<0.1, significance (P<0.05) denoted with an asterisk

6.5 Nesting Studies

The measures available to judge healthy aging in mice are legion [246]. Given the apparent differences observed in physical measures of healthspan such as those included in section 6.3, we decided to explore whether there were any overt differences between genotype which might inform our knowledge of cognitive and behavioural function. As an exploratory measure, we chose to perform nesting studies on the mice.

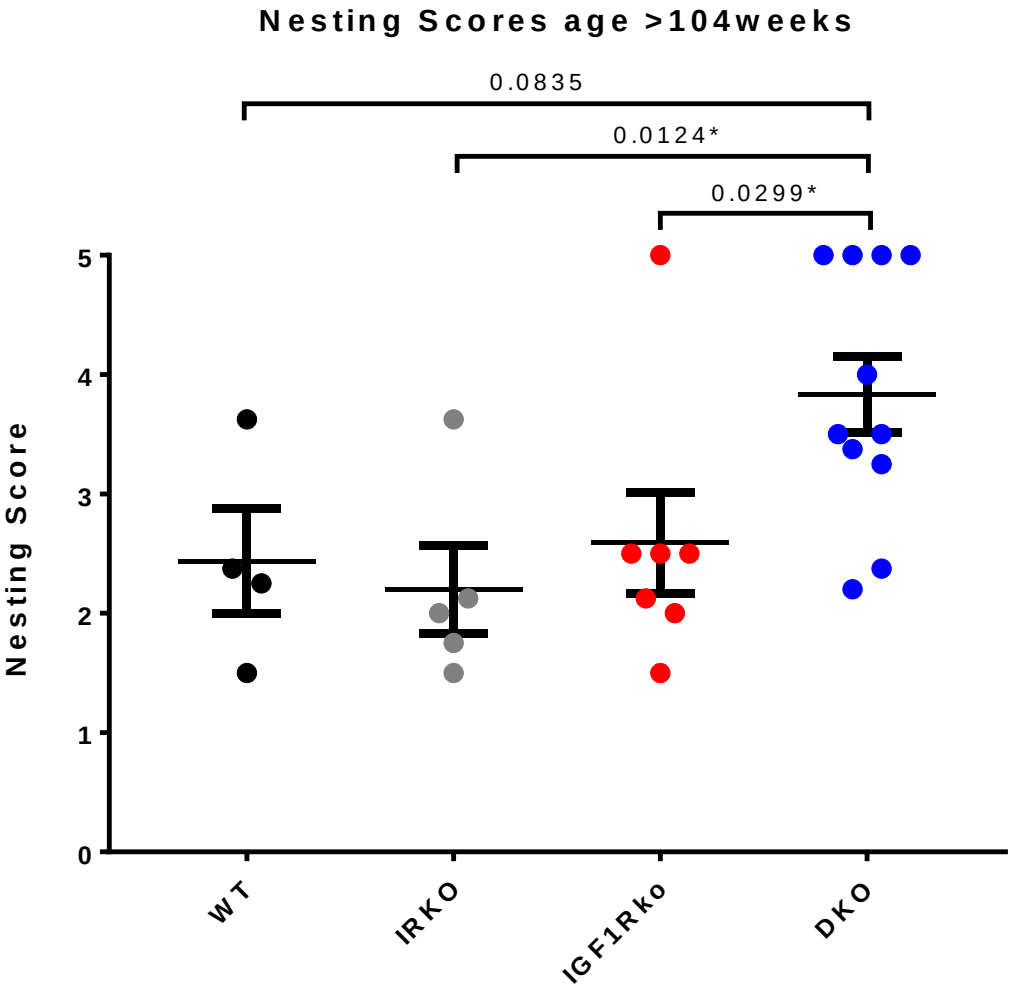

Figure 6.17: Nesting Scores in Mice > 90 Weeks of Age

See section 4.10.5 for scoring system. N=4(WT), 5(IRKO), 7(IGF1Rko), 11(DKO). P values <0.1 included on figure, statistical significance is highlighted with an asterisk.

As these data are not normally distributed, the Mann-Whitney U test was used to analyse the data [246]. DKO animals scored significantly higher than both IRKO and IGF1Rko, with no significant differences between the other genotypes (DKO mean score 3.84[0.32] Vs IRKO 2.2[0.37, P=0.0124; DKO Vs IGF1Rko 2.59[0.43], p=0.0299). There was a strong trend towards a similar difference between DKO and WT (DKO 3.84[0.32] Vs WT 2.44[0.44], P=0.0835). Given that nests may be constructed to conserve body heat, we decided to plot body weight against nesting score having found DKO and IRKO to be significantly lighter than the other groups (see section 6.2.1).

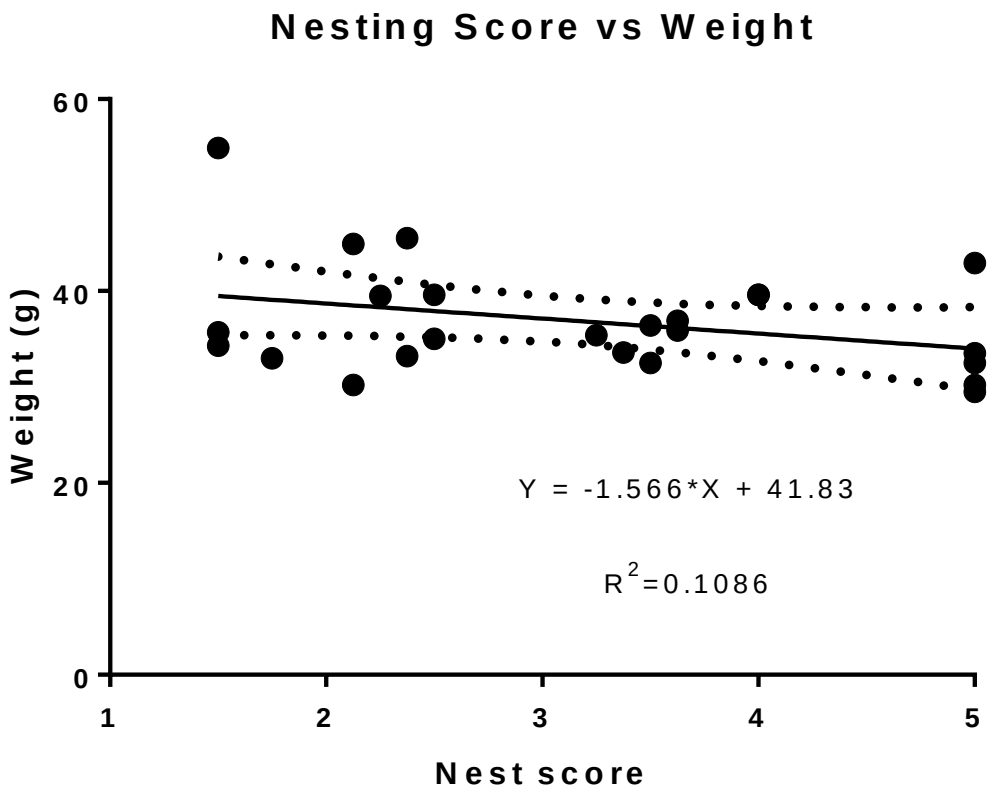

Figure 6.18: Nesting Score Versus Body Weight
N=24

The two variables correlate poorly, with linear regression indicating that there is no significant deviation from zero.

Chapter 7 **Discussion**

7.1 **Summary of Key Findings**

This thesis presents data examining the role of the insulin and insulin-like growth factor-1 receptors (IR, IGF-1R) in vascular regeneration and aging. We used a colony of transgenic mice to investigate our hypothesis that reduced IGF-1R expression in the setting of global haploinsufficiency of the IR (IRKO) would be associated with improved vascular repair and regeneration, and healthspan when compared with IRKO animals.

We found no significant differences in measures of glucose or insulin homeostasis between the genotypes in young adult mice (age 8-13 weeks), although a significant difference in body weight was noted at this age, with double knockout (DKO, i.e. $IR^{+/-}$:$IGF\text{-}1R^{+/-}$) animals lighter than both wild type (WT) and IRKO littermates.

We found DKO animals to have significantly augmented re-endothelialisation after denuding femoral artery wire injury compared with IRKO. Interestingly, these mice had superior recovery of perfusion to both IRKO and WT mice following induction of hind-limb ischaemia, indicating a markedly favourable vascular reparative phenotype in contrast to that seen in IRKO.

Studies *in vitro* demonstrated no significant difference in the number of circulating progenitor cells (CPCs) between groups, or in the number of myeloid

angiogenic cells (MACs) cultured from mouse blood and spleen samples. A significant increase in the number of MACs cultured from DKO bone marrow samples compared with IRKO led us to undertake more detailed investigation of blood and bone marrow leukocytes. We found no significant difference in the number or proportion of any of the cell types quantified from blood samples, but interesting differences were noted between genotypes on bone marrow analysis. We found significantly fewer CD11b+ cells, a greater percentage of non-leukocyte cells, with strong trends towards fewer neutrophils and monocytes in DKO marrow compared with IRKO. Notably, there were significantly fewer inflammatory monocytes in the DKO marrow than in IRKO samples.

Functional assays demonstrated a surprising impairment in scratch wound healing *in vitro* in DKO pulmonary endothelial cells (PECs) compared with IRKO, in contrast to the findings of improved vascular repair *in vivo*. A sprouting angiogenesis assay demonstrated significantly reduced sprout length in IRKO PEC-coated beads compared with WT, a difference abrogated in the DKO samples.

Studies in an aging cohort of mice provided further insights into the metabolic influence of the IR and IGF-1R over time. Interestingly IRKO and DKO animals appear to be protected from weight gain, which occurs in WT C57Bl6 and IGF1Rko (IGF-$1R^{+/-}$) mice. This is mirrored by a corresponding significant enhancement in glucose and insulin tolerance in these groups which correlates with body weight. Healthspan is significantly prolonged in the DKO animals compared with WT. Preliminary behavioural data show a significant

improvement in nesting score in elderly DKO mice compared with IRKO, with trends towards a similar difference between DKO and WT. Exploratory insights from quantitative RT-PCR suggest that DKO animals have important differences in the expression of FOXO targets known to influence the aging process.

7.2 Vascular Repair and Regeneration

7.2.1 Metabolic Phenotyping in Young Mice

The metabolic profile of the mice included in this study was investigated with body weight, systolic blood pressure, and glucose and insulin tolerance testing. These parameters were recorded in mice aged 8-13 weeks. Further metabolic studies have been performed in mice in the aging cohort, and will be discussed in section 7.3.1.

7.2.1.1 Body Weight

In this cohort, DKO animals were significantly lighter than both IRKO and WT animals. Previous work has noted only a trend towards IRKO being lighter than WT without statistical significance [146]. Of note, the number of animals studied in this project was greater than in the previous investigation (15 per group Vs 8), which may have led to the detection of a small, but significant difference between the genotypes. This thesis presents the first characterisation of body weight in mice with global haploinsufficiency for both the IR and IGF-1R. In that DKO animals have reduced expression of two key growth factor receptors, it is not necessarily surprising that they are lighter than both IRKO and WT littermates. The Kahn laboratory has recently published data from mice with inducible adipocyte-specific knockout of the IR and or IGF-1R, indicating that the insulin

receptor is essential for adipogenesis [225]. These mice were found to have significant glucose intolerance until proliferation of preadipocytes and rapid regeneration of both brown and white adipocytes normalised their phenotype 10-30 days following tamoxifen injection. Data from our IRKO:IGF1Rko colony indicates no such difference in glucose homeostasis, (see section 7.2.1.3), indicating that there appear to be tissue-specific effects of reduced IR expression, and indeed that the level of IR or IGF-1R reduction (i.e. complete knockout versus haploinsufficiency) appears important.

Further work to characterise the nature of the observed differences in weight will be important to learn more about this phenotype. I plan to study wet organ weights as a crude measure of body composition in future cohorts, with dual-energy X-ray absorptiometry (DEXA) scanning an alternative technique which could allow more accurate determination of fat mass as well as providing additional information such as bone density [249]. Magnetic resonance imaging would be another possible imaging modality, allowing longitudinal assessment of body composition across the healthspan of an animal [250]. I also plan to characterise the metabolic phenotype of these animals in greater detail using a comprehensive lab animal monitoring system which allows for activity assessments, food and water intake and output measurement, along with O_2 consumption/CO_2 production and temperature monitoring [250].

7.2.1.2 Systolic Blood Pressure

Systolic blood pressure did not differ between groups, which contrasts with findings from previous studies indicating that IRKO mice are hypertensive in

comparison with WT littermates [146]. It is possible that genetic drift is responsible for these divergent observations, although other aspects of the phenotype have remained consistent with previous studies (see vascular injury section 7.2.2). Certainly the technique of tail cuff plethysmography can lead to a broad spread of results, and a variety of factors such as the comfort of the mice under conscious restraint and their body temperature during the experiment can have a profound effect on the observed blood pressure [251]. Whilst every effort was made to ensure consistency in the approach to the mice, with a minimum of 2 acclimatisation cycles during the week preceding the final experiment, and the use of a temperature-controlled incubator throughout the study, it is possible that minor differences in these factors could have led to a wider spread of data. Indeed, it is possible that the numbers used for this study are insufficient to demonstrate a difference (i.e. type II error) in BP between groups, although this would not be consistent with previous studies in IRKO mice where 8 mice per group was sufficient to record a significantly greater BP in the animals compared to WT [146]. Regardless, on examining the data presented, we decided not to add further mice to the dataset as we could not justify the additional discomfort to the numbers of experimental animals we would have needed to definitively exclude a significant difference between groups. In future work, implantable telemetry [251] could be used in order to provide another approach to assess BP, although the potential for increased accuracy and the avoidance of conscious restraint would have to be balanced against the possibility of surgical complications and any unintended haemodynamic effects of the implanted device itself.

7.2.1.3 Glucose and Insulin Homeostasis

Previous work has characterised glucose and insulin homeostasis in IRKO [146] and DKO animals [123]. No significant difference was found in fasting blood glucose, or with insulin or glucose tolerance testing (GTT and ITT respectively) [123, 146]. My results are consistent with these findings, confirming that (at this age) the animals have no significant difference in glucose or insulin homeostasis, despite the observed differences in their body weight. Further characterisation of these animals as they age is presented in section 7.3.1. One key difference between IRKO and WT animals noted previously is an elevated insulin level following glucose load [146]. It will be important to measure this parameter in my cohort to compare DKO with IRKO. Options for more detailed assessment of glucose and insulin homeostasis in these animals include hyperinsulinaemic-euglycaemic clamping [142].

7.2.2 Vascular Injury

In keeping with previous data [80], we have demonstrated that IRKO animals have impaired re-endothelialisation after denuding femoral artery wire injury. One of the most significant novel findings within this thesis is the discovery that animals haploinsufficient for both the IR and IGF-1R (DKO) have vascular repair comparable to WT levels. This intriguing observation fits with previous data indicating a favourable vascular phenotype in these animals, with greater nitric oxide bioavailability, and reduced expression of insulin-resistant IR:IGF-1R hybrid receptors [123] compared with IRKO mice. Previous work from our group has demonstrated that haploinsufficiency of the IGF-1R leads to augmented recovery following vascular injury compared with WT animals, possibly via an

enhanced capacity of bone marrow-derived cells to promote repair [148]. The results displayed in section 5.3 are the first data to describe the consequences of reduced IGF-1R expression in the setting of whole body insulin resistance. It is well-understood that patients with insulin resistance have impaired wound healing and recovery after vascular events. As such, these data, indicating a rescue of the negative vascular phenotype seen in mildly insulin-resistant animals via concomitant reduction of the IGF-1R, highlight a possible therapeutic avenue for exploration in future work.

Clearly, murine studies alone cannot be directly extrapolated to indicate likely benefits in patients, and the germline mutations used in these models do not mirror the use of a therapeutic once insulin resistance develops in later life, e.g. due to type 2 diabetes. Nonetheless, these interesting data provide a basis for further investigation. In the first instance, our group is optimising the use of the Cre-Lox system to induce IGF-1R haploinsufficiency in adult mice via tamoxifen administration (unpublished). Employing this technology we can then investigate whether reducing IGF-1R expression could improve or even reverse the impaired vascular repair and regeneration seen in adult IRKO mice. This could then be used with other models across the spectrum of insulin resistance such as high fat-fed obese animals or with ob/ob or db/db mice. Pharmacological reduction of IGF-1R expression could also be investigated in these models, and we plan to study the effects of the human monoclonal IgG1 antibody IMC-A12 which binds with high affinity to the IGF-1R, blocks its activity, and promotes internalisation and degradation of the receptor [252]. We also plan to trial a new generation of small molecule inhibitors of IR:IGF-1R hybrid receptor formation being developed in our group.

7.2.3 Vascular Regeneration

A key positive finding from this project is the demonstration of improved recovery of perfusion after induction of hind-limb ischaemia (HLI) in DKO mice compared with both IRKO and WT littermates. Given the favourable vascular phenotype displayed by DKO [123], and the previous finding from our group that recovery following HLI is impaired in IRKO mice [247] we hypothesised that reduced IGF-1R expression in the setting of haploinsufficiency for the IR would abrogate the reduced recovery of perfusion seen in IRKO. Remarkably, not only did our data support this hypothesis, they also indicated supraphysiological (i.e. better that WT) recovery of perfusion in the DKO animals. This finding was unexpected, and suggests an important role for IR/IGF-1R signalling in vascular regeneration. Certainly DKO animals have an improved healthspan compared with WT animals (see section 6.3), therefore improved resistance to stress in the vasculature may, in part, explain some of this difference. It should be noted that laser Doppler perfusion imaging results may be markedly affected by small changes in a variety of factors such as the depth and duration of anaesthesia, temperature of the animals and the positioning of the hind-limbs for analysis. Having said this, a great deal of care was taken in order to ensure consistency between measurements, and no significant differences were noted in body temperature readings taken during imaging or in total duration of anaesthesia between groups (data not presented). Histological quantification of capillary density is a more robust indicator of recovery following induction of HLI, and analysis of samples of gastrocnemius muscle taken following the experiments is ongoing. Significant differences in these samples coupled with the results of the laser Doppler studies would provide strong evidence in favour of a key role of the IGF-1R in vascular regeneration. Further imaging with either ultrasound or MRI perfusion studies

would allow for comparisons of recovery following HLI in future studies, with the potential for greater anatomical detail. Micro-CT is considered the gold standard test to quantify arteriogenesis in ischaemic hind-limbs, although technical factors, such as adequate perfusion of the limb with contrast, present a challenge to operators [253].

It should be noted that results from HLI experiments are not directly comparable with human vascular disease, such as acute limb ischaemia. In this case, peripheral arteries are occluded either due to thromboembolisation (e.g. in the setting of atrial fibrillation) or more commonly due to atherothrombosis in arteries already affected by atherosclerosis. In the latter case, chronic, progressive occlusion of conduit vessels leads to the gradual development of collaterals over time, whereas the HLI procedure renders previously normal vessels acutely ischaemic through immediate vascular ligation and removal. As such, the results of such studies should be considered exploratory, and future work investigating the effects of reduced IGF-1R expression should also be considered in other models of vascular disease such as atherosclerosis-prone animals (e.g. ApoE knockout) and with other assays such as coronary artery ligation/occlusion, including in larger animals.

7.2.4 Progenitor Cell Studies

Previous work has shown that progenitor cells contribute to vascular repair and regeneration and that insulin signalling has a strong influence on this process [153]. Despite previous work identifying a deficiency in circulating progenitor cells (CPCs) and a reduction in the number of myeloid angiogenic cells (MACs)

cultured from the monocyte fraction of blood from IRKO mice [80], these findings were not reproduced in the present study. Genetic drift could help explain these divergent results although, as previously mentioned, other features of the IRKO phenotype have been recapitulated in this project, such as the vascular repair and regeneration data. There is an inherent degree of variability in the method used by Kahn *et al* to culture MACs from mononuclear cells, and although the number of cells plated down for culture is standardised across experiments, small differences in the subsequent handling of samples could possibly have influenced the final results. Both assays are subject to a degree of variability, given that the serum concentration and activity state of the white cells studied is likely to differ depending on the inflammatory condition of the experimental animals. Whilst the mice were from pathogen-free colonies, and housed in cages with isolated, HEPA (high efficiency particulate air) filtered air, it is impossible to discount the possibility of differences in inflammatory state between animals contributing to the variability of the results.

It is interesting to note that the bone marrow-derived MACs were more abundant in the DKO animals when compared to IRKO. Differences in the bone marrow environment and its influence on vascular repair and regeneration will be discussed in section 7.2.5.

It should be noted that although CPC abundance has been negatively correlated with cardiovascular disease event rates in humans [171], and murine transfusion studies have demonstrated the reparative potential of C-kit$^+$ cells in HLI and vascular injury assays [80], the importance of these cells in human

pathophysiology has not been proven. Indeed, MACs are a form of cell only derived thus far through *in vitro* methods, and studied under laboratory conditions. Whether these cells occur naturally *in vivo* has not yet been elucidated, and any potential role of MACs in human physiology remains undetermined. Nonetheless, the associations seen with CPC and MAC abundance in health and disease make them reasonable surrogate markers for vascular repair potential [171]. These exploratory experiments will inform future work which will aim to elucidate further the role of the IR and IGF-1R in vascular repair and regeneration.

7.2.5 Quantification of Leukocyte Populations

In section 5.5.2 we showed a greater number of MACs were derived from bone marrow monocytes from DKO mice than IRKO. As such, we decided to perform more detailed experiments with flow cytometry to examine leukocyte populations in the blood and bone marrow of the mice studied. There were no significant differences between genotypes in the number or proportions of the different cell populations in the blood samples tested. The marrow samples did produce some interesting findings, however. Overall, there were trends towards fewer monocytes and neutrophils, and a lower proportion of CD11b+ cells as a percentage of total CD45+ cells in the DKO animals compared with IRKO. Indeed, the number of CD11b+ cells was significantly fewer in the DKO than IRKO. In contrast to this, the proportion of non-leukocyte cells in the bone marrow of DKO animals was significantly greater than in IRKO, with a similar non-significant trend versus WT. Of note, the number of monocytes considered inflammatory (i.e. Ly-6C^{high}) was significantly lower in the DKO than IRKO, with

a trend indicating a skewing of the DKO monocyte populations towards a lower ratio of inflammatory to reparative cells. Mirroring the results from section 5.5.1 showing no difference in the abundance of Sca1(+) or C-Kit (+) cells in blood samples, there was no difference seen in the absolute number or proportion of Lin(-) Sca1(+) C-kit(+) (LSK) cells from bone marrow.

It should be noted that this dataset is not yet complete, as previous work done by our group has indicated a sample size of 10-15 mice per group is of appropriate power to detect significant differences between genotypes (unpublished data). As such, it is possible that some of the trends seen may become significant as the numbers are increased in the dataset. In particular, it will be interesting to see if any differences are uncovered between the cell populations in the blood samples, given the bone marrow environment certainly seems to differ in the DKO animals compared with IRKO. Already there are several significant differences between groups in the marrow samples, with the overall impression being of fewer leukocytes in the DKO bone marrow compared with IRKO, and an already significant increase in non-leukocyte cells. Further characterisation of these cells will be important in future work. Given the favourable phenotype of vascular repair and regeneration seen in DKO compared with IRKO, it is interesting to note that fewer inflammatory monocytes were seen in DKO compared with IRKO, and that there is a trend towards a lower ratio of these cells compared to reparative monocytes. Recent data from Gamrekelashvili *et al* indicates that interactions between the vascular endothelium and monocytes, particularly in niches such as the bone marrow and spleen, influence their cell fate [191]. Notch2 was shown to regulate conversion of Ly-6C^{high} cells (inflammatory monocytes) to the Ly-6C^{low} reparative (or

patrolling) phenotype. This process was found to be controlled by DLL1 (delta-like ligand 1), a Notch ligand. Given the importance of endothelial Notch and Delta-like ligands in angiogenesis (see section 1.4.3.1), these factors provide a possible mechanism for the differences seen in vascular repair and regeneration between genotypes.

Previous work by Xia *et al* has demonstrated the importance of insulin signalling in the bone marrow for the determination of lineage of multipotent progenitor cells [254]. They found that after inducible knockout of the IR in bone marrow LSK cells, there was a skewing of the myeloid/lymphoid ratio towards a greater number of myeloid (CD11b+) cells. Although BM cells in our work are haploinsufficient for rather than fully lacking the IR, there are trends in our (as yet incomplete) dataset towards similar findings between IRKO and WT. The significant reduction in CD11b+ cells shown in DKO compared with IRKO therefore indicates possible re-sensitisation of bone marrow cells to insulin in these mice, which may help explain the markedly improved phenotype of vascular repair and regeneration displayed by the DKO group.

As outlined in section 1.5.3, caloric restriction is associated with reduced IR/IGF-1R signalling [219]. Cheng *et al* [255] have published work linking prolonged fasting with a reduction in serum IGF-1 levels and a subsequent reduction in aging-associated myeloid bias. As such, there appear to be close links between the IR and IGF-1R signalling pathways and the bone marrow environment, in keeping with the preliminary results we have outlined in section 5.5.3. Completion of this dataset may lead to further progress towards understanding

the complex relationship between IR/IGF-1R signalling and those marrow-derived cells which may influence vascular repair and regeneration.

Clearly more work is required to examine potential differences in Notch signalling between genotypes *in vitro* and *in vivo*, and experiments such as immunofluorescence of tip and stalk cells, e.g. as imaged in murine retinae, or from angiogenic beads (see section 4.9.2) may help further this project. Bone marrow transplantation studies could also provide valuable insights into the relationships between IR and IGF-1R expression and vascular repair and regeneration. An obvious limitation of the studies in this project is the lack of human blood or bone marrow data thus far. As mentioned elsewhere, these experiments have been exploratory in nature, and the results will help develop hypotheses which might explain the significantly augmented vascular phenotype seen in the DKO animals. Now that we have observed interesting differences in the bone marrow environment of the animals studied, further work with samples from insulin-resistant patients and glucocompetent controls will be crucial to further the work towards possible new therapies. Quantification of cells from patients' blood and marrow with flow cytometry, in similar fashion to the murine studies conducted thus far, would be the first priority in this regard. Studies to transfuse human cells (e.g. C-kit+) into immunodeficient mice following HLI or femoral artery wire injury could provide important insights, with samples from those with insulin resistance being compared with healthy controls. Were a difference to be found between these groups, techniques such as lentiviral transduction of the cells with IGF-1R shRNA, or indeed pharmacological treatment with an IGF-1R antagonist [252], could be employed to explore the

therapeutic potential of reducing IGF-1R expression in the setting of human insulin resistance.

7.2.6 Studies with Murine Pulmonary Endothelial Cells

As described above, the endothelium has important actions which influence the fate of cells known to contribute to vascular repair and regeneration [191]. Moreover, the endothelium itself directs both re-endothelialisation and angiogenesis, with previous work from our group having identified a significant impairment in IRKO recovery following denuding injury to the femoral artery [80] and after induction of hind-limb ischaemia [247]. As such, we sought to investigate whether there were any differences in endothelial cell phenotype which might account for those differences, and whether cells from DKO animals might outperform IRKO in any of the functional indices tested.

We used the scratch wound assay to examine the properties of migration and proliferation in endothelial cells. Interestingly, despite the improved vascular repair seen *in vivo*, we noted a significant reduction in scratch wound closure in the DKO cells compared with WT, with a trend towards a similar reduction in IRKO PEC wound closure. Whilst we might have expected the IRKO PECs to have impaired migration and proliferation based on previous work (unpublished data), it is surprising to see an apparent impairment in proliferation and/or migration in the DKO PECs. This implies that the mechanism of the enhanced re-endothelialisation seen in DKO mice relies on factors other than the ability of endothelial cells to proliferate or migrate. In order to investigate which of these two factors is primarily responsible for impaired scratch wound closure, we plan

to perform a proliferation assay using flow cytometry to quantify Alexa Fluor 647-labelled EdU (5-ethynyl-2′-deoxyuridine) incorporation into PECs in culture. We can also consider migration studies, e.g. using a Boyden chamber to assess migration across a VEGF gradient. It should also be noted that we have only used one type of endothelial cell for these studies, and although PECs provide an excellent model to study the behaviour of microvascular ECs [256], further work should be undertaken in cells of large vessel origin, as well as human cell lines such as HUVECs.

Using a modified bead assay (from Nakatsu *et* al [243]) we investigated sprouting angiogenesis in murine pulmonary endothelial cells. The ability to form angiogenic sprouts is a key property of endothelial cells, and we saw that sprouts from IRKO cells were significantly shorter than those from WT animals. This difference was abrogated in the DKO animals, indicating that reduced IGF-1R expression in the setting of whole body IR haploinsufficiency improves the stability of angiogenic sprouts from tip cells. No difference was observed in the number of sprouts per bead, with the data being rather variable (standard error ~20% of mean value). We concluded that it would take many more mice in order to definitively exclude a difference between genotypes with this measurement, given the inherent variability, and decided that it would be unethical to do so as we had already demonstrated significance in a different parameter.

It is counterintuitive to a certain extent that we note improvements in sprouting in the DKO mice compared with IRKO, whereas there was no observed difference in scratch wound closure between these groups. Evidence from

Kennedy *et al* suggests that reduced insulin/IGF-1R signalling promotes migration in other cell types, a process which is effected through altered FOXO activity (see section 6.4). As such, our findings from the sprouting assay are in keeping with these observations, despite the scratch wound data not showing a difference. Therefore it is possible that differences between genotypes in proliferation, rather than migration, might explain some of the divergent results of these two assays. Further experiments to investigate proliferation and migration in greater detail (as outlined above) should help our understanding of the contribution of endothelial cells to the augmented vascular repair and regeneration seen in DKO animals.

Whilst bead assays such as the one used for these experiments are well-accepted methods to study sprouting angiogenesis *in vitro* [253], it is obvious that findings in this setting cannot be extrapolated directly to the far more complex systems active *in vivo*. Such a controlled environment provides a unique opportunity to examine endothelial cell properties in isolation, without the influence of other cell types which are involved in the development of new blood vessels. Having said that, complementary studies must also be undertaken in order to investigate the influence of IGF-1R reduction on angiogenesis. In this thesis we provide data from three different murine models of blood vessel repair, with these *in vitro* findings being explored further in HLI and femoral artery wire injury models. As such, we have noted significant improvements in the vascular reparative phenotype in DKO animals across a spectrum of different measures, indicating a robust association between IGF-1R reduction in the setting of IR haploinsufficiency and improved vascular repair and regeneration. Whilst further murine assays such as retinal angiogenesis studies [253] could be undertaken

to explore the DKO phenotype in more detail, a key focus of our work will involve cells from patients and healthy volunteers to find whether these interesting findings can be replicated in a setting more directly related to human disease. We also plan to use inducible models (described earlier) of IGF-1R reduction, along with pharmacological inhibitors of the receptor to explore the therapeutic potential of this approach to augment vascular repair and regeneration in insulin resistant states.

7.2.7 Summary for Vascular Repair and Regeneration

As outlined in chapter 1, insulin resistance and type 2 diabetes are increasing in global prevalence year on year, and are associated with a significantly increased risk of cardiovascular disease, and a far poorer prognosis following a vascular event such as MI or stroke. As such, a greater understanding of the mechanisms which promote vascular repair and regeneration could yield novel therapies to target insulin resistant vascular disease.

In chapter 5, we present important novel data highlighting a key role for the IGF-1R in vascular repair and regeneration. We have found that reduced IGF-1R expression abrogates the impaired recovery following vascular injury seen in IRKO, and identified supraphysiological recovery of perfusion following induction of hind-limb ischaemia in the DKO mice. We note some interesting differences in endothelial cell sprouting which help to explain the augmented vascular phenotype seen in the DKO group, although the lack of a difference in scratch wound recovery across genotypes suggest that other cell types may also be

involved in the process. Given the models studied exhibit global, rather than endothelial-cell specific IR and IGF-1R haploinsufficiency, a broad range of cell types could be responsible for the observed differences in vascular repair and regeneration. Early results from studies in bone marrow cells indicate an important role for IR/IGF-1R signalling in the determination of myeloid cell fate, which may help explain the differences seen in sections 5.3 and 5.4.

Overall, we have highlighted a key role for IR/IGF-1R signalling in vascular repair and regeneration. Further work to build on these interesting observations will be important to extend our understanding of this complex area of vascular biology and to work towards the development of novel therapeutic paradigms to treat insulin resistant vascular disease.

7.3 Aging Cohort

We selected 15 consecutively born mice from each of the four possible genotypes from the IRKO-IGF1Rko colony and observed them throughout their healthspan (see section 6.1).

7.3.1 Metabolic Phenotyping in Older Mice

In section 6.2 we provide fascinating data detailing the body weight of the aging cohort throughout their healthspan. Whilst studies have been conducted into the lifespan of IGF-1R$^{+/-}$ animals [224] and mice with fat cell-specific reduced IR expression [223], to our knowledge this is the first project to study in detail the metabolic phenotype of animals with global haploinsufficiency of one or both

receptors. We noted a significant reduction in weight in the DKO compared with all other genotypes in early adulthood (age 8-13 weeks). This difference was maintained long-term in these animals versus WT and IGF1Rko mice, although by middle age IRKO and DKO weights are similar. As such, it appears that as mice age, reduced IR expression results in a lower weight, with a synergistic effect of reduced IGF-1R expression seen in early adulthood. Although insulin resistance in humans is normally associated with obesity, this simplified model indicates that reduced IR signalling in IRKO mice leads to decreased weight gain over time, a discovery which is perhaps not surprising given the important role of the IR as a nutrient sensor and of the actions of insulin as a growth factor. It is certainly intriguing that DKO animals exhibit such a markedly different phenotype to the IFG1Rko animals as they age, with the most obese mice in the colony all belonging to either WT or IGF1Rko groups, (weight > 45g), and the maximum weight of IRKO and DKO only 40.7g and 39.8g respectively. Incredibly the highest single values recorded for weight in the WT and IGF1Rko groups (59.1g and 57.3g respectively) were approaching 20g heavier than the genotypes with reduced IR expression. As such it appears that the IR is a key determinant of weight gain over the healthspan of mice, and reduction in its expression appears to protect from obesity.

We decided to investigate glucose and insulin homeostasis in the aging colony. Although no differences were found in young adult mice (see section 5.2.4), given the marked divergence in weight across the genotypes we performed fasting glucose measurements along with glucose and insulin tolerance testing (GTT and ITT respectively) on the mice once they had exceeded 80 weeks of age. Fasting glucose was significantly lower in the DKO group compared with

IGF1Rko, with a similar trend toward a lower value versus WT. IRKO animals also showed a trend towards a lower fasting glucose compared with WT and IGF1Rko mice. GTT results indicated significantly better glucose tolerance in DKO and IRKO compared with IGF1Rko, with DKO having significantly lower glucose area under the curve (AUC) than WT and IRKO approaching significance in a similar trend. ITT results were similar, with IRKO having significantly better insulin sensitivity than WT and IGF1Rko, and DKO having significantly lower glucose AUC than IGF1Rko, and a similar non-significant trend versus WT. Given the differences we identified in body weight, we decided to explore correlations between weight and ITT and GTT results. There was a strong positive correlation in both cases, indicating that reduced IR expression protects from insulin and glucose intolerance at least in some part due to its effect on weight gain.

These novel data provide fascinating insights into the importance of the IR and IGF-1R to weight gain and glucose homeostasis across the healthspan of mice. Clearly there is scope for far greater phenotyping of these animals, but as we were monitoring healthspan in this cohort, we were keen to avoid invasive or distressing tests as much as possible. Given the differences noted previously in IRKO plasma insulin levels following a glucose bolus [146], this measurement would be important in future studies. We felt that taking blood samples (other than 1-2 microlitre tail vein samples for GTT and ITT) could artificially decrease the healthspan of the mice studied, therefore we elected not to conduct this assay or other assessments requiring larger volumes of blood on this colony.

Further investigation into the body composition of these animals would be valuable in future work. Although longitudinal non-invasive measurements of body fat content are available in our institution, the circumstances in our laboratory necessitate removal of the mice from the most sterile area of the animal facility if they undergo imaging e.g. MRI for body composition. Although they would still be kept in clean conditions, we felt that it would be inappropriate to potentially expose the animals to pathogens whilst monitoring their healthspan. Furthermore, the anaesthetic risk associated with any imaging technique, albeit low with mice, was considered to be too great (particularly in the severely obese animals) for the purposes of this study. Organs were harvested at post mortem for further analysis, however given the greatly different healthspans of the animals studied, we felt that assessment of organ weight at this stage would be misleading. In future studies, we plan to age a certain number of mice to a particular time point (e.g. 18 months), then cull them for detailed study at the same age. Clearly there are several limitations of the present work, as detailed above. In particular, murine studies cannot be directly extrapolated to human disease, however it should be noted that the entire aging study is exploratory in nature. Notwithstanding the limitations of the project, these results provide an important insight into the role of the IR and IGF-1R and represent a platform for further investigation.

7.3.2 Healthspan

Animals from the aging cohort were observed throughout their healthspan as defined in section 4.10.3. This study is still ongoing, with 1 WT, 4 IRKO, 2 IGF1Rko and 3 DKO still being within their healthspan. As such, the data

presented are the results up to 1/8/17. The DKO animals had a significantly longer healthspan than WT, with no other inter-group differences. There is well-established evidence for an increase in longevity in mice haploinsufficient for the IGF-1R [224] and with fat-specific IR-knockout (FIRKO) [223]. Indeed, Nelson *et al* have previously demonstrated that IRKO mice have similar longevity to WT, but noted an increase in the maximum lifespan of male animals [226]. To our knowledge, the data presented in section 6.3 are the first to show an improvement in healthspan in animals with reduced expression of both IR and IGF-1R versus wild-type. It is interesting to note that reduction in either receptor in isolation does not appear to confer such an advantage, hinting at a synergistic effect of reduction of both receptors.

Tumour prevalence and cause of death data are clearly not powered to detect a significant difference between genotypes, and are provided for illustrative purposes only. We cannot exclude the possibility that some of the early deaths were due to fighting within cages as part of the establishment of social order, a recognised factor in younger adult male mice [224]. Post mortem examinations were performed on all mice once they had either died spontaneously or reached a healthspan endpoint, after which point they were euthanised. Macroscopic examination to look for the presence of a tumour was undertaken throughout the thorax, abdomen and skull at this time. This gross assessment has the potential to miss the presence of small tumours, therefore if cancer prevalence is to be investigated in future studies other methods e.g. micro-CT or other imaging modality could be undertaken in order to investigate this in further detail.

Looking closely at the data, there appears to be a trend towards a small initial decrease in healthspan in the IRKO and DKO when compared to WT. As noted in section 4.10.3, fighting to establish social order is common in young male mice, and therefore antagonistic pleiotropy could be a factor, with those animals which are lighter being more vulnerable to physical violence in their youth, but surviving longer into old age due to an improved metabolic phenotype.

It should be noted that, in keeping with the rest of the aging data presented, these results represent preliminary findings of an exploratory study, and therefore firm conclusions cannot be drawn from these data. Nonetheless, these interesting findings indicate an important role for IR/IGF-1R signalling in healthy aging and warrant investigation in further detail (see section 7.5).

7.3.3 Quantitative PCR for FOXO Targets

Exploratory analyses in samples from young adult mice (age 8-15 weeks) were undertaken to explore the effects of haploinsufficiency for the IR, IGF-1R or both receptors on the levels of a range of FOXO targets. It should be noted that these results are very much preliminary findings, with no samples yet processed from IGF1Rko animals. Nonetheless, we identified some interesting signals in these samples, with ATM (ataxia telangiectasia mutated) elevated in aortic samples from both IRKO and DKO compared with WT. Interestingly ATM was elevated in fat from DKO animals compared with WT, but not in the corresponding IRKO samples, hinting at tissue-specific effects of IR and IGF-1R signalling on FOXO targets. ATM is a key activator of the DNA damage response in the face of DNA

double-strand breaks (DSBs), with a mutation in the gene causing the condition ataxia telangiectasia (hence its name) which features a severe phenotype of genomic stress leading to multisystem dysfunction and morbidity [257]. We saw significant increases in DKO frataxin and rictor compared to WT in aorta and fat respectively, with a significant increase in Myc seen in IRKO versus WT. Myc is a determinant of cell proliferation, and levels are elevated in a range of cancers, with this oncogene being primarily responsible for Burkitt's Lymphoma [248]. Rictor is involved in protein synthesis through its companionship with mTOR, with Rapamycin being well-known to prolong life [235]. Overall, we have identified several interesting readouts in the limited dataset completed thus far. Further work to increase numbers across all genotypes will give greater insight into the role of the IR and IGF-1R in the expression of FOXO targets.

We also plan to perform similar analyses in samples from the aging colony, although we first sought to look at the levels of the FOXO targets in younger animals in order to establish a baseline for further investigation. This also has the advantage that these samples are all from animals of a similar age. The fact that, for example, WT animals were much younger than DKO on reaching their healthspan endpoint, at which point their tissue was collected, means that comparison of levels of FOXO targets at this stage would not be standardised to age. Future work will need to involve a larger cohort of animals from whom samples can be taken at different standardised time points, e.g. 3, 6, 12 and 18 months for analysis. Although we have identified some interesting readouts thus far, completing the dataset may well yield further results of note. Overall, we have seen signals in a range of different target genes suggesting that reduction of IR and IGF-1R expression appears to affect downstream FOXO signalling,

with a range of factors implicated which may help explain the apparent differences seen in healthspan between groups. Future work will, in the first instance, require completion of the existing studies with processing and analysis of samples from IGF1Rko mice as well as more tissue from the other genotypes. Assuming we continue to identify interesting differences between groups, more detailed analysis e.g. with RNA sequencing to explore the full spectrum of gene transcripts in the organs studied would provide more comprehensive and unbiased data from which to seek mechanistic insights to explain the differences noted in healthspan. We are currently processing samples to quantify markers of senescence such as p21 and p16 in the IRKO-IGF1Rko colony. Future aging studies may include such analyses, with measures such as leukocyte telomere length and telomerase activity providing additional possible approaches to study the phenotype in greater detail. Overall, these preliminary results are limited by the lack of a complete dataset and by the narrow scope of the FOXO targets studied. Nonetheless, they provide interesting insights into the influence of the IR and IGF-1R on key determinants of aging, and provide a basis for further exploratory and mechanistic studies.

7.3.4 Nesting Studies

Following on from our findings of increased healthspan and augmented resilience of the DKO animals to stressors on the vasculature, we decided to investigate whether these mice exhibited other signs associated with healthy aging. There are a broad range of possible assays available to study this (reviewed in [246]). As a starting point we performed nesting studies on the older mice in the cohort according to an established protocol [245] in order to explore

the possible effects of reduced IR and IGF-1R expression on cognition and motivation. We found the DKO animals outperformed both IRKO and IGF1Rko in these experiments, with a strong trend towards an improvement versus WT. These preliminary findings are intriguing, and hint at a key role for the IGF-1R in healthy aging from a neurocognitive perspective. This assay is a broad assessment of a variety of different factors. Mice have an instinctive desire to build nests for protection from predators, to facilitate reproduction and to conserve heat [245]. To build a nest of high quality mice need motivation, planning skills, coordination, manual dexterity, and physical strength amongst other attributes. As such, the results of the assay give a gross assessment of a variety of factors which typically diminish with aging. It was interesting to note that, despite the differences highlighted in section 6.2.1, body weight did not correlate with nesting score across genotypes. Therefore, it appears the impressive performance by the DKO group cannot simply be attributed to a greater need for warmth due to their low body weight, although it should be noted that we have not measured core temperatures in these animals. Indeed, IRKO mice have a similar body weight to DKO at this age, yet score significantly worse in the nesting assay. Clearly these are preliminary findings, and further work must be undertaken to clarify the situation in greater detail. The first priority will be to study younger adult mice (age 8-15 weeks) to see if the differences observed in the aging cohort are also apparent at this age. Should this not be the case, longitudinal study of animals as they age will be required to visualise changes in behaviour over time. Moving on from this gross assessment, future investigations could include physical tests such as grip strength and wheel running, assessments of co-ordination such as rotor rod walking, and further cognitive assays such as burrowing or maze performance (reviewed in [246]).

7.3.5 Summary for Aging Cohort

In chapter 6 we present novel data indicating a key role for the IR and IGF-1R in healthy aging. Previous work by other investigators has studied the relationship between insulin and IGF-1 signalling and longevity in both global and tissue-specific murine models [223, 224] . Extensive work across multiple other species has highlighted similar findings [231-234] (reviewed in [235]). To our knowledge, however, this is the first data to describe the effects of reduction (rather than complete deletion) of both IR and IGF-1R on measures of healthy aging in mice. We found a significant improvement in the healthspan of DKO animals versus WT, and have highlighted some other interesting differences between genotypes, with IRKO and DKO being protected from weight gain, and having superior glucose and insulin tolerance compared with the other two genotypes. In keeping with previous findings in the literature [230, 235], we saw some interesting readouts suggesting divergent FOXO signalling between groups, which might help explain some of the observed differences in healthspan. Whilst our nesting studies give only a gross overall neurocognitive assessment of the animals in the aging cohort, they provide interesting data indicating a key role for the IR and IGF-1R in preservation of cognitive and physical abilities through aging.

Although many metabolic aspects of the IRKO and DKO mice are similar in these analyses (weight, GTT, ITT results), and there was no difference found in healthspan between these two genotypes, it is important to highlight the other factors which differ between them. Importantly, as outlined in chapter 5, IRKO have a blunted response to stressors on the vascular system. A feature of the

phenotype which is abrogated in the DKO animals. Previous work from other labs has shown that IGF1Rko animals have augmented resistance to stressors such as paraquat [224], and the DKO mice studied here appear to have augmented resilience to stressors on the vascular system along with an improved metabolic phenotype as they age, and indeed an increased healthspan. In that they also appear to have an improved neurocognitive phenotype, compared with IRKO, it appears that the combination of reduced IR and IGF-1R signalling confers additive benefit to a reduction in either receptor type alone across a variety of different factors.

7.4 General Limitations

In addition to the factors mentioned in the individual sections above, it is important to recognise the general limitations of the research presented in this thesis. Firstly, the data presented are largely exploratory, and several datasets remain incomplete. Clearly further work will be required in the coming months to complete these datasets and to perform some of the other assays crucial to understanding some of the preliminary findings outlined in chapters 5 and 6.

Although animal studies have been used extensively to model insulin resistance and diabetes in humans (reviewed in [62], [258]) it is important to recognise that whilst these approaches provide excellent, standardised experimental conditions to test hypotheses, they can never fully mimic the conditions seen in patients. IRKO mice are a relatively simple model of insulin resistance, and exhibit only some of the features of the human metabolic syndrome. Insulin resistance in

humans is a highly complex multi-level phenomenon, therefore transgenic animals with changes in the expression of only one or two receptor types can never fully recapitulate the physiology seen in the clinic. Indeed, it would be misleading to suggest that the findings identified in these animals could be directly extrapolated to other models of insulin resistance or diabetes, and further work with e.g. high fat-fed, leptin deficient, or even streptozotocin-treated mice will be required before results can be generalisable to wider murine physiology. Clearly studies in animals with physiology closer to that of humans would be required before any translation of this work into the clinical environment. Nonetheless, future work with human cells (see section 7.5) should help inform our understanding of the relevance of our *in vitro* and murine studies to disease in man.

A limitation of our aging cohort data is that we only included male mice in this study, although previous work has indicated gender-specific roles for IGF-1R [224] and IR signalling [226]. We chose to perform this exploratory work in male animals first, as all of the other assays performed in the IRKO:IGF1Rko colony thus far had been conducted on males to avoid cyclic effects of oestrogen on the vasculature. Nonetheless, it will be important to include females in future studies in order to investigate the effects of reduced IR and IGF-1R signalling in a broader cohort.

A potential criticism of the work presented from this project is that of the small sample sizes used in many of the assays. Whilst studies in the clinical cardiology environment now routinely include several thousand patients in each treatment

arm (e.g. [259, 260]), it is important to note that large-scale clinical trials are powered to prove hard outcomes with novel agents which have already undergone rigorous examination in a broad range of experimental settings, often over several decades. In contrast, some of the data presented in this thesis are intended to be exploratory, and therefore a pragmatic approach to the numbers used for each experiment has been taken. Aside from issues of cost, in order to comply with the ethical principles of the, “3 Rs”, it is the duty of Home Office Personal License holders to reduce the use of mice, refine experiments, and replace animal models with other techniques where possible. As such, in hypothesis generating experiments where we have achieved statistical significance in our datasets with the numbers used (even if these are relatively few), we have avoided adding extra data so as to reduce the number of mice exposed to regulated procedures. Whilst greater experimental numbers would provide more robust evidence of the findings generated, we have attempted to balance scientific rigour with the ethical considerations inherent to animal work.

Overall, the data presented largely represent exploratory studies into the relationships between the IR and IGF-1R in the context of vascular regeneration and aging. A broad portfolio of further work will be required to prove conclusively the associations shown in this thesis, with many more years of research required to elucidate the mechanisms which underpin the observed differences and to translate any positive findings towards clinical applications. Nonetheless, the interesting descriptive readouts identified thus far merit further investigation and provide a platform for future, more detailed study.

7.5 Future Directions

In addition to the specific approaches outlined in the sections above, a number of broader goals will be important to build on the work produced in this project. Initially, there are a number of datasets which remain incomplete, and therefore the first priority will be to complete these experiments in order to address the hypotheses outlined in section 2. Following this, there are a number of possible avenues for exploration in order to characterise the DKO phenotype further and to elucidate the possible mechanisms for some of the observations made.

Chapter 5 highlights a remarkable phenotype of augmented re-endothelialisation following denuding femoral artery injury, and supraphysiological vascular regeneration after induction of hind-limb ischaemia in DKO animals. Whilst there is more work to do in terms of histological corroboration of the findings seen with laser Doppler imaging, the results thus far indicate that reduction of the IGF-1R has important effects on the ability of the vasculature to repair itself. In order to help elucidate possible mechanisms for the observed favourable phenotype, we could measure local growth factor concentrations in ischaemic muscle, and use similar techniques to those employed in section 5.5.3 to study leukocyte populations in the blood and muscle of animals which have recently had induction of hind-limb ischaemia. As mentioned in section 7.2.6, it will be interesting to use both pharmacological and inducible genetic models to investigate the effect of reduced IGF-1R expression in adult animals with established insulin resistance. Translation of these findings towards possible therapeutics to benefit patients with insulin resistance will mandate exploration of the role of the IGF-1R in other animal models (including larger animals), and

indeed in human cells. Work from our department has employed lentiviral vectors to transduce human umbilical vein endothelial cells (HUVECS) as well as ECFCs with shRNA to reduce both IR and IGF-1R expression (unpublished). Functional assays with these cells such as scratch wound closure, proliferation, and bead sprouting studies will help elucidate the role of the IGF-1R in cells with reduced IR expression. Indeed, the effect of reduced IGF-1R expression in ECFCs following lentiviral transduction could be investigated *in vivo* with transfusion of these cells into mice following femoral artery wire injury or induction of hind-limb ischaemia [153]. Furthermore, ECFCs isolated from populations of patients known to be insulin resistant, such as South Asians, and those with established cardiovascular disease, could be treated with IGF-1R shRNA in order to investigate the therapeutic potential of such an approach.

Chapter 6 details some fascinating novel insights into the effects of long-term reduction of IR and/or IGF-1R expression on glucose and insulin homeostasis and on healthy aging. More detailed metabolic phenotyping of a future colony would help extend our knowledge beyond the exploratory analyses conducted thus far. Measures of glucocompetence could be conducted in longitudinal fashion, with ITT and GTT at multiple ages e.g. 6, 12, 18 months to examine the relationships between IR and IGF-1R expression and glucose homeostasis over time. More detailed analyses such as hyperinsulinaemic-euglycaemic clamping [142] could also be undertaken to provide further insights. As mentioned in section 7.2.1, measurements of plasma insulin following glucose bolus would be important, given the previously noted differences in IRKO mice [146]. We also plan to characterise the metabolic phenotype of these animals in greater detail using a comprehensive lab animal monitoring system [250]. Imaging to assess

body composition throughout aging e.g. MRI scanning could also be useful in order to help us understand the differences we have observed in weight gain between genotypes.

The healthspan data, whilst exploratory, are certainly interesting and indicate an important role for IR and IGF-1R signalling in healthy aging. Future work could include assessment of lifespan, in addition to healthspan, which would give us a greater understanding of the natural history of these animals. This would obviously require a larger sample size and an appropriate project license, but could yield important results. In addition to this, more detailed assessment of the vascular health of the mice studied would be important in future work. Imaging to examine vascular aging, e.g. coronary calcification on micro-CT, might improve our understanding of the role of the IR and IGF-1R in the development of vascular disease. Brain imaging with CT or MRI to look for evidence of intracranial pathology, e.g. cerebral involution/micro/macrovascular ischaemia, might help explain the poor performance of IRKO and WT in behavioural tests compared with DKO. The results from the quantitative PCR experiments indicate that divergent FOXO activity may be linked to the observed differences in healthspan. More detailed analysis, e.g. with RNA sequencing would help identify key factors involved in this process.

Overall, this thesis presents data which indicate an important role for the IR and IGF-1R in vascular regeneration and healthy aging. Future studies will aim to build upon the interesting exploratory findings identified thus far and to provide novel insights into this important field of vascular biology.

7.6 Concluding Remarks

As outlined in chapter 1, the rising prevalence of type 2 diabetes (T2DM) and insulin resistance represents a huge challenge to global healthcare providers. Despite significant improvements in the treatment of cardiovascular disease over recent years, there remains a significant disparity in outcomes between those with and without diabetes (DM). People with DM are twice as likely to suffer myocardial infarction (MI) and stroke and these events occur on average 15 years earlier than in the general population [5, 6]. Not only do cardiovascular events occur prematurely and more frequently in those with DM; patients have a far poorer prognosis if they develop heart disease, with double the risk of mortality following MI or in the setting of chronic heart failure (CHF) [9, 10]. As such, there is an urgent need for novel therapies to address the divergent cardiovascular outcomes seen in those with and without diabetes.

Our data indicate that reducing IGF-1R in setting of insulin resistance abrogates some of the negative findings identified in previous studies such as an impaired ability to repair damaged blood vessels [80] and to regenerate the vasculature of ischaemic tissue [247]. Further work will be needed to explore these findings in a wider variety of settings, but the insights presented here have highlighted possible mechanisms for these observations and provide a solid foundation on which to build future studies

Aging is a complex, multifactorial process with many factors affecting longevity and healthspan. Clearly, as the population gets older, it is important to consider ways in which people might be kept healthy into old age in order to mitigate the

significant morbidity associated with advancing years. Given the apparently accelerated phenotype of vascular disease in patients with DM, [6] it is important to gain a greater understanding of the factors which influence healthy aging in these individuals. Our exploratory work with insulin resistant mice with or without concomitant reduction of IGF-1R expression provides interesting insights into the relationship between healthspan and signalling through both of these receptors. There is a broad evidence base to support the importance of insulin and IGF-1 signalling in longevity ([223, 224] reviewed in [235]), and the exploratory findings detailed in this thesis point towards a key role for the IR and IGF-1R in healthy aging in mice. Further studies will aim to explore the phenotype of these animals in far greater detail including thorough metabolic and vascular assessments. More extensive neurocognitive analyses as well as behavioural and physical studies will aim to explore the effects of reduced IR and IGF-1R signalling beyond the vasculature.

Overall, this project provides important data to suggest a key role for the IR and IGF-1R in vascular health, along with preliminary insights into the importance of these signalling nodes on healthy aging *per se*. Ongoing work will aim to extend these findings beyond the interesting initial results presented, examine the influence of these receptors across broader settings, and work towards a greater understanding of the complex signalling processes which underpin insulin and IGF-1 biology. Greater mechanistic knowledge of these systems could yield novel therapeutic targets to help patients with insulin resistance and vascular disease in the future.

References

1. Federation ID. IDF Diabetes Atlas. 2015. http://www.diabetesatlas.org/.
2. Organisation WH. Global Report on Diabetes. 2016. http://apps.who.int/iris/bitstream/10665/204871/1/9789241565257_eng.pdf?ua=1.
3. Organisation WH. WHO global database on body mass index. http://apps.who.int/bmi/index.jsp (accessed 4/11/2014.
4. Rawshani A, Rawshani A, Franzen S, et al. Mortality and Cardiovascular Disease in Type 1 and Type 2 Diabetes. *The New England journal of medicine* 2017; 376(15): 1407-18.
5. Emerging Risk Factors C, Seshasai SR, Kaptoge S, et al. Diabetes mellitus, fasting glucose, and risk of cause-specific death. *The New England journal of medicine* 2011; 364(9): 829-41.
6. Booth GL, Kapral MK, Fung K, Tu JV. Relation between age and cardiovascular disease in men and women with diabetes compared with non-diabetic people: a population-based retrospective cohort study. *Lancet* 2006; 368(9529): 29-36.
7. Ovbiagele B, Markovic D, Fonarow GC. Recent US Patterns and Predictors of Prevalent Diabetes among Acute Myocardial Infarction Patients. *Cardiology research and practice* 2011; 2011: 145615.
8. From AM, Leibson CL, Bursi F, et al. Diabetes in heart failure: prevalence and impact on outcome in the population. *The American journal of medicine* 2006; 119(7): 591-9.
9. Cubbon RM, Adams B, Rajwani A, et al. Diabetes mellitus is associated with adverse prognosis in chronic heart failure of ischaemic and non-ischaemic aetiology. *Diabetes & vascular disease research : official journal of the International Society of Diabetes and Vascular Disease* 2013; 10(4): 330-6.
10. Cubbon RM, Wheatcroft SB, Grant PJ, et al. Temporal trends in mortality of patients with diabetes mellitus suffering acute myocardial infarction: a comparison of over 3000 patients between 1995 and 2003. *European heart journal* 2007; 28(5): 540-5.
11. Walker A, Cubbon R, Kearney M. Contemporary treatment strategies for Type 2 diabetes-related macrovascular disease. *Expert Rev Endocrinol Metab* 2014; 9(6): 641-58.
12. Wheatcroft SB, Williams IL, Shah AM, Kearney MT. Pathophysiological implications of insulin resistance on vascular endothelial function. *Diabetic medicine : a journal of the British Diabetic Association* 2003; 20(4): 255-68.
13. Decode Study Group EDEG. Is the current definition for diabetes relevant to mortality risk from all causes and cardiovascular and noncardiovascular diseases? *Diabetes care* 2003; 26(3): 688-96.
14. Reaven GM. Banting lecture 1988. Role of insulin resistance in human disease. *Diabetes* 1988; 37(12): 1595-607.
15. Executive Summary of The Third Report of The National Cholesterol Education Program (NCEP) Expert Panel on Detection, Evaluation, And Treatment of High Blood Cholesterol In Adults (Adult Treatment Panel III). *JAMA : the journal of the American Medical Association* 2001; 285(19): 2486-97.
16. Selvin E, Marinopoulos S, Berkenblit G, et al. Meta-analysis: glycosylated hemoglobin and cardiovascular disease in diabetes mellitus. *Annals of internal medicine* 2004; 141(6): 421-31.

17. Intensive blood-glucose control with sulphonylureas or insulin compared with conventional treatment and risk of complications in patients with type 2 diabetes (UKPDS 33). UK Prospective Diabetes Study (UKPDS) Group. *Lancet* 1998; 352(9131): 837-53.
18. Group AC, Patel A, MacMahon S, et al. Intensive blood glucose control and vascular outcomes in patients with type 2 diabetes. *The New England journal of medicine* 2008; 358(24): 2560-72.
19. Duckworth W, Abraira C, Moritz T, et al. Glucose control and vascular complications in veterans with type 2 diabetes. *The New England journal of medicine* 2009; 360(2): 129-39.
20. Holman RR, Paul SK, Bethel MA, Matthews DR, Neil HA. 10-year follow-up of intensive glucose control in type 2 diabetes. *The New England journal of medicine* 2008; 359(15): 1577-89.
21. Action to Control Cardiovascular Risk in Diabetes Study G, Gerstein HC, Miller ME, et al. Effects of intensive glucose lowering in type 2 diabetes. *The New England journal of medicine* 2008; 358(24): 2545-59.
22. Yakubovich N, Gerstein HC. Serious cardiovascular outcomes in diabetes: the role of hypoglycemia. *Circulation* 2011; 123(3): 342-8.
23. Effect of intensive blood-glucose control with metformin on complications in overweight patients with type 2 diabetes (UKPDS 34). UK Prospective Diabetes Study (UKPDS) Group. *Lancet* 1998; 352(9131): 854-65.
24. Boussageon R, Bejan-Angoulvant T, Saadatian-Elahi M, et al. Effect of intensive glucose lowering treatment on all cause mortality, cardiovascular death, and microvascular events in type 2 diabetes: meta-analysis of randomised controlled trials. *Bmj* 2011; 343: d4169.
25. Boussageon R, Supper I, Bejan-Angoulvant T, et al. Reappraisal of metformin efficacy in the treatment of type 2 diabetes: a meta-analysis of randomised controlled trials. *PLoS medicine* 2012; 9(4): e1001204.
26. Hemmingsen B, Schroll JB, Lund SS, et al. Sulphonylurea monotherapy for patients with type 2 diabetes mellitus. *The Cochrane database of systematic reviews* 2013; 4: CD009008.
27. Spigoni V, Picconi A, Cito M, et al. Pioglitazone improves in vitro viability and function of endothelial progenitor cells from individuals with impaired glucose tolerance. *PloS one* 2012; 7(11): e48283.
28. Werner C, Kamani CH, Gensch C, Bohm M, Laufs U. The peroxisome proliferator-activated receptor-gamma agonist pioglitazone increases number and function of endothelial progenitor cells in patients with coronary artery disease and normal glucose tolerance. *Diabetes* 2007; 56(10): 2609-15.
29. Gensch C, Clever YP, Werner C, et al. The PPAR-gamma agonist pioglitazone increases neoangiogenesis and prevents apoptosis of endothelial progenitor cells. *Atherosclerosis* 2007; 192(1): 67-74.
30. Trombetta A, Togliatto G, Rosso A, et al. Increase of palmitic acid concentration impairs endothelial progenitor cell and bone marrow-derived progenitor cell bioavailability: role of the STAT5/PPARgamma transcriptional complex. *Diabetes* 2013; 62(4): 1245-57.
31. Nissen SE, Wolski K. Effect of rosiglitazone on the risk of myocardial infarction and death from cardiovascular causes. *The New England journal of medicine* 2007; 356(24): 2457-71.
32. Home PD, Pocock SJ, Beck-Nielsen H, et al. Rosiglitazone evaluated for cardiovascular outcomes in oral agent combination therapy for type 2 diabetes

(RECORD): a multicentre, randomised, open-label trial. *Lancet* 2009; 373(9681): 2125-35.
33. Richter B, Bandeira-Echtler E, Bergerhoff K, Clar C, Ebrahim SH. Rosiglitazone for type 2 diabetes mellitus. *The Cochrane database of systematic reviews* 2007; (3): CD006063.
34. Dormandy JA, Charbonnel B, Eckland DJ, et al. Secondary prevention of macrovascular events in patients with type 2 diabetes in the PROactive Study (PROspective pioglitAzone Clinical Trial In macroVascular Events): a randomised controlled trial. *Lancet* 2005; 366(9493): 1279-89.
35. Skyler J. PROactive: A Sad Tale of Inappropriate Analysis and Unjustified Interpretation. *Clinical Diabetes* 2006; 24: 63-5.
36. Richter B, Bandeira-Echtler E, Bergerhoff K, Clar C, Ebrahim SH. Pioglitazone for type 2 diabetes mellitus. *The Cochrane database of systematic reviews* 2006; (4): CD006060.
37. Lincoff AM, Wolski K, Nicholls SJ, Nissen SE. Pioglitazone and risk of cardiovascular events in patients with type 2 diabetes mellitus: a meta-analysis of randomized trials. *JAMA : the journal of the American Medical Association* 2007; 298(10): 1180-8.
38. Kernan WN, Viscoli CM, Furie KL, et al. Pioglitazone after Ischemic Stroke or Transient Ischemic Attack. *The New England journal of medicine* 2016; 374(14): 1321-31.
39. Turner RM, Kwok CS, Chen-Turner C, et al. Thiazolidinediones and associated risk of Bladder Cancer: a Systematic Review and Meta-analysis. *British journal of clinical pharmacology* 2013.
40. Erdmann E, Charbonnel B, Wilcox RG, et al. Pioglitazone use and heart failure in patients with type 2 diabetes and preexisting cardiovascular disease: data from the PROactive study (PROactive 08). *Diabetes care* 2007; 30(11): 2773-8.
41. Gallwitz B, Guzman J, Dotta F, et al. Exenatide twice daily versus glimepiride for prevention of glycaemic deterioration in patients with type 2 diabetes with metformin failure (EUREXA): an open-label, randomised controlled trial. *Lancet* 2012; 379(9833): 2270-8.
42. Marso SP, Daniels GH, Brown-Frandsen K, et al. Liraglutide and Cardiovascular Outcomes in Type 2 Diabetes. *The New England journal of medicine* 2016; 375(4): 311-22.
43. Green JB, Bethel MA, Armstrong PW, et al. Effect of Sitagliptin on Cardiovascular Outcomes in Type 2 Diabetes. *The New England journal of medicine* 2015; 373(3): 232-42.
44. White WB, Cannon CP, Heller SR, et al. Alogliptin after acute coronary syndrome in patients with type 2 diabetes. *The New England journal of medicine* 2013; 369(14): 1327-35.
45. Scirica BM, Bhatt DL, Braunwald E, et al. Saxagliptin and cardiovascular outcomes in patients with type 2 diabetes mellitus. *The New England journal of medicine* 2013; 369(14): 1317-26.
46. Pfeffer MA, Claggett B, Diaz R, et al. Lixisenatide in Patients with Type 2 Diabetes and Acute Coronary Syndrome. *The New England journal of medicine* 2015; 373(23): 2247-57.
47. Ingelfinger JR, Rosen CJ. Cardiac and Renovascular Complications in Type 2 Diabetes--Is There Hope? *The New England journal of medicine* 2016; 375(4): 380-2.

48. Komoroski B, Vachharajani N, Boulton D, et al. Dapagliflozin, a novel SGLT2 inhibitor, induces dose-dependent glucosuria in healthy subjects. *Clinical pharmacology and therapeutics* 2009; 85(5): 520-6.
49. Zinman B, Wanner C, Lachin JM, et al. Empagliflozin, Cardiovascular Outcomes, and Mortality in Type 2 Diabetes. *The New England journal of medicine* 2015; 373(22): 2117-28.
50. Sattar N, McLaren J, Kristensen SL, Preiss D, McMurray JJ. SGLT2 Inhibition and cardiovascular events: why did EMPA-REG Outcomes surprise and what were the likely mechanisms? *Diabetologia* 2016; 59(7): 1333-9.
51. Bonner C, Kerr-Conte J, Gmyr V, et al. Inhibition of the glucose transporter SGLT2 with dapagliflozin in pancreatic alpha cells triggers glucagon secretion. *Nature medicine* 2015; 21(5): 512-7.
52. Pfeifer M, Townsend RR, Davies MJ, Vijapurkar U, Ren J. Effects of canagliflozin, a sodium glucose co-transporter 2 inhibitor, on blood pressure and markers of arterial stiffness in patients with type 2 diabetes mellitus: a post hoc analysis. *Cardiovascular diabetology* 2017; 16(1): 29.
53. Tikkanen I, Narko K, Zeller C, et al. Empagliflozin reduces blood pressure in patients with type 2 diabetes and hypertension. *Diabetes care* 2015; 38(3): 420-8.
54. Fitchett D, Zinman B, Wanner C, et al. Heart failure outcomes with empagliflozin in patients with type 2 diabetes at high cardiovascular risk: results of the EMPA-REG OUTCOME(R) trial. *European heart journal* 2016; 37(19): 1526-34.
55. Costa J, Borges M, David C, Vaz Carneiro A. Efficacy of lipid lowering drug treatment for diabetic and non-diabetic patients: meta-analysis of randomised controlled trials. *Bmj* 2006; 332(7550): 1115-24.
56. Tight blood pressure control and risk of macrovascular and microvascular complications in type 2 diabetes: UKPDS 38. UK Prospective Diabetes Study Group. *Bmj* 1998; 317(7160): 703-13.
57. Patel A, Group AC, MacMahon S, et al. Effects of a fixed combination of perindopril and indapamide on macrovascular and microvascular outcomes in patients with type 2 diabetes mellitus (the ADVANCE trial): a randomised controlled trial. *Lancet* 2007; 370(9590): 829-40.
58. Arguedas JA, Leiva V, Wright JM. Blood pressure targets for hypertension in people with diabetes mellitus. *The Cochrane database of systematic reviews* 2013; 10: CD008277.
59. Group AS, Cushman WC, Evans GW, et al. Effects of intensive blood-pressure control in type 2 diabetes mellitus. *The New England journal of medicine* 2010; 362(17): 1575-85.
60. Bangalore S, Messerli FH, Wun CC, et al. J-curve revisited: An analysis of blood pressure and cardiovascular events in the Treating to New Targets (TNT) Trial. *European heart journal* 2010; 31(23): 2897-908.
61. Wing RR, Bolin P, Brancati FL, et al. Cardiovascular effects of intensive lifestyle intervention in type 2 diabetes. *The New England journal of medicine* 2013; 369(2): 145-54.
62. Cubbon RM, Mercer BN, Sengupta A, Kearney MT. Importance of insulin resistance to vascular repair and regeneration. *Free radical biology & medicine* 2013; 60: 246-63.
63. Luscher TF. The endothelium and cardiovascular disease--a complex relation. *The New England journal of medicine* 1994; 330(15): 1081-3.

64. Palmer RM, Ferrige AG, Moncada S. Nitric oxide release accounts for the biological activity of endothelium-derived relaxing factor. *Nature* 1987; 327(6122): 524-6.
65. Radomski MW, Palmer RM, Moncada S. An L-arginine/nitric oxide pathway present in human platelets regulates aggregation. *Proceedings of the National Academy of Sciences of the United States of America* 1990; 87(13): 5193-7.
66. Bhardwaj R, Page CP, May GR, Moore PK. Endothelium-derived relaxing factor inhibits platelet aggregation in human whole blood in vitro and in the rat in vivo. *European journal of pharmacology* 1988; 157(1): 83-91.
67. Sneddon JM, Vane JR. Endothelium-derived relaxing factor reduces platelet adhesion to bovine endothelial cells. *Proceedings of the National Academy of Sciences of the United States of America* 1988; 85(8): 2800-4.
68. Kubes P, Suzuki M, Granger DN. Nitric oxide: an endogenous modulator of leukocyte adhesion. *Proceedings of the National Academy of Sciences of the United States of America* 1991; 88(11): 4651-5.
69. Heller R, Polack T, Grabner R, Till U. Nitric oxide inhibits proliferation of human endothelial cells via a mechanism independent of cGMP. *Atherosclerosis* 1999; 144(1): 49-57.
70. Garg UC, Hassid A. Nitric oxide-generating vasodilators and 8-bromo-cyclic guanosine monophosphate inhibit mitogenesis and proliferation of cultured rat vascular smooth muscle cells. *The Journal of clinical investigation* 1989; 83(5): 1774-7.
71. Murohara T, Asahara T, Silver M, et al. Nitric oxide synthase modulates angiogenesis in response to tissue ischemia. *The Journal of clinical investigation* 1998; 101(11): 2567-78.
72. Kuhlencordt PJ, Gyurko R, Han F, et al. Accelerated atherosclerosis, aortic aneurysm formation, and ischemic heart disease in apolipoprotein E/endothelial nitric oxide synthase double-knockout mice. *Circulation* 2001; 104(4): 448-54.
73. Lowenstein CJ, Morrell CN, Yamakuchi M. Regulation of Weibel-Palade body exocytosis. *Trends in cardiovascular medicine* 2005; 15(8): 302-8.
74. Celermajer DS, Sorensen KE, Gooch VM, et al. Non-invasive detection of endothelial dysfunction in children and adults at risk of atherosclerosis. *Lancet* 1992; 340(8828): 1111-5.
75. Joannides R, Haefeli WE, Linder L, et al. Nitric oxide is responsible for flow-dependent dilatation of human peripheral conduit arteries in vivo. *Circulation* 1995; 91(5): 1314-9.
76. Dimmeler S, Fleming I, Fisslthaler B, et al. Activation of nitric oxide synthase in endothelial cells by Akt-dependent phosphorylation. *Nature* 1999; 399(6736): 601-5.
77. Perry JM, Marletta MA. Effects of transition metals on nitric oxide synthase catalysis. *Proceedings of the National Academy of Sciences of the United States of America* 1998; 95(19): 11101-6.
78. Andrew PJ, Mayer B. Enzymatic function of nitric oxide synthases. *Cardiovascular research* 1999; 43(3): 521-31.
79. Zeng G, Nystrom FH, Ravichandran LV, et al. Roles for insulin receptor, PI3-kinase, and Akt in insulin-signaling pathways related to production of nitric oxide in human vascular endothelial cells. *Circulation* 2000; 101(13): 1539-45.

80. Kahn MB, Yuldasheva NY, Cubbon RM, et al. Insulin resistance impairs circulating angiogenic progenitor cell function and delays endothelial regeneration. *Diabetes* 2011; 60(4): 1295-303.
81. Ross R. Atherosclerosis--an inflammatory disease. *The New England journal of medicine* 1999; 340(2): 115-26.
82. Hynes RO, Wagner DD. Genetic manipulation of vascular adhesion molecules in mice. *The Journal of clinical investigation* 1996; 98(10): 2193-5.
83. Cross SS, Underwood JCE. Underwood's pathology : a clinical approach. 6th ed. Edinburgh: Churchill Livingstone Elsevier; 2013.
84. Bell GI, Pictet RL, Rutter WJ, et al. Sequence of the human insulin gene. *Nature* 1980; 284(5751): 26-32.
85. De Meyts P. Insulin and its receptor: structure, function and evolution. *BioEssays : news and reviews in molecular, cellular and developmental biology* 2004; 26(12): 1351-62.
86. Chan SJ, Keim P, Steiner DF. Cell-free synthesis of rat preproinsulins: characterization and partial amino acid sequence determination. *Proceedings of the National Academy of Sciences of the United States of America* 1976; 73(6): 1964-8.
87. Fu Z, Gilbert ER, Liu D. Regulation of insulin synthesis and secretion and pancreatic Beta-cell dysfunction in diabetes. *Current diabetes reviews* 2013; 9(1): 25-53.
88. Crane RK. Hypothesis for mechanism of intestinal active transport of sugars. *Federation proceedings* 1962; 21: 891-5.
89. Kellett GL, Helliwell PA. The diffusive component of intestinal glucose absorption is mediated by the glucose-induced recruitment of GLUT2 to the brush-border membrane. *The Biochemical journal* 2000; 350 Pt 1: 155-62.
90. Itoh N, Okamoto H. Translational control of proinsulin synthesis by glucose. *Nature* 1980; 283(5742): 100-2.
91. Bass J, Chiu G, Argon Y, Steiner DF. Folding of insulin receptor monomers is facilitated by the molecular chaperones calnexin and calreticulin and impaired by rapid dimerization. *The Journal of cell biology* 1998; 141(3): 637-46.
92. De Meyts P, Whittaker J. Structural biology of insulin and IGF1 receptors: implications for drug design. *Nature reviews Drug discovery* 2002; 1(10): 769-83.
93. Belfiore A, Frasca F, Pandini G, Sciacca L, Vigneri R. Insulin receptor isoforms and insulin receptor/insulin-like growth factor receptor hybrids in physiology and disease. *Endocrine reviews* 2009; 30(6): 586-623.
94. Cubbon RM, Kearney MT, Wheatcroft SB. Endothelial IGF-1 Receptor Signalling in Diabetes and Insulin Resistance. *Trends in endocrinology and metabolism: TEM* 2016; 27(2): 96-104.
95. Kimura KD, Tissenbaum HA, Liu Y, Ruvkun G. daf-2, an insulin receptor-like gene that regulates longevity and diapause in Caenorhabditis elegans. *Science* 1997; 277(5328): 942-6.
96. Goren HJ, White MF, Kahn CR. Separate domains of the insulin receptor contain sites of autophosphorylation and tyrosine kinase activity. *Biochemistry* 1987; 26(8): 2374-82.
97. Kasuga M, Zick Y, Blithe DL, Crettaz M, Kahn CR. Insulin stimulates tyrosine phosphorylation of the insulin receptor in a cell-free system. *Nature* 1982; 298(5875): 667-9.

98. Taniguchi CM, Emanuelli B, Kahn CR. Critical nodes in signalling pathways: insights into insulin action. *Nature reviews Molecular cell biology* 2006; 7(2): 85-96.
99. Yamaguchi Y, Flier JS, Yokota A, et al. Functional properties of two naturally occurring isoforms of the human insulin receptor in Chinese hamster ovary cells. *Endocrinology* 1991; 129(4): 2058-66.
100. Yamaguchi Y, Flier JS, Benecke H, Ransil BJ, Moller DE. Ligand-binding properties of the two isoforms of the human insulin receptor. *Endocrinology* 1993; 132(3): 1132-8.
101. Delibegovic M, Bence KK, Mody N, et al. Improved glucose homeostasis in mice with muscle-specific deletion of protein-tyrosine phosphatase 1B. *Molecular and cellular biology* 2007; 27(21): 7727-34.
102. Ebina Y, Ellis L, Jarnagin K, et al. The human insulin receptor cDNA: the structural basis for hormone-activated transmembrane signalling. *Cell* 1985; 40(4): 747-58.
103. Watson RT, Pessin JE. Subcellular compartmentalization and trafficking of the insulin-responsive glucose transporter, GLUT4. *Experimental cell research* 2001; 271(1): 75-83.
104. Kim JA, Montagnani M, Koh KK, Quon MJ. Reciprocal relationships between insulin resistance and endothelial dysfunction: molecular and pathophysiological mechanisms. *Circulation* 2006; 113(15): 1888-904.
105. Laron Z. Insulin-like growth factor 1 (IGF-1): a growth hormone. *Molecular pathology : MP* 2001; 54(5): 311-6.
106. Katznelson L, Jr ERL, Melmed S, et al. Acromegaly: An Endocrine Society Clinical Practice Guideline. *The Journal of Clinical Endocrinology & Metabolism* 2014; 99(11): 3933-51.
107. Clemmons DR. Metabolic actions of insulin-like growth factor-I in normal physiology and diabetes. *Endocrinology and metabolism clinics of North America* 2012; 41(2): 425-43, vii-viii.
108. Moses AC, Young SC, Morrow LA, O'Brien M, Clemmons DR. Recombinant human insulin-like growth factor I increases insulin sensitivity and improves glycemic control in type II diabetes. *Diabetes* 1996; 45(1): 91-100.
109. Juul A, Scheike T, Davidsen M, Gyllenborg J, Jorgensen T. Low serum insulin-like growth factor I is associated with increased risk of ischemic heart disease: a population-based case-control study. *Circulation* 2002; 106(8): 939-44.
110. Laughlin GA, Barrett-Connor E, Criqui MH, Kritz-Silverstein D. The prospective association of serum insulin-like growth factor I (IGF-I) and IGF-binding protein-1 levels with all cause and cardiovascular disease mortality in older adults: the Rancho Bernardo Study. *The Journal of clinical endocrinology and metabolism* 2004; 89(1): 114-20.
111. Ruidavets JB, Luc G, Machez E, et al. Effects of insulin-like growth factor 1 in preventing acute coronary syndromes: the PRIME study. *Atherosclerosis* 2011; 218(2): 464-9.
112. van Bunderen CC, van Nieuwpoort IC, van Schoor NM, et al. The association of serum insulin-like growth factor-I with mortality, cardiovascular disease, and cancer in the elderly: a population-based study. *The Journal of clinical endocrinology and metabolism* 2010; 95(10): 4616-24.
113. Schneider HJ, Klotsche J, Saller B, et al. Associations of age-dependent IGF-I SDS with cardiovascular diseases and risk conditions: cross-sectional

study in 6773 primary care patients. *European journal of endocrinology / European Federation of Endocrine Societies* 2008; 158(2): 153-61.
114. Gatenby VK, Imrie H, Kearney M. The IGF-1 receptor and regulation of nitric oxide bioavailability and insulin signalling in the endothelium. *Pflugers Archiv : European journal of physiology* 2013; 465(8): 1065-74.
115. Pashmforoush M, Chan SJ, Steiner DF. Structure and expression of the insulin-like peptide receptor from amphioxus. *Molecular endocrinology (Baltimore, Md)* 1996; 10(7): 857-66.
116. Zeng G, Quon MJ. Insulin-stimulated production of nitric oxide is inhibited by wortmannin. Direct measurement in vascular endothelial cells. *The Journal of clinical investigation* 1996; 98(4): 894-8.
117. Johansson GS, Chisalita SI, Arnqvist HJ. Human microvascular endothelial cells are sensitive to IGF-I but resistant to insulin at the receptor level. *Molecular and cellular endocrinology* 2008; 296(1-2): 58-63.
118. Li G, Barrett EJ, Wang H, Chai W, Liu Z. Insulin at physiological concentrations selectively activates insulin but not insulin-like growth factor I (IGF-I) or insulin/IGF-I hybrid receptors in endothelial cells. *Endocrinology* 2005; 146(11): 4690-6.
119. Soos MA, Field CE, Siddle K. Purified hybrid insulin/insulin-like growth factor-I receptors bind insulin-like growth factor-I, but not insulin, with high affinity. *The Biochemical journal* 1993; 290 (Pt 2): 419-26.
120. Federici M, Porzio O, Lauro D, et al. Increased abundance of insulin/insulin-like growth factor-I hybrid receptors in skeletal muscle of obese subjects is correlated with in vivo insulin sensitivity. *The Journal of clinical endocrinology and metabolism* 1998; 83(8): 2911-5.
121. Federici M, Lauro D, D'Adamo M, et al. Expression of insulin/IGF-I hybrid receptors is increased in skeletal muscle of patients with chronic primary hyperinsulinemia. *Diabetes* 1998; 47(1): 87-92.
122. Federici M, Giaccari A, Hribal ML, et al. Evidence for glucose/hexosamine in vivo regulation of insulin/IGF-I hybrid receptor assembly. *Diabetes* 1999; 48(12): 2277-85.
123. Abbas A, Imrie H, Viswambharan H, et al. The insulin-like growth factor-1 receptor is a negative regulator of nitric oxide bioavailability and insulin sensitivity in the endothelium. *Diabetes* 2011; 60(8): 2169-78.
124. Imrie H, Viswambharan H, Sukumar P, et al. Novel role of the IGF-1 receptor in endothelial function and repair: studies in endothelium-targeted IGF-1 receptor transgenic mice. *Diabetes* 2012; 61(9): 2359-68.
125. Duncan ER, Crossey PA, Walker S, et al. Effect of endothelium-specific insulin resistance on endothelial function in vivo. *Diabetes* 2008; 57(12): 3307-14.
126. Cusi K, Maezono K, Osman A, et al. Insulin resistance differentially affects the PI 3-kinase- and MAP kinase-mediated signaling in human muscle. *The Journal of clinical investigation* 2000; 105(3): 311-20.
127. Cai W, Sakaguchi M, Kleinridders A, et al. Domain-dependent effects of insulin and IGF-1 receptors on signalling and gene expression. *Nature communications* 2017; 8: 14892.
128. Lammers R, Gray A, Schlessinger J, Ullrich A. Differential signalling potential of insulin- and IGF-1-receptor cytoplasmic domains. *The EMBO journal* 1989; 8(5): 1369-75.
129. Kalloo-Hosein HE, Whitehead JP, Soos M, et al. Differential signaling to glycogen synthesis by the intracellular domain of the insulin versus the insulin-

like growth factor-1 receptor. Evidence from studies of TrkC-chimeras. *The Journal of biological chemistry* 1997; 272(39): 24325-32.
130. Jiang ZY, Lin YW, Clemont A, et al. Characterization of selective resistance to insulin signaling in the vasculature of obese Zucker (fa/fa) rats. *The Journal of clinical investigation* 1999; 104(4): 447-57.
131. Williams KJ, Wu X. Imbalanced insulin action in chronic over nutrition: Clinical harm, molecular mechanisms, and a way forward. *Atherosclerosis* 2016; 247: 225-82.
132. Kubota N, Kubota T, Kajiwara E, et al. Differential hepatic distribution of insulin receptor substrates causes selective insulin resistance in diabetes and obesity. *Nature communications* 2016; 7: 12977.
133. Bence KK, Delibegovic M, Xue B, et al. Neuronal PTP1B regulates body weight, adiposity and leptin action. *Nature medicine* 2006; 12(8): 917-24.
134. Delibegovic M, Zimmer D, Kauffman C, et al. Liver-specific deletion of protein-tyrosine phosphatase 1B (PTP1B) improves metabolic syndrome and attenuates diet-induced endoplasmic reticulum stress. *Diabetes* 2009; 58(3): 590-9.
135. Mosthaf L, Vogt B, Haring HU, Ullrich A. Altered expression of insulin receptor types A and B in the skeletal muscle of non-insulin-dependent diabetes mellitus patients. *Proceedings of the National Academy of Sciences of the United States of America* 1991; 88(11): 4728-30.
136. Sesti G, Marini MA, Tullio AN, et al. Altered expression of the two naturally occurring human insulin receptor variants in isolated adipocytes of non-insulin-dependent diabetes mellitus patients. *Biochemical and biophysical research communications* 1991; 181(3): 1419-24.
137. Kellerer M, Sesti G, Seffer E, et al. Altered pattern of insulin receptor isotypes in skeletal muscle membranes of type 2 (non-insulin-dependent) diabetic subjects. *Diabetologia* 1993; 36(7): 628-32.
138. Krook A, O'Rahilly S. Mutant insulin receptors in syndromes of insulin resistance. *Bailliere's clinical endocrinology and metabolism* 1996; 10(1): 97-122.
139. Kitamura T, Kahn CR, Accili D. Insulin receptor knockout mice. *Annual review of physiology* 2003; 65: 313-32.
140. Kubota T, Kubota N, Kadowaki T. Imbalanced Insulin Actions in Obesity and Type 2 Diabetes: Key Mouse Models of Insulin Signaling Pathway. *Cell metabolism* 2017; 25(4): 797-810.
141. Wu KK, Huan Y. Streptozotocin-induced diabetic models in mice and rats. *Current protocols in pharmacology* 2008; Chapter 5: Unit 5 47.
142. Haywood NJ, Cordell PA, Tang KY, et al. Insulin-Like Growth Factor Binding Protein 1 Could Improve Glucose Regulation and Insulin Sensitivity Through Its RGD Domain. *Diabetes* 2017; 66(2): 287-99.
143. Lindstrom P. The physiology of obese-hyperglycemic mice [ob/ob mice]. *TheScientificWorldJournal* 2007; 7: 666-85.
144. Accili D, Drago J, Lee EJ, et al. Early neonatal death in mice homozygous for a null allele of the insulin receptor gene. *Nature genetics* 1996; 12(1): 106-9.
145. Joshi RL, Lamothe B, Cordonnier N, et al. Targeted disruption of the insulin receptor gene in the mouse results in neonatal lethality. *The EMBO journal* 1996; 15(7): 1542-7.

146. Wheatcroft SB, Shah AM, Li JM, et al. Preserved glucoregulation but attenuation of the vascular actions of insulin in mice heterozygous for knockout of the insulin receptor. *Diabetes* 2004; 53(10): 2645-52.
147. Duncan ER, Walker SJ, Ezzat VA, et al. Accelerated endothelial dysfunction in mild prediabetic insulin resistance: the early role of reactive oxygen species. *American journal of physiology Endocrinology and metabolism* 2007; 293(5): E1311-9.
148. Yuldasheva NY, Rashid ST, Haywood NJ, et al. Haploinsufficiency of the insulin-like growth factor-1 receptor enhances endothelial repair and favorably modifies angiogenic progenitor cell phenotype. *Arteriosclerosis, thrombosis, and vascular biology* 2014; 34(9): 2051-8.
149. Folkman J. Tumor angiogenesis: therapeutic implications. *The New England journal of medicine* 1971; 285(21): 1182-6.
150. Ye W. The Complexity of Translating Anti-angiogenesis Therapy from Basic Science to the Clinic. *Developmental cell* 2016; 37(2): 114-25.
151. Cubbon RM, Ali N, Sengupta A, Kearney MT. Insulin- and growth factor-resistance impairs vascular regeneration in diabetes mellitus. *Current vascular pharmacology* 2012; 10(3): 271-84.
152. Hutter R, Carrick FE, Valdiviezo C, et al. Vascular endothelial growth factor regulates reendothelialization and neointima formation in a mouse model of arterial injury. *Circulation* 2004; 110(16): 2430-5.
153. Cubbon R, Yuldasheva N, Viswambharan H, et al. Restoring Akt1 activity in outgrowth endothelial cells from south asian men rescues vascular reparative potential. *Stem cells* 2014; 32(10): 2714-23.
154. Hagensen MK, Shim J, Thim T, Falk E, Bentzon JF. Circulating endothelial progenitor cells do not contribute to plaque endothelium in murine atherosclerosis. *Circulation* 2010; 121(7): 898-905.
155. Hagensen MK, Raarup MK, Mortensen MB, et al. Circulating endothelial progenitor cells do not contribute to regeneration of endothelium after murine arterial injury. *Cardiovascular research* 2012; 93(2): 223-31.
156. Asahara T, Murohara T, Sullivan A, et al. Isolation of putative progenitor endothelial cells for angiogenesis. *Science* 1997; 275(5302): 964-7.
157. Kalka C, Masuda H, Takahashi T, et al. Transplantation of ex vivo expanded endothelial progenitor cells for therapeutic neovascularization. *Proceedings of the National Academy of Sciences of the United States of America* 2000; 97(7): 3422-7.
158. Jain RK. Molecular regulation of vessel maturation. *Nature medicine* 2003; 9(6): 685-93.
159. Carmeliet P, Jain RK. Molecular mechanisms and clinical applications of angiogenesis. *Nature* 2011; 473(7347): 298-307.
160. Potente M, Gerhardt H, Carmeliet P. Basic and therapeutic aspects of angiogenesis. *Cell* 2011; 146(6): 873-87.
161. Augustin HG, Koh GY, Thurston G, Alitalo K. Control of vascular morphogenesis and homeostasis through the angiopoietin-Tie system. *Nature reviews Molecular cell biology* 2009; 10(3): 165-77.
162. Maisonpierre PC, Suri C, Jones PF, et al. Angiopoietin-2, a natural antagonist for Tie2 that disrupts in vivo angiogenesis. *Science* 1997; 277(5322): 55-60.
163. Phng LK, Gerhardt H. Angiogenesis: a team effort coordinated by notch. *Developmental cell* 2009; 16(2): 196-208.

164. Jakobsson L, Franco CA, Bentley K, et al. Endothelial cells dynamically compete for the tip cell position during angiogenic sprouting. *Nature cell biology* 2010; 12(10): 943-53.
165. Krebs LT, Shutter JR, Tanigaki K, et al. Haploinsufficient lethality and formation of arteriovenous malformations in Notch pathway mutants. *Genes & development* 2004; 18(20): 2469-73.
166. Fantin A, Vieira JM, Gestri G, et al. Tissue macrophages act as cellular chaperones for vascular anastomosis downstream of VEGF-mediated endothelial tip cell induction. *Blood* 2010; 116(5): 829-40.
167. Strilic B, Kucera T, Eglinger J, et al. The molecular basis of vascular lumen formation in the developing mouse aorta. *Developmental cell* 2009; 17(4): 505-15.
168. Fishman JA, Ryan GB, Karnovsky MJ. Endothelial regeneration in the rat carotid artery and the significance of endothelial denudation in the pathogenesis of myointimal thickening. *Laboratory investigation; a journal of technical methods and pathology* 1975; 32(3): 339-51.
169. Clopath P, Muller K, Staubli W, Burk RR. In vivo and in vitro studies on endothelial regeneration. *Haemostasis* 1979; 8(3-5): 149-57.
170. Zampetaki A, Kirton JP, Xu Q. Vascular repair by endothelial progenitor cells. *Cardiovascular research* 2008; 78(3): 413-21.
171. Werner N, Kosiol S, Schiegl T, et al. Circulating endothelial progenitor cells and cardiovascular outcomes. *The New England journal of medicine* 2005; 353(10): 999-1007.
172. Peichev M, Naiyer AJ, Pereira D, et al. Expression of VEGFR-2 and AC133 by circulating human CD34(+) cells identifies a population of functional endothelial precursors. *Blood* 2000; 95(3): 952-8.
173. Medina RJ, Barber CL, Sabatier F, et al. Endothelial Progenitors: A Consensus Statement on Nomenclature. *Stem cells translational medicine* 2017; 6(5): 1316-20.
174. Hirschi KK, Ingram DA, Yoder MC. Assessing identity, phenotype, and fate of endothelial progenitor cells. *Arteriosclerosis, thrombosis, and vascular biology* 2008; 28(9): 1584-95.
175. Hill JM, Zalos G, Halcox JP, et al. Circulating endothelial progenitor cells, vascular function, and cardiovascular risk. *The New England journal of medicine* 2003; 348(7): 593-600.
176. Hur J, Yang HM, Yoon CH, et al. Identification of a novel role of T cells in postnatal vasculogenesis: characterization of endothelial progenitor cell colonies. *Circulation* 2007; 116(15): 1671-82.
177. Yoder MC, Mead LE, Prater D, et al. Redefining endothelial progenitor cells via clonal analysis and hematopoietic stem/progenitor cell principals. *Blood* 2007; 109(5): 1801-9.
178. Hur J, Yoon CH, Kim HS, et al. Characterization of two types of endothelial progenitor cells and their different contributions to neovasculogenesis. *Arteriosclerosis, thrombosis, and vascular biology* 2004; 24(2): 288-93.
179. Prokopi M, Pula G, Mayr U, et al. Proteomic analysis reveals presence of platelet microparticles in endothelial progenitor cell cultures. *Blood* 2009; 114(3): 723-32.
180. Medina RJ, O'Neill CL, O'Doherty TM, et al. Myeloid angiogenic cells act as alternative M2 macrophages and modulate angiogenesis through interleukin-8. *Molecular medicine (Cambridge, Mass)* 2011; 17(9-10): 1045-55.

181. Lin Y, Weisdorf DJ, Solovey A, Hebbel RP. Origins of circulating endothelial cells and endothelial outgrowth from blood. *The Journal of clinical investigation* 2000; 105(1): 71-7.
182. Cubbon RM, Yuldasheva NY, Viswambharan H, et al. Restoring Akt1 activity in outgrowth endothelial cells from South Asian men rescues vascular reparative potential. *Stem cells* 2014; 32(10): 2714-23.
183. Cubbon RM, Murgatroyd SR, Ferguson C, et al. Human exercise-induced circulating progenitor cell mobilization is nitric oxide-dependent and is blunted in South Asian men. *Arteriosclerosis, thrombosis, and vascular biology* 2010; 30(4): 878-84.
184. Nahrendorf M, Swirski FK, Aikawa E, et al. The healing myocardium sequentially mobilizes two monocyte subsets with divergent and complementary functions. *The Journal of experimental medicine* 2007; 204(12): 3037-47.
185. Nahrendorf M, Swirski FK. Monocyte and macrophage heterogeneity in the heart. *Circulation research* 2013; 112(12): 1624-33.
186. van Furth R, Cohn ZA. The origin and kinetics of mononuclear phagocytes. *The Journal of experimental medicine* 1968; 128(3): 415-35.
187. Robbins CS, Chudnovskiy A, Rauch PJ, et al. Extramedullary hematopoiesis generates Ly-6C(high) monocytes that infiltrate atherosclerotic lesions. *Circulation* 2012; 125(2): 364-74.
188. Swirski FK, Nahrendorf M, Etzrodt M, et al. Identification of splenic reservoir monocytes and their deployment to inflammatory sites. *Science* 2009; 325(5940): 612-6.
189. Yona S, Kim KW, Wolf Y, et al. Fate mapping reveals origins and dynamics of monocytes and tissue macrophages under homeostasis. *Immunity* 2013; 38(1): 79-91.
190. Sunderkotter C, Nikolic T, Dillon MJ, et al. Subpopulations of mouse blood monocytes differ in maturation stage and inflammatory response. *Journal of immunology* 2004; 172(7): 4410-7.
191. Gamrekelashvili J, Giagnorio R, Jussofie J, et al. Regulation of monocyte cell fate by blood vessels mediated by Notch signalling. *Nature communications* 2016; 7: 12597.
192. Jung K, Kim P, Leuschner F, et al. Endoscopic time-lapse imaging of immune cells in infarcted mouse hearts. *Circulation research* 2013; 112(6): 891-9.
193. Tsujioka H, Imanishi T, Ikejima H, et al. Impact of heterogeneity of human peripheral blood monocyte subsets on myocardial salvage in patients with primary acute myocardial infarction. *Journal of the American College of Cardiology* 2009; 54(2): 130-8.
194. Fadini GP, de Kreutzenberg SV, Boscaro E, et al. An unbalanced monocyte polarisation in peripheral blood and bone marrow of patients with type 2 diabetes has an impact on microangiopathy. *Diabetologia* 2013; 56(8): 1856-66.
195. Fu Y, Moore XL, Lee MK, et al. Caveolin-1 plays a critical role in the differentiation of monocytes into macrophages. *Arteriosclerosis, thrombosis, and vascular biology* 2012; 32(9): e117-25.
196. Paneni F, Diaz Canestro C, Libby P, Luscher TF, Camici GG. The Aging Cardiovascular System: Understanding It at the Cellular and Clinical Levels. *Journal of the American College of Cardiology* 2017; 69(15): 1952-67.

197. Statistics OfN. Ageing of the UK population. 2014. http://webarchive.nationalarchives.gov.uk/20160105160709/http://www.ons.gov.uk/ons/rel/pop-estimate/population-estimates-for-uk--england-and-wales--scotland-and-northern-ireland/mid-2014/sty-ageing-of-the-uk-population.html (accessed 25/5/2017.
198. North BJ, Sinclair DA. The intersection between aging and cardiovascular disease. *Circulation research* 2012; 110(8): 1097-108.
199. Heidenreich PA, Trogdon JG, Khavjou OA, et al. Forecasting the future of cardiovascular disease in the United States: a policy statement from the American Heart Association. *Circulation* 2011; 123(8): 933-44.
200. Camici GG, Savarese G, Akhmedov A, Luscher TF. Molecular mechanism of endothelial and vascular aging: implications for cardiovascular disease. *European heart journal* 2015; 36(48): 3392-403.
201. Newman AB, Naydeck BL, Ives DG, et al. Coronary artery calcium, carotid artery wall thickness, and cardiovascular disease outcomes in adults 70 to 99 years old. *The American journal of cardiology* 2008; 101(2): 186-92.
202. Kuller LH, Lopez OL, Mackey RH, et al. Subclinical Cardiovascular Disease and Death, Dementia, and Coronary Heart Disease in Patients 80+ Years. *Journal of the American College of Cardiology* 2016; 67(9): 1013-22.
203. Vita JA, Treasure CB, Nabel EG, et al. Coronary vasomotor response to acetylcholine relates to risk factors for coronary artery disease. *Circulation* 1990; 81(2): 491-7.
204. Celermajer DS, Sorensen KE, Spiegelhalter DJ, et al. Aging is associated with endothelial dysfunction in healthy men years before the age-related decline in women. *Journal of the American College of Cardiology* 1994; 24(2): 471-6.
205. Zieman SJ, Melenovsky V, Kass DA. Mechanisms, pathophysiology, and therapy of arterial stiffness. *Arteriosclerosis, thrombosis, and vascular biology* 2005; 25(5): 932-43.
206. Vita JA, Treasure CB, Ganz P, et al. Control of shear stress in the epicardial coronary arteries of humans: impairment by atherosclerosis. *Journal of the American College of Cardiology* 1989; 14(5): 1193-9.
207. Tschudi MR, Barton M, Bersinger NA, et al. Effect of age on kinetics of nitric oxide release in rat aorta and pulmonary artery. *The Journal of clinical investigation* 1996; 98(4): 899-905.
208. Taddei S, Virdis A, Ghiadoni L, et al. Age-related reduction of NO availability and oxidative stress in humans. *Hypertension* 2001; 38(2): 274-9.
209. Yang YM, Huang A, Kaley G, Sun D. eNOS uncoupling and endothelial dysfunction in aged vessels. *American journal of physiology Heart and circulatory physiology* 2009; 297(5): H1829-36.
210. Delp MD, Behnke BJ, Spier SA, Wu G, Muller-Delp JM. Ageing diminishes endothelium-dependent vasodilatation and tetrahydrobiopterin content in rat skeletal muscle arterioles. *The Journal of physiology* 2008; 586(4): 1161-8.
211. Berkowitz DE, White R, Li D, et al. Arginase reciprocally regulates nitric oxide synthase activity and contributes to endothelial dysfunction in aging blood vessels. *Circulation* 2003; 108(16): 2000-6.
212. Higashi Y, Noma K, Yoshizumi M, Kihara Y. Endothelial function and oxidative stress in cardiovascular diseases. *Circulation journal : official journal of the Japanese Circulation Society* 2009; 73(3): 411-8.

213. Shi Y, Camici GG, Luscher TF. Cardiovascular determinants of life span. *Pflugers Archiv : European journal of physiology* 2010; 459(2): 315-24.
214. Watanabe S, Kawamoto S, Ohtani N, Hara E. Impact of senescence-associated secretory phenotype and its potential as a therapeutic target for senescence-associated diseases. *Cancer science* 2017; 108(4): 563-9.
215. Colman RJ, Anderson RM, Johnson SC, et al. Caloric restriction delays disease onset and mortality in rhesus monkeys. *Science* 2009; 325(5937): 201-4.
216. Kennedy BK, Steffen KK, Kaeberlein M. Ruminations on dietary restriction and aging. *Cellular and molecular life sciences : CMLS* 2007; 64(11): 1323-8.
217. McCay CM, Crowell MF, Maynard LA. The effect of retarded growth upon the length of life span and upon the ultimate body size. 1935. *Nutrition (Burbank, Los Angeles County, Calif)* 1989; 5(3): 155-71; discussion 72.
218. Vermeij WP, Dolle ME, Reiling E, et al. Restricted diet delays accelerated ageing and genomic stress in DNA-repair-deficient mice. *Nature* 2016; 537(7620): 427-31.
219. Bonkowski MS, Rocha JS, Masternak MM, Al Regaiey KA, Bartke A. Targeted disruption of growth hormone receptor interferes with the beneficial actions of calorie restriction. *Proceedings of the National Academy of Sciences of the United States of America* 2006; 103(20): 7901-5.
220. Bartke A, Wright JC, Mattison JA, et al. Extending the lifespan of long-lived mice. *Nature* 2001; 414(6862): 412.
221. Kojima T, Kamei H, Aizu T, et al. Association analysis between longevity in the Japanese population and polymorphic variants of genes involved in insulin and insulin-like growth factor 1 signaling pathways. *Experimental gerontology* 2004; 39(11-12): 1595-8.
222. Pawlikowska L, Hu D, Huntsman S, et al. Association of common genetic variation in the insulin/IGF1 signaling pathway with human longevity. *Aging cell* 2009; 8(4): 460-72.
223. Bluher M, Kahn BB, Kahn CR. Extended longevity in mice lacking the insulin receptor in adipose tissue. *Science* 2003; 299(5606): 572-4.
224. Holzenberger M, Dupont J, Ducos B, et al. IGF-1 receptor regulates lifespan and resistance to oxidative stress in mice. *Nature* 2003; 421(6919): 182-7.
225. Sakaguchi M, Fujisaka S, Cai W, et al. Adipocyte Dynamics and Reversible Metabolic Syndrome in Mice with an Inducible Adipocyte-Specific Deletion of the Insulin Receptor. *Cell metabolism* 2017; 25(2): 448-62.
226. Nelson JF, Strong R, Bokov A, Diaz V, Ward W. Probing the relationship between insulin sensitivity and longevity using genetically modified mice. *The journals of gerontology Series A, Biological sciences and medical sciences* 2012; 67(12): 1332-8.
227. Stephen AG, Esposito D, Bagni RK, McCormick F. Dragging ras back in the ring. *Cancer cell* 2014; 25(3): 272-81.
228. Borras C, Monleon D, Lopez-Grueso R, et al. RasGrf1 deficiency delays aging in mice. *Aging* 2011; 3(3): 262-76.
229. Slack C, Alic N, Foley A, et al. The Ras-Erk-ETS-Signaling Pathway Is a Drug Target for Longevity. *Cell* 2015; 162(1): 72-83.
230. Webb AE, Kundaje A, Brunet A. Characterization of the direct targets of FOXO transcription factors throughout evolution. *Aging cell* 2016; 15(4): 673-85.

231. Kenyon C, Chang J, Gensch E, Rudner A, Tabtiang R. A C. elegans mutant that lives twice as long as wild type. *Nature* 1993; 366(6454): 461-4.
232. Lin K, Dorman JB, Rodan A, Kenyon C. daf-16: An HNF-3/forkhead family member that can function to double the life-span of Caenorhabditis elegans. *Science* 1997; 278(5341): 1319-22.
233. Ogg S, Paradis S, Gottlieb S, et al. The Fork head transcription factor DAF-16 transduces insulin-like metabolic and longevity signals in C. elegans. *Nature* 1997; 389(6654): 994-9.
234. Tatar M, Kopelman A, Epstein D, et al. A mutant Drosophila insulin receptor homolog that extends life-span and impairs neuroendocrine function. *Science* 2001; 292(5514): 107-10.
235. Kenyon CJ. The genetics of ageing. *Nature* 2010; 464(7288): 504-12.
236. Shimokawa I, Komatsu T, Hayashi N, et al. The life-extending effect of dietary restriction requires Foxo3 in mice. *Aging cell* 2015; 14(4): 707-9.
237. Morris BJ, Willcox DC, Donlon TA, Willcox BJ. FOXO3: A Major Gene for Human Longevity--A Mini-Review. *Gerontology* 2015; 61(6): 515-25.
238. Passtoors WM, Beekman M, Deelen J, et al. Gene expression analysis of mTOR pathway: association with human longevity. *Aging cell* 2013; 12(1): 24-31.
239. Migliaccio E, Giorgio M, Mele S, et al. The p66shc adaptor protein controls oxidative stress response and life span in mammals. *Nature* 1999; 402(6759): 309-13.
240. Pagnin E, Fadini G, de Toni R, et al. Diabetes induces p66shc gene expression in human peripheral blood mononuclear cells: relationship to oxidative stress. *The Journal of clinical endocrinology and metabolism* 2005; 90(2): 1130-6.
241. Berniakovich I, Trinei M, Stendardo M, et al. p66Shc-generated oxidative signal promotes fat accumulation. *The Journal of biological chemistry* 2008; 283(49): 34283-93.
242. Feng M, Whitesall S, Zhang Y, et al. Validation of volume-pressure recording tail-cuff blood pressure measurements. *American journal of hypertension* 2008; 21(12): 1288-91.
243. Nakatsu MN, Davis J, Hughes CC. Optimized fibrin gel bead assay for the study of angiogenesis. *Journal of visualized experiments : JoVE* 2007; (3): 186.
244. Ullman-Cullere MH, Foltz CJ. Body condition scoring: a rapid and accurate method for assessing health status in mice. *Laboratory animal science* 1999; 49(3): 319-23.
245. Deacon RM. Assessing nest building in mice. *Nature protocols* 2006; 1(3): 1117-9.
246. Richardson A, Fischer KE, Speakman JR, et al. Measures of Healthspan as Indices of Aging in Mice-A Recommendation. *The journals of gerontology Series A, Biological sciences and medical sciences* 2016; 71(4): 427-30.
247. Mercer B, Walker A, Warmke N, et al. T2 Systemic insulin resistance without dysglycaemia impairs angiogenesis (oral presentation abstract). *Heart* 2016; 102: A1.
248. Finver SN, Nishikura K, Finger LR, et al. Sequence analysis of the MYC oncogene involved in the t(8;14)(q24;q11) chromosome translocation in a human leukemia T-cell line indicates that putative regulatory regions are not altered. *Proceedings of the National Academy of Sciences of the United States of America* 1988; 85(9): 3052-6.

249. Ackert-Bicknell CL, Anderson LC, Sheehan S, et al. Aging Research Using Mouse Models. *Current protocols in mouse biology* 2015; 5(2): 95-133.
250. Luk CT, Shi SY, Cai EP, et al. FAK signalling controls insulin sensitivity through regulation of adipocyte survival. *Nature communications* 2017; 8: 14360.
251. Batchu SN, Smolock EM, Dyachenko IA, Murashev AN, Korshunov VA. Autonomic dysfunction determines stress-induced cardiovascular and immune complications in mice. *Journal of the American Heart Association* 2015; 4(5).
252. Rowinsky EK, Youssoufian H, Tonra JR, et al. IMC-A12, a human IgG1 monoclonal antibody to the insulin-like growth factor I receptor. *Clinical cancer research : an official journal of the American Association for Cancer Research* 2007; 13(18 Pt 2): 5549s-55s.
253. Simons M, Alitalo K, Annex BH, et al. State-of-the-Art Methods for Evaluation of Angiogenesis and Tissue Vascularization: A Scientific Statement From the American Heart Association. *Circulation research* 2015; 116(11): e99-132.
254. Xia P, Wang S, Du Y, et al. Insulin-InsR signaling drives multipotent progenitor differentiation toward lymphoid lineages. *The Journal of experimental medicine* 2015; 212(13): 2305-21.
255. Cheng CW, Adams GB, Perin L, et al. Prolonged fasting reduces IGF-1/PKA to promote hematopoietic-stem-cell-based regeneration and reverse immunosuppression. *Cell stem cell* 2014; 14(6): 810-23.
256. Viswambharan H, Yuldasheva NY, Sengupta A, et al. Selective Enhancement of Insulin Sensitivity in the Endothelium In Vivo Reveals a Novel Proatherosclerotic Signaling Loop. *Circulation research* 2017; 120(5): 784-98.
257. Shiloh Y, Ziv Y. The ATM protein kinase: regulating the cellular response to genotoxic stress, and more. *Nature reviews Molecular cell biology* 2013; 14(4): 197-210.
258. Nandi A, Kitamura Y, Kahn CR, Accili D. Mouse models of insulin resistance. *Physiological reviews* 2004; 84(2): 623-47.
259. McMurray JJ, Packer M, Desai AS, et al. Angiotensin-neprilysin inhibition versus enalapril in heart failure. *The New England journal of medicine* 2014; 371(11): 993-1004.
260. Sabatine MS, Giugliano RP, Wiviott SD, et al. Efficacy and safety of evolocumab in reducing lipids and cardiovascular events. *The New England journal of medicine* 2015; 372(16): 1500-9.